Subduction initiation from the earliest stages to self-sustained subduction: Insights from the analysis of 70 Cenozoic sites

Serge Lallemand, Diane Arcay

Subduction initiation from the earliest stages to self-sustained subduction: Insights from the analysis of 70 Cenozoic sites.

Serge Lallemand[a] and Diane Arcay[a]

[a] Géosciences Montpellier, Université de Montpellier, CNRS, Montpellier, France

Abstract

To address the question of the initiation and mechanisms involved in the process of subduction zone formation, we explored most of the available evidence for the subduction initiation (SI) during the Cenozoic. For this, we targeted a total of 70 candidate sites for subduction initiation cumulating ~70,000 km of trench, two thirds of which are still active and a majority still immature. Our strategy is to define four stages reached for each subduction initiation site (SIS) from the incipient-diffuse stage through incipient-localized stage and early arc magma production to self-sustained subduction. We have paid special attention to prematurely extinguished, i.e., aborted, subduction attempts in order to better understand the reasons for the termination of the process, and thus to clarify the conditions of success. The failure of SI results from a combination of hindering parameters (e.g., lithosphere cooling, frictional resistance, unfavorable age contrasts for intra-oceanic SISs) and insufficient external forcings (e.g., too low convergence velocity). From this comprehensive study, we find that new subduction zones regularly nucleate, at a mean rate of about once every Myr, and with a success rate of more than 70% to reach subduction maturity, generally in less than ~15 Myr, ~3-8 Myr for the shortest time between the very early stage and the self-sustained stage. A majority forms at the transition between an ocean and a continent, plateau or volcanic arc, demonstrating that large differences in composition, topography and/or lithospheric weaknesses favor the localization of the strain. Lithospheric forces are required to ensure the success of the process in the early (immature) stages, with the help of mantle forces in a third of the cases. Multiple triggers are common. Stress during the SI process is compressive in most, if not all, cases and oriented obliquely to the nascent plate boundary in more than half of the cases. The incipient plate boundary generally reactivates an old lithospheric fault, most often with a change in its kinematics, i.e., conversion of a transform plate boundary, a former normal or a detachment fault, or even a former spreading center. Sometimes, the new lithospheric fault reactivates a former subduction fault. There is no rule concerning the age of the subducting plate which varies from 0 to 140 Ma in the examples studied. In the same vein, the subducting plate is not necessarily older than the overriding plate when it is oceanic. Both situations are equally observed.

Keywords: Subduction initiation, Cenozoic, strain localization, subduction duration, forced subduction, lithological contrast

Introduction

Nowadays, it is agreed that the excess mass of most oceanic slabs older than ~10 Ma, with respect to the surrounding mantle, drive them deep into the mantle but "how does a subduction initiate ?" still remains a fundamental question. This query has been addressed in the past by multiple authors adopting different approaches. Based on the Wilson cycle theory, named in honor of J. Tuzo Wilson by Dewey and Spall (1975), most orogenic belts preserve evidence for ocean closing after spreading (Wilson, 1968). For many authors, the corollary of this theory is that the oceanic plate begins to subduct in the mantle as it densifies and plate thickens while ageing (e.g., Hynes, 1982). Uyeda and Kanamori (1979) have emphasized the difference between two end-member subduction types: the Chilean type where a young slab dips shallowly under a compressing overriding plate versus the Mariana type where an old slab dips vertically beneath an extending upper plate. Does this mean that we should consider that the density contrast between continental and oceanic crust, or between two adjacent oceanic lithospheres, may be enough for initiating the sinking and further subduction of the old oceanic lithosphere? It is also observed that young subduction zones often locate in the vicinity of collision zones providing regional stress changes forcing convergence and subsequent subduction in weak areas (e.g., Crameri et al., 2020a), sometimes attested by the presence of ophiolites (Casey & Dewey, 1984). For Cloetingh et al. (1989), the lack of preservation of back-arc basins tends to indicate that very young oceanic regions are favorable for the development of subduction zones if they are pre-stressed.

In this study, we focus on the early stages of subduction initiation before the generation of a magmatic arc. The questions addressed here are: Under which conditions the subduction of an oceanic lithosphere may start? Are gravitational forces enough to trigger a subduction? The debate has long been focused on the question whether nascent subduction zones are induced/forced by external forces or not. Even now, the concept of “spontaneous” subduction initiation, i.e., driven only by gravity without external forcing, is still popular (e.g., Arculus et al., 2015; Stern and Gerya, 2018; Reagan et al., 2019; Maunder et al., 2020; Zhang and Leng, 2021; Zhou and Wada, 2021). However, Cenozoic examples of such mechanisms are either rare or absent (Arcay et al., 2020; Crameri et al., 2020a). Despite several regional studies (e.g., Izu-Bonin-Mariana forearc) showing relics of “infant arc” magmatism or physical models testing subduction initiation processes (e.g., Stern and Gerya, 2018), no exhaustive quantitative study on subduction initiation modes has been conducted yet. Here, we aim to shed light on the conditions which prevailed at early stages of subductions that initiated during Cenozoic time, even if they soon failed because we consider that those conditions are critical and can be easily compared with parametric physical models. We then attempt to characterize the most likely initial conditions in order to classify them and further address the mechanical processes that best explain the observations.

1. Previous studies on subduction initiation processes

1.1. Conceptual model(s) of subduction initiation: the controversy

There is a relative consensus on the fact that subduction may initiate anywhere along a weak zone if significant compressive tectonic forces are applied on an oceanic lithosphere or at an ocean-continent transition (Fig.1ab; e.g., Cloetingh et al., 1989). Self-sustaining subduction is achieved as the slab pull force exerted by the downgoing oceanic lithosphere overcomes the resisting forces (Oxburgh and Parmentier, 1977; Hassani et al., 1997; Gurnis et al., 2004). Since the 70's, another mechanism, based on the gravitational instability of an old oceanic lithosphere without any external tectonic forces, was also proposed to account for subduction initiation (Fig.1cde; e.g., Vlaar and Wortel, 1976; Turcotte et al., 1977; Hynes, 1982). This last process, even if never directly observed, is still popular because it explains the occurrence of some magmatic supra-subduction sequences along the Izu-Bonin-Mariana (IBM) subduction system for example (e.g., Stern and Bloomer, 1992). Review studies often refer to these two initiation modes, also described as forced vs spontaneous (e.g., Stern, 2004). In their last review paper, Stern and Gerya (2018) classify for example the Izu-Bonin-Mariana arc, the Tonga Arc, the Central America Arc, the Antilles Arc and the Gibraltar Arc as resulting from the collapse (understand spontaneous) at a transform fault, margins of a plume head or a passive margin respectively. They mention only one Cenozoic example of induced (understand forced) subduction which is the Solomon Arc. The present study will show that the concept of spontaneous subduction has been over-emphasized in the literature for several decades and is far from reflecting the main stream of ongoing processes involved in subduction initiation.

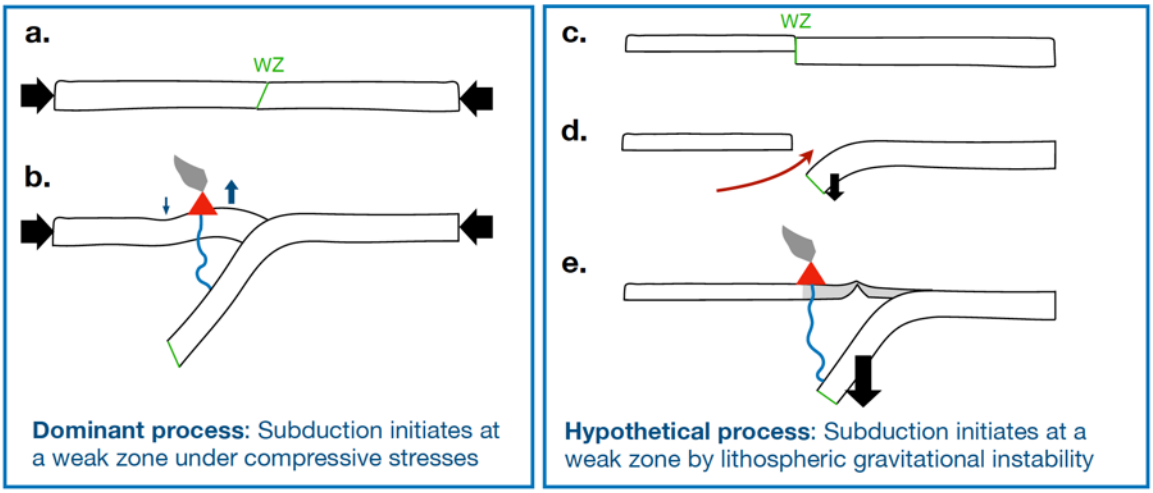

Fig.1: left sketch: dominant mode of subduction initiation with external forcing, right sketch: alternative mode without external forcing, unlikely nowadays. WZ: weakness zone, highlighted in green. Lithospheric deformations and mantle flows are depicted in dark blue and dark red, respectively. Lithospheric forces driving subduction initiation are represented with black arrows. The grey area in (e) represents the new crust often called "forearc basalts" or "early basalts".

1.2. Petro-chemical processes involved in subduction initiation

Petrological arguments were largely used by the community who advocate the process of gravitational collapse of a lithosphere denser than the asthenosphere (Fig.1cd). Given that the main driving force of a slab is its negative buoyancy with respect to the asthenosphere, density contrast reflecting compositional contrast within the lithosphere

should favor subduction initiation. Such compositional contrast exists at edges of buoyant oceanic plateaus, at passive continental margins or occasionally at transform faults (Niu et al., 2003), but the question is "Is the gravitational force enough to overcome the resisting forces including the lithosphere, the asthenosphere, and the plate boundary respective strengths?". To answer this question, sampling of rocks on both sides of the young subduction is required. Since one side has disappeared in subduction, scientists generally sample the leading edge of the overriding plate. Then, a second bias may exist if the subduction is active for millions of years because in this case, attention should be paid on whether the initial forearc has been preserved or not. From a petrological point of view, Whattam and Stern (2011) have established that most ophiolites form above a subduction zone during subduction initiation since they show a magmatic chemostratigraphic sequence from less to more HFSE[1]-depleted and LILE[2]-enriched compositions, reflecting the progressive influence of mantle melting with slab enrichment (Fig.1e). This petrological evolution has been qualified by the authors as the "subduction initiation rule". This rule may apply similarly to the Tethyan ophiolites and the IBM forearc but not to the Ligurian and Chilean ophiolites (Whattam and Stern, 2011). The stratigraphic section of the IBM forearc crust consists, from bottom to top, of peridotites, gabbroic rocks, sheeted dike complex, basaltic lava flows, boninites and their differentiates, transitional high-Mg andesites, tholeiitic and calc-alkaline arc lavas (Ishizuka et al. 2014). The basaltic series underlying the boninites were also called "forearc basalts" since Reagan et al. (2010) and others have sampled them at several forearc locations all along the IBM arc (Reagan et al., 2013). Unfortunately, similar lavas of the same age and composition were drilled in the backarc region during IODP[3] Expedition 351 west of the Kyushu-Palau Ridge (Arculus et al. 2015), making the reference to "forearc" for these basalts no more justified. In this regard, Crameri et al. (2020a), in their review study, prefered the term “early basalts” to “forearc basalts” to avoid misconceptions about their emplacement. In addition, boninites with compositions of MORB[4] enriched in slab volatiles (Bougault et al., 1981; Crawford et al., 1989) are also found in other settings than forearcs including arcs and backarcs, above mature subductions (Kamenetsky et al., 1997; Deschamps and Lallemand, 2003).
The "subduction initiation rule" as defined by Whattam and Stern (2011), Stern et al. (2012) or Whattam et al. (2020) is thus questioned. Indeed, the youngest natural case supporting the rule is ~50 Ma old. Hence, the petrological sequence supposed to be representative of subduction infancy might not be in a forearc position when subduction is initiated. One may notice that the only modern example of incipient subduction cited in the study of Whattam and Stern (2011), i.e., Macquarie Island (see section 3.2), doesn't satisfy the rule as it is entirely composed of young MORB without any enrichment from a sub-forearc mantle melt. Another scenario in which the typical "subduction infancy" magmatic sequence forms in a rear-arc position has been proposed by Deschamps and Lallemand (2002, 2003) and Lallemand (2016). This scenario scopes for the process of tectonic erosion that was responsible for the consumption of ~200 km of overriding plate leading edge along most of the western Pacific forearcs since their formation (Bloomer, 1983; von Huene and Lallemand, 1990; Lallemand, 1995). Furthermore, the scenario

[1] HFSE : High Field Strength Elements (Hf, Zr, Ti, Nb, Ta)
[2] LILE : Large Ion Lithophile Elements (K, Rb, Sr, Cs, Ba, Eu, Pb)
[3] IODP : International Ocean Discovery Program
[4] MORB : Mid-Ocean Ridge Basalt

required to form such a magmatic sequence in a forearc position implies that the forearc spreading center (sub)parallels the arc (Fig.1e, Stern, 2004; Stern and Gerya, 2018) which was never observed in modern subduction zones. Active rifting and magmatism is therefore presently observed south of the Mariana forearc but it is perpendicular to the strike of the arc (Ribeiro et al., 2015), as it was the case in the proto-Philippine Sea Plate during Early Eocene (Deschamps and Lallemand, 2002, 2003). In other words, convergence in one direction can coexist with extension in a perpendicular direction.

The second petrological criteria used to promote the spontaneity of IBM or Tethyan subduction initiation is the short time lag between initial lower plate burial and the subsequent upper plate extension (Fig.1e) because it is supposed that near-trench seafloor spreading occurs within 2-3 Myr after plate collapse and before arc volcanism establishes at a larger distance from the trench (Ishizuka et al., 2011; Reagan et al., 2013). Estimating this time lag is difficult because either we focus on the earliest magmatic products still accessible in the forearcs leading to controversies on both their dating and significance (e.g., Reagan et al., 2019; Deschamps and Lallemand, 2003), or by chance we have access to both the upper and lower plate relics of incipient subduction stages. Thanks to the exceptional exposure of the Semail ophiolite of Oman, it has been demonstrated using Lu-Hf and U-Pb geochronology that the burial of the metamorphic sole ophiolite predates by at least 8 Myr the Semail oceanic crust (Guilmette et al., 2018; Agard et al., 2016). Such a significant time span rebuts subduction initiation by rapid gravitational collapse and argues for far-field forced subduction initiation.
Considering that the supposedly typical supra-subduction zone (SSZ) sequence characterizing some ophiolites and the IBM forearc may be discarded to testify for subduction infancy, what petrological record should attest for subduction initiation in the neo-forearc and arc? Matthew & Hunter Islands region in the SW Pacific provide an ideal case of a nascent subduction zone reaching the stage where the first subduction-related magmas are erupting, since it is the youngest known volcanically-active subduction system (Patriat et al., 2019). Incidentally, both geodetic and seismic data attest for convergence across the former subduction-transform edge propagator (STEP) fault caused by the collision of the Loyalty Ridge with the New Hebrides Arc (Patriat et al., 2015). Melting of the upwelling asthenospheric mantle together with the subducted oceanic crust is recorded at a short distance (~ 100km) from the new trench. The geodynamic setting of the Matthew & Hunter incipient subduction is representative of a very non-unique but specific subduction initiation context (see section 3.2). Boninites sampled along the Hunter Ridge are probably relics of the old Vitiaz Arc (Danyushevsky et al., 2006). Backarc basalts characterize the Eissen spreading center trending oblique to the neo-trench. Asthenospheric-derived MORB-like decompression melts, slab melts (adakites) and their mixing products are observed in the 80 km long en-échelon trench-parallel Monzier rift which connects the Eissen spreading center with the infant arc (Patriat et al., 2019). The lack of precise datings of the boninites in particular makes the interpretation of these lavas difficult. The simplest interpretation being eruptive products at the intersection between a backarc spreading center and a volcanic arc above a subducting slab. Similarly with the northern termination of the Lau basin, backarc MORB-like basalts juxtaposed with boninites, are expected in the context of a STEP fault which sits both at the edge of - and above - a subduction zone, adjacent to a spreading backarc basin (Deschamps and Lallemand, 2003). However, the presence of

adakites requires hot geotherms in the slab which may be the case at the tip of a newly formed slab but which is also characteristics of flat subduction, subducting spreading centers, STEP faults or slab windows in general (Gutscher et al., 2000; Abratis and Wörner, 2001).

To summarize, the presence of either boninites or adakites found in association (or not) with backarc basalts undoubtedly reflects the existence of a subducting slab (e.g., Turner et al., 2014) but not necessarily the early stage of a subduction process. Consequently, the compatibility of a magmatic sequence with the conceptual model of gravitational collapse does not mean that the model is true as such a magmatic sequence can be found in other settings and other conceptual models also satisfy the observations. In the next sections 2 and 3, we observe a wide spectrum of magmatic products associated with early subduction and report a wide range of geodynamic settings characterizing subduction initiation.

1.3. Physical processes involved in subduction initiation: Externally driven vs gravitational instability

1.3.1 Forces at stake

To apprehend the processes involved during trench formation, let us consider the balance of forces governing at first order subduction initiation (Fig. 2). Driving forces may include, when present, the negative buoyancy of the oceanic plate (highly variable), the ridge push (~1 to $4*10^{12}$ N/m, Parsons and Richter, 1980) and other forces resulting from the considered geodynamic setting. For instance, discontinuities in uncompensated topography and/or in crust thickness (detailed in section 1.3.5.1), are assumed to generate a driving force of at most $3*10^{12}$ N/m (Turcotte and Schubert, 1982). On the other hand, the main forces resisting subduction first include the (elastic) plate resistance to bending, which rises with the ocean-floor age. This implies that the tectonic force necessary to initiate trench formation must increase with the age of the incoming plate, possibly between ~10^{12} N/m and 10^{13} N/m (McKenzie, 1977; McNutt and Menard, 1982; Wiens and Stein, 1983; Hall et al., 2003; Gurnis et al., 2004). Second, subduction initiation requires the development of a main shear zone or proto-subduction plane (e.g., Thielman and Kaus, 2012). In the least favorable situation of a homogeneous plate, it can be approximated by plate failure, for which the necessary force also increases with the oceanic plate age, between ~1 and 4.5 $*10^{13}$ N/m for a lithosphere aged between 20 and 100 Ma, this for favorable dip angle and frictional properties (Mueller and Phillips, 1991). In a more propitious setting when a weakness zone preexists such as a weak oceanic fault, the shear on the main fault was suggested to be lower than ~20 MPa, in order to decrease the integrated shear strength by one order of magnitude (Toth and Gurnis, 1998) otherwise the ridge push alone is not sufficient to overcome it (Hall et al., 2003). Third, the forming slab sinking is resisted by the viscous strength of the underlying asthenosphere (Davies, 1980), the latter possibly implying a resistant force at most equal to $2*10^{12}$ N/m (Mueller and Phillips, 1991).

1.3.2. The need of external forcing

Therefore, the main driving forces being insufficient in most cases, extra compressive forces are invoked to overcome the sum of resisting efforts (e.g., Mahatsente and

Ranalli, 2004). The additional engine may come from near- of far-field lithospheric tectonics, such as congestion of a neighboring subduction zone (Mueller and Phillips, 1991), kinematic changes (e.g., Uyeda and Ben-Avraham, 1972), or a driving shear resulting from mantle drag at the base of the lithosphere (e.g., Forsyth and Uyeda, 1975; Kemp and Stevenson, 1996). Then, upon initiation, subduction velocity must overcome a minimum rate of ~1 cm/yr to limit the hindering effect of thermal diffusion (McKenzie, 1977; Toth and Gurnis, 1998). The process becomes self-sustained when the incipient slab is long enough for the resulting excess weight (slab pull) to exceed the sum of the forces resisting convergence, that is, for slab lengths encompassed between ~225 and 300 km for reasonable friction coefficients along the subduction plane (Hassani et al., 1997). The transition from forced-convergence to self-sustained subduction could necessitate low stresses along the subduction plane, lower than 20 MPa (Hall et al., 2003). Eclogitization of the oceanic crust could help to achieve subduction sustainability (Faccenna et al., 1999; Doin and Henry, 2001; Hall, 2018).

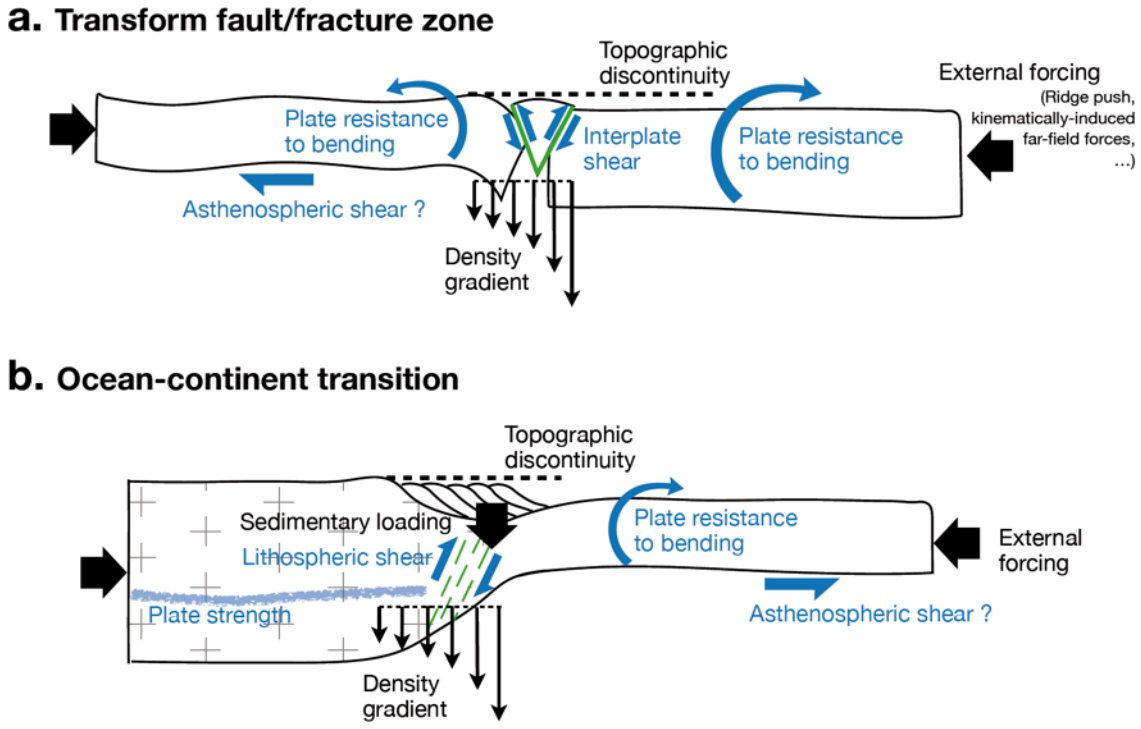

Fig.2 : Balance of intrinsic forces acting at a transform fault (a) and at an ocean-continent transition (b). The driving terms are depicted in black, and the resistant ones in blue. Weak and/or damaged areas are sketched in green. Note that the asthenosphere strength is here displayed as a force competing against subduction (passive mantle flow), but it may act as a driving term in some specific geodynamic settings (see sections 1.3.5.2 and 4.2.2).

1.3.3. Localization of deformation and weakening processes

In terms of deformation, subduction initiation (SI) succeeds if the compressive strain eventually localizes efficiently enough to form a convergent plate boundary. Shemenda (1992) showed that when an elasto-plastic passive margin is shortened, a buckling instability first develops within the oceanic plate, before deformation localizes away from the margin. Deformation localization is enhanced by weakening processes, which by the way reduce the necessary compressive stresses and thus further favor SI. A local

decrease in plate strength and/or thickness away from the OCT promotes the concentration of deformation (Shemenda 1992, later confirmed by Boutelier and Oncken's experiments, 2011). Similarly, the required compressive stresses are much lesser when subduction initiates on a preexisting dipping fault with a reduced strength or frictional properties, than when occurring on a homogenous plate (Shemenda, 1992; Toth and Gurnis, 1998; Doin and Henry, 2001). Gurnis et al. (2004) moreover note that compression of a homogeneous lithosphere prevents subduction from reaching a self-sustained state. Hence, as aforementioned the strength of the weak fault accommodating convergence could be limited to a few tens of MPa only (Hall et al., 2003), which suggests, as argued by numerous authors, that at least one process of mechanical weakening and/or localization must take place, such as strain softening (Boutelier and Oncken 2011), pore fluid pressure (Bercovici, 1998; Hall et al., 2003), shear heating (Yuen et al., 1978; Doin and Henry 2001; Crameri and Kaus, 2010; Thielmann and Kaus, 2012), low temperature plasticity (Regeneauer-Lieb et al., 2001; Auzemery et al., 2020), damage and grain size reduction (Bercovici and Ricard, 2005; Linckens et al., 2011), hydration and hydrous minerals formation, such as amphibole and talc (Soret et al. 2016) or serpentine (Hilairet et al., 2007; Shimabukuro et al., 2012). These weakening processes have not to be all activated, but a minimum softening may be required such that viscosities within the forming shear zones accommodating shortening would remain encompassed between ~10^{19} and ~10^{20} Pa.s (Agard et al., 2016; 2020), in agreement with the strength inferred for well-developed subduction "channel" (Arcay, 2017; Billen and Arredondo, 2018; Sandiford and Moresi, 2019).

1.3.4. Numerical modeling of subduction initiation: insights for various geological settings

In intra-oceanic domain, transform faults (TF) and fracture zones (FZ) represent structures that display not only contrast in plate thickness, hence in plate density, but also weak zones likely to localize shortening (Uyeda and Ben Avraham, 1972; Hilde et al., 1977; Mueller and Philipps, 1991). When subduction is forced at a TF, Hall et al. (2003) noted that in the absence of a weak zone at the plate boundary, compressive strain is accommodated by the thinner plate until a shear zone promotes the underthrusting of the oldest plate. Leng and Gurnis (2011) have highlighted three different modes of thick plate subduction at a TF as a function of the plate rheology: repeated slab breakoffs for the weakest one, continuous subduction resulting in backarc spreading for moderately weak plates, and continuous without significant upper plate deformation for the strongest plates. They show that the age of the thicker plate (i.e., of the older one) does not significantly change the result, but that pushing onto the thick plate by applying constant stresses instead of constant velocity prevents the backarc from spreading as extensional stresses are released by the downgoing plate acceleration.

In the vicinity of an ocean-continent transition (OCT), some authors consider that subduction initiation (SI) should be promoted in continents since continental lithospheres are usually weaker than oceanic ones (e.g., Ellis, 1988). Passive margins appear as preferential sites for subduction nucleation because of topographic discontinuities, sedimentary loading and/or lateral compositional buoyancy contrast (Fig. 2). Numerical experiments of imposed convergence at passive margin have shown that convergence

localization is modelled in the oceanic plate if it is younger than ~40 Myr, and rather occurs at the OCT for older oceanic plates (Zhong and Li, 2019; Auzemery et al., 2020). The required boundary force increases with the ocean-floor aging (Zhong and Li, 2019), but SI always fails for oceanic plates older than 90 Myr for reasonable forces imposed to foster convergence (Zhong and Li, 2019; Auzemery et al., 2020). Using analogue experiments of kinematically-driven SI at a passive margin, Faccenna et al. (1999) have evidenced three different modes of deformation when shortening is imposed, from diffuse folding to fast subduction and trench rollback, that depend on the negative buoyancy of the oceanic plate, and of the amount of (uncompensated) lateral pressure gradient. If the latter is high, continental collapse occurs and loads the oceanic plate, triggering a fast SI. They emphasized the role of the lower ductile continental plate since it is the layer that must accommodate the initial depression at the OCT, as also suggested by Auzemery et al. (2020). Nevertheless, Crameri et al. (2020a) considered that trench formation at passive margins are scarcely observed, possibly because the OCT strength (both in the brittle and ductile realms), is too high to be overcome, despite sedimentary loading as well as elevational and crustal discontinuity (Mueller and Phillips, 1991).

1.3.5. The concept of “spontaneous” subduction

1.3.5.1. Physical considerations and successive steps

Vlaar and Wortel (1976) proposed that subduction initiates by gravitational instability by noting that the age of the oceanic plate at trench and the maximum depth of seismicity were positively correlated at subduction zones. Arguing that the oceanic plate age also controls the plate weight excess, they inferred that a high degree of gravitational instability was favored for the oldest plates (>70 Ma). The threshold age above which a cooling oceanic lithosphere becomes denser than the underlying asthenosphere has been argued to be ~40 Myr (e.g., Oxburgh and Parmentier, 1977), and the maximum negative buoyancy for old oceanic plates could be limited to ~35 kg/m³ only (Afonso et al., 2007). SI by gravitational collapse, at a transform fault or at an ocean-continent transition (OCT), is a concept assuming that lateral variations of density and/or of elevation generate a lateral pressure gradient across the plate boundary (Fig. 2), that can lead to lithospheric gravitational instability (“vertical forcing”, Crameri et al. 2020) if the resulting tensional forces are high enough (Erickson and Arkani-Hamed, 1993; Kemp and Stevenson, 1996). This would facilitate the first stage of “spontaneous” subduction, that is trench formation by plate bending initiation (Fig.1d). In 3D, the setup may be less favorable as the margin curvature affects the direction of the lateral pressure gradient and can hinder spontaneous subduction triggering (Marques et al., 2014).

A successful SI then implies to decouple the two adjacent plates to avoid the downward dragging of the overriding plate along with the incipient subducting plate (« ablative subduction”, Tao and O’Connell, 1992, or « two-sided subduction », Gerya et al., 2008). This critical step is usually achieved by an asthenosphere upward flow along the subducting plate surface, filling the gap between the two plates up to the surface (Kemp and Stevenson, 1996). The resulting asthenospheric outcropping is quite fast and occurs over an widening area (Leng and Gurnis, 2011; Fig. 1d), which should be associated with a significant mantle melting by decompression. In some cases, plate decoupling eventually occurs thanks to the weakening of the oceanic plate surface resulting from

the water release at asthenospheric depth (Gerya et al., 2008; Nikolaeva et al, 2010). Otherwise, in numerous experiments plate decoupling does not occur and either the gravitational downgoing motion prematurely stops, or the two adjacent plates are only partly dragged together downward (Faccenna et al., 1999; Gerya et al., 2008; Arcay et al., 2020). When modelled "spontaneous" subduction usually proceeds fast (< 1 to 6 Myr, Hall and Gurnis, 2003; Gurnis et al., 2004; Gerya et al., 2008; Nikolaeva et al., 2010; Lu et al., 2015; Marques and Kaus, 2016; Zhou et al. 2018). This swiftness has been an additional argument to advocate for subduction initiation by gravitational instability to explain an assumed fast triggering of arc magmatism in IBM (Reagan et al., 2013, Maunder et al., 2020, see section 1.2).

1.3.5.2. Preferential sites invoked for spontaneous subduction

Passive margins have been suggested to be a suitable site for this mode of "spontaneous" subduction because they intrinsically display several promising specificities, as mentioned in the previous section. First, the differences in crust composition and thickness between continental and oceanic lithospheres imply a high lateral density gradient (Niu et al., 2003), but also a rheological contrast possibly favoring strain localization. Analogue experiments have shown that the ductile continental plate must be soft enough (~100 times weaker than the underlying asthenosphere, Mart et al., 2005; Goren et al., 2008) to promote flowing on top of the oceanic side. This condition is achieved when the Moho temperature is close to the crust solidus (Nikolaeva et al., 2010), which requires an additional heating process, such as rifting or a plume head impact. Second, the topographic discontinuity at the OCT that is not elastically supported exerts a push onto the oceanic plate during viscous relaxation, possibly of the order of the ridge push force (Turcotte and Schubert, 1982), that would further enable the viscous spreading of the continental crust on the oceanic side and initiate subduction if the spreading width extended up to a few hundreds of km (Lévy and Jaupart 2012). Third, the potential role of sedimentary loading in passive margin collapse (Dewey, 1969) has been extensively explored. Cloetingh et al. (1982, 1984) concluded that the most propitious conditions corresponded to a young (<20 Myr old) and soft passive margin undergoing a sedimentary loading high enough to allow tensile failure, and that oceanic plate aging mainly prevented trench formation by cooling-induced strengthening. Plasticity was shown to enable plate failure by sedimentary loading when specific, perhaps extreme, conditions were assumed. For instance by combining a low to moderate (< 25 km) elastic thickness and an excessive sedimentary loading, equivalent to a 100 Myr old margin (Branlund et al., 2000); or when low temperature plasticity (Peierls'stress) and shear heating interplay in combination to an additional weakening process lowering by at least 2 orders of magnitude the plate viscous strength, possibly resulting from olivine hydration (Regenauer-Lieb et al., 2001). Lastly, the potential role of basal shear to trigger the OCT destabilization was addressed by Mulyukova and Bercovici (2018): a significant weakening by fast grain-size reduction and grain-sensitive diffusion creep has to be activated to offset the thermally-induced strengthening of the passive margin. This implies, in addition to ridge push, a high basal shear stress (>10 MPa) that cannot be modeled using classical asthenospheric viscosities (<10^{20} Pa.s).

Far away from passive margins, the process of lithospheric gravitational instability was investigated at transform faults (TF) and fracture zones. The older plate spontaneously

sinks for a significant offset in plate thickness and a limited viscosity contrast (between 10 and 10^3) between lithospheres and the underlying asthenosphere when thermal diffusion is neglected (Matsumoto and Tomoda, 1983). Nonetheless, “spontaneous” subduction fails when thermal conduction is considered, even in the most propitious case of an old and thick plate facing a section of the asthenosphere (Hall et al., 2003; Baes and Sobolev, 2017). To successfully model the instability of the thicker plate, density contrasts at the TF must be maximized. This is reached either by adding a thick and buoyant crust at the thinner plate top (Leng and Gurnis, 2015) mimicking the edge of an oceanic plateau (Niu et al., 2003), or/and by imposing at the TF an extremely thin younger plate (≤1 Myr old), either in 2D (Nikolaeva et al., 2008) or in 3D (Zhu et al., 2009, 2011; Zhou et al., 2018). Additionally, subduction initiation by gravitational instability always needs a soft domain in the vicinity of the plate interface with adequate mechanical weakness. This condition is modelled thanks to the dehydration of the incipient slab if the released fluids yield a strong lubrication and mechanical decoupling between the two plates, but simultaneously the lithospheric plates have to be strong enough (Gerya et al., 2008), possibly to prevent localization outside the plate boundary. Alternatively, the necessary plate surface weakening can be reached by pore fluid pressure increase with sea water downward percolation if the matrix permeability is assumed to be low enough (≤10^{-21} m^2, Dymkova and Gerya, 2013).

Generally, models show that trench formation at TFs and OCTs without any external compressive forcing requires not only very particular and favorable geodynamical settings but also additional processes of enhanced plate weakening, the amount of which may be extreme and likely not reasonable (Arcay et al. 2020). The concept of spontaneous subduction has thus been advocated to not apply in the vast majority of recorded subduction infancies under present-day Earth’s conditions (Fig.1): significant compressive stresses must somehow come into play to drive subduction initiation (McKenzie, 1977; Mueller and Phillips, 1991; Hall et al. 2003; Arcay et al. 2020; Crameri et al., 2020a).

2. Four stages and three fates of subduction initiation: our definitions

In this study, the subduction initiation (SI) process is not limited to onset but includes all immature stages preceding the mature subduction stage. Indeed, our strategy consists of learning from the detailed examination of the maturation stages from the very early symptoms including the failing modes before reaching the self-sustained state. The terminology used in this study includes three immature (or maturation) stages of SI: "incipient-diffuse SI", "incipient-localized SI", and "achieved SI" and, ultimately, a mature stage called "self-sustained subduction". At each stage, the fate of the process could be either currently active or inactive. If it is inactive, we make a difference between an early stop in the SI process at an immature stage and call it abortion, and a stop of the subduction at an advanced mature stage and call it extinction (Fig.3).

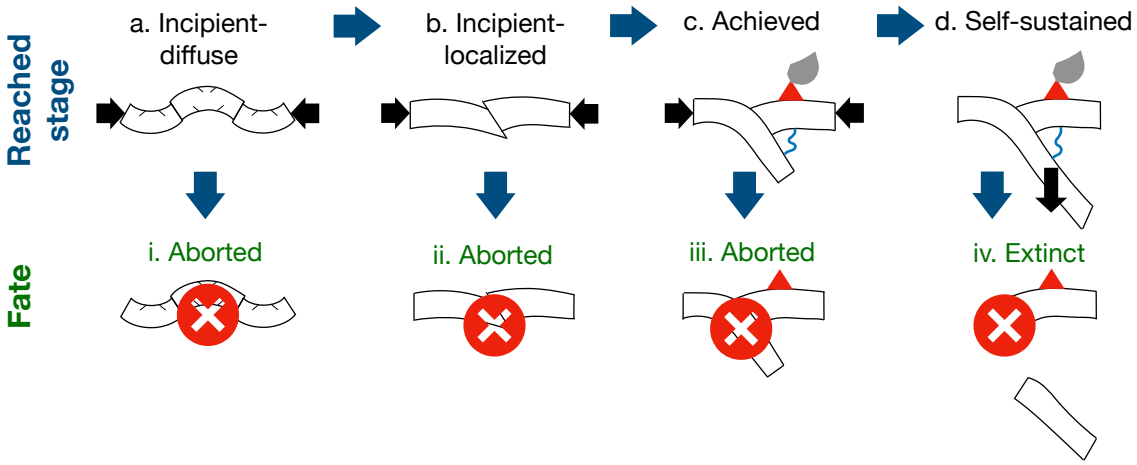

Fig.3: SI proceeds through three different immature stages a, b and c before reaching the final mature stage d, all being active at present-day in this cartoon. The process may stop at each of these stages either prematurely (i, ii, iii) or after a period of self-sustained activity (iv). Smoking/non-smoking volcanoes symbolize active and extinct subduction magmatism. Each of the further 70 Cenozoic SI sites corresponds to one of these active or inactive stages depending on their present-day status.

SI may be suspected when significant lithospheric deformation, either compressive or producing highs and lows, is observed in a restricted area which did not previously suffer such deformation. Buckling of the oceanic lithosphere under compression often precedes the failure (Fig.3a). If compressive stress overcomes the lithospheric strength in a homogeneous lithosphere, neo-formed conjugate thrusts form and accommodate the shortening (Shemenda, 1992; Gerbault, 2000). The same evolution is expected if normal faults inherited from crustal accretion at a mid-ocean ridge are oriented sub-perpendicular to the principal stress. Typically, E-W trending normal faults in the Indian Ocean started to reactivate into reverse faults around 9 Ma (Delescluse et al., 2008). There, a N-S compressive stress comes from the collision in the Himalaya as the Indian continent subducts beneath Eurasia to the north (Cloetingh and Wortel, 1985). Today, the ~20-60 km of shortening still distributes over a wide area (~800 x 500 km) and strain localization has not been completed (Delescluse and Chamot-Rooke, 2007). The eastern passive margin of the Japan Sea, off Tohoku and Hokkaido, is another example of tectonic inversion of normal faults caused by E-W shortening since 1.8 Ma (Nakamura, 1983). Today, the shortening is accommodated over a ~100 km-wide area along several east and west-dipping thrusts (Tamaki and Honza, 1985). Strain localization along one main lithospheric thrust fault is not yet accomplished there (van der Werff, 2000).
We will call this stage **"incipient - diffuse SI"**. At this stage, nobody knows yet if a new subduction will proceed in the near future or if it will stop (Fig.3i).

We will talk about **"incipient - localized SI"** when deformation localizes on a single convergent proto-plate boundary (Fig.3b). As a case example, the region off the East-Taiwan coast exhibits ~19 km of cumulated slip along a single NS-trending flat thrust (the Chimey Canyon thrust) (Hsieh et al., 2020). Here, the collision between the northern

Luzon Arc and the Chinese continental platform caused an ongoing reversal of subduction polarity since ~3 Myr (Chemenda et al., 1997). Compressive deformation and shortening first occurred in the northern Luzon forearc and then flipped ~2 Ma ago in the rear-arc region (Malavieille et al., 2002). Underthrusting of the oceanic Huatung Basin beneath the deformed Luzon Arc (E-Taiwan Coastal Range) is supported by regional tomography imaging and seismicity (Lallemand, 2014). Nowadays, ~3 cm/yr of convergence is accommodated offshore, essentially along the Chimey Canyon thrust. As for incipient-diffuse SI, no one can predict the future evolution of such systems.

Once the deformation localizes on a single proto-plate boundary, the process either aborts (Fig.3ii), fossilizing the scars of the SI reached stage, or proceeds until the downgoing plate reaches the depth of the asthenospheric wedge and triggers primitive arc magmatism through mantle wedge metasomatism.

We will consider the **SI as "achieved"** once arc magmatism starts (Fig.3c). The southernmost Ryukyu subduction zone (SZ) developed during the last 8 Myr by westward lateral propagation of the Ryukyu slab (Lallemand et al., 2001). Arc volcanism started less than 2 Ma as the Southern Okinawa Trough opened (Sibuet et al., 1995). Another case may be represented by Matthew & Hunter (see section 1.2). Slab melts or MORB-like melts enriched in volatiles have been dredged at some distance from the new trench (Patriat et al., 2019). If further datings demonstrate that these lavas containing slab-derived volatiles are less than 1.8 Ma old, one may consider that this new SZ has reached the achieved state. The process of SI can still stop at this stage (Fig.3iii) or proceed forward.

The next step for the subduction initiation process is the one of maturity, i.e., becoming **self-sustained** as the forced slab reaches the length for which its excess weight somehow overcomes the forces competing against subduction (Fig.3d). This is the case for the Izu-Bonin-Mariana, Aleutians or Tonga-Kermadec subduction systems. Any cessation of activity of a mature subduction, like the Vitiaz SZ (see section 3.2), will be considered as an extinction (Fig.3iv).

Unlike other studies which generally focus on SI giving rise to mature subductions, we consider here that understanding why short-lived subduction failed shed light on SI processes. For each natural case, we aim to date the early strain exerted over a narrow area (≲ 200 km), then localized on a single lithospheric fault and finally give birth to the early arc volcanism. We will only treat in this study the cases of SZ initiation where the subducting plate is oceanic, whatever could be their later evolution.

Glossary

The terminology used by each (group of) author(s) generally depends on the approach and objectives. The same term or acronym can have different meanings. Below we clarify what we mean by some of the key terms in our study.

***SZ**: Subduction zone.*

***Immature SZ**: Any SZ the initiation of which is still "in progress" or whose evolution has not yet reached a self-sustained state.*

***Mature SZ**: Any SZ having reached a self-sustained stage.*

***SI**: Subduction initiation. It designates the process of initiating a SZ in a generic manner from the onset to the last stage before self-sustained subduction.*

***SIS**: Subduction initiation site. In this study, SIS concerns all sites where significant lithospheric deformation, prone to evolve into a new subduction zone, is suspected. It thus includes the subduction zone initiation (SZI) events defined by Crameri et al. (2020a&b) but also all sites where a SZ propagates/expands laterally, resumes from a former SZ or fails before reaching a self-sustained state.*

***OT**: Oceanic Transition. For the purpose of this study, we sometimes use the generic term OT to designate the transition between oceanic crust and continental crust (generally called OCT), but also plateau crust (OPT) or arc crust (OAT). We thus extend the 'OCT' terminology to the transition with arc crust or oceanic plateau crust because in all these cases, we observe a large compositional and/or topographic difference. As a consequence, OT may be used indifferently in classical oceanic settings (typically around a remnant arc fringed by oceanic crust) or in continental settings at the edge of a passive margin.*

***Oceanic subduction**: Any subduction where an oceanic plate is subducting (Lallemand, 2016b). Note that it does not imply the overriding plate to be oceanic.*

***Ridge**: any elongated buoyant oceanic feature, such as a seamount chain or an aseismic plateau, that is always distinct from a spreading ridge.*

3. A review of Cenozoic examples of SI

In this chapter, we have attempted to list most subduction initiation sites (SISs) recorded during the Cenozoic (Table 1). For some of them, the geodynamic context is well constrained but we are fully aware that many of them are model-dependent. It happens that geological and geophysical evidence may be incomplete leading to controversies between authors. We have tried to list the essentials of the published scenarii, sometimes adding our own analysis.

NW Pacific (30, 21480 km)		SW Pacific (17, 26880 km)		Atlantic Ocean (6, 1990 km)	
C- & W-Aleutians	1700	N-Melanesian	3000	Saint Paul	100
Bowers Ridge	380	Vitiaz	2800	Romanche	380
Proto-Kamtchatka	550	Pocklington (S-Melanesian)	3300	N-Iberia	700
Komandorsky	400	Samoa-Gilbert-Ralik (Micronesian)	4200	SW Iberia (incl. Gorringe)	250
Kamtchatka	550	N-Solomon	700	Barracuda	380
Kuril	1500	New Britain - San Cristobal (incl. S-Solomon)	2300	Tiburon	180
E-Japan Sea	850	Trobriand	650		
Ryukyus-Nankai	1650	New Hebrides	1350	**Mediterranean & surroundings (5, 6100 km)**	
S-Ryukyus	400	Ambrym (incl. Pentecost-Maewo)	200	Carpathians	1000
Zenisu	220	Matthew & Hunter	380	W-Mediterranean	3200
Gagua - E-Luzon Trough	900	d'Entrecasteaux Zone	600	Gibraltar	200
Manila	1000	Loyalty - Three Kings (New Caledonia)	2100	Calabria	600
Taiwan E-coast	100	Tonga-Kermadec	3500	N-Maghrebides (Alboran to Sicily)	1100
Negros	180	Puysegur	500		
Cotobato	380	McDougall	550	**Indian Ocean & surroundings (3, 6900 km)**	
Philippines	1380	Macquarie	200	Sumatra - Java (Sunda)	3800
NW-Borneo - Cagayan	930	Hjort	550	C-Indian Ocean	1100
Flores	570			Banda (incl. Seram)	2000
Wetar	350	**NE Pacific (1, 1050 km)**			
Sula	100	Cascadia	1050	**Scotia Plate (2, 1500 km)**	
Sulu	200			Endurance Collision Zone	700
N-Sulawesi	440	**Caribbeans & surroundings (6, 4450 km)**		S-Sandwich	800
Tolo	250	S-Caribbeans	1700		
Sangihe	1300	N-Panama	700	**SI reached stage : incipient-diffuse, incipient-localized, achieved, self-sustained - Present SZ status : active, aborted (when self-sustained stage was never reached), extinct**	
Halmahera	700	Puerto-Rico (incl. E-Hispaniola & Virgin Islands)	700		
Izu-Bonin-Mariana	2530	Muertos	700		
Yap	600	Nicaragua Rise	250		
Palau	220	Beata Ridge	400		
Lyra	550				
Mussau	600	**Trench length of 70 subduction zone sites initiated during Cenozoic cumulating 70350 km**			

Table 1: List of studied Cenozoic SISs with their respective lengths in km (measured at present, not at the time of SI). Each SIS labelled with colored characters corresponds to a stage reached either today or when it ceased to be active. Simple underlining refers to aborted cases and double underlining to extinct cases.

3.1. Northwest Pacific area

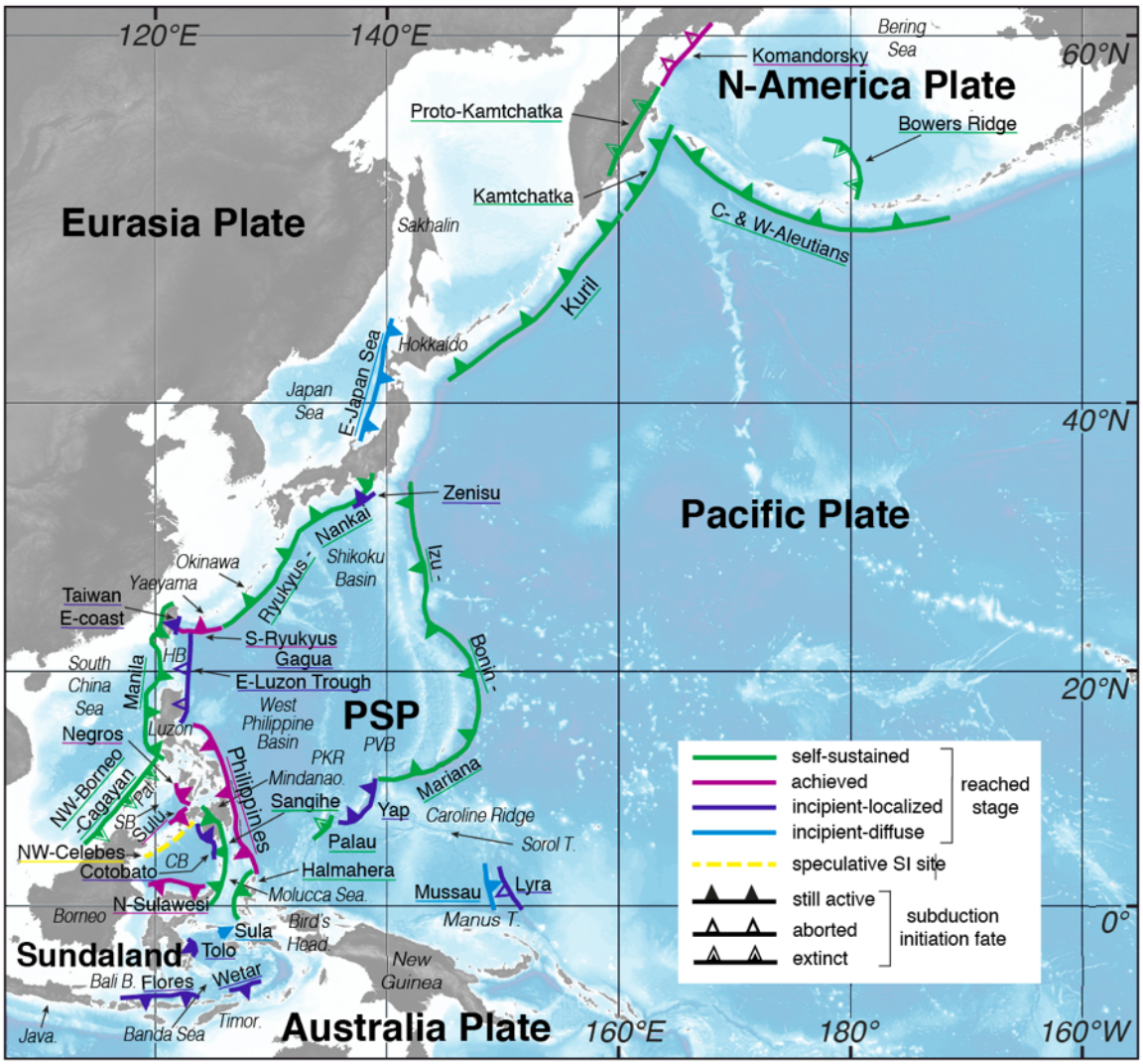

Fig.4: Map of Cenozoic SISs in the NW Pacific region. Some of them have expanded or shrunk since their initiation but only their present-day trace is represented here. The color code representing the stage reached after SI onset is the same as in Table 1. The solid triangles on the upper plate side indicate that the mature or immature SZ is still active. Open triangles indicate that the SI process aborted at an immature stage. Solid combined with open triangles correspond to extinct mature SZs. The yellow dotted line outlines a speculative paleo-SIS. Each SIS is underlined with the adequate color and labelled with plain letters, whereas toponymy appears in italic. Main plates are in bold letters. C- & W-: Central & Western, E-: Eastern, NW-: Northwest, N-: North, B.: Basin, T.: Trough or Trench, HB: Huatung Basin, Pal.: Palawan, CB: Celebes Basin, SB: Sulu Basin, PKR: Palau-Kyushu Ridge, PVB: Parece-Vela Basin.

Central and Western Aleutians - Bowers Ridge

Convergent plate boundaries have profoundly evolved in the NW Pacific area throughout the Cenozoic (Fig. 4). During Paleocene, the Kula (and Kronotsky) plate(s) subducted northward beneath the North-American plate (NAM) along southern Alaska (same as today's location) and Beringian margin in the Bering Sea, while the Eurasia plate subducted southward beneath the Izanagi (and Olyutorsky) plate(s) away from Siberia, producing the Olyutorsky arc (OA, Scholl et al., 1992; Konstantinovskaya, 2001; Domeier et al., 2017; Vaes et al., 2019). Following the collision between the OA against proto-Kamtchatka around 55-50 Ma, the Central and Western Aleutian SZ initiates within the Kula plate, either along a TF as suggested by its small circle shape (Vaes et al.,

2019) or spreading center segments of the Kula-Pacific ridge (Seton et al., 2015; Domeier et al., 2017) or both. The oldest arc volcanism of the Aleutian arc has been dated to 46 Ma (Jicha et al., 2006). During this process, part of the Late Cretaceous Kula plate called Aleutia (Scholl et al., 1992) or Aleutian Basin (Vaes et al., 2019) was trapped and incorporated into the NAM plate. Since the vergence has changed from the earlier Olyutorsky SZ to the Aleutian one, we can describe the process as a flip of subduction including polarity reversal, even if the distance from the earlier subduction varies from the rear-arc to 1700 km away. Later, in the Oligocene, the collision of part of the Kronotsky arc with the Central Aleutian SZ might have triggered some local intra-Aleutia southwest-dipping subduction at the origin of the Bowers Ridge as attested by the 34-26 volcanic arc rocks dredged on the ridge (Wanke et al., 2012). The presence of adakitic-like material might reflect either very oblique subduction (Wanke et al., 2012) or simply reflect the effect of STEP faults that might have accompanied this narrow (~380 km) back-arc subduction (Vaes et al., 2019).

Proto-Kamtchatka - Komandorsky - Kamtchatka - Kuril

The Kamtchatka Peninsula has recorded several arc collisions. The Olyutorsky arc (also called Achaivayam-Valaginskaya Arc in the north and Nemuro-Vitiaz in the south) docked against the Asian continent, i.e., Kamtchatka-Hokkaido-Sakhalin orogen, diachronously starting near south-Kamtchatka at ~55-65 Ma (Konstantinovskaya, 2001) or ~55-50 Ma (Vaes et al., 2019) and around ~45 Ma both northward along Kamtchaka and southward until Hokkaido and Sakhalin (Konstantinovskaya, 2001; Vaes et al., 2019). As a result of this diachronous collision, SE-vergent initial subduction flipped on the other side of the Olyutorsky Arc initiating new segments of NW-vergent SZs : the proto-Kamtchatka SZ first around 55 Ma and then the Kuril SZ around 45 Ma. The oldest granodiorite belonging to the Kuril arc has been dated to ~31 Ma (De Grave et al., 2016). Later, the Kronotsky arc, carried by the Pacific plate, was supposed to both (1) drag the western Aleutian arc, inducing a 400 km-long westward subduction of the Komandorsky Basin, further called Komandorsky SZ, beneath North Kamtchatka between 20 and 13 Ma, and (2) collide and accrete against the South Kamtchatka margin around 13 Ma at the origin of a subduction jump back of the Kronotsky arc, further called Kamtchatka SZ (Konstantinovskaya, 2001; Vaes et al., 2019).

Eastern margin of Japan Sea

The N-S-trending eastern margin of the Japan Sea undergoes strong E-W compression at an estimated shortening rate increasing from 0 off North Sakhalin to 15 mm/yr off Central Japan (Wei & Seno, 1998). Normal faults inherited from the Oligo-Miocene Japan Sea rifting and spreading are reactivated into reverse faults since about 1.8 Ma (Nakamura, 1983; Seno, 1983; Kobayashi, 1983; Tamaki & Honza, 1985; Lallemand & Jolivet, 1985; Okamura et al., 1995, 2005; Sato et al., 2014). Four thrust earthquakes, with magnitudes Mw ranging from 7.5 and 7.8 occurred during the last century (Okamura et al., 2005) along this margin, which is considered by several authors as an incipient SZ still in a stage of strain localization, as the ~100 km-wide shortening area off Tohoku exhibits both vergences (Okada et al., 1985; Tamaki & Honza, 1985; van der Werff, 2000). The reactivated margin merges with the transform boundary between the Eurasia and North America plates at the time of the opening of the Japan Sea. E-W compression across this former plate boundary began about 3.5 Ma ago, possibly as a result of clockwise rotation of the AMUR Plate (Lallemand and Jolivet, 1985). Another

cause for E-W compression could be the resistance of the upper mantle underlying the Pacific slab to escape, preventing trench roll back and slab sinking or the flattening of the Pacific slab far from its edges (Lallemand, 1998; Lallemand et al., 2005; Schellart, 2020).

Nankai - Ryukyus - S-Ryukyus

The Ryukyus subduction system is composed of two main segments (Kizaki, 1986), possibly across an inherited N-S-trending shear zone which has accommodated the opening of the Japan Sea (Le Pichon, pers. comm. 1997). The longest one starts from Izu Peninsula to the south of Okinawa Island, including the Nankai Trough as well as the Northern and Central Ryukyus. It is the geological continuation of the Mesozoic-Eocene Shimanto accretionary complex observed in SW Japan. The record of arc magmatism along the main segment is discontinuous throughout the Cenozoic (Kimura et al., 2005; 2014). The quiescence of the volcanism between 27 and 15(?) Ma and between 12 and 6 Ma have been interpreted respectively by Kimura et al. (2005, 2014) as periods of transform faulting rather than subduction, accommodating the clockwise rotation of the Philippine Sea plate and Shikoku Basin opening (e.g., Hall, 1996) and creeping of the Izu-Bonin arc beneath the margin. If true, it means that the Ryukyu subduction has ceased and resumed at least once during the Cenozoic era. The shortest segment corresponds to the Southern Ryukyus including the Yaeyama Islands. The geology there is comparable to those of Taiwan with HP metamorphic rocks (Faure et al., 1988). Furthermore, Shinjo (1999) considers that the absence of any subduction-related since the Middle Miocene magmatic record on the Yaeyama islands suggests that the western part of the southern Ryukyus was not a SZ at this time. Based on global tomography data, Lallemand et al. (2001) have demonstrated that the southernmost Ryukyu margin was formerly the northern passive margin of the South China Sea during its Oligo-Miocene spreading. Then, around 8 Ma, the Ryukyus SZ propagated laterally through a STEP fault that developed along the ocean-continent transition formed by the rifted margin of the South China Sea. The trigger of the lateral subduction propagation could have been the full consumption of the TF that separated the NW-dipping Ryukyus SZfrom the SE-dipping Manila SZ (Lallemand et al., 2001). The westward lateral translation of the Central Ryukyus broad slab significantly complicates the setting of arc volcanism there. The oldest volcanic rocks attributed to this new SZ are 2 Ma old (Sibuet et al., 1995) making this case intermediate between achieved and self-sustained.

Zenisu

About 50 km away from the trench at the northernmost edge of the Philippine Sea Plate, shortening is undergoing within the Shikoku Basin resulting in a 2 km high – 220 km long intra-oceanic sliver called Zenisu (Le Pichon et al., 1987; Chamot-Rooke and Le Pichon, 1989). Intraplate shortening started about 2 Ma ago and localized along a series of low-angle thrusts cutting through the entire crust and a single lithospheric thrust which already accommodated 9 km of reverse slip (Mazzotti et al., 2002). The lithospheric character of the thrust is supported by the 5 km vertical offset of the Moho according to Nakanishi et al. (1998, 2002). This restricted deformation caused by the differential motion of the subducting oceanic basin with respect to the buoyant Izu-Bonin Ridge potentially led to earlier accretion of oceanic slivers at the margin by subduction jump from the previous plate boundary to the developing intraplate thrust since Early Miocene (Lallemand et al., 1992). Based on refined geophysical data (Park et al., 2003; Kodaira

et al., 2004; Dessa et al., 2004), Lallemand (2014) has reinterpreted the structure of the ridge and do not exclude distributed crustal shortening of the oceanic crust with low-angle thrusts branching in depth onto a decoupling layer at transition between the crust and the mantle. The location of the deforming zone at the rear of the Izu-Bonin arc may not be fortuitous since it may be weakened by ascending fluids from the subducting Pacific Plate.

Gagua Ridge - East Luzon Trough

The Gagua Ridge is an N-S-trending narrow striking feature overhanging the abyssal plain off southeast Taiwan which has been interpreted by Mrozowski et al. (1982) as an uplifted sliver of oceanic crust possibly bounding a fracture zone. Based on further investigations, Deschamps et al. (1998, 2000) have confirmed the origin of the feature as a former transform fault separating a piece of Early Cretaceous oceanic crust (Huatung Basin) trapped between Taiwan and the ridge from the Eocene West Philippine Basin. The observations that the magnetic lineations are perpendicular to the west but oblique to the ridge as well as the presence of the deepest – now filled – trough fringing the ridge on the east side are pieces of evidence that a significant amount of West Philippine Basin oceanic crust has been underthrusted beneath the ridge with an increasing cumulative slip in the south near Luzon island (Deschamps and Lallemand, 2002). The East Luzon Trough is supposed to have accommodated significant shortening until the Late Oligocene (Lewis and Hayes, 1983; Yumul et al., 2003). The vergence and the timing of the past subduction as well as the age of the subducting plate have been constrained – and confirmed - by further gravity models built from detailed seismic structure of the ridge (Deschamps et al., 1998; Eakin et al., 2015). One or two subduction initiation episodes have been proposed depending on assumptions: one around 50-40 Ma ago involving the subduction of a very young oceanic crust (~5 Ma) and another around 24 Ma involving a ~25 Ma subducting oceanic crust. The western edge of the Philippine Sea Plate underwent transpression during most of its rotating northward motion from the Equator to its present position (Deschamps and Lallemand, 2002). It seems highly possible that the weak zone formed by this former transform plate boundary has accounted for two shortening episodes during the Cenozoic. Lavas, recently grabbed at the top of the Gagua Ridge by a Chinese ROV in 2018, indicate Early Cretaceous subduction-related arc magmatism (Qian et al., 2021). Furthermore, the presence of 0.25 to 2.45 Ga trapped zircons xenocrysts in the lavas implies that the Gagua Ridge basement is partially composed of continental material of Cathaysian affinity that drifted away from the Eurasian margin during the opening of the Huatung Basin, southern China. Since there is no evidence of Cenozoic infant arc volcanism, we conclude that Cenozoic subduction inception stopped prematurely at the incipient-localized stage. The new discovery of continental relics beneath the ridge, despite its narrowness and linearity is puzzling, and questions the representativeness of the sampling at a unique site.

Manila – Taiwan East coast

The 1000 km long Manila SZ formed during the last spreading phase of the South China Sea around 18 Ma ago as attested by the oldest age of arc volcanism (16 Ma according to Yang et al., 1995, 1996). The end of spreading is debated within a range from 18 to 12 Ma, due to the fact that late volcanism dated 6-10 Ma superimposes with the last spread crust in the basin axis (Briais et al., 1993; Li et al., 2014; Koppers, 2014;

Barckhausen et al., 2014; Sibuet et al., 2016; Zhao et al., 2018; Huang et al., 2018). The simplest geodynamic setting prior to the initiation of subduction was a major N-S-trending transform fault bounding the South China Sea on its eastern edge (Huang et al., 2019), then transpression occurred in the Middle Miocene along this transform plate boundary and oblique subduction initiated, involving the active spreading center of the South China Sea. Yumul et al. (2003) have proposed that the Manila SZ initiation resulted from the counter-clockwise rotation of Luzon in response to the collision of the Palawan microcontinental block with the Philippine mobile belt. The northern segment of the Manila SZ involves the Chinese continental platform since 3 to 5 Ma promoting the Taiwan orogeny (Lu and Hsü, 1992; Malavieille et al., 2002). Based on analog modeling, Chemenda et al. (2001a) have proposed that the convergence should flip from an eastward-dipping slab to a westward one on the other side of the orogen. Evidence for such subduction flip along the eastern coast of Taiwan is observed from bathymetry and seismic imaging (Lallemand et al., 1999, 2013). Shortening is maximal beneath northeastern Taiwan and underthrusting of the Huatung Basin beneath the East coast propagates southward along the East coast of Taiwan. It is accommodated by buckling and thrusting of the Philippine Sea Plate over a ~100 km-wide area with strain localization along a new plate boundary offshore Hualien in a rear-arc position with respect to the accreted North Luzon arc (Lallemand, 2014). About 3 cm/year of shortening has been accommodated there since less than 1 Ma and ~20 km of shortening have already been accommodated on a single thrust at the foot of the Coastal range (Hsieh et al., 2020). The incipient subduction propagates southward concomitantly with the breakoff of the Eurasian slab (Lallemand et al., 2001; Gautier et al., 2019)

Negros – Cotobato - Philippines

The Negros and Cotobato SZs probably developed contemporaneously with the Manila Trench around Middle Miocene from a series of N-S-trending transform boundaries fringing the Miocene Sulu and Eocene Celebes marginal basins on their east side, due to a change in the Philippine Sea Plate motion (Pubellier et al., 2014). Arc volcanism landward of Cotabato Trench belongs to the Sangihe Arc (Molucca Sea long-lived slab and not the <100 km-long Celebes Sea slab) according to Hall (2018). Perez et al. (2018) suggest that the ~45 Ma Zambales ophiolitic rocks may represent early stages of an east-dipping subduction offshore Mindanao as they show boninitic affinities but further investigations are needed to establish which subduction was associated with these Eocene relics. Recently based on a new age compilation, Lai et al. (2021) challenged this interpretation suggesting that subduction of the SE Sulu Sea along the Negros-Sulu trenches may have started in ~4 Myr forming the Plio-Pleistocene arc and adakitic volcanism in SW Philippines. E-W-trending Palawan/Cagayan and Sulu continental ridges bounding the marginal basins collided with the Philippine archipelago in late Miocene slowing the convergence across the Negros and Cotobato trenches and inducing a flip of subduction on the other side of the Philippine arc along the incipient Philippine Trench (Lallemand et al., 1998). Failure within the Philippine Sea plate started either near Mindanao, propagating in both directions (Lallemand et al., 1998) or in the

north, propagating southward (Macpherson, 2008). Hall (2018) proposes an alternate mechanism, based on extensional features observed in the margin and on the fact that the Cotobato SZ is not "needed" as the Sangihe and Philippine SZs already accommodate the convergence. He suggests that margin's failure loaded the crust of the Celebes Basin up to a point where the oceanic crust is sufficiently depressed to transform into eclogite and then sinks.

Sangihe - Halmahera

Many studies refer to a wide oceanic basin called Molucca Sea having almost entirely subducted both westward beneath the Sangihe arc since 25 to 30 Ma and eastward beneath the Halmahera arc, beneath and south of Mindanao Island, Philippines since about 10 Ma (Silver & Moore, 1978; Hall, 1987; Lallemand et al., 1998; Rangin et al., 1999; Zahirowicz et al., 2014; Hall & Spakman, 2015; Wu et al., 2016; van der Meer et al., 2018). Its total width, cumulating both slabs and based on tomography, has been first estimated at 3400 km by Rangin et al. (1999) and further revised to 1500 km by Wu et al. (2016) and van der Meer et al. (2018). The reconstruction of the initial geodynamic setting before subduction is uncertain but Wu et al. (2016) observe that unfolded Philippine and Halmahera slabs edges fit exactly, suggesting that both subducting plates belonged to the same mother plate and that subduction might have initiated along a transform boundary sometime in late Miocene. Hall (2018) proposes that the former Molucca Sea formed a quasi-rectangular basin north of the Australian promontory (Sula Spur and Bird's Head). This large oceanic basin was forced to close in mid-Miocene due to the reorganization of Sundaland following the India-Australia ongoing collision. Two opposite-verging SZs, turning their back, initiated along passive margins on the two small sides of the rectangle, while the two transform faults accommodated the closure along the long sides. Yang et al. (2016) proposed an alternate cause involving a slab avalanche through the 660 km discontinuity in Early Miocene, which is supposed to trigger basin inversion across the southern Sundaland.

Northwest Borneo-Cagayan (Palawan) – Sulu – North Sulawesi - Tolo - Sula

Just like the lost Molucca Sea, another oceanic basin: the proto South China Sea, has entirely disappeared from Eocene to Miocene by subduction beneath NW Borneo and the Cagayan Ridge (Pubellier & Meresse, 2013; Pubellier and Morley, 2014; Wu et al., 2016). These authors propose that the start of subduction along its southern rifted margin coincided with the onset of India-Sundaland collision at 47 Ma. However, Encarnacion et al. (1995) and Keenan et al. (2016), based on precise dating of the metamorphic sole at the base of the Palawan ophiolite rather suggest a SI at ~35 Ma ending at ~17 Ma, as an accommodation of the South China Sea opening. The geodynamic setting at the start of the Palawan SZ is either a TF for Encarnacion et al. (1995) or a spreading-center for Keenan et al. (2016). Yang et al. (2016) suggested another trigger, or at least another contributor, for the SI of the proto-South China Sea, i.e., the mantle dynamics, since the start of the compression at the southern margin of the basin coincided with a huge slab avalanche in the lower mantle beneath southern Sundaland. The N-S shortening jumped to the southern rim of the young Sulu Basin around 12-15 Ma as the Palawan continental Block collided with the Cagayan arc (Pubellier & Meresse, 2013; Pubellier and Morley, 2014; Wu et al., 2016) triggering the birth of the Sulu subduction zone. We must mention here an alternate scenario which

assumes that the Palawan Continental Terrane start of accretion at ~21 Ma was first accommodated by a NW-dipping Celebes Sea subduction prior than a SE-dipping Sulu Sea subduction which formed later at ~4 Ma (Lai et al., 2021). In the present study, we do not consider the existence of a NW-dipping Celebes Sea subduction (see the yellow dotted line in Fig.4) beneath the Sulu Ridge because of the lack of structural constraints along the Sulu Ridge SE margin. However, we recognize that further offshore investigations should unveil the reality of this subduction episode. NW-Borneo might still accommodate some convergence according to geodetic measurements (Simons et al., 2007). To the south of these basins, the direct influence of the Australian platform collision triggered a complex microblock reorganization including the initiation of new SZs as the N Sulawesi one in Late Miocene or the Tolo one during Pliocene. The age of subducting oceanic crust at SI varies from less than 17 Ma for the Sulu Basin or the North Banda Basin to 40 Ma for the Celebes Basin. As for Cotobato, Hall (2018) observes similar extensional features along the margins of N-Sulawesi and Tolo that are supposed to have loaded the adjacent oceanic crust and triggered its sinking. According to Hall (2018), many of these short subduction zones are initiated at the transition between thick and hot continental or arc crust and oceanic crust triggered by loading of the transition zone as the result of the collapse of the thick crust. The earliest stage is reflected by the Sula Deep in the young North Banda Sea.

Flores - Wetar

Backthrusting in the South Banda back-arc basin of the Eastern Sunda Arc has been first noticed by Hamilton (1979). A detailed geophysical survey then helped to map the newly formed trench north of Sumbawa-Flores and Wetar Islands. Silver et al. (1983) described the two main north-directed backthrusts over 570 km for the Sumbawa-Flores segment and 350 km for the Wetar segment, pointing out lateral propagation both in between the two former segments and west of the system in the Bali Basin. Shortening across the incipient-localized Flores and Wetar thrusts is attested by seismicity (McCaffrey and Nabelek, 1984) and has been estimated to be 30 and 10 km respectively by Silver et al. (1983). Based on geodetic measurements, Koulali et al. (2016) characterized a 2000 km long line of active deformation running from East Java to east of Wetar Island accounting for 5 to 40 % of the total convergence between the Australia plate and the Sunda Block. The convergence rate across this line of deformation increases eastward up to ~3 cm/yr concomitantly with the westward decreasing of the convergence accommodated from 7 cm/yr along the Java Trench to 3 cm/yr near 123°E, rapidly decreasing westward along Timor trough. The ~30-40% of convergence obliquity between major plates is accommodated by ~37% of lateral shear along the backthrusts (right-lateral north of Flores and left-lateral north of Wetar, Koulali et al., 2016). According to most authors, collision between the arc and the Australian continent is the main driver but do not totally explain the particular location of the thrusts, especially the westernmost segment facing the oceanic part of the Australian Plate (Silver et al., 1983). The westward propagation of the lithospheric thrust along the rear-arc might be caused by the subduction of the Roo Rise, a massif of seamounts which locally increases the interplate friction (Silver et al., 1983). Polarity reversal (subduction flip) occurred at the rear of the East Sunda Arc at the ocean-continent transition with

young oceanic basins, i.e., > 13 Ma for the Flores basin and < 6.5 Ma for the South Banda Basin (Hinschberger et al., 2001; 2005).

Izu-Bonin-Mariana

The Izu-Bonin-Mariana (IBM) system is often cited as an example of subduction which developed from a transform plate boundary between the Pacific and the Izanagi (or Kula) oceanic plates in early Eocene (e.g., Uyeda and Ben-Avraham, 1972). The IBM arc built on a composite substratum made of Cretaceous remnant arc rocks, mostly observed today in the Amami-Daito-Oki-Daito region but also in the IBM arc itself (Matsuda et al., 1975; Hickey-Vargas, 2005), and of ~48-52 Ma basalts observed today both in the forearc and the back-arc area (Ishizuka et al., 2011; 2018). Boninitic lavas attesting for the presence of subduction-derived fluids started to erupt almost simultaneously around 51 Ma (Reagan et al., 2019). The composition of the lavas evolved from high-Si to transitional boninites and then typical tholeiites. This magmatic sequence was described by several authors as a typical supra-subduction zone ophiolite interpreted as resulting from the sinking of the old oceanic plate under its weight excess allowing asthenosphere invasion in the early stages of subduction initiation (e.g., Stern and Bloomer, 1992, see section 1.2). This scenario is refuted by Lallemand (2016) and Arcay et al. (2020) because it neglects the fact that a significant portion of the initial IBM margin has been removed by subduction erosion and it is very unlikely from a mechanical point of view, unless using unrealistic weak lithologies. Regardless of this controversy (see section 1.1), most people agree that subduction initiated along an oceanic transform or fracture zone and arc volcanism started around 50-52 Ma. Furthermore, significant age contrast between the two plates and the presence of buoyant features on the overriding plate are very probable. Depending on the mechanical process (spontaneous or forced), the initiation either started simultaneously with asthenosphere invasion, because such process is known to be catastrophic (Maunder et al., 2020; Arcay et al., 2020), or a few Myrs – typically after 100 km of convergence - before accounting for strain localization of the TF area under compressive stress (Hall and Gurnis, 2003). Several triggers have been invoked for the birth of the IBM subduction zone which preceded the major change in Pacific plate motion around 43-50 Ma (e.g., Whittaker et al., 2007) or the Oki-Daito plume around 48 Ma (Ishizuka et al., 2013). Both events should result from IBM's inception rather than the opposite (Faccenna et al., 2010; 2012). A good candidate is the subduction of the Izanagi-Pacific spreading center beneath East Asia around 60-55 Ma (Whittaker et al., 2007). Spreading segments were supposed to align sub-parallel with the East Asia margin so that the Izanagi plate should have detached from the Pacific one soon after its subduction triggering a chain reaction of tectonic plate reorganization including major changes in plate-driven forces and mantle flow (Lallemand, 2016a).

Yap – Palau – Lyra - Mussau

The Yap SZ has been described as immature by Kim et al. (2009) based on a bunch of observations such as the absence of arc volcanism, the lack of deep (> 70 km) Benioff zone, evidence of obduction of the overriding plate with exposure of the oceanic crust of Parece-Vela (PV) Basin on the inner trench slope (Fujiwara et al., 2000; Kobayashi, 2004) and a narrow strip of non-isostatically compensated region compared with mature SZs. Collision of the proto-Yap-Mariana margin with the Caroline Ridge began about 25 Ma ago, changing the spreading direction of the PV Basin around 19 Ma. Data indicate

two distinctive short episodes of arc volcanism between 25 and 20 Ma and 11 and 7 Ma (Ohara et al., 2002; Gaina and Muller, 2007). Only the western limb of the PV Basin exists at the latitude of the Yap Basin suggesting either that (1) the last oblique phase of spreading (19-15 Ma) offset the southern part of the basin (Okino et al., 1998), (2) strong tectonic erosion has removed the eastern limb until the fossil spreading center as the result of Caroline Ridge collision (Fujiwara et al., 2000), or (3) the subduction zone jumped from an eastward initial position to the spreading center, consuming the eastern limb of the PV Basin in the subduction. None of these scenarii is fully satisfying but the coincidence between the fossil PV spreading center with the present-day trench together with the absence of a developed slab is in favor of a combination of (1) and (3).

The Palau Arc formed during the Eocene as attested by the presence of tholeiites and boninites that were dated to the mid to late Eocene (Ozima et al., 1977; Hawkins and Castillo, 1998). Subduction coincides with the start of Caroline Basin spreading around 36 Ma (Gaina and Müller, 2007) but probably ending around 26 Ma, so that the subduction is presently extinct. The asymmetry of the Caroline Basin as well as numerous ridge jumps might indicate the influence of the Manus hotspot. It shares some characteristics with the Yap Trench such as low seismicity, no forearc and a very small trench-arc distance (Gaina and Müller, 2007). Subduction might have been initiated along a transform boundary if it is contemporaneous with the IBM subduction zone, since the Palau arc coincides with the Palau-Kyushu Ridge which was the proto-IBM Arc (Gaina and Müller, 2007).

The Lyra Trough is supposed to have been active in the Oligocene time together with the Palau SZ. It marked the boundary between the Pacific plate and the newly opening Caroline Basin back, and north, of the Caroline Arc. As it was normal to the Sorol Trough, a fossil spreading center of the Caroline Basin, one may hypothesize that subduction initiated along the former transform boundary allowing the old Pacific plate to subduct beneath the young Caroline Basin (Hegarty et al., 1983; Gaina and Müller, 2007; Kim et al., 2009).

The Mussau trench forms the present eastern boundary between the Caroline and the Pacific plates. Hegarty et al. (1983) have shown that the Caroline plate thrusts under the Pacific one along that trench, whereas the polarity changes northward along a paleo-transform fault called the “Disrupted zone” by the authors. If the Mussau system very well fits the bathymetric profile of an incipient subduction, those of the disrupted zone are characterized by numerous closely spaced (2-5 km across) east-vergent thrust faults distributed over a > 100 km wide area. Because of their trend with respect to the Sorol Trough, Hegarty et al. (1983) propose that convergence localized along a former TF which started about 1 Ma ago at a rate varying from 1.0 cm/yr in the north to 1.6 cm/yr in the south accommodating a maximum of 11 km of shortening. Seismicity level is low with only shallow earthquakes. The start of E-W compression in the area of the Mussau system may be related to the collision between the Caroline Ridge (remnant arc) with the Yap margin. Depending on the authors, the Oligocene East Caroline Basin starts to subduct either beneath itself along an intra-basin TF (Hegarty et al., 1983, based on the similarity of the crust across the nascent trench) or beneath the Late Jurassic Pacific plate adjacent to the Ontong-Java Plateau (Gaina and Müller, 2007).

The singularity of this region including Yap, Palau, Lyra and Mussau systems is that it evolved under the double influence of the Manus and Caroline plumes throughout the Cenozoic (Macpherson and Hall, 2001; Wu et al., 2016).

3.2. Southwest Pacific area

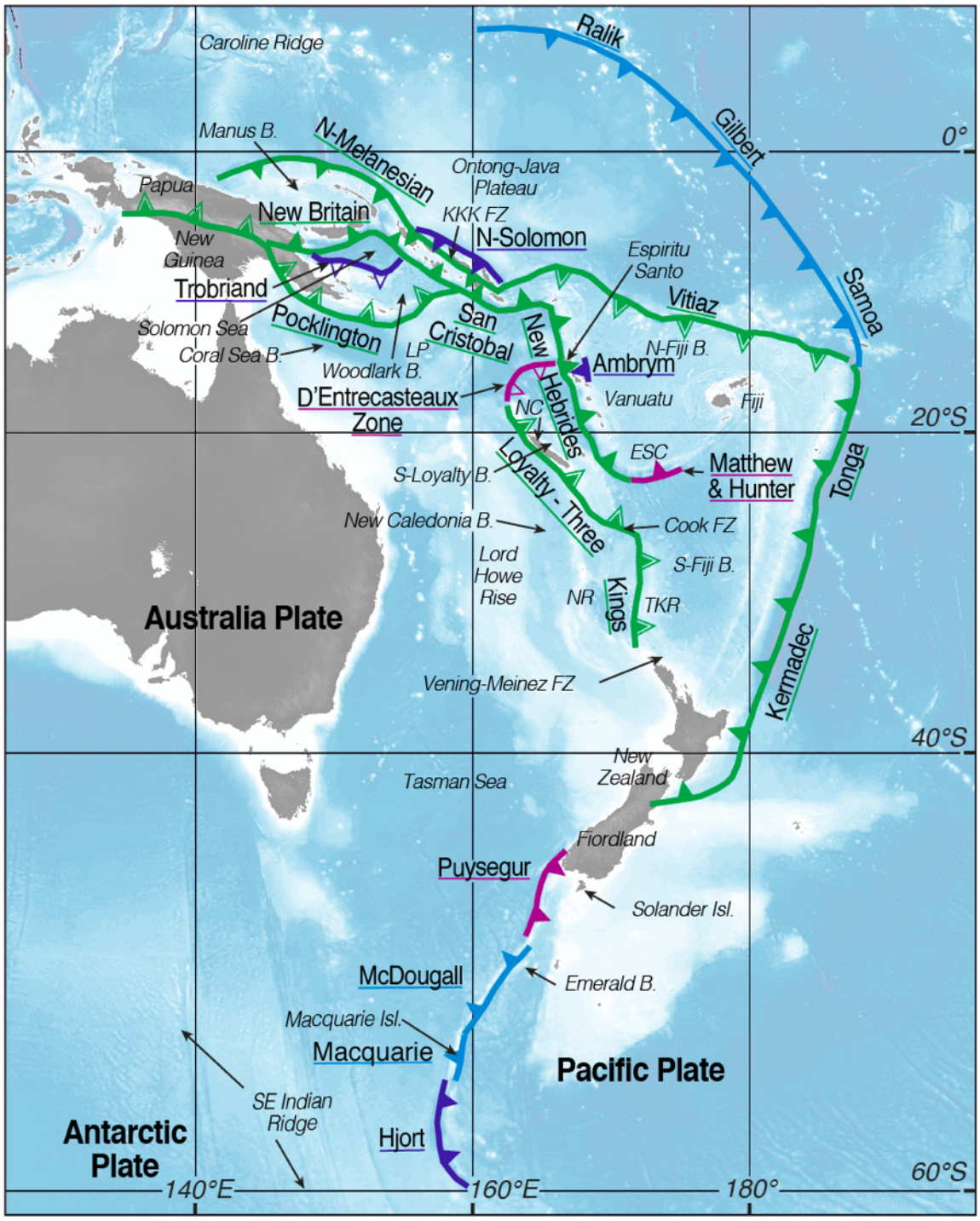

Fig.5: Map of Cenozoic SISs in the SW Pacific region. See the legend in Fig.4. KKK FZ: Kia-Kaipito-Korigole Fault Zone, LP: Louisiade Plateau, NC: New Caledonia, ESC: Eissen Spreading Center, FZ: Fracture Zone, NR: Norfolk Ridge, TKR: Three-Kings Ridge, Isl.: Island, SE: Southeast.

(New Guinea -) Pocklington (South Melanesian)

The initial Melanesian Arc can be traced from New Guinea to the east over thousands of kilometers (Fig. 5). It was flanked on its southern margin by a northeast-dipping subduction called the New Guinea - Pocklington SZ. Schellart and Spakman (2015)

dates its activity from 71-65 to 50 Ma. It has contributed to the rapid northward motion of the Australian plate together with the Sunda subduction zone especially between 59 and 52 Ma with a phase of plate acceleration from 64 to 59 Ma as the slab lengthened supported by numerical modeling (Schellart, 2017). Kinematic reconstructions support a very slow convergence between 71 and 64 Ma at a rate of 0.2 - 0.4 cm/yr (Schellart & Spakman, 2015). The SZ has consumed more than 1000 km of a back-arc basin oceanic crust called Emo backarc Basin in reference to the Maastrichtian Emo metamorphics outcropping in Papua-New Guinea (Worthing & Crawford, 1996; Baldwin et al., 2012). The geodynamic context for the initiation of the New Guinea - Pocklington SZ is poorly constrained but many authors consider that the East Australian margin was fringed by a west to southwest dipping SZ since early Cretaceous which accounted for widespread extension and drift of many ridges and plateaus (see Schellart et al., 2006 for details). This fragmentation of microcontinental ribbons from the eastern part of Gondwana, i.e., Australia continent, was probably triggered by a major mantle plume at ~100 Ma beneath the southern part of the Lord Howe Rise and East Tasmania region (Crawford et al., 2003). In this perspective, the New Guinea - Pocklington subduction might have resulted from a polarity reversal (flip) of an opposite-dipping SZ.

North Melanesian - Vitiaz

The same Melanesian Arc s.l. was supposed to extend from Papua-New-Guinea to the north of New Zealand through Fiji, but here, we will only discuss the 5800 km long section trending WNW-ESE from New-Guinea to Fiji. We distinguish a western segment from Manus to San Cristobal Islands, hereafter called Melanesian Arc s.s., and an eastern segment from San Cristobal to Fiji, hereafter called Vitiaz Arc (Petterson et al., 1999). The basement of this elongated archipelago attests for a complex Cenozoic tectono-magmatic history involving multiple subduction arcs or terranes collage (Petterson et al., 1999) with continental origin as attested by Early Cretaceous to Archean zircons (Tapster et al., 2014). According to Hall (2002), the N-Melanesian-Vitiaz southwest-dipping SZ is initiated by flip (polarity-reversal) of an opposite-dipping SZ after collision of older arcs as attested by the Papua and Sepik ophiolites for example. The collision was followed by slab detachment at 52-49 Ma in the western part (New Guinea region) as attested by the rapid slowdown of the Australian plate (Schellart & Spakman, 2015). The age of subducting Pacific oceanic lithosphere was estimated to be ~70 Ma by Gaina & Müller (2007). The collision and subsequent N-Melanesian-Vitiaz SI occurred diachronously from west to east sometime between 50 and 40 Ma, concomitantly with the acceleration of the northward motion of the Australian plate. The lateral propagation might have been facilitated by the high obliquity of the convergence (~50°). Ongoing seismicity delineating the Pacific slab attests for some residual activity along the N-Melanesian s.s. SZ, even after subduction polarity reversal occurred following the collision with the Ontong-Java Plateau (Mann and Taira, 2004). By contrast, the Vitiaz segment ceased to be active soon after the collision of an eastern extent of the Ontong-Java Plateau with the Melanesian Arc around 16 Ma ago.

New Hebrides - New Britain - San Cristobal (including South Solomon)

The largest and thickest oceanic plateau on Earth, i.e., the Ontong-Java Plateau carried by the Pacific plate, collided first in the east against the Vitiaz margin (Vanuatu, Fiji) between 16 and 10 Ma (Mann & Taira, 2004). It has to be said that the collision started

sooner around 20-25 Ma for other authors (e.g., Yan and Kroenke, 1993; Petterson et al., 1999). Here, we adopt the chronology of Mann and Taira (2004) since it results from a comprehensive geological and geophysical study. The last igneous intrusion attributed to the Vitiaz SZ was dated to 16 Ma in the ancient Vanuatu Arc (Carney and Macfarlane, 1982). This earlier collision is responsible for the flip of the subduction across the Vanuatu Arc with an opposite polarity around 10-8 Ma (Auzende et al., 1988). We believe that the arc-plateau collision occurred soon after 16 Ma, otherwise the time between the arc-plateau collision and the beginning of spreading in the North-Fiji Basin at ~8 Ma would have been extremely short. Another puzzling observation concerns the full subduction of the eastern part of the plateau beneath the former Vitiaz Arc, maybe indicative of an eastward-tapered thinner plateau. The new Vanuatu Arc, also called New Hebrides Arc, rotated clockwise about a pivot point located east of San Cristobal Island (Auzende et al., 1995). The ~70-80° rotation was accommodated by a lengthening left-lateral STEP fault connecting the southern termination of the New Hebrides northeast-dipping subduction zone with Fiji Island. The earlier arc volcanics related to the new subduction on Vanuatu islands were dated at 7 Ma (Carney and Macfarlane, 1982) and the oldest magnetic anomaly identified in the North Fiji Basin is An4, i.e., ~8 Ma (Malahoff et al., 1979; Auzende et al., 1988).

Then, the collision propagated from east to west and reached the Solomon Islands region around 10 Ma ago. The flip of polarity across the Solomon Islands from southwest-dipping to northeast-dipping subduction occurred probably soon after 10 Ma since the earlier arc volcanics attributed to the San Cristobal subduction are dated to 6 Ma (Petterson et al., 1999). Based on geological observations related to sedimentary facies, Mann and Taira (2004) considered that arc-plateau collision occurred later around 6-4 Ma, i.e. after the earlier arc magmatism. If they are right, one may reconcile their observations considering that the New Hebrides SZ propagated northwestward to the longitude of the Solomons before the arrival of the Ontong Java Plateau.

The New Britain SZ is supposed to form at the same time (Mann and Taira, 2004). The slab pull originating beneath New Britain has been invoked by Taylor et al. (1995) as an additional cause for the spreading of the Woodlark Basin since 5 Ma (Yoneshima et al., 2005). The slab beneath New Britain reaches a depth of 575±100 km according to van der Meer et al. (2018) corresponding to a subduction starting between 15 (Wu et al., 2016) and 10 Ma (Hall, 2002). Despite its youthfulness (≤ 5 Ma), the oceanic crust of the Woodlark basin subducts beneath the Solomon Islands at a high dip angle probably in response to the high stress originating from the collision of the Ontong Java Plateau in the north (Yoneshima et al., 2005).

We shall notice that the northeast-dipping New Britain - S-Solomon - San Cristobal - New Hebrides subduction occupies the same locus than the former eastern part of the Pocklington SZ (Hall, 2002) which ceased its activity at ~50 Ma (Schellart and Spakman, 2015). If true, the subduction thus resumed after ~40 Myr of quiescence.

Trobriand

The Trobriand Trough, south of the Solomon Sea, has accommodated shortening between the Late Eocene - Early Oligocene Solomon Sea backarc basin and the SE Papuan Peninsula and Trobriand islands (Lock et al., 1987; Mortimer et al., 2014). It is

considered a south-dipping SZ which ceased its activity around 0.5 Ma ago (Mann & Taira, 2004) as attested by the low level of seismicity compared with the nearby New Britain SZ. The authors differ on the period of activity of the Trobriand subduction as well as on the causes for its initiation. Schellart et al. (2006) attributes the initiation to the collision in the north between the Ontong Java Plateau and the Solomon Arc ~15 Ma ago. For them, the Trobriand subduction was initiated prior to the New Britain - San Cristobal one as the result of a jump from the N-Melanesian Trench to the south of the Solomon Sea. They also speculate that the opening of the Woodlark Basin was triggered by the rollback along the Trobriand Trench, in contrast to Taylor et al. (1995) who suggested that the basin opened in response to the slab pull of the Solomon Sea slab beneath New Britain. For Schellart et al. (2006), large parts of the Solomon Sea have been consumed along the Trobriand Trough. For Mann and Taira (2004), the Trobriand converging system played a minor role from 2 to 0.5 Ma only.
Here, we adopt the scenario of Schellart et al. (2006) because most backarc basins open above a subducting slab within an upper plate undergoing extension.

North Solomon (s.s.)

As discussed in a section above, some activity remains along the southwest-dipping N-Melanesian s.s. SZ (Mann and Taira, 2004). The 33 km-thick Early Cretaceous Ontong-Java Plateau partly docked against the Solomon Arc since 4 Ma. The suture zone is represented by the Kia-Kaipito-Korigole (KKK) Fault Zone (Fig.5) which delimits the Pacific Province also called Malaita accretionary prism, including the Malaita, Ulawa and the northeastern flank of Santa Isabel islands, composed of oceanic plateau rocks (Hugues and Turner, 1977; Kroenke et al., 1986) while a southwest-dipping thrust system develops offshore northward. This system has been called the proto-N-Solomon SZ by Mann and Taira (2004). Here we consider the N-Solomon s.s. deformation front as an incipient-localized subduction (Taira et al., 2004) which initiated 2 Ma ago after a jump of the initial N-Melanesian s.s. SZ from the KKK Fault to about 80 km northward. Geophysical data tend to show that the south-dipping décollement connected with the frontal thrusts is rather shallow, i.e., 1 km of sedimentary rocks and 6 km of upper crystalline part of the plateau (Phinney et al., 2004). The lower 80% of the plateau crust appears not affected by the accretionary process, remaining attached to the main body of the plateau (Miura et al., 2004). The fact that only the 20% upper section is accreting may be explained by a weaker rheology caused by hydrothermal alteration or fracturing as the bending is developed approaching the trench (Kerr et al., 1997; Phinney et al., 1999). The cause for this subduction jump backward of the former deformation front may be local, considering the Pacific Province as a crustal-scale accretionary prism, or as another flip of subduction across the Solomon Arc as a consequence of the compressive stress exerted by the subduction of the Louisiade Plateau at San Cristobal Trench.

Samoa - Gilbert - Ralik (Micronesian)

The region extending northeast of the Australian continent underwent several flips of subduction across the Melanesian Arc during the Cenozoic (Schellart et al., 2006) from S-dipping to N-dipping (New Guinea - Pocklington SZ), then S-dipping (N-Melanesian - Vitiaz SZ), and N-dipping again (New Britain - S-Solomon - San Cristobal - New Hebrides SZ). Okal et al. (1986) have speculated that a new flip toward a new S-dipping subduction was undergoing 1000 to 2000 km northward of the present New Britain - S-

Solomon - San Cristobal - New Hebrides SZ. In their scenario, a ~4000 km long line extending from the Caroline Ridge to Samoa Island through Gilbert Island and Ralik FZ could host in the future a new S-dipping subduction of the Pacific plate beneath the Ontong Java Plateau and surrounding oceanic plate. This idea was also defended by Kroenke and Walker (1986) who named this incipient SZ the "Micronesian Trench". This hypothesis is supported by the intraplate seismic activity recorded along this line with several events of body-wave magnitudes up to 6 showing horizontal compressional stress oriented NNE-SSW, and the low geoid between Fiji and Gilbert Island which could be explained by buckling and eventual mantle delamination beneath Gilbert Island. The source of this compressive stress would originate from the numerous buoyant features entering the N-dipping New-Britain - Britain - S-Solomon - San Cristobal - New Hebrides SZ, such as the Louisiade Plateau, Renell Ridge, d'Entrecasteaux Zone or Loyalty Ridge. The oceanic domain located between the New Britain - New Hebrides SZ and the Samoa - Gilbert - Ralik line would thus be the locus of distributed shortening presently accommodated by downward flexure of the plate over a great distance and incipient faulting localization along the northern line, following a scenario close to the situation in the Indian Ocean.

Ambrym (including Pentecost & Maewo)

The New Hebrides Arc has undergone severe shortening at the latitude of Espiritu Santo Island, the largest and highest island of the archipelago, since the late Pliocene. Collot et al. (1985) described the deformation by plastic plane strain theory applied to the indentation of the arc by the D'Entrecasteaux Zone buoyant ridge. The western chain including Espiritu Santo Island is pushed forward and uplifted as a result of its interaction with the ridge at trench (Chung and Kanamori, 1978). The 9-10 cm/yr of AUS-PAC convergence rate fell down to 3.5 - 4 cm/yr at the New-Hebrides Trench, while the remaining 5-6 cm/yr are accommodated in the rear-arc offshore the rising Eastern chain (Maewo and Pentecost Islands) and the volcanic Central Chain (Ambrym Island), as shown by GPS studies (Calmant et al., 2003). Between the two rising eastern and western chains, the Aoba Basin is flexed down as a large syncline (Pelletier et al., 1994). Seismicity, neotectonic and deep-sea drilling studies revealed that a backarc thrust belt developed over a length of 200 km since 2-3 Ma (Taylor et al., 1987; Louat and Pelletier, 1989; Pelletier et al., 1994). A Mw 7.5 thrust earthquake occurred in 1999 east of Ambrym Island along the main backthrust which outcrops as a 2 km-deep, 40 km-long, 1 km-high scarp on the seafloor (Régnier et al., 2003; Lagabrielle et al., 2003). The upper bound of the total shortening across this backarc thrust belt has been estimated to be 54 km. It could correspond to the very early stages of an incipient-localized subduction according to Régnier et al. (2003) or intraplate crustal shortening with permanent creation of relief, i.e., 4 mm/yr of uplift rate for the past 8 kyrs (Lagabrielle et al., 2003).

Matthew & Hunter

The southern termination of the New Hebrides Trench connects with a left-lateral transform system accommodating the E-W recent opening of the North Fiji Basin and the subsequent clockwise rotation of the trench (Auzende et al., 1988; Louat and Pelletier, 1989; Pelletier et al., 1998). In detail, this transform system does not satisfy all the characteristics of a STEP Fault (Patriat et al., 2015). In particular, the seismicity and

deformation close to its connection with the southern termination of the New Hebrides Trench is not typical of a strike-slip fault as it could be north of the Tonga Trench for example. Thrust-type events with a P-axis sub-perpendicular to the fault are observed (e.g., Louat and Pelletier, 1989; Patriat et al., 2015). The Loyalty Ridge, which is an Eocene volcanic Arc (Cluzel et al., 2001) collides with the southern termination of the New Hebrides Trench since ~1.8 Myr (Patriat et al., 2015). The collision has been dated assuming its contemporaneity with the development of the Eissen Spreading Center and en-échelon Monzier Rift in the backarc (e.g., Monzier et al., 1993). Backarc extension facing the collision zone has been interpreted as a tension gash associated with southward lateral extrusion of an upper plate sliver. Subsequently, a young piece of the oceanic upper plate rotated clockwise overriding the older (~28 Ma, Mortimer et al., 2014) South Fiji Basin along the newly formed trench, down to 7.3 km depth (Patriat et al., 2015). In the region of SI, the upper plate is composite. The ~400 km-long Hunter Ridge, running from Matthew island to Conway Reef, is probably composed of dismembered remnants of the >10 Ma old Vitiaz Arc (Danyushevsky et al., 2008). As such, Matthew & Hunter region provides a good illustration of the proposal of Leng and Gurnis (2015), originally elaborated in the context of Izu-Bonin-Mariana subduction, that the close juxtaposition of the nascent plate boundary with relic oceanic arcs is a key factor localizing initiation of a new SZ. The proto-arc and forearc of the Matthew and Hunter subduction zone is a collage of the old Vitiaz arc crust, young (< 2 Ma) back-arc type oceanic crust forming at the Eissen spreading center and a wide range of primitive subduction-related magmas mixing asthenospheric derived MORB-like decompression melts and slab melts, including adakites and boninites in the region of the Monzier Rift splitting the Hunter Ridge in its central portion (Monzier et al., 1993; Sigurdsson et al., 1993; Deschamps and Lallemand, 2003; Danyushevsky et al., 2006, 2008; Patriat et al., 2019). Based on plate kinematics, Patriat et al. (2015) suggest that the total amount of convergence accommodated across this new plate boundary averages ~90 km which would be just enough to trigger partial melting of the supra-slab mantle wedge. For us, this early arc magmatism marks the transition from incipient-localized to achieved subduction initiation, prior to a self-sustained stage which may be reached if the slab pull force becomes high enough to drive the subducting plate.

Loyalty - Three Kings (New Caledonia) - d'Entrecasteaux Zone

According to Schellart et al. (2006), wide Late Cretaceous to Paleogene backarc basins, including Pocklington, New Caledonia, South Loyalty and Coral Sea basins, opened in response to the northeast- and eastward rollback of a proto-Melanesian-Vitiaz-Tonga southwest- and west-dipping subduction zone. Based on observations from the New Caledonia ophiolite, Cluzel et al. (2001) and Crawford et al. (2003) proposed that a subduction of the western part of the South Loyalty basin beneath the eastern part initiated in the Late Paleocene. Later, Cluzel et al. (2012), based on petrological arguments, demonstrated that subduction initiated along the South Loyalty fossil (or dying) spreading center. This east-dipping subduction, indifferently called the New Caledonia, the Loyalty - Three Kings or the South Loyalty SZ, extended far south to the Northland (New Zealand) when it abuted against the Vening-Meinez FZ (Schellart et al., 2009). Its northern termination consisted in the d'Entrecasteaux FZ around which the slab edge tore during its westward roll back (Schellart and Spakman, 2012). Dated amphibolites, representing the metamorphic sole of the ophiolitic nappe, suggest

subduction initiated prior ~56 Ma, i.e., simultaneously with the lastly erupted backarc basalts (Poya Terrane, Cluzel et al., 2012). South of New Caledonia, the SZ was supposed to be sinistrally offset along the Cook FZ, so that the associated volcanic arc was represented by the Loyalty Islands in the north and the offset Three Kings Ridge further south (Schellart et al., 2006; Patriat et al., 2018). In the same way as in the recent Matthew & Hunter achieved SZ, slab-derived melts (adakites, boninites) intruded the forearc mantle soon after initiation from ~55 to 50 Ma (Arndt, 2003; Cluzel et al., 2012; Meffre et al., 2012). Schellart et al., (2006) proposed that subduction be initiated at the rear of the Tonga-Kermadec arc around 50 Ma ago in apparent contradiction with Cluzel et al. (2012) who advocated an initiation at a spreading center around ~57 Ma based on petrological data. Both models could be reconciled when considering the boninites as the expression of slab melts erupting at the intersection between a volcanic arc and a backarc spreading center similarly with the situation in the actual Tonga rear-arc (Danyushevsky et al., 1995; Deschamps and Lallemand, 2003). Subduction ceased when the continental New Caledonia-Norfolk Ridge collided at ~41 Ma, resulting in ophiolite obduction at the latitude of New Caledonia from 41 to 33 Ma (Cluzel et al., 2006; 2012; Lagabrielle et al., 2013). The trigger of the Loyalty - Three Kings SZ is generally attributed to a change in the Pacific-Australia relative motion either during the Early Eocene (~50 Ma; Schellart et al., 2006) or the Late Paleocene (~60-55 Ma) which may have various origins among which the sinking of the Izanagi slab beneath East Asia (Whittaker et al., 2007; Seton et al., 2015; Lallemand, 2016a). The slab produced by this Paleogene subduction has been identified below the Tasman Sea (Schellart et al., 2009; Schellart and Spakman, 2012; van der Meer et al., 2018).

The D'Entrecasteaux Zone (DEZ) is a 600 km-long singular intraoceanic feature prolongating the Loyalty Ridge to the north and changing strike clockwise by 90° before colliding with the Vanuatu Arc. It is composed of two-parallel ridges (North DEZ and South-DEZ) and troughs. The Bougainville Guyot, presently colliding with the Vanuatu margin (Maillet et al., 1983; Collot et al., 1992; Greene and Collot, 1994), is an Eocene arc edifice (~40 Ma old) which belongs to the South-DEZ. Primitive arc tholeiites of Eocene age (34-56 Ma) sometime close to E-MORB backarc basalts were dredged on a 370 km strike length of the North-DEZ. Based on their composition, it has been suggested that the North-DEZ represented the forearc of the South-DEZ Arc (Coltorti et al., 1994; Mortimer et al., 2014). If the trough north of the North-DEZ marks the paleo-trench, the arc-trench gap is unreasonably narrow (Mortimer et al., 2014). This observation together with the trend of this zone led Daniel et al. (1977, 1978) to compare the North-DEZ with the present Hunter Fracture Zone (see above section). The trend of the DEZ perpendicular to the main Loyalty - Three Kings SZ, similar to the Matthew & Hunter incipient to achieved subduction may explain the presence of E-MORB backarc basalts and primitive arc basalts within a narrow arc-forearc position if the backarc spreading center paralleled the Loyalty Arc. Because of its narrowness, one may believe that this paleo-plate boundary accommodated first as a STEP Fault as suggested by Schellart and Spakman (2012) experimenting a short-lived right-lateral transform motion, it certainly also accommodated a subduction component as revealed by the volcanic rocks sampled along the DEZ consuming ~300 km of the trapped South Loyalty Basin crust (Seton et al., 2016).

Tonga-Kermadec

Despite its more than 3000 km length, the activity of the Tonga-Kermadec SZ prior to the mid-Eocene is largely debated including west- or east-dipping SZ, transform boundary or even no plate boundary (see Schellart et al., 2006 for discussion). Even the age of SI is debated varying from 85 (e.g., Schellart et al., 2006) to 27 Ma (e.g., Yan and Kroenke, 1983; van de Lagemaat et al., 2018) because reconstructions are plate-circuit dependent. We take note from the conclusions of Schellart et al. (2006) that the simplest way for an E-W opening of the South Loyalty backarc basin between 85 and ~50 Ma is the presence of a west-dipping Pacific SZ, i.e., a proto-Tonga-Kermadec SZ. At the same time, the oldest igneous rocks collected in the Tonga forearc were dated around 48-52 Ma in the south becoming younger to the north (Meffre et al., 2012). Based on the fact that their composition is that of backarc basalts, not forearc, Meffre et al. (2012) suggested that these rocks were formed in the backarc of the Loyalty-Three Kings east-dipping SZ, i.e., in the South Loyalty Basin, and they were trapped later in the forearc of the newly formed Tonga SZ. In this study, we consider that the presence of backarc basalts in a forearc position can be more simply explained by the strong tectonic erosion which characterizes this subduction zone (von Huene and Scholl, 1991; Lallemand 1995; Clift and Vanucchi, 2004) in a way similar to forearc basalts of backarc composition observed in the forearc of IBM SZ without requiring any east-dipping former subduction (Lallemand, 2016a). Furthermore, most authors consider that the Loyalty-Three Kings SZ started no later than 50-55 Ma ago (see section above) invalidating Meffre et al. 's hypothesis. Matthews et al. (2015) predict in their kinematic reconstructions that the relative motion between Pacific and Australia plates was purely a transform one between 52 and 45 Ma and turned into oblique convergence across the PAC-AUS boundary after 45 Ma. This time was retained by Sutherland (1995) as the starting time for Tonga-Kermadec SZ resuming. Such reconstruction and timing have been recently questioned by Sutherland et al. (2017) based on seismic-reflection data acquired in the Tasman Sea, Lord Howe Rise, Southern New Caledonia Trough and Norfolk Ridge. They demonstrate that a widespread continental and oceanic compressional failure, called Tectonic Event in the Tasman Sea (TECTA), occurred there between 53-48 Ma and 37-34 Ma. Such setting is clearly distinct from those recorded back of the IBM SZ after SI where extension prevailed, but the synchronicity in SI can hardly be a coincidence and likely results from a change in Pacific plate absolute motion (Sharp and Clague, 2006). Here, we have decided to follow the interpretation of Sutherland et al. (2010, 2017) that the Tonga-Kermadec SZ initiated around 53 Ma ago, possibly along a former west-dipping SZ, as a result of PAC-AUS convergence. They suggest a mechanism of lower crust delamination beneath the thickened Norfolk Ridge by gravitational instability under compressive stress.

Puysegur - McDougall - Macquarie - Hjort (Macquarie Ridge Complex)

The Macquarie Ridge (MCR) Complex defines the ~1800 km long transpressive plate boundary between Australian and Pacific plates, south of New Zealand. This plate boundary, marked by a prominent ridge bordered by troughs, runs from Fiordland (South Island, New Zealand) in the north to the Pacific-Antarctic Ridge in the south (Massel et al., 2000). It is composed of several segments from north to south: Puysegur (~500 km), McDougall (~550 km), Macquarie (~200 km) and Hjort (~550 km). The pattern of fracture zones in the South Tasman Sea adjacent to the ridge allowed Lamarche et al. (1997) to identify a progressive change in the AUS-PAC rotation pole from 31 to 12 Ma resulting in

the conversion from a divergent (MCR) to a transcurrent plate boundary by coalescence of the fracture zones and spreading segments reduction. The MCR stopped spreading at ~25 Ma. Today, the shear zone offsets laterally more than 700 km of both sides of the initial South Tasman and Emerald Basins so that the ~40 to ~10 Ma old crust is observed on both sides of the plate boundary only north of Macquarie Island around 54°S. South of 54°S, the crust east of the MCR Complex still belongs to the Emerald Basin but those on the west side originate from the Southeast Indian Ridge, i.e., aged from 0 at the ridge near 62°S up to 30 Ma near 54°S (Meckel et al., 2003; Keller, 2004). Today, the oceanic crust is thus ~20 Ma older on the west near Macquarie island (~30 vs ~10 Ma), has similar ages on both sides near 57°S (Northern Hjort segment, ~20 Ma) and is 20 Ma older on the east near 59°S (Southern Hjort segment, ~10 vs ~30 Ma).
In their reconstruction, Lamarche and Lebrun (2000) and Lebrun et al. (2003) suggested that the Puysegur SZ nucleated at ~20 Ma along the Balleny transpressive relay, south of Fiordland, soon after inception of the Alpine Fault at ~23 Ma. Oceanic crust abutted continental crust there and subduction probably nucleated where the density contrast was the greatest (Collot et al., 1995; Gurnis et al., 2019). According to Lebrun et al., (2003), ~200 km (downdip) and ~600 km (along strike) of Solander oceanic lithosphere is supposed to have been underthrust beneath the thinned continental crust of the Puysegur Bank from 20 to 15 Ma. The subduction front jumped westward from the Balleny fault system to a fracture zone belonging to the Australian plate, which will become the Puysegur Trench, sometime during the last 5-10 Ma (Lebrun et al., 2003). Meckel et al. (2005) predicted that ~65 km of convergence preceded lithospheric failure at the northern Puysegur Trench. The transition from underthrusting to partitioned thrust and strike-slip in the southern Puysegur Trench results from a decreased angle of convergence from ~40° to 25°. Collot et al. (1995) and Lamarche and Lebrun (2000) described the process of southward propagation of the subduction as transverse shortening increased during the last 10 Myr, including differential uplift, interplate coupling drop as subduction proceeded and capture of an Australian terrane at the front of the Pacific upper plate during the localization process as the slab first started to subduct in the north. Today, the slab exhibits a plowshare shape with a maximum length of 200 km beneath Fiordland decreasing to zero near 50°S (Hayes et al., 2009). In this study, we consider that the Puysegur subduction initiation is just achieved as andesitic eruptions, at Solander and Little Solander islands south of Fiordland, occurred during the last 350 kyrs (Sutherland et al., 2006; Mortimer et al., 2013). These andesites and trachy-andesites show geochemical affinities with modern adakites (Foley et al., 2013).
A broad zone of penetrative deformation extending ~150 km into the plate interior from the Ridge Complex has been mapped by Hayes et al. (2009). It accounts for plate boundary evolution since ~25 Ma from divergence to translation.
Not only the Puysegur region was concerned by incipient subduction but all the MCR Complex down to its connection with the Pacific-Antarctic Ridge has been affected by the kinematic change in PAC-AUS plate motion near ~25-30 Ma (Keller, 2004). The whole complex originates from the Macquarie spreading center, whose motion became dominantly translational by ~20-25 Ma (Cande and Stock, 2004; Hayes et al., 2009). Today, strike-slip motion is observed all along the ridge but convergence and underthrusting is mainly observed along the Puysegur, Macquarie and Hjort segments. The McDougall segment is the only section without any thrusting evidence (Massell et

al., 2000). Even at the latitude of Macquarie Island, Meckel et al. (2005) consider that lithospheric failure has not been achieved yet, explaining why the ridge is the highest along this central segment, as compressional stress has not been relaxed yet. Transition from strike-slip to oblique convergence occurred at ~6 Ma along Macquarie Ridge (Meckel et al., 2005), much later than in the Puysegur region, resulting in a rapid uplift of the ridge and formation of adjacent troughs (Massell et al., 2000). The deepest troughs are located east of the MCR along the McDougall and Macquarie segments, possibly because of the weakening of the crust as a result of the denser fracture zones on the east side (Meckel et al., 2005). Based on their observations all along the intra-oceanic MCR, Meckel et al. (2005) conclude that the first ~100 km of convergence give rise to distributed ridge (tectonic uplift) and troughs before lithospheric failure, then thrust faults appear when angle of convergence becomes larger than 30°. At the time of SI, the age of the oceanic crust on both sides was almost similar.
Along the southern part of the MCR Complex (Hjort region), the deepest trough is again located west of the ridge as in the northern Puysegur segment (Massell et al., 2000). The arcuate shape of the plate boundary there allows distinguishing the northern Hjort segment mostly transformational and the southern Hjort segment where the oblique convergence is partitioned between thrust and strike-slip (Meckel et al., 2005). Lithospheric thrusting imposed by PAC-AUS relative plate motion change south of the MCR along the southern Hjort Trench is concomitant with the formation of the Macquarie microplate, independent from the Australian plate south of 52.5°S, i.e., west of the Macquarie and Hjort trenches, ~6 Ma ago (De Mets et al., 1994; Cande and Stock, 2004; Meckel et al., 2005). With the active TF between the Macquarie plate and the Pacific plate located at the crest of the Hjort Ridge, the trench on the west side formed via a shallow splay capturing a sliver of Macquarie plate crust (Meckel et al., 2003). Meckel et al. (2005) estimated that 150-200 km of shortening was accommodated across the southern Hjort segment, half of which having occurred diffusely between 11 and 6 Ma. Only ~50 km of Southeast Indian crust underthrust beneath the Northern Hjort segment and less along the Southern Hjort segment according to Meckel et al. (2003). For these authors, the formation of the northern Hjort Trench rather results from the translation of the crust underthrust at the southern Hjort trench than resulting from plate boundary convergence which is not enough due to its azimuth. The lack of early arc magmatism and the decrease in convergence rate since 6 Ma along this incipient subduction offers little hope of achieving a self-sustained subduction here in the near future. In that way, one may draw a parallel between Hjort and Gagua ridges (see previous section).

The MCR Complex offers a unique setting of the recent SI process along an intra-oceanic transform plate boundary. The length of the ridge, the latitudinal (and time) variations in azimuth, angle of convergence vector, oceanic age contrast across the plate boundary or starting age for convergence provide a bunch of situations that can be used for constraining thermo-mechanical models.

3.3. Northeast Pacific area

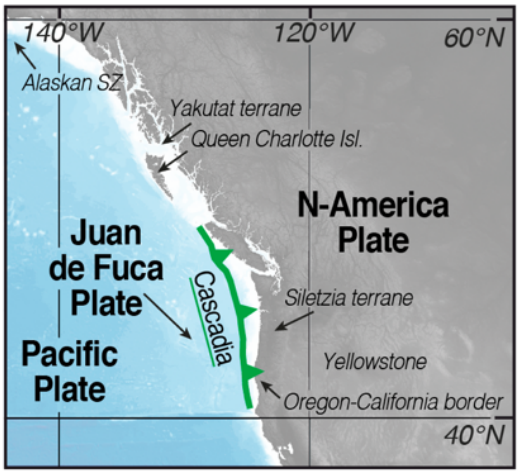

Fig.6: Map of Cenozoic SISs in the NE Pacific region. See the legend in Fig.4. SZ: Subduction Zone.

Cascadia

Subduction of the Farallon plate beneath the North American plate stopped and resumed seaward after accretion of the Siletzia oceanic plateau around 53 Ma (Wells et al., 2014; Stern and Dumitru, 2019, Fig.6). Based on kinematic reconstructions from Seton et al. (2012), the Siletzia as well as the Yakutat plateaus formed symmetrically from the Kula-Farallon or Resurrection-Farallon spreading center at the head of the Yellowstone plume between 56 and 49 Ma (Wells et al., 2014). Soon after and during their formation, the Siletzia plateau collided at ~53 Ma near the present Oregon-California border margin, while the Yakutat plateau collided at ~50 Ma farther north near the Queen Charlotte Islands. The Yakutat Plateau then travelled northwestward along the margin until it subducted beneath the northern termination of the Alaskan SZ. We thus do not strictly consider that the Early Eocene docking, lateral translation and then underthrusting of the Yakutat terrane illustrates the birth of a new subduction zone. However, the seaward migration of the volcanic arc after accretion of the Siletzia terrane further south between 50 and 45 Ma separated by a quiescent period has been interpreted by Schmandt and Humphreys (2011) as an evidence of initiation of a new subduction back of the plateau. Following plate kinematic reconstructions of Seton et al. (2012), the new subduction initiated at or near the Kula-Farallon or Resurrection-Farallon spreading center (if the Resurrection plate existed between the Kula and Farallon plates - see Wells et al., 2014 for more details). The presence of an active spreading ridge prone to subduct in the Early Eocene is controversial. It should be noted that, based on the magnitude of the high seismic velocity anomaly attributed to the tip of the Farallon plate having been subducted 50 Ma ago, its initial age should be within the range 20-50 Ma (Schmandt and Humphreys, 2011). Recently Stern and Dumitru (2019) have proposed a variant of the above model, considering the quasi-synchronicity between the formation of the oceanic plateau and the collision. In their model, the plume head rose partly under the subducting Farallon Plate and partly under the overriding North America plate within a pre-existing Columbia embayment, in a way similar to the Yellowstone plume in the Early Miocene. The global story does not differ much from other authors, except that the initial geometry of the margin includes a larger embayment and that the plume-head might have controlled the process of SI.

3.4. Caribbean area

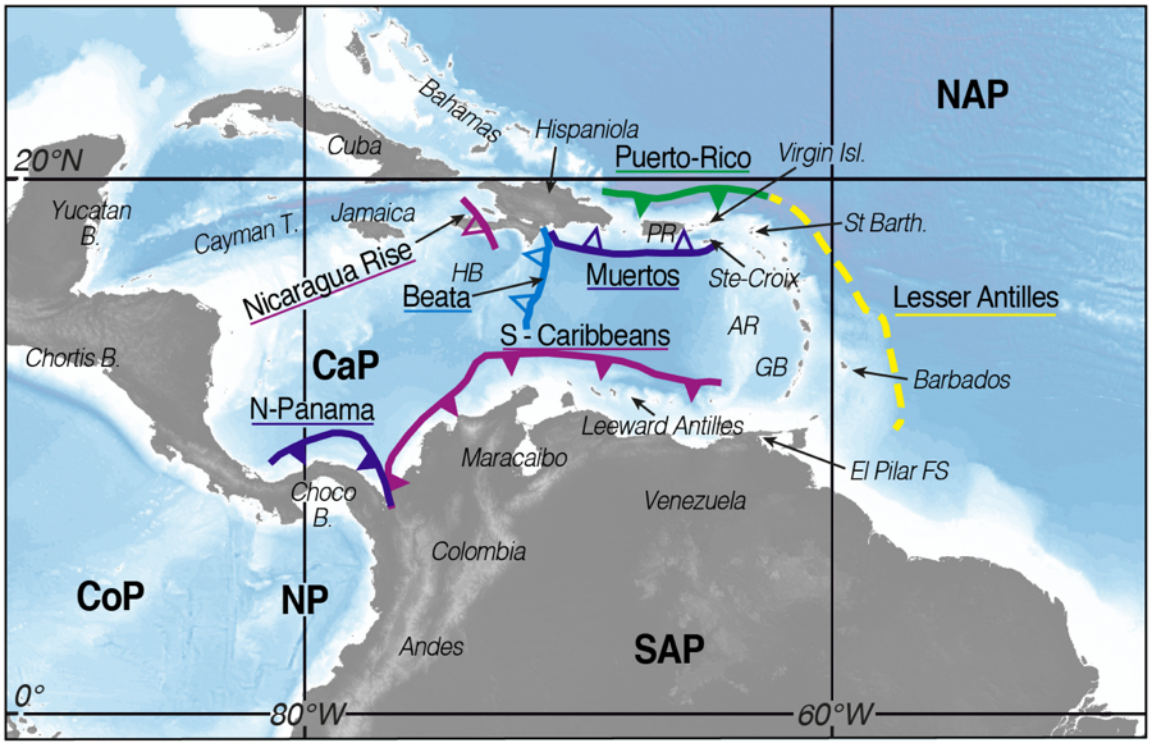

Fig.7: Map of Cenozoic SISs in the Caribbean region. See the legend in Fig.4. The yellow dotted line outlines a speculative paleo-SIS. T.: Trough, Isl.: Island, St Barth.: Saint Barthelemy Island, PR: Puerto-Rico, HB: Haiti Basin, AR: Aves Ridge, GB: Grenada Basin, FS: Fault System, B.: Block.

The Caribbean region has been the locus of several SIs during the Cenozoic, among which most of them are either weakly active or even inactive today (Fig. 7). The plate itself is composed of a mosaic of structural units including an oceanic plateau, further called CLIP for Caribbean Large Igneous Province. The CLIP is mainly aged 95-85 Ma (Whattam & Stern, 2015) with a later magmatic stage occurring around 75 Ma (Dürkefälden et al., 2019). The plateau lies above an oceanic plate, supposed to be a cannibalized portion of the Farallon plate aged of 190-125 Ma (Boschman et al., 2019) and various continental or arc blocks such as the Nicaraguan Rise, the Chortis or Choco blocks (Pindell & Kennan, 2001; 2009; Mann, 2007). The Caribbean plate was individualized when the two west- and east-verging SZs acted simultaneously. These two main SZs, outlined by the Central America and Greater Antilles (GAA) arcs, probably formed in the Late Cretaceous but their starting time is still heavily debated. Most people consider that the Lesser Antilles SZ corresponds to the remaining central segment of a longer west-verging SZ (GAA) which resulted from a flip of an older east-verging subduction zone around 70-60 Ma (Burke, 1988), 90-75 Ma (Cardona et al., 2011; Hastie et al., 2013; 2021; Gomez et al., 2018), 90 Ma (Mauffret et al., 2001; Vallejo et al., 2006; Mann, 2007; Wright & Wyld, 2011) or 120-125 Ma (Pindell & Kennan, 2009; Boschman et al., 2019). The polarity reversal, at the origin of the GAA, might have been caused by the collision of the plateau with a proto-Central America Arc. Other authors consider that the westward subduction initiated immediately after the eruption of the plateau, which means that the plume might have a causal role in subduction initiation (Vallejo et al., 2006; Whattam & Stern, 2015). The proto-Central

America east-verging SZ initiated around 100 Ma in an intra-oceanic setting for Pindell & Kennan (2001), Weber et al. (2015), Boschman et al. (2019), or later around 72-75 Ma for Mann (2007) or Wright & Wyld (2011). In any case, those SI contexts will not be detailed in this study as they did not occur during the Cenozoic.

South Caribbeans

In Early Cenozoic, the domain between South and North America was occupied by the proto-Caribbean ocean in the middle of which a spreading center separating both plates was either dying (Pindell & Kennan, 2001, 2009) or already no longer active (Mann, 2007). The westward motion of both America plates with respect to a quasi-fixed Caribbean plate in a hot spot reference frame, since its decoupling from the Farallon and Phoenix plates, resulted in a severe deformation of the former GAA at both contacts with the passive margins of the Americas (e.g., Pindell & Kennan, 2001). The lateral slip of the Caribbean plate with respect to the America plates since 75 Ma was very probably accommodated by STEP faults allowing the oceanic part of America plates for subducting whereas continental parts remained unsubducted. Numerous outcrops attest for the accretion of terranes with CLIP affinities along the Colombian margin (e.g., Cédiel et al., 2003; Montes et al., 2005, 2019) since 75-65 Ma (Vallejo et al., 2006). The subduction of the Caribbean plate beneath NW South America started in the Late Cretaceous. Terranes composed of CLIP, arc and continental rocks docked first along the northernmost Andean margin (Western Cordillera of Colombia - Chocos block). The subducted part of the CLIP is still attached to the Chocos block beneath Maracaibo according to Taboada et al. (2000). CLIP southward thrusting underneath the Caribbean coast of Colombia (Maracaibo region) is documented only since the Paleogene (Pindell & Kennan, 2001). The onset of CLIP subduction beneath the Caribbean coast of Colombia is estimated around 65-55 Ma by Ayala et al. (2012), Pindell et al. (2012), van der Meer et al. (2018) or Montes et al. (2019) based on deformation within the Maracaibo block or present length of subducted plateau (~800-1200 km). Montes et al. (2019) reported a post-collisional short-lived Paleocene magmatic arc attesting that the subduction process reached the achieved stage. The fact that the magmatism abruptly shut-down during the Eocene may be caused by the underthrusting of the buoyant plateau inhibiting volcanism. Here, the length of the slab is probably counterbalanced by its buoyancy, so that the slab pull is probably not enough to consider that subduction as self-sustained. It should be mentioned that, based on the detailed analysis of offshore seismic lines and wells, Escalona and Mann (2011) propose a younger age, ~44 Ma, for the reversal of subduction polarity along the northern Colombia margin, allowing the southward subduction of the CLIP. The subduction of the Caribbean plate beneath North Colombia might have been facilitated by a thinner oceanic crust as suggested by the smaller crustal thickness off the North Colombia margin (Sanchez et al., 2019). The South Caribbean trench probably appeared during the Paleocene, following the STEP Fault initiation and eastward propagation. Its length thus grew up to 1500 km off the north coast of South America including the Leeward Antilles (Kroehler et al., 2011). Today, the surface trace of the STEP Fault is represented by the El Pilar Fault system fringing the northern coast of Venezuela and ending somewhere south of the Barbados

accretionary prism (Deville & Mascle, 2012; Padron et al., 2021b). The thinning of the South America plate, south of the Leeward Antilles and Grenada Basin, by delamination induced by the tear (STEP Fault) as suggested by Levander et al. (2014) should have facilitated subduction initiation. Nowadays, transpression is localized onshore south of the Grenada Basin (Audemard and Castilla, 2016) but the southeastward flexure of the Grenada Basin basement under the load of the South America margin (Escalonna & Mann, 2011; Garrocq et al., 2021) should favor the westward propagation of the S-Caribbean trench in a near future. Today, the S-Carribean trench ends west of the Aves Ridge.

North Panama

The North Panama SZ propagated northwestward during Pliocene time from a lithospheric SW-dipping thrust originating from the collision of the Choco Block with South America at the end of the Middle Eocene (40-38 Ma; Barat et al., 2014). The Choco Block is supposed to represent the initial Late Cretaceous - Paleocene Arc associated with the NE-dipping Farallon slab beneath the Caribbean Plate. The Choco Block first accreted against South America (present NW corner of Colombia) throughout Eocene, Oligocene and Miocene and the lithospheric backthrust then propagated along the rear of the former deforming arc above the subducting active Cocos-Nazca spreading center (Barat et al., 2014; Montes et al., 2019). Based on hypocenters, the Caribbean slab reaches up to 80 km in depth (Camacho et al., 2010) which is neither enough to generate arc volcanism, nor being self-sustained (Silver et al., 1990). Its present trench length reaches at least 600 km and even 800 km when considering the whole North Panama Thrust Belt (Silver et al., 1990). As proposed by these authors, NWward thrusting of the Choco Block over the Caribbean Plate probably accommodates its bending as an elastic beam as it collides with South America.

Beata Ridge

The Beata Ridge is a SW-trending thicker (up to 23 km, Nunez et al., 2016) crustal part of the Caribbean magmatic plateau extending from the island of Hispaniola, where it outcrops, across the Caribbean Sea. It results from a dual magmatic plume event from 95 to 74 Ma (Révillon et al., 2000; Dürkefälden et al., 2019a&b) followed by extension at the origin of the Haiti Basin which flanks the Beata Ridge to the west (Driscoll and Diebold, 1998; Diebold, 2009). Its deformed eastern flank attests for lithospheric oblique thrusting of the western part (Colombian microplate) onto the eastern one (Venezuelan microplate) since the Early Miocene under a NE-SW compressive stress (Driscoll and Diebold, 1998; Mauffret and Leroy, 1999). Such compression, which caused the most severe reduction in space in the Caribbean area, started around ~23-25 Ma and has been attributed by Müller et al. (1999) to the differential accelerated convergence between the two Americas, increasing from east to west. Distributed compressional and wrench faults result in a shortening increasing toward the north (Mauffret and Leroy, 1999). These compressional faults may have reactivated former normal faults inherited from earlier extensional episodes at ~75 Ma (Driscoll and Diebold, 1998) and ~55 Ma (Révillon et al., 2000). Based on a detailed study of the morphostructure at the junction between the Beata Ridge and the GAA, Granja-Bruna et al. (2014) call into question the models supporting the transpression in the northern Beata Ridge.

Nicaragua Rise

The Nicaragua Rise extends to the east of the Chortis continental and oceanic block to Jamaica (Baumgartner et al., 2008). Dredges have shown that the Nicaragua Rise is at least partly of oceanic origin (Late Cretaceous Caribbean Plateau). During the Paleocene, this region underwent left-lateral shearing under transpressive stress as the Caribbean plate inserted into the Americas until strike-slip motion localized to the north in the Early Eocene (Pindell and Kennan, 2009). The area of the Caribbean Plate has considerably reduced since its birth in the Late Cretaceous. Tectonic reconstructions generally consider that most of the lost area was located in the south of the plate but, as for the ~200 km shortening in the Beata Ridge region, a significant area (500-800 km long and a few hundred km wide slab) is supposed to have disappeared between the present Nicaragua Rise, including Jamaica and South Hispaniola, and North Hispaniola during the Paleogene (van Fossen and Channell, 1988; Müller et al., 1999). The existence of a nearby subduction is attested by relics of Paleocene to Early Eocene continuous arc volcanism including adakite-like rocks derived from Caribbean oceanic plateau crust that underthrust Jamaica in the early Tertiary (Arden, 1975; Pindell and Barrett, 1990; Hastie et al., 2010). Other reconstructions involve oblique shortening and possible subduction at the southern edge of the Nicaragua Rise at the same period (Pindell and Kennan, 2009; Mann, 2007). New insights from tomographic images of ancient slabs indicate that if a slab developed between the Nicaragua Rise/Jamaica and North Hispaniola, it was very small (~300 km maximum; van Benthem et al., 2013). Finally, some geological and geophysical evidences support the idea that a short-lived subduction developed within the Caribbean plateau during the Paleocene - Early Eocene accommodating the collision between the Caribbean and North America plates at a distance from the main plate boundary which will further localize to the north along the Cayman Trough (Leroy et al., 2000).

Puerto-Rico (including East Hispaniola and Virgin Islands)

The Puerto-Rico SZ formed by lateral propagation of the Lesser Antilles SZ since the Eocene. The Cretaceous Proto-Caribbean Sea subducted westward beneath the GAA from Cuba to the Leeward Antilles during the Paleocene, until the Bahamas transitional crust first collided with the Cuba margin in Eocene (Pindell and Kennan, 2001; Boschman et al., 2014). Zircon and apatite (U-Th)/He ages revealed that deformation associated with arc-continent collision started around 52 Ma in the Early Eocene in the western part of Puerto-Rico and propagated gradually eastward reaching the Virgin Islands around 21-24 Ma at the Oligo-Miocene transition (Roman et al., 2020). Puerto-Rico might be positioned south of Hispaniola in the Early Eocene, before being left-laterally offset to its present location east of Hispaniola (Pindell et al., 2006). Indeed, the new E-W trending transform plate boundary formed between Cuba and Hispaniola, to account for the docking of Cuba and the adjacent Yucatan Basin to the North American Plate, during the Early Eocene. The ~1000 km left-lateral plate motion across this N-Caribbean new plate boundary has been recorded in the magnetic lineations of the Cayman Trough, a pull-apart basin which started to open around 49 Ma (Leroy et al., 2000). The deformation thus started with the underthrusting of the Bahamas transitional

crust beneath Hispaniola and then Puerto-Rico and the Virgin Islands, followed by the Cretaceous oceanic crust of the Proto-Caribbean Sea. The remnant North American slab beneath Cuba might have detached (van Benthem et al., 2013) as intraslab E-W shearing proceeded to account for the new transform motion. The intense deformation of the colliding plates is reflected today in the very peculiar seismicity down to a depth of ~200 km from Central Hispaniola to Puerto-Rico (Rodriguez-Zurrunero et al., 2020). The seismic slab beneath Puerto-Rico reaches a maximum depth of 200 km but could be longer, even reaching the 660 km depth based on tomography (Harris et al., 2018). The Puerto-Rico SZ thus developed progressively starting from a continental subduction in the Eocene and Oligocene and evolving into an oceanic subduction in the Miocene as the trench lengthened, concomitantly with the Cayman Trough spreading. It is hard to trace the arc volcanism which can be specifically attributed to this new subduction segment because of the highly oblique and slow convergence in which most of the fluids are released by the slab to the east before reaching the central and western part (Calais et al., 1992). Based on the seismic activity, the length of the slab and despite the lack of clear associated arc volcanism, we will consider this segment as active and self-sustained in this study.

Muertos

The Muertos Trough is a 650 km-long south-vergent deformation front marking the backthrusting of the East Hispaniola - Puerto-Rico - Sainte Croix Block, part of the Cretaceous to Early Eocene GAA, onto the Caribbean plate (ten Brink et al., 2009). The age of initial convergence is unknown but likely coincides with the major uplift phase of the arc in the Eocene and Oligocene (Larue, 1994), in response to the collision of the GAA with the Bahamas platform from Late Paleocene to mid-Eocene (Stanek et al., 2009). New (U-Th)/He data on zircon and apatite from Puerto-Rico from Roman et al. (2020) reveal that deformation associated with arc-continent collision started in the Early Eocene (~52 Ma). An alternative scenario has recently been proposed, based on numerical simulations (Cerpa et al., submitted). Just after the early Eocene jump of the SZ from NE Cuba to the NW of the Lesser Antilles, the sharp transition between the newly formed northern strike-slip boundary (N Hispaniola) and the eastern SZ of the Lesser Antilles could have locally promoted high compressive stresses and underthrusting, resulting in the Muertos Trough formation. The lack of slab in the tomography (van Benthem et al., 2013) as well as the absence of related-volcanism (Pindell and Kennan, 2009) indicate that subduction was never achieved despite continuous activity since initial lithospheric thrusting (Granja Bruna et al., 2014). Strain partitioning must occur considering the highly oblique relative motion between North American and Caribbean plates, but evidence for strike-slip was found neither within the Muertos accretionary wedge nor the upper slope. The strike-slip component seems to be accommodated to the north along the Hispaniola - Puerto-Rico northern margins (ten Brink et al., 2009) or within the subducting north-American plate itself.

Lesser Antilles

On one side, the oldest robust ages of supra-subduction arc lavas along the W-dipping Lesser Antilles Arc (LAA) vary from 38 Ma from a dacite dyke in Grenada Island in the

south (White et al., 2017) to 40 Ma for an andesitic intrusion in St. Barthelemy Island in the north (Legendre et al., 2018). On the other side, the youngest W-dipping subduction-related rocks, located 100-300 km inward of the LAA, attesting to the volcanic activity of the GAA are supposed to be 59 Ma (Neill et al., 2011). So far, no arc volcanics have been documented during the ~20 Myr from Late Paleocene to Middle Eocene, but W-dipping subduction might have occurred since the Grenada Basin rifted and spread between the two arcs (LAA & GAA) during this period (Pindell & Kennan, 2009; Aitken et al., 2011; Padron et al., 2021a). Some authors thus consider that the Lesser Antilles subduction resumed in Late Eocene (see the yellow dotted line in Fig.7), but here we suggest that the subduction of the proto-Caribbean Sea beneath the former GAA never stopped but subduction-related volcanism from 58 to 41 Ma is either buried beneath the sediment of the Grenada Basin younger than mid-Eocene or beneath the arc or forearc of the LA (Allen et al., 2019; Garrocq et al., 2021). An alternative scenario would be a decrease, or even a gap, in the volcanic activity during the middle Eocene active backarc spreading as suggested by Magni (2019). Since the eastern front of the Caribbean plate expanded during the Grenada Basin opening (Pindell & Kennan, 2009), the new LAA occupies a larger area than the former GAA but in fine, the W-dipping subduction in this region initiated before the Cenozoic despite the apparent 20 Myr volcanic gap.

3.5. Atlantic Ocean

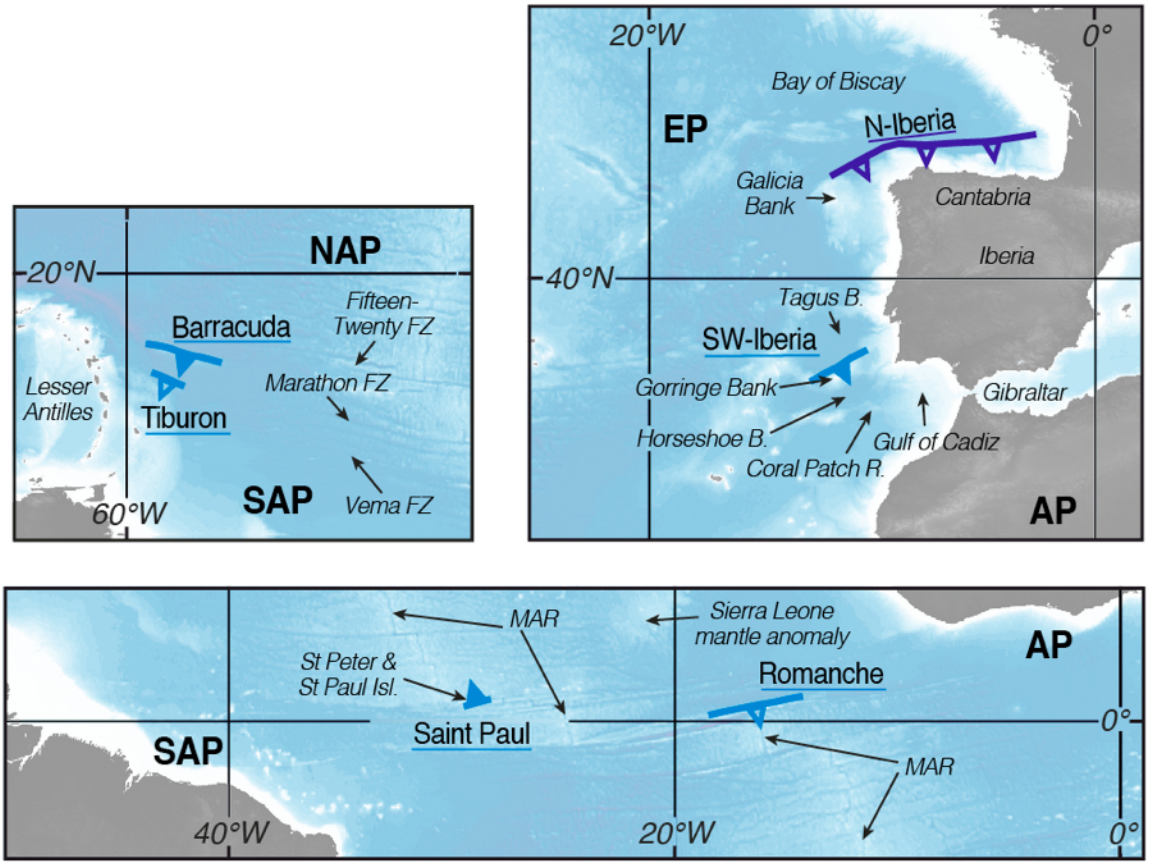

Fig.8: Map of Cenozoic SISs in the Atlantic region. See the legend in Fig.4. B.: Basin, R.: Ridge, FZ: Fracture Zone, Isl.: Island, MAR: Mid-Atlantic Ridge, EP: Eurasian Plate, AP: African Plate, NAP: North-America Plate, SAP: South-America Plate.

North Iberia

The North Iberian margin underwent a short period of compression during the Paleocene-Miocene period, as a result of the partial closure of the Bay of Biscay (Le Pichon and Sibuet, 1971; Boillot and Malod, 1988; Roest and Srivastava, 1991; Alvarez-Marron et al., 1997, Fig.8), which opened from 125-118 to 112-80 Ma ago (Srivastava et al., 1990; Sibuet et al., 2004; Gong et al., 2008) accommodating the counter-clockwise rotation of Iberia. This is attested by a well-developed accretionary wedge now buried beneath a post-tectonic sediment cover (Gallastegui et al., 2002; Fernandez-Viejo et al., 2012). Based on detailed seismic stratigraphy, Gallastegui et al. (2002) restricted the time of compressive deformation from Upper Eocene to Middle Miocene. Wide-angle imagery revealed that normal faults inherited from the Bay of Biscay rifting were inverted during the compression episode. A Mesozoic crustal scale extensional detachment within the thinned Iberian crust played the role of a weakness zone allowing the ~ 80 Ma-aged lower transitional crust to slide southward under the upper crust indenting the Cantabrian margin (crocodile-style). As a consequence, southward subduction (lithospheric sinking in the mantle) never developed. However, about 90 km of shortening was absorbed through lower-crustal indentation/underthrusting, allowing the northward subduction of Iberia to occur at deeper levels while thickening the Cantabria margin by duplicating crustal levels (Gallastegui et al., 2002; Fernandez-Viejo et al., 2012). No related volcanism has been documented. Shortening decreased westward and vanished off the Galicia Bank, north of which less than 40 km of shortening was estimated (Alvarez-Marron et al., 1997). Africa-Eurasia plate convergence stopped along the North Iberian margin as plate boundary jumped to South Iberia after the Late Oligocene (Roest and Srivastava, 1991).

Southwest Iberia (including Gorringe)

To the west, the diffuse plate boundary between Eurasia and Africa plates goes through the Gulf of Cadiz where it is still compressional accommodating about 1.5 to 5.8 mm/yr of shortening (e.g., Nocquet and Calais, 2004; Serpelloni et al., 2007; Koulali et al., 2011). The southwest Iberia margin (SIM) is composed of a mosaic of highly heterogeneous crusts which originally dealt with both the Alpine-Tethys history and the North and Central Atlantic opening (Martinez-Loriente et al., 2014). It attests for an initial rifting setting as a transform margin during the Early Jurassic following the continental break-up in the Central Atlantic, then oblique rifting and spreading occurred between Iberia and Africa from about 170 Ma ago until the start of the North Atlantic Basin at about 140 Ma (Sallarès et al., 2011). The Gorringe Bank is the most prominent surface expression of a larger area of distributed shortening, 450 x 450 km wide, NE-SW-trending, thrust system described by several authors (e.g., Terrinha et al., 2009; Duarte et al., 2013). The Gorringe Bank is bounded to the north by a 150 km long southward shallow dipping thrust, allowing Early Cretaceous serpentinized mantle peridotites and gabbros to be exhumed along a 5 km high scarp (Duarte et al., 2013). Total amount of crustal shortening across the Bank has been estimated by Hayward et al. (1999) to be 50 km at the most. Most of the shortening occurred in the Late Miocene as attested by an unconformity in the surrounding Tagus and Horseshoe basins (Zitellini et al., 2009).

Reactivation of former lithospheric structures beneath the Gorringe Bank, the Horseshoe Abyssal Plain or the SW margin of Iberia is revealed by a high level of seismicity down to a depth of 50 km (Fukao, 1973; Gutscher et al., 2002; Civiero et al., 2018; Hensen et al., 2019). About 10% of additional shortening has also been revealed south of the Gorringe Bank across the Jurassic Coral Patch Ridge and surrounding abyssal plains (Hayward et al., 2009; Martinez-Loriente et al., 2013, 2014, 2018). Today, the SW-Iberia margin region primarily appears as a compressive relay between the transform focused plate boundary (Gloria Fault) to the west and the distributed compressive one (Betic and Rif-Tell fault zones) to the east (Zitellini et al., 2009). Its connection with the Gibraltar system (see next section) has been highlighted by Duarte et al. (2013). They suggest that the westward movement of the Gibraltar Arc may contribute to the compression observed in the area in addition to the WNW-ESE convergence between Africa and Eurasia. The trend of the thrusts is compatible with the direction of convergence between Africa and Eurasia and oblique to the former normal faults inherited from North Atlantic spreading. Some of them thus appear to have been neoformed during mid-Miocene (Hayward et al., 1999), whereas structures inherited from Late Jurassic – Early Cretaceous continental mantle denudation might have also been reactivated (Sallarès et al., 2013; Martinez-Loriente et al., 2014). Ongoing lithospheric mantle delamination localized beneath a serpentinized front of crust and upper mantle of Horseshoe abyssal plain has been suspected and modelled by Duarte et al. (2019) based on a new tomographic imagery after NEAREST seismic survey (Monna et al., 2015; Civiero et al., 2018) which supports the hypothesis of Fukao (1973) of incipient northward dipping subduction beneath Horseshoe abyssal plain revealed by M_s7.9 1969 thrust earthquake. This hypothesis needs to be confirmed by further investigations but if true, it would indicate an unusual way of SI starting at deep levels by delamination of the mantle part of an oceanic lithosphere sandwiched between two transform faults before localizing at shallower depths.

Barracuda - Tiburon

The Barracuda Ridge results from a tectonic uplift of the Atlantic crust along the Fifteen Twenty FZ following the northward migration of the rotation pole between North and South America plates (Roest and Collette, 1986; Müller and Smith, 1993). A change in the direction of North America relative to South America plate motion during the middle-late Miocene caused ~N-S compression within the oceanic lithosphere east of the Lesser Antilles Trench (Roest and Collette, 1986). There, the weak zones sub-perpendicular to the compressive stress are the Central Atlantic Fifteen-Twenty, Marathon and Vema fracture zones. Roest and Collette (1986) estimated ~16 km of N-S shortening across the ridge and adjacent trough within the last 7 Ma. The timing for the compression has been further revised by Patriat et al. (2011) with a start of the deformation since the Early Pleistocene (~2.3 Ma), based on a reflection seismic survey and Deep-Sea Drilling biostratigraphic correlations. The deformed area comprises not only the Barracuda Ridge and Trough but also the Tiburon Rise further south over a total area of 200 x 500 km. Pichot et al. (2012), after careful analyses of the seismostratigraphic sequences in this area, have concluded that the deformation was diachronous starting in the South with an uplift (< 2 km) of the Tiburon Rise between 13 and 5.3 Ma, then migrating to the north with a larger uplift (> 2 km) of the Barracuda Ridge during the last 2.3 Ma. Here, the ~N-S shortening has been partly accommodated

by flexure but the wavelength of the buckling, expected to be around 80-100 km according to the Late Cretaceous age of the Atlantic crust, is mostly controlled by the spacing of the vertical fracture zones (>100 km) localizing the deformation. The finite shortening across the deformed region has not been measured by Pichot et al. (2012) but is probably quite small (< 10 km). Today, compression still occurs around the Barracuda Ridge but has stopped at Tiburon Ridge. Diffuse deformation thus first affected the Marathon FZ resulting in the rise of the Tiburon Ridge in mid-late Miocene and then migrated north to the Fifteen Twenty FZ where deformation is the most active since the Early Pleistocene. The maximum uplift is seen at the bulge of the subducting plate seaward of the trench indicating that, not only the convergence between the North American and South American plates, but also the flexure of the downgoing plate is responsible for the deformation.

Saint Paul - Romanche

Two large-offset transform faults in the equatorial Atlantic have been subject to compressional tectonic uplift and thrusting in the Late Miocene. In both cases, transtension and transpression have produced transverse ridges culminating at 3 to 4 km above the adjacent seafloor. The ridges distribute along non-straight transform boundaries and are caused by regional changes in ridge/transform geometries. The Romanche transform has jumped from a ~800-km long paleo-valley to its present location about 8-10 Ma ago. Transpressional deformation occurred during the migration time from one site to the other with the rise of a ~300-km transverse ridge which emerged above sea-level at ~5 Ma, then it subsided until present (Bonatti et al., 1994). The same transverse ridge is observed along the Saint-Paul system about 1000 km west of the Romanche ridges. Here, St Peter and St Paul islets still emerge today, attesting to compressive deformation since ~10 Myr (Maia et al., 2016). Age of the oceanic crust is young and almost similar on both sides at the time of transpressional activity. According to Maia et al. (2016), a change in plate motion at ~11 Ma initially triggered extension in the left-stepping transform, then long-lived compression occurred at the origin of the ~100-km-long transverse ridge, facilitated by enhanced melt supply at the ridge axis above the Sierra Leone mantle anomaly rather than changes in the far-field stress regime.

3.6. (Peri-)Mediterranean area

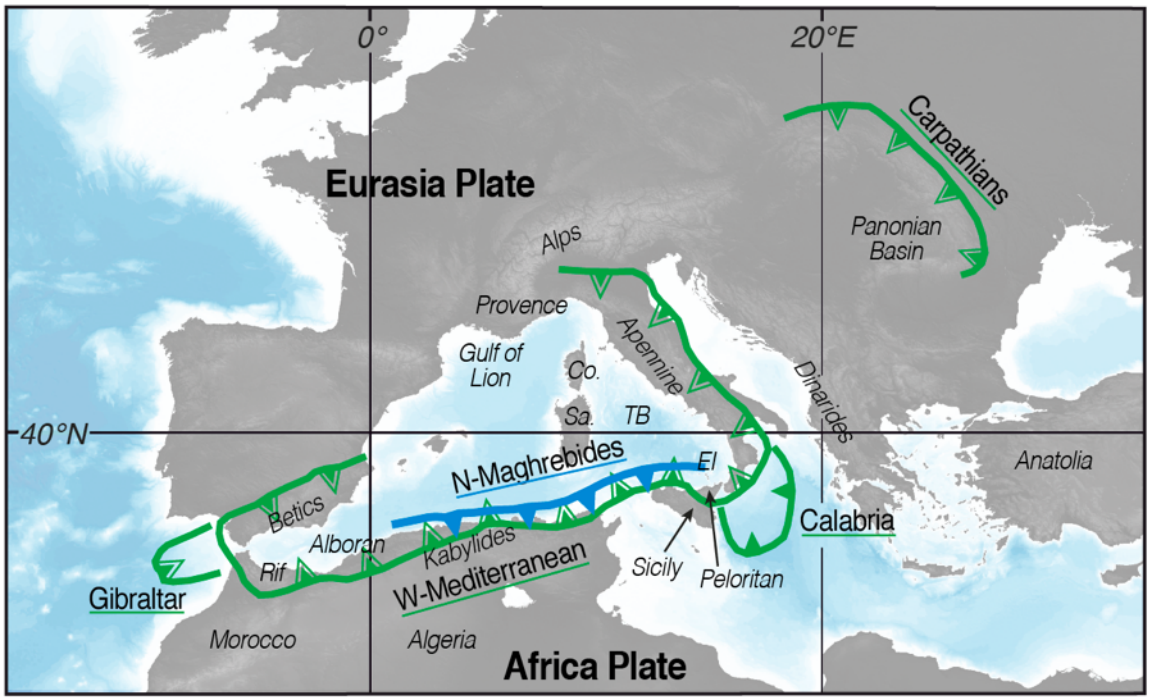

Fig.9: Map of Cenozoic SISs in the Mediterranean region. See the legend in Fig.4. PB: Pannonian Basin, Co.: Corsica, Sa.: Sardinia, TB: Tyrrhenian Basin, EI: Eolian Islands, EP: Eurasia Plate, AP: African Plate.

Western Mediterranean - Gibraltar - Calabria

The Alpine orogen in the Mediterranean region displays characteristics of collisional (e.g., Alps) and subduction (e.g., Apennine, Maghrebides, Rif, Betic in the Western Mediterranean Arc) orogens (Royden and Faccenna, 2018) as well as a series of orogenic curvatures (e.g., Gibraltar, Calabria, Fig.9) (Rosenbaum, 2014). They initially result from the indentation of Adria into Europe and then, second- and third order oroclines developed as convergence proceeds since Late Cretaceous (~85 Ma) following the transform motion between Africa and Iberia from ~120 to 85 Ma (van Hinsbergen et al., 2014). Based on tomographic and kinematic reconstructions, the preferred scenario is that shortening initiated along the transform fault that accommodated pre-85 Ma translation, first at a very slow rate between 85 and 45 Ma followed by the onset of deep-northward dipping underthrusting, later called Western Mediterranean SZ, at ~45 Ma culminating in roll-back since ~27 Ma (van Hinsbergen et al., 2014, 2020; van der Meer et al., 2018). The localization phase from 85 to 45 Ma is a matter of debate, especially regarding the vergence of the initial subduction/underthrusting, either northward (e.g., Faccenna et al., 2001; Schettino and Scotese, 2002; van Hinsbergen et al., 2014) or southward (e.g., Handy et al., 2010; Molli and Malavieille, 2010), while the Eocene onset of real northward subduction, along the northern passive margin of the Ligurian-Piemont Ocean beneath East Iberia and Provence region, is generally accepted by most authors (see discussion in Royden and Faccenna, 2018). The oldest arc volcanism in Sardinia has been dated to around 38 Ma by Lustrino et al. (2009), meaning that Apennine SZ – which belongs to the Western Mediterranean SZ - was initiated in the mid-Eocene around 49-42 Ma. Extension first recorded in the Gulf of Lion around 30 Ma attests for its roll-back with respect to Eurasia since the Oligocene (Faccenna et al., 2014). In his review paper about the Gulf of Lion evolution, Seranne (1999) envisaged an alternative scenario with a change of

subduction polarity from southward north of Cap Corse in Corsica (Malavieille and Molli, 2014) to northwestward south of it until Late Eocene. Then, the northwestward-dipping subduction trapped the Cap Corse by lateral propagation around 35 Ma. Throughout the Cenozoic, the length and curvature of the Western Mediterranean subduction boundary increased as trench retreated, back-arc basins developed and slab tore (Rosenbaum, 2014). It is difficult to precisely date the formation of the present Gibraltar and Calabria SZs as they both result from the progressive lateral propagation and local invaginations of the former Western Mediterranean SZ. As a rough estimate, the length of the present trench trace (~4000 km) is at least twice the one of the former SZ (~1700 km). However, the timing of formation of those two oroclinal bends differs. The Gibraltar orocline developed progressively, probably since 45 Ma (van der Meer, 2018), and then accelerated its westward migration by trench roll-back accompanying the Alboran block extrusion, contemporaneously with the last E-W spreading phase of the Algerian Basin from 16 to 8 Ma (Leprêtre et al., 2013), and then possibly accommodating the northward motion of Africa promontory through the activation of conjugate strike-slip faults in a way similar to the extrusion of Anatolia caused by the push of Arabia (e.g., Nocquet, 2012). Present activity of the Gibraltar subduction is debated (see discussion in Gutscher et al., 2012) since no active subduction volcanism is observed since ~9 Ma (Wilson and Bianchini, 1999; Fullea et al., 2010) or even ~6 Ma (Booth-Rea et al., 2018), contrary to the Calabria SZ which still feeds volcanism in the Eolian islands. As the Gibraltar SZ, the Calabria SZ derived from a segment of the former Western Mediterranean SZ, and acquired its tightly curved shape when migrating westward as trench rolled-back and the Tyrrhenian Basin opened during the last 5 Ma (Sartori, 1990; Milia et al., 2018). Both Gibraltar and Calabria SZs are still connected with long slabs and accommodate ultra-low convergence rates (Serpelloni et al., 2007; Nocquet, 2012). It is admitted that the subducting oceanic crust in both cases corresponds to the last remnants of the Tethyan ocean of Jurassic or older (Permo-Triassic?) age (Sallarès et al., 2011, Stampfli, 2000). Gibraltar and Calabria segments are represented separately from the W-Mediterranean main SZ in Fig.9 for clarity even though they are part of it.
We see that the initial stages of the Western Mediterranean SZ are not definitely constrained. Questions remain about the respective role of the pre-85 Ma transform plate boundary between Africa and Iberia, the weak zone represented by the northern passive margin of the Ligurian-Piemont Ocean or the possible consumption of the Valaisian Ocean prior to inception of the northward subduction (Molli and Malavieille, 2010), during SI. Since the oldest arc magmatism attributed to the Western Mediterranean SZ is dated to the Late Eocene, we will treat it as a Cenozoic subduction.

Carpathians

Accompanying the northward drift and collision of the Adriatic microplate with the European platform around 25-20 Ma, subduction of the Peninnic-Magura (Late Jurassic – Early Cretaceous Meliata-Maliac Ocean of Schmid et al., 2008) basement initiated beneath the Carpathian belt as attested by active thrusting at the front of the accretionary prism at 20-18 Ma (Konecny et al., 2002). According to paleo-reconstructions (Ustaszewski et al., 2008), the Mid-Hungarian transform plate boundary between opposite-verging Alps (including Western Carpathians) and Dinarides orogens might have been the locus of subduction nucleation around 20 Ma ago. Since no relics of the subducted basement were preserved, its nature is not clear but the presence of radiolarian cherts in the early accreted rocks indicates that the subducted lithosphere

was likely oceanic (Royden and Faccenna, 2018). Subduction-related calc-alkaline magmatism was dated to 17.5 to 9.5 Ma in the northwestern part of Eastern Carpathians and 14.5 to 1 Ma in the southeastern part (Konecny et al., 2002). The slab has been progressively detached from north to south since 9 Myr. Early Miocene back-arc transtension within the Pannonian Basin coupled with asthenospheric upwelling is supposed to have been triggered by the rapid sinking of the dense oceanic lithosphere. The width and length of the subducting slab has been estimated to ~500 km x ~500 km (Konecny et al., 2002) while the present surface trace reaches ~1000 km.

North Maghrebides (Alboran to Sicily)

The north-directed Western Mediterranean subduction beneath the Maghrebides stopped around 10 Ma ago following slab break-off (Wortel and Spakman, 2000; Faccenna et al., 2004) after having consumed about 1000 km of oceanic lithosphere (Royden and Faccenna, 2018). Thrusting polarity reversal occurred about 11 Ma ago off Morocco (d'Acremont et al., 2020), 8 Ma ago off Algeria (Deverchère et al., 2005) and propagated eastward to Sicily less than 1 Ma ago (Serpelloni et al., 2007; Billi et al., 2011). Shortening does not exceed yet a few tens of kilometers, making this margin the locus of incipient south-verging subduction (Royden and Faccenna, 2018). The flip of subduction polarity across the western segment of “AlKaPeCa” (Alboran-Kabylides-Peloritan-Calabria) drifted continental blocks of European affinity, started 11.6 Ma ago along the South Alboran Ridge which is supposed to represent the surface expression of the former STEP fault which accommodated the westward Miocene Tethysian slab roll-back (d'Acremont et al., 2020). Reactivation started around 8 Ma ago at the foot of the North Algerian margin in a rear-arc structural setting (Hamai et al., 2015, 2018). The collision of the AlKaPeCa arc with the North Africa continental margin occurred during Middle Miocene as attested by the coastal uplift and emergence of the Algiers and Sahel Ridge massifs as well as the folding and subsequent uplift of the South Alboran Ridge (van Hinsbergen et al., 2014; Authemayou et al., 2017; Gomez de la Pena et al., 2018; d'Acremont et al., 2020). Offshore Algeria, diffuse shortening might have begun in the late Miocene but probably localized at the toe of the margin only 5 to 2 Ma ago (Kherroubi et al., 2009; Strzerzynski et al., 2010). The structure of the margin reflects the last phase of E-W basin opening (16 to 8 Ma ago) off Algeria, while it has been strongly deformed off Morocco (d'Acremont et al., 2020). It is thus those of a transform margin off Algiers (Leprêtre et al., 2013) but previous transform faults like Jebha and Nekor in Morocco were reactivated after the Tortonian (d'Acremont et al., 2020). Detachment faults from the earlier rifting phase (35-25 Ma ago) might have been reactivated into south-dipping thrust faults (Strzerzynski et al., 2010). A thermal anomaly, observed beneath the thinned continental margin, possibly as a result of slab rupture starting around 15 Ma, might have facilitated the strain localization (Hamai et al., 2015, 2018; Aïdi et al., 2018; Garzanti et al., 2018). The minimum area concerned by lithospheric flexure under N-S compressional stress, accommodating 2.7 to 3.9 mm/yr of shortening distributed both onshore and offshore, is about 600 km long north of Algeria (Serpelloni et al., 2007; Hamai et al., 2015). The total lateral extent of compressive deformation may reach 1100 km including the northwestern margin’s slope of Sicily which undergoes 2.1 cm/yr of localized shortening since ~0.5 Ma (Billi et al., 2011; Serpelloni et al., 2007; Chiarabba & Palano, 2017). The shortening rate recorded in the sedimentary cover around the South Alboran Ridge off Morocco has decreased from 1 mm/yr 11.6 Ma ago

to 0.2 mm/yr today (d'Acremont et al., 2020). The minimum amount of shortening there is at least 8.5 km.

3.7. Indian Ocean

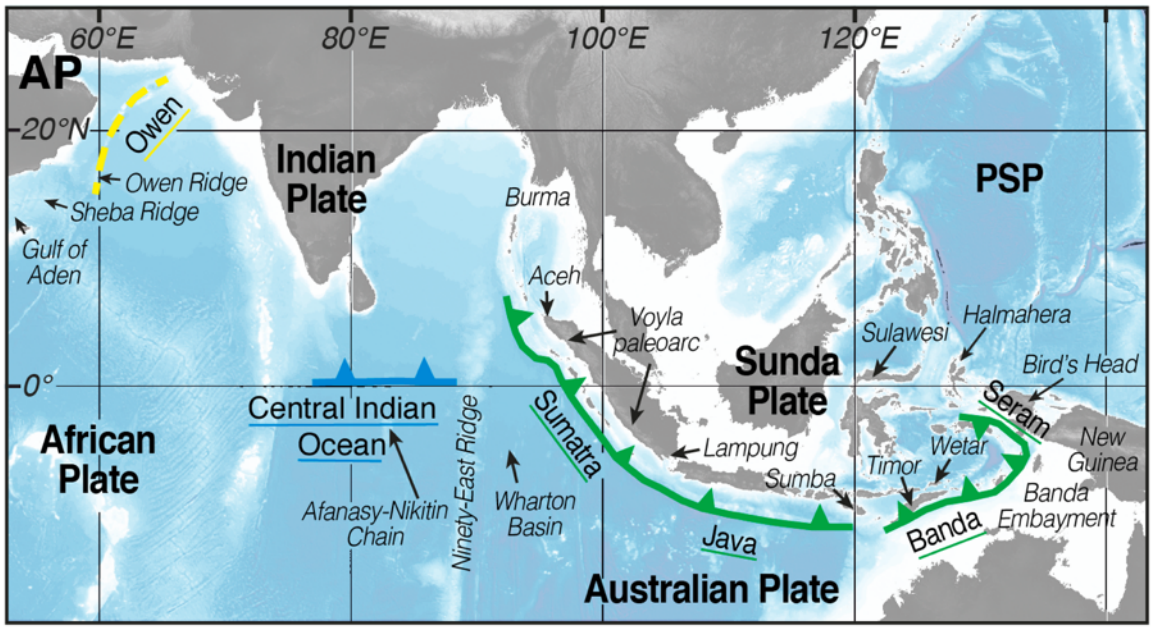

Fig.10: Map of Cenozoic SISs in the Indian Ocean region. See the legend in Fig.4. The dotted yellow line outlines the Owen fracture zone which has been proposed as an incipient SI case by Gurnis et al. (2004) but we consider here that it is speculative. The vergence of incipient subduction in the Central Indian Ocean is random since the deformation is still diffuse without any localization yet. AP: Arabian Plate, PSP: Philippine Sea Plate.

Central Indian Ocean

It has long been observed that intraplate seismicity, long wavelength (~150-300 km) folding and dense thrusting associated with high heat-flow attest for intra-oceanic compressional deformation in the northeastern Indian Ocean (Weissel et al., 1980). Deformation there was compared to the buckling of an elastic plate under N-S compression originating from the continental subduction and collision between India and Asia. Based on driving and resistive forces balance over the Indo-Australian plate, Cloetingh and Wortel (1985, 1986) have documented a concentration of compressive forces of the order of a few kbars in the Ninetyeast Ridge area (Fig.10). Cloetingh et al. (1989) concluded that the folding of the oceanic lithosphere amplified by sediment loading might be a preparatory stage for SI. Shemenda (1992) has provided further constraints using 4D physical modeling of a horizontal oceanic lithosphere mimicking the Indo-Australian plate geometry under compression. Further seismic and deep-sea drilling investigations were used to establish a constrained scenario for the intraplate deformation (Krishna et al., 1998; Delescluse and Chamot-Rooke, 2007, 2008). Purely compressive deformation is distributed over a - ~1000-km-wide ~2000-km-long E-W trending band centered on the Afanasy Nikitin Chain in the Central Indian Ocean. The Ninetyeast Ridge appears as a major strain discontinuity separating the compressive area from the area under strike-slip centered on the Wharton Basin which enters into subduction beneath Sumatra (Delescluse and Chamot-Rooke, 2007). They suggest that

intraplate deformation started about 8.0 Ma ago when Australia detached from India along the left-lateral oceanic shear band centered around the Ninetyeast Ridge and accelerated its northward motion. About 110-140 km of left-lateral finite strain has been estimated by the authors. Modeling of various processes authorized Delescluse and Chamot-Rooke (2008) to conclude that exothermic serpentinization, triggered by the onset of deformation through vigorous hydrothermal circulation, is the main factor explaining a heat-flow 30 mW/m^2 higher than expected from plate cooling of a Cretaceous oceanic lithosphere. Sub-Moho reflections down to 15 km attest for a serpentinization front. Such syn-tectonic crustal weakening should logically favor strain localization in the near future. Another factor of weakness is given by the E-W orientation of the normal paleofaults which were inverted at the very onset of deformation at ~9 Ma. Most of the densely spaced (~3 km) small-offset faults were no more reactivated after ~7 Ma while deformation then localized on a few of them with larger (~20-30 km) spacing (Delescluse et al., 2008).

Sumatra - Java (Sunda)

The tectonic evolution of the Sunda region is quite complex to reconstruct and certainly needs further exploration. Hall (2012)'s reconstruction is based on tremendous geological data constraints onshore as well as plate kinematics and tomographic considerations validated by van der Meer et al. (2018) after Hall and Spakman (2015). Subduction of the Meso-Tethys beneath the Sunda plate (Burma and Sumatra) occurred from Late Jurassic to Late Cretaceous until the eastern segment of the Woyla Arc, fringing the Meso-Tethys Plate, collided with Sumatra. Then, plate reorganization occurred with the inception of a new N-S-trending India-Australia transform allowing the northward motion of the India Plate to the west and cessation of NE-directed subduction beneath Sumatra to the east. The margin south of Sumatra and Java thus became passive or transform until ~50-45 Ma ago, where subduction resumed as Australia started to move northward. The Indo-Australian oceanic crust thus subducted northeastward from Sumatra to Halmahera along a ~3000-km long former trench, abandoned 45 Myr before, after the docking of an arc terrane. According to van der Meer et al. (2018), the Sunda slab reaches the base of the upper mantle but does not connect with deeper anomalies. It is disconnected from the Burma slab to the north and possibly contiguous with the Banda slab to the east. Later, Zahirovic et al. (2014) refined the motions of India and Australia, thanks to an update of magnetic anomaly data. Their model confirms the cessation of the Sunda subduction but only during 10 Myr from 75 and 65 Ma. They argue that their model better fits some geological data such as continuous calc-alcaline and shoshonitic volcanic products, from Aceh to Lampung, whose ages range from ~63 Ma to recent times (Bellon et al., 2004). The predicted age of the subducting oceanic crust varies from ~70 to ~10 Ma from north to south and the convergence rate is incredibly fast (~15 cm/yr) in Zahirovic et al. (2014)'s reconstructions.

Banda (including Seram)

As a result of the collision between Sulawesi and the Kolonodale microcontinent, the Java-Sumatra SZ propagated east at about 15 Ma along the ocean-continent transition allowing the oceanic crust that opened west of New Guinea in Jurassic to Early Cretaceous times - also called Banda embayment - for subducting northward (Rangin et al., 1999; Hall, 2012). Volcanic activity on Wetar Island related to this new subduction started at ~12 Ma (Abbott and Chamalaun, 1981). The Banda Trench s.s. runs from Sumba to the Bird's Head western Peninsula of New Guinea. Some authors (e.g., van der Meer et al., 2018) consider that the Banda slab has a cusp shape and is continuous with the Seram slab since their lengths are equivalent, i.e., 675 km. Opposingly, Hinschberger et al. (2005) suggest that the Seram subduction zone initiated 9 Ma ago along a paleo-transform at right-angle from the Banda subduction which recently became less and less active as the northern Australia continental platform clogged the plate interface, transferring the convergence into the backarc (Nugroho et al., 2009, see section 3.1). The Seram SZ, still active, is supposed to have consumed a hypothetical "Timor-Seram" ocean (Linthout et al., 1997). Slab breakoff is recorded at 4 Ma and the last evidence of Banda arc volcanism is dated to 3.3 Ma (Ely et al., 2011; Zhou et al., 2018).

Owen

The Owen Fracture Zone is a large-offset fracture zone (~300 km) between a Paleocene oceanic crust on the east and a poorly constrained Late Jurassic to Eocene oceanic crust on the west (Fournier et al., 2011). As such, it was supposed to be prone to initiate a new SZ (Gurnis et al., 2004). It exhibits mantle peridotites along steep scarps attesting for tectonic uplift (Bonatti, 1978) that probably occurred after the initiation of seafloor spreading in the Gulf of Aden about 20 Ma ago (Fournier et al., 2010). Coast Range Ophiolite in California shares the same petrological characteristics and was interpreted by Choi et al. (2008) as a relic of a large-offset fracture zone along which the proto-Franciscan subduction initiated. Johnston et al. (2011) have examined the normal compressive stress in magnitude and direction near many large-offset fracture zones and they concluded that most of these regions including the Owen FZ are not associated with enough far-field compressive stress and thus could not evolve into incipient subduction. Indeed, a detailed survey of the Owen Fracture Zone in 2009 has revealed a 800-km long system of ridges (~2000 m higher than surrounding seafloor) and troughs between the Sheba Ridge and the Gulf of Aden (Fournier et al., 2011). Since ~3-6 Ma, the plate boundary runs in the troughs with strike-slip fault segments separated by releasing and restraining bends outlining a small circle centered on the Arabia-India pole of rotation (Fournier et al., 2011). A 90-km long, 35-km wide pull-apart basin flanks the Owen Ridge near 20°N (Rodriguez et al., 2013). Minor compressional structures and folds are observed adjacent to restraining bends (Fournier et al., 2011) but nothing indicates a subduction initiation process there.

3.8. Scotia area

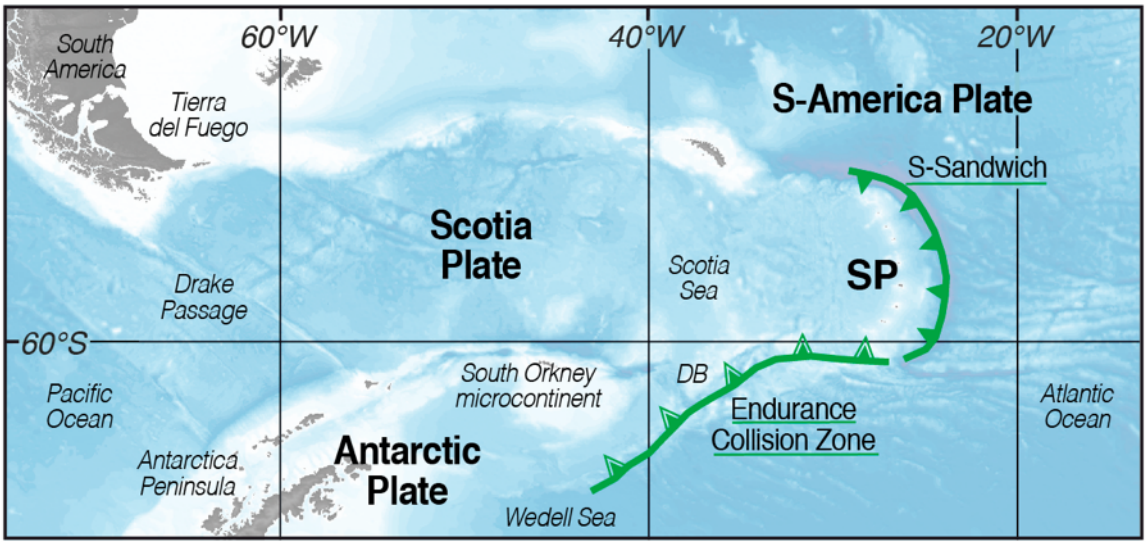

Fig.11: Map of Cenozoic SISs in the Scotia Sea region. See the legend in Fig.4. DB: Discovery Bank, SP: Sandwich Plate.

Endurance Collision Zone

During Paleogene, the Drake Passage between South America and Antarctica continents opened a gate between the Pacific and the Atlantic oceans not only at shallow levels with the break-up of the land bridge allowing the water masses to circulate (Livermore et al., 2005; Lagabrielle et al., 2009; Maldonado et al., 2014), but also at deeper levels in the asthenosphere allowing the Pacific upper mantle to invade the Atlantic area (Shemenda & Grokhol'skiy, 1986; Shemenda, 1994; Barker, 2001, Fig.11). The first record of a northeast-vergent SI of the Atlantic crust (Weddell Sea) beneath the continental land bridge, called Osmond Land composed of the South Orkney microcontinent and other continental blocks, is dated prior to 55 Ma (van der Meer et al., 2018). The age for the onset of subduction with an active Scotia slab is supposed to coincide with the onset of extension in Tierra del Fuego (Ghiglione et al., 2008), i.e., between 55 and 45 Ma. The passive margin southwest of the Osmond Land was probably inverted following a change in South-American - Antarctic plate motion from north- to northwest-directed around ~70-65 Ma (Barker et al., 1991; Eagles, 2010). One may notice the presence of two spreading centers that might have eased the SI process: one off the southern termination of the incipient trench within the subducting plate with a transform connecting the spreading center to the trench, and another on the Pacific side where the Phoenix-Penas active ridge was subducting beneath the Scotia Sea (Scalabrino et al., 2009; Vérard et al., 2012). Such a geodynamic setting might have weakened the overriding plate by asthenospheric upwelling above a slab window. This section of the Endurance Collision Zone became inactive about 10 Ma ago as the Weddell Sea spreading ridge subducted and the slab broke (Eagles & Jokat, 2014).

South Sandwich

The South Sandwich margin results from the lateral propagation of the Endurance Collision Zone northward prior to 33 Ma as 29-33 Ma calc-alkaline volcanism was erupting north of Discovery Bank (Barker, 1995; Livermore et al., 1994; Eagles & Jokat, 2014). Van de Lagemaat et al. (2021) recently revised the chronology with a slow onset of the Endurance SZ as early as ~80 Ma ago, followed, ~10 to 30 Myr after, by the

delamination of the South American continental lithosphere, leading to its northward lateral propagation at the origin of the South Sandwich SZ. The normal component of convergence allows significant lithosphere subduction only since 50 Ma, when the absolute plate motion of South America changed from south to west-northwest (van de Lagemaat et al., 2021). Eagles (2010) invoked the presence of a Mesozoic fracture zone that might have facilitated the lateral propagation but it could have also been a passive margin in the continuation of those that have been reactivated along the Endurance Collision Zone 20 Myr earlier. The triggering factor for such lengthening of the trench (from 700 to 1500 km) by lateral propagation of the SZ might have come from mantle flow as suggested by Eagles & Jokat (2014). As mentioned in the previous section (Endurance Collision Zone), the break-up of the long-lived continuous east-directed slab from the Andes to the Antarctica Peninsula during Paleogene has allowed the confined sub-Pacific upper mantle to escape toward the east (Shemenda & Grokhol'skiy, 1986; Shemenda, 1994; Lallemand, 1998; Barker, 2001). Such mantle flow probably favored the rollback of the west-dipping slab beneath the Endurance Collision Zone subduction, as well as the downwelling of the sub-Atlantic mantle dragged by the slab. Today, the trench is limited to the South Sandwich section (800 km long) as the Atlantic crust stopped subducting at the Endurance Collision zone about 10 Ma ago.

4. Toward a comprehensive classification of subduction initiation sites

Classifying the SI modes is a challenge because settings, processes and deformation modes are generally associated like for example "spontaneous or forced subduction by conversion of a TF" (Dickinson & Seely, 1979; Karig, 1982; Stern, 2004; Gerya, 2011; Stern & Gerya, 2018). To overcome this complexity, we successively examine each situation based on the geodynamic setting, the driving processes and the deformation style, although all aspects are relevant to describe the context of any candidate area.

4.1. Classification based on geodynamic settings

In terms of rheological discontinuities, a distinction should be made between domains setting at the transition between a continent, a plateau or an arc and an ocean, hereafter called: ocean transition (OT) and intra-oceanic domains far from an OT (Fig.12, see glossary in section 2). However, whatever the distance from the OT, the deformation always localizes along weak zones inherited from the crustal fabric, tectonic or magmatic history (Cloetingh et al., 1982).

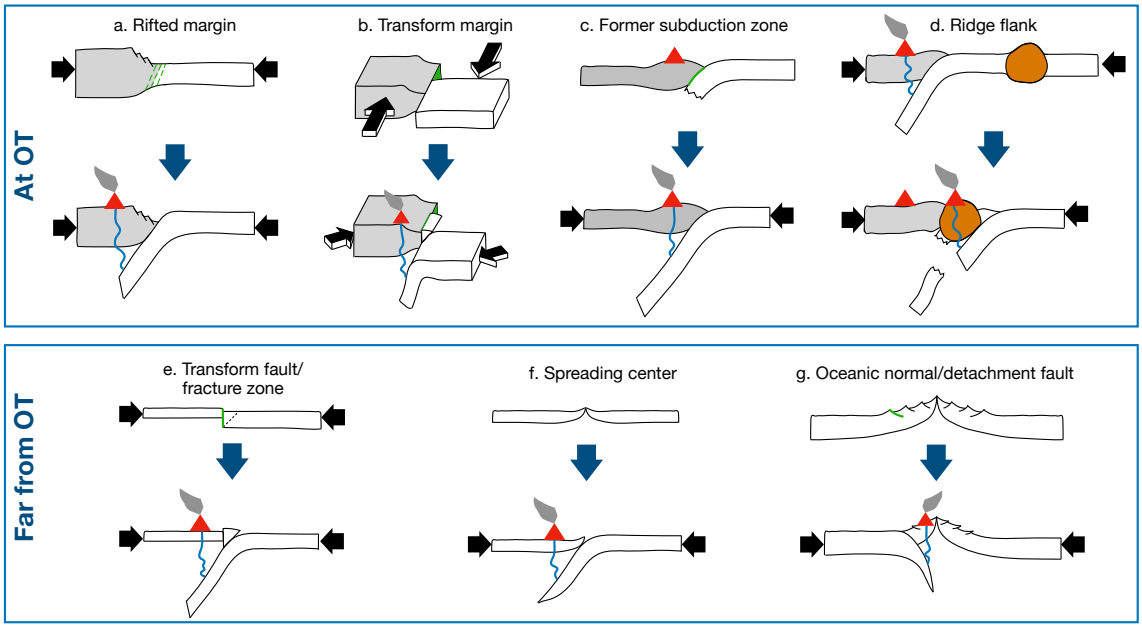

Fig.12: Schematic representation of geodynamic settings where subduction has initiated, either close to an ocean-continent/plateau/arc transition (OT, top row), or far away from it (bottom row). Grey domains represent tectonic plates different from typical oceanic lithospheres such as a continent, a former volcanic arc, or an oceanic plateau. The brown feature in panel (d) represents a geological structure unable to subduct, such as a buoyant oceanic (aseismic) ridge. For other legend details see Figs.1 & 3 captions.

4.1.1. At an oceanic transition (OT)

In this study, we extrapolate the notion of ocean-continent transition (OCT) to the juxtaposition of an oceanic lithosphere with any buoyant feature such as a continental lithosphere, an oceanic plateau, an aseismic ridge or a volcanic arc (grey and brown patterns in Fig.12). Note that “spreading ridges” are excluded from our definition of oceanic transition (OT). We then distinguish four main settings.

4.1.1.1. Rifted margin

Passive or rifted margin represent the most frequently observed setting for SZ initiation. A typical example is provided by the North Iberian (Cantabrian) margin which underwent successive tectonic regimes of rifting, passive and finally active margin (Gallastegui et al., 2002). Based on seismic imagery, the authors suggest that a Mesozoic extensional detachment was reactivated into a thrust during the Upper Eocene. Plate convergence stopped in the mid-Miocene after less than 90 km of shortening, freezing the initial stages of tectonic inversion of a passive margin. In the absence of an initial detachment fault, whose geometry likely fits with a subduction plane, normal faults of the rifted margin may be tectonically inverted as seen along the eastern margin of the Japan Sea (Okamura et al., 1995, Fig.4). The region where the normal faults were recently reactivated into reverse ones is now considered as a case of incipient-diffuse SI, whereas the Cantabrian margin reached the stage of incipient-localized SI before aborting in the Early Miocene (see sections 3.1 & 3.5).

4.1.1.2. Transform margin (including ocean-continent STEP fault)

Intrinsically, transform margins have narrower transitional areas between oceanic and continental lithospheres making them, a priori, more prone to be destabilized under a tectonic or gravitational stress (Boutelier and Beckett, 2018). The Owen transform plate boundary for example (Fig.10) is subject to an important vertical deformation since the Pliocene but its kinematics is purely strike-slip (Fournier et al., 2011). Today, the 1200 km long left-lateral Philippine Fault cutting through the main islands of the Philippine Archipelago (Fig.4) is still active (Yu et al., 2013). Plate reconstructions indicate that another major shear zone was active offshore west of the archipelago, known as the Philippine mobile belt, including Cathaysian continental slivers, during Eocene-Oligocene time (Rangin et al., 1990; Shao et al., 2015; Huang et al., 2019; Qian et al., 2021). This major shear zone is supposed to have accommodated, to the east, the N-S opening of several marginal basins such as the Celebes Basin, the Sulu Basin and the South China Sea (Rangin et al., 1990). It also accommodated the drift of the Philippine Sea Plate with respect to the Eurasia Plate during part of the Cenozoic (Wu et al., 2016). Compression across this transform margin occurred during the Miocene, resulting in the eastward subduction of all these basins.
Some transform margins result from the propagation of a subduction-transform boundary at their edge (STEP fault) above a retreating subducting slab (Govers and Wortel, 2005). They potentially represent excellent candidates for SI compared with regular transform margins by reason of the weakening of the continental plate as the STEP fault propagates, which may strongly enhance localization and further oceanic subduction (Baes et al., 2011). Such contexts may apply, for example, to the Northern Maghrebides or the Southern Caribbeans (see sections 3.4 & 3.6 and Figs.7 & 9, Levander et al., 2014).

4.1.1.3. Former subduction zone

Former subduction zones can potentially cease to be active for a period and then resume. Based on the record of arc volcanism, a few subduction zones are known to have switched between periods of activity and quiescence. Cessation of volcanic activity for long periods may occur either because characteristics of the subduction change like slab flattening (Gutscher et al., 2000) or backarc spreading (Magni, 2019) or simply because the plate convergence changes in azimuth or magnitude. This might happen along the Central Ryukyus - Nankai subduction system (Fig.4) during the Cenozoic as suggested by Kimura et al. (2014). The eastern border of mainland China including the continental platform showed various episodes of arc volcanism alternating with quiescent periods. Focusing on the recent times, a gap in central and northern Ryukyus arc volcanism was interpreted as an episode of slab break-off and cessation of subduction for a few Myrs, followed by the resumption of the activity since about 8 Ma (Lallemand et al., 2001; Faccenna et al., 2018). Similarly, Sutherland (1995) or Gurnis et al. (2004) suggested that the Tonga-Kermadec subduction (Fig.5) initiated along the Gondwana subduction boundary inferred to have ceased during the Cretaceous period. Subduction of the Tethys Ocean beneath Indonesia ceased at 90 Ma following the collision between the Woyla intra-oceanic arc and the Sumatra margin (Hall, 2012). It resumed ~45 Myr later as the Australia plate moved faster to the north.

4.1.1.4. Ridge flank

Terrane accretion is often interpreted as the result of a jump of subduction from a position on the foreside of a buoyant feature (microcontinent, plateau or ridge) carried by an oceanic plate, to its backside. A typical example is illustrated by the Caribbean Plateau which has been partly accreted to the NW corner of South America during the Paleogene as the Caribbean Plate (Fig.7) moved eastward through the seaway between the North and South America plates (Pindell & Kennan, 2001; Kroehler et al., 2011). To be considered as a new subduction, the whole lithosphere carrying the buoyant feature needs to be accreted, not only the crustal layer. This happened with the docked Choco Block forming the western cordillera of Colombia to which the slab is still attached (Taboada et al., 2000). The failure here possibly occurred in an area of a thinner plateau as suggested by Sanchez et al. (2019).

4.1.2. Far from an oceanic transition (OT)

4.1.2.1. Transform fault / fracture zone (including oceanic STEP fault)

Oceanic TFs, either active or fossil (fracture zones), are likely weak lithospheric features prone to localize deformation when stressed as seen in section 3.5 with the Fifteen Twenty, Marathon and Vema fracture zones (Pichot et al., 2012) or the Saint Paul fracture zone (Maia et al., 2016) which are all subject to vertical motions since mid-Miocene caused by small plate kinematic changes (Fig.8). Many examples of TFs or fracture zones exist which were used as guides for SI during the Cenozoic (Table 2). The most cited example of a TF which turned in the Early Eocene into a SZ is the Izu-Bonin-Mariana Trench (e.g., Uyeda and Ben Avraham, 1972, Fig.4). Similarly with section 4.1.1.2, STEP faults may develop in intra-oceanic domains and may serve as locus for SI if compression occurs across the transform plate boundary like in the Matthew & Hunter region (Patriat et al., 2015).

4.1.2.2. Spreading center

Spreading centers are among the weakest features at the surface of the Earth where subduction may initiate (Gurnis et al., 2004). They are supposed to represent diverging motion between plates, not converging ones. Furthermore, a second problem arises which is the buoyancy of the very young lithosphere that may oppose subduction (Mueller & Phillips, 1991). This appears to be not a hindrance to SI if a far-field force rises as demonstrated by Keenan et al. (2016) in Palawan (Philippines, Fig.4) with SI along the former spreading center of the Proto-South China Sea around 34 Ma as a result of the India-Asia collision transmitted along the Red River Fault. Another Cenozoic case of SI along a former spreading center is given by the Macquarie Ridge Complex (Fig.5) south of New Zealand (Gurnis et al., 2004) but, before being inverted into a SZ during the Miocene, the spreading center has been turned into a strike-slip boundary for millions of years (Lebrun et al., 2003).

4.1.2.3. Oceanic normal/detachment fault

Such geodynamic context has been used to explain the emplacement of the Jurassic ophiolites in Albania and Greece along a ridge-parallel detachment fault in the western Neotethys (Maffione et al., 2015; Maffione and van Hinsbergen, 2018). There are only a few Cenozoic examples of reactivation of well-oriented oceanic normal paleofaults into reverse ones far from any ocean-continent transition. We could mention the Central

Indian Basin around the Afanasy Nikitin Chain south of Ceylan (Delescluse and Chamot-Rooke, 2007, Fig.10). Based on the observation of heat-flow in excess in the deformed area together with thermal modeling, Delescluse and Chamot-Rooke (2008) have shown that vigorous hydrothermal circulation closely followed the onset of deformation around ~9 Ma triggering exothermic serpentinization reactions at Moho depths. Densely spaced faults were soon abandoned around ~7 Ma while deformation localized onto fewer faults with larger spacing (Delescluse et al., 2008). However, it cannot be excluded that SI cases known as originating from spreading centers have started on intra-oceanic detachment faults.

4.2. Classification based on triggers

Another way to characterize SI may focus on the forcings responsible for strain localization which may be expressed through various modes. We distinguish here the forcings transmitted within the lithosphere from those originating from the mantle (Fig. 13). In some specific cases, the SI trigger is deemed to come locally from the lithospheric structures themselves (e.g., sedimentary loading).

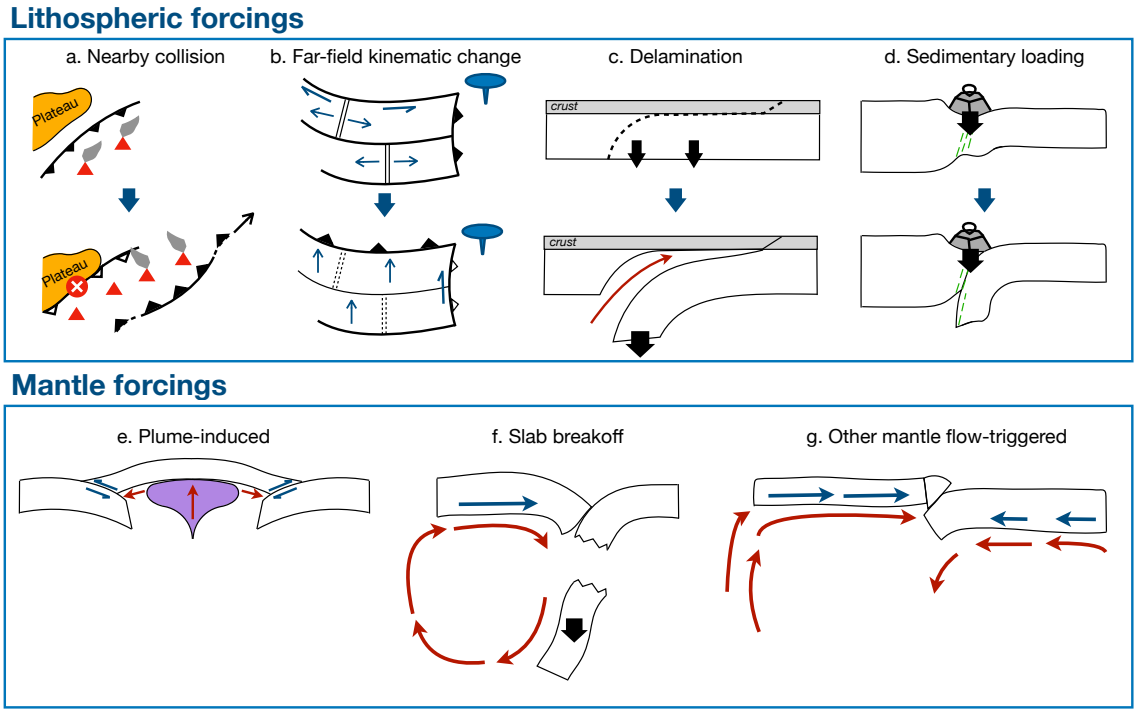

Fig.13: Schematic representation of engines driving SI, originating from lithospheric (top row) and mantle processes (bottom row). The black, blue and red arrows represent lithospheric forces, lithospheric motions and mantle flows, respectively. The damaged and weakened zones are represented in green. Smoking/non-smoking volcanoes symbolize active and extinct subduction magmatism.

4.2.1. Lithospheric forcing

4.2.1.1. Local or nearby collision

We show in section 3 that numerous SISs occurred in collisional settings during the Cenozoic, making collision one of the two major triggers together with far-field kinematic

change. The collision of the Ontong-Java Plateau with the Melanesian-Vitiaz Arc during Miocene triggered for example the flip of the convergence from south-directed Pacific plate (Vitiaz) subduction to the north-directed Australian plate (New Hebrides-San Cristobal - New Britain) subduction during Miocene (Mann & Taira, 2004, Fig.5). Similarly, the Australian platform started to collide with the Sunda Arc and was responsible for incipient south-directed subduction of the Flores and S-Banda basins beneath the Sunda Arc since Middle and Late Miocene respectively (Silver et al., 1983; Hinschberger et al., 2001, 2005). Sometimes, a distant collision may change one plate kinematics and thus create the conditions for local convergence. The resistance of the India plate colliding with Eurasia creates for example, the conditions for N-S compression within the Central Indian Ocean (Fig.10) which may favor SI in a near future (Cloetingh et al., 1989).

4.2.1.2. Far-field kinematic change

Far-field kinematic change is often invoked to explain a sudden change in regional stress in the absence of a local trigger. The Pleistocene shortening across the eastern margin of the Japan Sea (Fig.4) has been attributed to a change in the Amurian plate kinematics in response to the India-Eurasia collision thousands of kilometers away (Lallemand and Jolivet, 1985). The change in the Pacific-Australia rotation pole from Oligocene to Middle Miocene modified the relative motion across the Macquarie Ridge Complex from strike-slip to transpression (Lamarche et al., 1997), giving rise to the Puysegur and Hjort trenches (Fig.5).

4.1.2.3. Delamination

Another mechanism, namely delamination, is more difficult to detect because it concerns the deep inaccessible layers of the lithosphere. Sub-horizontal delamination of the mantle layer of an oceanic lithosphere may be facilitated by serpentinization of the uppermost mantle when lying above a dehydrating subducting slab along the Zenisu Ridge off Nankai or the eastern coast of Taiwan (Lallemand, 2014, Fig.4). Other mechanisms of delamination of transpressional regions at an OCT, based on seismic imagery and/or geochemical constraints from magmatic records, were described. It may result from the propagation of a STEP fault, localized at the transition between a continent and an ocean when subjected to compressive stress. Such geodynamic context is observed south and north of the Alboran basin in the Mediterranean Sea (Duggen et al., 2005, Fig.8) and south of the Grenada Basin beneath the northern Venezuelan margin (Fig.7). The STEP fault follows the slab as it rolls back but the tear within the overriding plate doesn't break through the whole lithosphere. Instead of that, it only cuts through the upper crustal section and then propagates horizontally within the lower crust of the plate. As a consequence, the slab, which is still attached to the continental mantle, drags it to depths causing its delamination (Levander et al., 2014). Under compressive stress, the weakened ocean-continent transition is then prone to host a new subduction (Hamai et al., 2015; d'Acremont et al., 2020). A singular mechanism of delamination has recently been proposed by Duarte et al. (2019) beneath the Horseshoe Abyssal Plain off SW Iberia (Fig.8). Based on tomographic models imaging a fast-velocity anomaly extending down to 250 km beneath the basin, parallel to the Azores-Gibraltar transpressional plate boundary, the authors suggest that the old Jurassic lithospheric mantle delaminates between two transform faults. 2-D numerical models indicate that delamination of an oceanic lithosphere is possible if the transform

faults as well as the uppermost mantle between them are weak enough. Since seismicity there is observed at depths larger than 50 km, it is hypothesized that the crust is made of highly altered basalts and water-rich sediment. They speculate that it can be the locus of a SI. Finally, Sutherland et al. (2010) proposed a dual mechanism of SI of the Tonga-Kermadec (Fig.5) during Eocene times as a combination of lower crust and mantle delamination beneath the New Caledonia Trough over a distance ≥ 300 km from the present-day trench connected at lithospheric mantle depths with the paleo-Gondwana subduction, extinct since Cretaceous. Such mechanism involves gravitational instability in which convergence caused lithospheric thickening east of Norfolk Ridge along a preserved weakness zone associated with the denser Gondwana slab.

4.1.2.4. Sedimentary loading

Sedimentary loading at passive margins has been invoked by several authors in the past to favor SI process by downflexing the adjacent oceanic lithosphere (Cloetingh et al., 1982; Faccenna et al., 1999) keeping in mind that gravitational stress may not be enough to trigger subduction (Mueller and Phillips, 1991). Southeast Asia hosted multiple stages of incipient, achieved or even self-sustained subduction during Cenozoic time, the initiation of which might have been enhanced by sediment loading (Hall, 2018). In all cases, deep oceanic basins, some of them very young, are juxtaposed with hot crust thickened by recent collision and/or arc activity along a narrow and steep margin leading to the following sequence of events : (1) slumping of the thick crust onto the oceanic crust along extensional detachments, (2) bending of the oceanic floor under the sedimentary load creating a depression which encourages (3) further margin's collapse and loading, (4) deeper continental/arc crust is progressively involved in the collapse, (5) extension in the upper plate may weaken it by thinning and heating, the depressed oceanic crust may transform into eclogite and ultimately (6) subduction initiates (Hall, 2018). The Sula Deep and Tolo Trough, located in the Late Miocene North Banda Sea (Fig.4), respectively illustrate stages (1) to (3) of the above sequence. The Cotobato and North Sulawesi Trenches reached more advanced stages (5) or even (6).

4.1.2.5. Lateral pressure gradient

As detailed in section 1.3 and depicted in Fig. 2, the horizontal density gradients at the proto-plate boundary may promote trench formation. This lateral density gradient between the two plates results from the differences in composition, thickness, and thermal structure associated with the age offset. Similarly, the topography differential between the two adjacent plates, isostatically compensated or not, yields a lateral pressure gradient that could favor SI. These pressure gradients are expected to take place in the vast majority of SISs and are likely to be generally checked. That is the reason why the horizontal offsets in density and topography are not listed with the other potential driving terms (Table 2) since we are basically aiming at identifying parameters varying from one SI event to another. One notable exception may nevertheless concern SISs occurring in the middle of a rather homogeneous lithosphere, at the incipient-diffuse SI stage where buckling is mainly occurring (see the discussion section 5.2), such as for the Tiburon/Barracuda FZ or the Central Indian Ocean (Figs. 4 & 10).

4.2.2. Mantle forcing

4.2.2.1. Plume-induced or spreading center-related

Hot buoyant mantle plume is a good candidate to trigger lithospheric instabilities (Ueda et al., 2008; Baes et al., 2020). Numerical models can reproduce single-slab or multi-slab subduction initiation under specific conditions like the age of the initial lithosphere or its rheological structure (Crameri and Tackley, 2016). The proximity of hot mantle plume from many SISs like Izu-Bonin-Mariana, Caribbeans or South China Sea challenges us (Ishizuka et al., 2013; Nerlich et al., 2014; Yu et al., 2018). Stern and Dumitru (2019) have recently proposed an alternative scenario to explain the presence of the Siletzia plateau terrane in the forearc of the Cascadia subduction zone (Fig.6). Instead of being emplaced by docking and jump of the SZ as proposed by Duncan (1982) or Wells et al. (2014), Stern and Dumitru (2019) argue for an in-situ rise of the Yellowstone plume as a source for the Siletzia Plateau, disrupting the former SZ in Paleocene, and triggering a lithospheric collapse along its western margin to form the modern Cascadia SZ. Prior to Cascadia, Whattam and Stern (2015) have proposed that the Central America, NW South America and the Leeward Antilles SZs (Fig.7) nucleated along the southern and western margins of the Caribbean Large Igneous Province (CLIP) during Late Cretaceous (~100 Ma). Recently, van Hinsbergen et al. (2021) argued that plumes may induce large plate rotation which, in turn, may initiate divergent or convergent plate boundaries far away from the plume head. They support their concept using torque balance modeling applied to the Indian and Africa cratons and the initiation of a ~12000 km long intra-oceanic subduction zone across the Cretaceous Neotethys. There, the pre-Deccan plume push is efficient because of the presence of deep cratonic keels beneath the cratons and at the end, the subsequent change in plate kinematics would be responsible for SI (Rodriguez et al., 2021). However, Perez-Diaz et al. (2020) discuss an error in the coincidence of the respective ages between the Deccan flood basalt eruption and the acceleration of the Indo-Atlantic plate as well as the brevity of the event, questioning the driving role of the plume. During the Cenozoic, many SZs started close to mantle plumes or spreading centers (see Table 2), but we rather consider that they represent a weakening factor for the lithosphere that may lead to SI along lithospheric discontinuities when combined with tectonic stresses in a modern Earth. Indeed, plume-induced subduction might happen on Venus or in the Archean Earth (Ueda et al., 2008; Gerya et al., 2015; Baes et al., 2016; Davaille et al., 2017; Smrekar et al., 2018) but is less probable in a cold Earth.

4.2.2.2. Slab breakoff-triggered

Slab breakoff may be a way to generate either a downward suction flow or an upward return flow depending on where the overlying target lithosphere is located. Contributions of slab breakoff to the process of SI may be examined in several places. The detachment of the Izanagi slab beneath East Asia margin during Paleocene is thought to have changed not only plate-driven forces such as slab pull, but it also affected the sub-

Pacific and sub-East Asia mantle flow (Whittaker et al., 2007; Zahirovic et al., 2014). Moreover, it could have generated diffuse shortening across the region accommodating the transform motion between the Mesozoic composite proto-PSP and the Pacific oceanic plate and thus triggered the formation of the new Izu-Bonin-Mariana SZ (Lallemand, 2016a, Fig.4). Beneath East Taiwan, the synchroneity between Eurasia slab breakoff (Lallemand et al., 2001) and incipient subduction (Lallemand et al., 2013) is intriguing as well as those along the North-Maghrebides between the Africa slab breakoff propagating from west to east during the last 11 Myr and the flip of subduction which occurred concomitantly across the arc with a delay of 2 to 3 Myr (Faccenna et al., 2004; Spakman and Wortel, 2004; Billi et al., 2011; Garzanti et al., 2018). Such a geodynamic sequence needs further exploration and modeling to be fully understood and to prove (or disprove) that there may be a causal link between these two processes.

4.2.2.3. Other mantle-flow-triggered

More generally, the regions undergoing SI are often characterized by complex 3-D mantle-flows at onset. This is especially the case at the edges of slabs where both horizontal (toroidal) and vertical (poloidal) flows are observed (e.g., Faccenna et al., 2014; Lin and Kuo, 2016; Kiraly et al., 2017). Secondary (“small-scale”) convection at the base of the lithosphere is unlikely to lead to plate failure and subduction under usual conditions, as this would require that the maximum stresses available to break the lithospheric lid be extremely low (a few MPa to at most ~30 MPa, Solomatov, 2004a,b; Wong and Solomatov 2015, 2016; Crameri and Tackley, 2016; Patočka et al., 2019), but the question is "Is mantle flow enough to trigger a new subduction ?". Baes & Sobolev (2017) and Baes et al. (2018) support the idea that subduction nucleation along passive margins or TFs is theoretically possible by means of nearby vigorous downward mantle flows. In the case of a passive margin, it should be a long-term process (tens of Myr), only under the mantle flow effect if a number of conditions are fulfilled such as an appropriate magnitude, location and domain size of the mantle suction flow, strength of the crust and mantle near the margin and topographic gradient. Argentina and US East Coast margins are the two better candidates for subduction initiation in a few tens of Myrs. According to them, these two sites are places at the stage of incipient-diffuse SI. Following Baes et al. (2018), mantle suction at TFs may come from nearby SZs or avalanches of slab remnants of former SZs but since one of the two adjacent lithospheres has to be very young, the proximity of a spreading center is also required. They suggest that Cenozoic examples of SI at TFs satisfying the conditions for mantle flow triggering are the South Sandwich and Tonga-Kermadec. Strong mantle upwellings, driven by a high thermal anomaly, were also shown to generate a basal dragging/pushing of the lithosphere, leading to SI if deformation localisation is favored (Lu et al., 2015). Based on kinematic reconstructions, Collins (2003) has shown that most SZs distribute around two cells (Pangean and Panthalassan) with about the same pattern since > 450 Ma, emphasizing the role played by mantle convection. Basin inversion and marine transgression have been described by Hall and Morley (2004) in southern Sundaland. Based on plate reconstructions and modeling, Yang et al. (2016) suggest that a wide slab stagnating in the transition zone beneath Southeast Asia before the Miocene began to penetrate through the 660 km boundary and finally produced a slab avalanche. This avalanche induced a strong downwelling mantle flow and Sundaland experienced broadscale compression and dynamic subsidence. Similarly, the mantle flows induced by avalanches of old slabs lying within the transition zone could

have helped polarity reversal and plate reorganisation in the New Hebrides region (Pysklywec et al., 2003) provided suitable mechanical conditions.

4.3. Geodynamic setting vs trigger SIS classification

Among the various criteria characterizing SI, we decided to cross four of them as illustrated in Table 2:

- Which type of geodynamic setting at the time of initiation: at or near an OT
- Which forcing or combination of forcings governed the initiation: lithospheric vs mantle?
- Which stage has been reached during the initiation process: incipient-diffuse, incipient-localized, achieved, or self-sustained?
- Which is the current state of the subduction: active, prematurely stopped (aborted) or stopped at a mature stage (extinct)?

			Triggers						
			Lithospheric forcing				Mantle forcing		
		SI forcings → / ↓ SI settings	Local or nearby collision	Far-field kinematic change	Delamination	Sedimentary loading	Plume- or SC-induced	Slab breakoff - triggered	Other mantle flow - triggered
Geodynamic settings	At OT	Rifted margin (including rear-arc)	Proto-Kamtchatka, Kuril, S-Ryukyus, Zenisu, Taiwan E-coast, Philippines, Flores, Wetar, Sula, Sulu, N-Sulawesi, Tolo, Sangihe, Halmahera, N-Melanesian, Vitiaz, New Britain-San Cristobal (incl. S-Solomon), Trobriand, New Hebrides, Ambrym (incl. Pentecost-Maeowo), S-Caribbeans, W-Mediterranean, Gibraltar, Calabria, N-Maghrebides (Alboran to Sicily)	E-Japan Sea, S-Ryukyus, NW-Borneo - Cagayan, Pocklington, New Britain-San Cristobal (incl. S-Solomon), Trobriand, New Hebrides, Loyalty - Three Kings, N-Iberia, SW Iberia (incl. Gorringe), Endurance Collision Zone	S-Caribbeans, SW Iberia (incl. Gorringe), N-Maghrebides (Alboran to Sicily)	Philippines, Sula, N-Sulawesi, Tolo	Pocklington	Taiwan E-coast, N-Melanesian, N-Maghrebides (Alboran to Sicily)	E-Japan Sea, NW-Borneo - Cagayan, Sangihe, Halmahera, New Hebrides, Endurance Collision Zone, Gibraltar, Calabria
		Transform margin (including ocean-continent STEP fault)	S-Ryukyus, Zenisu, Gagua - E-Luzon Trough, Manila, Philippines, Sula, Sangihe, Halmahera, Banda (incl. Seram), S-Caribbeans, Muertos, Puerto-Rico, Nicaragua Rise, Carpathians, W-Mediterranean, Gibraltar, Calabria, N-Maghrebides (Alboran to Sicily)	E-Japan Sea, S-Ryukyus, Gagua - E-Luzon Trough, Manila, Negros, Cotobato, NW-Borneo - Cagayan, Tonga-Kermadec, Puysegur, Puerto-Rico, SW Iberia (incl. Gorringe)	Tonga-Kermadec, S-Caribbeans, SW Iberia (incl. Gorringe), N-Maghrebides (Alboran to Sicily)	Cotobato, Philippines, Sula, Tonga-Kermadec	Manila, Negros, Tonga-Kermadec	Puerto-Rico, N-Maghrebides (Alboran to Sicily)	E-Japan Sea, NW-Borneo - Cagayan, Sangihe, Halmahera, Tonga-Kermadec, Gibraltar, Calabria
		Former subduction zone	Komandorsky, Kamtchatka, Cascadia, New Britain-San Cristobal (incl. S-Solomon), New Hebrides, Sumatra-Java, Banda (incl. Seram)	Ryukyus-Nankai, New Britain-San Cristobal (incl. S-Solomon), New Hebrides, Tonga-Kermadec	Tonga-Kermadec	Tonga-Kermadec	Cascadia, Tonga-Kermadec	Ryukyus-Nankai	New Hebrides, Tonga-Kermadec
		Ridge flank (terrane)	Cascadia, N-Solomon, S-Caribbeans, N-Panama, Muertos, Nicaragua Rise, Beata Ridge				Cascadia		
	Far from OT	Transform fault / Fracture zone (including oceanic STEP fault)	C- & W-Aleutians, Bowers Ridge, Gagua - E-Luzon Trough, Yap, Mussau, Samoa-Gilbert-Ralik, Matthew & Hunter, Carpathians	Gagua - E-Luzon Trough, Izu-Bonin-Mariana, Yap, Palau, Lyra, Mussau, Samoa-Gilbert-Ralik, Matthew & Hunter, d'Entrecasteaux, Tonga-Kermadec, Puysegur, McDougall, Macquarie, Hjort, Saint Paul, Romanche, Barracuda, Tiburon, S-Sandwich	Samoa-Gilbert-Ralik, Tonga-Kermadec, S-Sandwich	Tonga-Kermadec	Izu-Bonin-Mariana, Yap, Palau, Lyra, Musseau, Matthew & Hunter, Tonga-Kermadec, Saint Paul	Izu-Bonin-Mariana	Tonga-Kermadec, S-Sandwich
		Spreading center	C- & W-Aleutians, Bowers Ridge, Yap, Cascadia	NW-Borneo - Cagayan, Yap, Loyalty - Three Kings, Puysegur, McDougall, Macquarie, Hjort, Endurance Collision Zone			Yap, Cascadia		NW-Borneo - Cagayan, Endurance Collision Zone
		Oceanic normal fault (incl. detachment fault)	C-Indian Ocean, Beata Ridge, W-Mediterranean						
			SI reached stage : incipient-diffuse, incipient-localized, achieved, self-sustained Present SZ status : active, aborted (when self-sustained stage was never reached), extinct						

Table 2 : Classification of areas where a SZ was initiated during the Cenozoic. Lines indicate the geodynamic setting at the time of subduction initiation. STEP = Subduction-Transform Edge Propagator; OT = Ocean-Continent/Plateau/Arc Transition. Columns list the subduction triggers at initiation sorted in two groups depending on whether the driving forces are lithospheric or originate from the mantle. SC = Spreading Center. Note that some SZs satisfy several settings or triggers either because there were multiple settings or triggers acting simultaneously or because initial settings or triggers are debated (see question marks in the supplementary Table). Colors indicate the SI stage reached by the system (see legend at the bottom of the table). If SI stops before reaching stage 4 = self-sustained, we consider that the process aborts, the name of the SZ is then underlined. If SI succeeds in reaching stage 4 and that subduction later stops, we consider that the SZis extinct; the name of the SZ is then double-underlined.

Such classification has the advantage of enabling combinations of settings and forcings, keeping the present state (underlining) and reached stage (color-coded fonts) unique and visible. A single SZ may thus appear in multiple boxes either because there were multiple involved settings or triggers acting simultaneously or because initial settings or triggers are debated. Indeed, it often appears that authors do not reach a consensus. In this case, we mention all interpretations except if we judge them too speculative, or if new data allow us to exclude some of them. In the supplementary Table, we specify our opinion on various authors' interpretations using question marks but here, we consider all interpretations equally. The implications that can be inferred from this way of SI classifying will be detailed in section 4.6.

4.4. Classification based on deformation

The above classification gives a brief glimpse of each SIS but fails to address the real nature of the deformation at the time of initiation. Hereafter, we aim to clarify the modes and spatial expression of the deformation (Fig. 14) even though it is sometimes difficult to decipher between various interpretations.

4.4.1 Deformation modes

4.4.1.1. Change in fault kinematics

Strain localization during the process of subduction initiation generally occurs along inherited crustal or lithospheric faults regardless of their type. Tectonic inversion of former normal, strike-slip, transform or STEP faults or even former axial rifts represents the dominant mode of SI (see sections 4.4.2.5, 4.4.2.6, 4.4.2.7 & 4.6.7).

4.4.1.2. Same fault kinematics

Changes in plate motion or driving forces may interrupt subduction for several Myr and then start again reactivating the same plate interface.

4.4.1.3. Fault neoformation

In the context of paleo-subduction initiation, it is difficult to prove a posteriori that a fault was neoformed but, in theory, we cannot exclude this situation. Most of the examples cited in this study for which we mention the possibility of new plate boundary formation, i.e., in the absence of previously known structural discontinuity, may not have been neoformed. It just means that we have no idea about the initial mechanical state of the lithosphere at the time of SI.

4.4.2 Deformation spatial expression

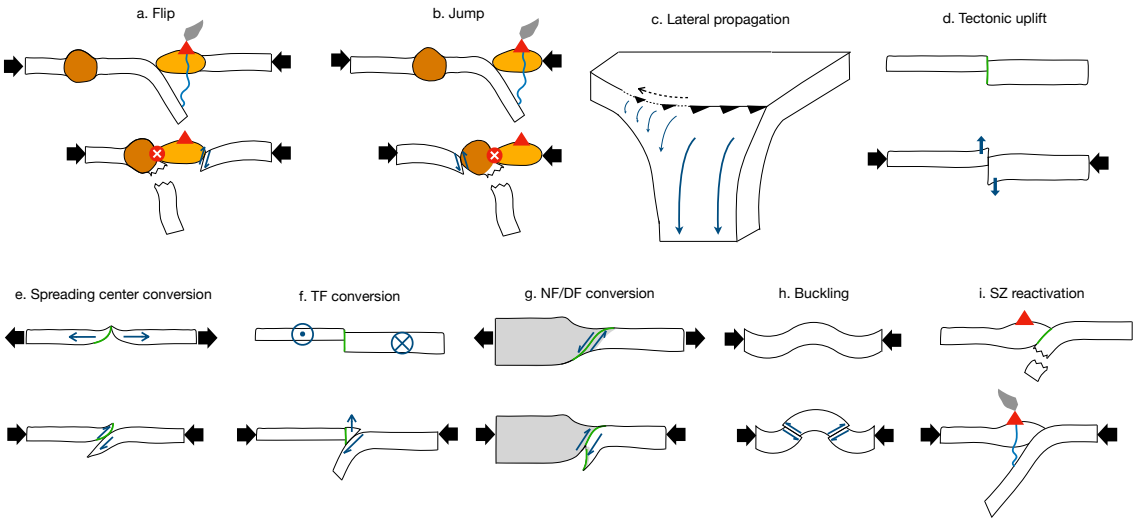

Fig.14: Simplified representations of the different deformation modes (deformation spatial expression) occurring as subduction initiates. The black and blue arrows represent lithospheric forces and motions, respectively. Weak zones are represented in green. Smoking/non-smoking volcanoes symbolize active and extinct subduction magmatism. The orange and brown domains depict an arc lithosphere and a buoyant structure unable to subduct. TF = transform fault; NF/DF = normal fault or detachment fault; SZ = subduction zone.

4.4.2.1. Flip

In this paper, we name flip any subduction polarity reversal across a subduction arc system. This widespread mechanism of SI often results from the collision of a buoyant feature: (micro)continent or plateau with an arc (Dickinson and Seely, 1979; Mitchell, 1984) which increases the compressive stresses in the overriding plate up to failure, that localizes in the arc lithosphere where the upper plate is the weakest (Chemenda et al., 1997). Based on numerical models, Baes et al. (2011) have shown for example that the mantle wedge should be at least one order of magnitude weaker than the average viscosity of the lithosphere for subduction polarity reversal to proceed. This process is facilitated if the back-arc lithosphere is oceanic and has previously spread (back-arc basin, Chemenda et al., 2001b). From 2D analog and numerical experiments of subduction-collision processes, the authors show that the failure direction depends on the trade-off between the opposite torques caused by interplate friction and interplate normal stress (Chemenda et al., 1997, 2001b; Tang and Chemenda, 2000; Tang et al., 2002). A typical example of flip associated with SI is the formation of the north vergent New Britain - San Cristobal - New Hebrides SZ following the diachronous collision of the Ontong-Java Plateau in the mid to late Miocene (Auzende et al., 1988, Pelletier et al., 1998, Fig.5). This collision caused the cessation of the south-vergent Vitiaz subduction first in the east and then in the west (Mann and Taira, 2004) and the new SZ soon became self-sustained. Recently, the d'Entrecasteaux Ridge carried by the Australian Plate collided with the New Hebrides Arc, triggering an incipient-localized SI stage of subduction polarity reversal at the foot of Ambrym - Pentecost Arc back of Espiritu Santo Island (Collot et al., 1985; Lagabrielle et al., 2003; Régnier et al., 2003).

4.4.2.2. Jump

We name jump any new SZ replacing a former one, in terms of accommodation of the convergence, keeping the same vergence. As for the flip, this situation generally

happens when a buoyant feature enters the subduction zone, stopping the convergence locally. This mechanism, which contributes to the growth of the continents through terrane accretion, was named transference by Stern (2004). Either the whole lithosphere fails back of the buoyant feature and a new subduction develops as in the Aleutians for example (Scholl et al., 1986) or delamination takes place if the lower crust of the buoyant feature is weak enough (Morency and Doin, 2004) to allow the crustal layer for being accreted while the mantle part subducts. The Central Aleutians SZ resulted from the accretion of the Bering Sea as the Olyutorsky arc collided with Kamtchatka during the Paleocene (Scholl et al., 1992). Delamination along the serpentinized uppermost mantle and crustal accretion is observed off the Nankai Trough at the Zenisu Ridge (Lallemand, 2014, Fig.4). This last situation resembles those occurring during a continental collision forming a crustal accretionary prism (thick-skin tectonics) with a decoupling level in the lower crust allowing the lithospheric mantle to subduct (Lallemand, 1999; 2016). The Siletzia Paleogene plateau accreted to North America by 50 Ma, triggering a backstepping subduction for Wells et al. (2014) (Fig. 6).

4.4.2.3. Lateral propagation

When reconstructing the Cenozoic history of the Mediterranean region, most authors initiate the subduction of Africa Plate (Ligurian Ocean) beneath Eurasia Plate sometime during the Paleocene along a Western Mediterranean SZ ~1700 km long, but summing the relics of that subduction from Gibraltar to Calabria and the Apennines at present leads to a total length of ~4000 km (e.g., Royden and Faccenna, 2018, Fig. 9). The SZ then necessarily expanded laterally. Taking a more recent example, the deepest Philippine Trench segment (~10 km) coincides with the oldest arc volcanism (~4 Ma) originating from the Philippine Sea Plate (PSP) subduction (Fig.4). Furthermore, the PSP slab length decreases from the middle part of the subduction to the edges. This has been interpreted by Lallemand et al. (1998) as evidence for northward and southward lateral propagation of the lithospheric failure, as a crack, from a mid-point off Mindanao Island since the Late Miocene. One-side lateral propagation of a mature subduction may also occur if kinematic conditions change. It has happened in the southernmost Ryukyus since 8 Ma as a TF connecting two opposite-verging subduction zones was totally consumed (Lallemand et al., 2001). A tear developed through the ocean-continent transition of the Eurasia plate in the prolongation of the former Ryukyus SZ, leaving space for the PSP slab to insert. Based on 3D numerical modeling, Zhou et al. (2020) have shown that SI propagation along passive continental margins requires a sufficiently weak OCT lithosphere and a large slab pull force, otherwise STEP faulting or slab-breakoff will result. However, the OCT curvature, if any, may induce an along-strike pressure gradient that could reduce the pressure difference perpendicular to the OCT, thus limiting subduction propagation (Marques et al., 2014). In the southern Ryukyus, all three processes might have occurred (Lallemand et al., 2001). The short-lived (~15 Ma) Banda subduction is another example of eastward lateral propagation of the Java Trench along a tear first cutting through the ocean-continent boundary (probably transform margin) and then across the Sula Spur which was the northernmost promontory of Australian continent (Hall, 2012; 2018, Fig.10). The tear is supposed to initiate at ~17 Ma as a result of margin's deformation following the arc-continent collision between the Sula Spur and North Sulawesi around 23 Ma.

4.4.2.4. Tectonic uplift

The terms "tectonic uplift" or "vertical tectonism" have been used by Bonatti in 1978 to explain anomalously (1 to 3 km) elongated highs fringing large oceanic TFs and fracture zones. Case examples cited by Bonatti included Vema, St. Paul, Romanche in the Atlantic Ocean, Owen in the Indian Ocean and Alula in the Gulf of Aden (Figs.8 & 10). Compressional and tensional horizontal stresses caused by small kinematic changes are common factors invoked to account for the rise of upper mantle ultramafic rocks in addition to thermal or visco-dynamic forces. Asymmetric rise of one limb of the lithospheric fault may coincide with a restraining bend along a major transform fault like the Owen Ridge or Saint-Paul Islets (Fournier et al., 2011; Maia et al., 2016), transpression like along Romanche fracture zone or Gorringe Bank (Bonatti et al., 1996; Tortella et al., 1997) or far-field compression like Tiburon or Barracuda FZs (Pichot et al., 2012). Such a setting juxtaposing oceanic crusts with contrasted ages and significant differences in elevation, especially if the lithosphere adjacent to the ridge bends downwards, may be theoretically prone to initiate a subduction. It happens for the Gagua Ridge in the westernmost Philippine Sea plate (Fig.4). The 300 km long, 20-30 km wide Gagua Ridge overhangs the adjacent abyssal plain by 2 to 4 km with a pronounced trough on its eastern side (Mrozowski et al., 1982). Based on seismic imagery and gravity modeling across this feature, Deschamps et al. (1998) and Eakin et al. (2015) have proposed two SI episodes at 50-40 Ma and 24 Ma that have rapidly aborted.

4.4.2.5. Spreading center (SC) conversion

Conversion of an oceanic spreading center to a SZ is generally suspected when similar ages are determined between the formation of the metamorphic soles and associated ophiolites. Such evidence was found, for example in the New Caledonia or Palawan ophiolites (Cluzel et al., 2012; Keenan et al., 2016, Fig.5). Despite the weakness and buoyancy of the newly formed oceanic crust, these relic ophiolites attest that extremely young crust can be forced into the nascent SZ which further became self-sustained. Indeed, the New Caledonia ophiolite is associated with the Loyalty-Three Kings SZ which lasted ~26 Myr, while the Palawan ophiolite related with the NW Borneo-Cagayan SZ which lasted ~18 Myr (Cluzel et al., 2012; Keenan et al., 2016). In both cases, the conversion from divergence to convergence was rapid. The onset of subduction in Palawan reveals that the oceanic crust was less than 1 my old when underthrust. This example shows that a very young and buoyant crust may be underthrust and plate motion may rapidly change from divergence to convergence (Keenan et al., 2016). Other cases were reported but they were deduced from kinematic reconstructions and subsequently subject to interpretation. The Macquarie Ridge Complex, which is nowadays a transpressional plate boundary between the Australian and the Pacific plates, was initially formed by succession of small spreading center segments and large-offset transform faults until Oligo-Miocene time before being inverted (Lamarche et al., 1997; Massel et al., 2000, Fig.5). The change in plate kinematics gave rise to the nascent Puysegur and Hjort trenches (Lebrun et al., 2003; Meckel et al., 2003). As shown by Beaussier et al. (2018), the geometry of SI at the spreading center (one main slab vs several contra-dipping slabs) is intrinsically governed by the three-dimensional setting and the degree of ridge asymmetry. Moreover, SI localizing at a spreading center is impeded if the time lag between ridge accretion and ridge compression is too long (~20 Myr, Beaussier et al. 2019). Based on 2D thermomechanical coupled numerical

models, Qing et al. (2021) confirmed that subduction may easily initiate at a spreading center with a cooling age less than ~20 Ma and a forced convergence rate larger than ~4 cm/yr.

4.4.2.6. Transform fault (TF) conversion

Conversion of a TF to a SZ is common because a TFor a fracture zone is known to be weak, possibly as a result of an enhanced serpentinization, over a significant width up to ~25 or 30 km away from the main fault (Searle 1983; Roland et al., 2010; Wolfson-Schwehr et al., 2014), prone to localize strain (Lowrie et al., 1986; Behn et al., 2002), and sensitive to small kinematic changes, often being at the verge of failure between strike-slip and reverse faulting (Boutelier and Beckett, 2018; Zhang et al., 2021). Slight compression across a TF generally results in a "tectonic" rise centered above the strike-slip fault (see section 4.4.2.4). Models tend to show that, when orthogonally compressed, two shear bands oppositely dipping develop from the deepest part of the vertical weak zone forming the TF toward the surface cutting through the lithosphere (Shemenda, 1992; 1994; Boutelier & Becket, 2018). Next, depending on the local mechanical conditions, one of the two conjugate shear zones becomes the predominant thrust fault, promoting the underthrusting either of the thick plate (Gurnis et al., 2004; Leng & Gurnis, 2011) or of the thin one (Boutelier & Becket 2018). Recent numerical models suggest that the SZ polarity could depend on the combination between the plate age offset at the TF, the plate strength, and the TF resistance (Zhang et al., 2021). Even neoformed, the resulting main thrust will be considered here as having nucleated from the TF. We will thus call this process "TF conversion" rather than a fault neoformation stricto sensu which supposes that the fault nucleates within a continuous medium. There exists a wealth of natural examples during the Cenozoic (see Table 3), the most famous being the birth of the Izu-Bonin-Mariana SZ (Uyeda and Ben Avraham, 1972, Fig.4). Conversion mechanisms are similar with Subduction Transform Edge Propagator (STEP) faults as they resemble TFs at distance from their edge (Govers and Wortel, 2005). Again, small kinematic changes from strike-slip to compression may facilitate the conversion to a SZ. A good example concerns the newly Matthew & Hunter SZ at the southern termination of the New Hebrides Trench (Patriat et al., 2015, Fig.5).
It was shown that if one side of the TF is very young (<5 Myr), the kinematically-imposed subduction of the thick plate reached self-sustained stage after 100 to 200 km of convergence only (depending on the assumed plastic weakening, Hall et al., 2003; Gurnis et al., 2004; Leng & Gurnis, 2011), the main force resisting subduction in this setup being the plate rigidity to bending. In contrast, if the young oceanic plate at the TF is not so young, plate resistance to shearing is the first force to overcome, and controls subduction polarity (Boutelier & Beckett 2018).

4.4.2.7. Normal/detachment fault (NF/DF) conversion

In theory, extensional detachment faults are excellent candidates for being converted to nascent SZs if boundary conditions change from extension to compression because they are weak and have the ideal geometry. Based on 2-D numerical models, Maffione et al. (2015) have shown that intra-oceanic serpentinized detachments are always weaker than spreading ridges. 3-D thermomechanical modeling supports this assumption. Shortening may be first accommodated by multiple pre-existing detachment

faults, before localization occurs at the base of the detachment faults to form the main thrust plane (Gülcher et al., 2019). In case of serpentinization, the resulting extreme weakness of detachment faults can localize deformation under perpendicular far-field forcing. However, natural examples mainly concern rifted margins like the N-Iberia margin south of the Bay of Biscay (Gallastegui and Pulgar, 2002, Fig.8) or the N-Maghrebides margin south of the Algerian Basin (Strzerzynski et al., 2010, Fig.9). Not only detachment but normal faults can also localize the deformation likely to evolve into a SZ. Tectonic inversion may happen either in an intra-oceanic setting such as the Central Indian Ocean (Delescluse et al., 2008, Fig.10) or along a rifted margin like along the eastern coast of the Japan Sea (Lallemand et al., 1985, Fig.4).

4.4.2.8. Buckling

Under compressive stress, buckling or flexure of the lithosphere is the most common tectonic sequence preceding lithospheric failure in a convergent setting (Shemenda, 1989). Buckling at a wavelength and maximum amplitude predicted by the elastic thickness of the lithosphere is expected and observed in physical models involving a homogeneous plate (Shemenda, 1992). Other studies suggest that brittle (plastic) deformation is the main driving mechanism of lithospheric buckling, the underneath viscous layer flowing passively or limiting buckling (Martinod and Davy, 1992). Buckling under compression is simulated when reverse faulting has propagated downward and once the stress yield of the competent layer is reached (Gerbault et al., 1999). Most of the time, pre-existing faults or lateral discontinuities tend to localize the flexure or faulting, if their orientation is compatible with the principal stress. In the Central Indian Ocean (Fig.10), long-wavelength (150-300 km) anticlinal basement structures with 1-2 km relief associated with tight folding and high-angle faulting (Weissel et al., 1980) appeared prior than 7.5 Ma as indicated by a widespread unconformity (Krishna et al., 1998). The deformation zone extends over almost 2000 km in a N-S direction while the basement folds trend E-W. Passive and transform margins may fail preferentially in the transition area between continental and oceanic lithospheres when stressed as observed in several regions. Based on velocity models across the north Algerian margin undergoing Africa-Eurasia convergence, Hamai et al. (2015) have shown that isostatic anomalies reflect opposite flexures of the Algerian Basin (Fig.9) and the Africa continent reaching a maximum amplitude at the margin's toe. The extremely low effective elastic thickness estimated from the amplitude and wavelength of the flexure reflects the relatively low strength of the lithosphere close to the incipient plate boundary. The North Algerian passive margin displays isostatic anomalies close to those of an active margin.

4.4.2.9. SZ reactivation

As described in section 4.4.1.2 focusing on the reactivation of major lithospheric faults with the same kinematics, it may happen that convergent motion vanishes at a SZ and resumes millions of years later if global kinematics requires it. The Melanesian Arc (Fig.5) is probably the best Cenozoic example of multiple flips of subduction alternatively on the northern and southern side of the arc throughout the Cenozoic, finally corresponding to successive reactivations of oppositely dipping thrusts since Late Cretaceous (Petterson et al., 1999; Schellart and Spakman, 2015, see section 3.2 and 4.1.1.3 for further details).

4.5 Deformation mode vs spatial expression classification

Our review of natural cases has highlighted common spatial expressions of the deformation which mainly result from the initial geodynamic setting but not exclusively. We thus felt the need to list those spatial expressions and combine them with the deformation modes. Here, we thus provide a complementary classification based on deformation characteristics (Table 3). We observe that most SZs initiate at or very near inherited faults. We specify below whether the former faults are reactivated the way they used to slip or if tectonic inversion occurred. The last category, corresponding to "fault neoformation", is ticked when we ignore if pre-existing faults localize the deformation. It doesn't mean that they were neoformed, it just means that we cannot exclude fault neoformation.

			Deformation spatial expression								
			Flip (polarity reversal)	*Jump (same polarity)*	*Lateral propagation*	*Tectonic uplift*	*SC conversion*	*TF conversion*	*NF/DF conversion*	*Buckling*	*SZ reactivation*
Deformation mode	fault reactivation	*Change in fault kinematics*	C- & W-Aleutians, Bowers Ridge, Proto-Kamtchatka, Kuril, E-Japan Sea, Philippines, NW-Borneo - Cagayan, Flores, Wetar, N-Sulawesi, Tolo, N-Melanesian, Vitiaz, Pocklington, Samoa-Gilbert-Ralik, New Britain-San Cristobal (incl. S-Solomon), New Hebrides, Ambrym (incl. Pentecost-Maeowo), Loyalty - Three Kings, Tonga-Kermadec, N-Panama, Muertos, Nicaragua Rise, W-Mediterranean, N-Maghrebides (Alboran to Sicily)	Zenisu, Gagua - E-Luzon Trough, Sulu, Yap, Trobriand, Sunda, S-Caribbeans, Nicaragua Rise, W-Mediterranean	S-Ryukyus, Manila, Negros, Cotobato, Philippines, Sula, Sulu, Sangihe, New Britain-San Cristobal (incl. S-Solomon), Vitiaz, Matthew & Hunter, d'Entrecasteaux, Puysegur, Hjort, Banda (incl. Seram), S-Caribbeans, N-Panama, Puerto-Rico, Endurance Collision Zone, S-Sandwich, W-Mediterranean, Gibraltar, Calabria, N-Maghrebides (Alboran to Sicily)	Zenisu, Gagua - E-Luzon Trough, McDougall, Macquarie, Hjort, Muertos, Beata Ridge, Saint Paul, Romanche, SW Iberia (incl. Gorringe), Barracuda, Tiburon	C- & W-Aleutians, Bowers Ridge, NW-Borneo - Cagayan, Yap, d'Entrecasteaux, Loyalty - Three Kings, Puysegur, Hjort, Beata Ridge	E-Japan Sea, Gagua - E-Luzon Trough, Manila, Negros, Cotobato, NW-Borneo - Cagayan, Sangihe, Halmahera, Izu-Bonin-Mariana, Yap, Palau, Lyra, Mussau, Samoa-Gilbert-Ralik, Matthew & Hunter, Tonga-Kermadec, Puysegur, McDougall, Macquarie, Hjort, Sumatra-Java, Banda (incl. Seram), Puerto-Rico, Saint Paul, Romanche, SW Iberia (incl. Gorringe), Barracuda, Tiburon, Carpathians, W-Mediterranean, Gibraltar, Calabria, N-Maghrebides (Alboran to Sicily)	E-Japan Sea, Mussau, C-Indian Ocean, Beata Ridge, N-Iberia, N-Maghrebides (Alboran to Sicily)	Zenisu, Samoa-Gilbert-Ralik, Ambrym (incl. Pentecost-Maeowo), C-Indian Ocean, Barracuda, Tiburon	
		Same fault kinematics	N-Melanesian, Vitiaz, Pocklington, New Britain-San Cristobal (incl. S-Solomon), New Hebrides, Ambrym (incl. Pentecost-Maeowo)	Komandorsky, Kamtchatka, Trobriand, Sumatra-Java	New Britain-San Cristobal (incl. S-Solomon), Vitiaz					Ambrym (incl. Pentecost-Maeowo)	Komandorsky, Kamtchatka, Ryukyus-Nankai, Halmahera, N-Melanesian, Vitiaz, Pocklington, New Britain-San Cristobal (incl. S-Solomon), New Hebrides, Ambrym (incl. Pentecost-Maeowo), Sunda
		Fault neoformation ?	C- & W-Aleutians, Bowers Ridge, Taiwan E-coast, Philippines, Tolo, Samoa-Gilbert-Ralik, N-Solomon, Ambrym (incl. Pentecost-Maeowo), Tonga-Kermadec, N-Panama, Muertos, Nicaragua Rise, W-Mediterranean	Zenisu, Cascadia, N-Solomon, Trobriand, Sunda, Nicaragua Rise, W-Mediterranean	Taiwan E-coast, Cotobato, Philippines, Sula, Sangihe, Matthew & Hunter, N-Panama, Puerto-Rico, W-Mediterranean	Zenisu, Muertos	C- & W-Aleutians, Bowers Ridge	Cotobato, Sangihe, Halmahera, Mussau, Samoa-Gilbert-Ralik, Matthew & Hunter, Tonga-Kermadec, Sunda, Puerto-Rico, W-Mediterranean	Mussau	Zenisu, Taiwan E-coast, Samoa-Gilbert-Ralik, Ambrym (incl. Pentecost-Maeowo)	Halmahera, Ambrym (incl. Pentecost-Maeowo), Tonga-Kermadec, Sunda

SI reached stage : incipient-diffuse, incipient-localized, achieved, self-sustained
Present SZ status : active, aborted (when self-sustained stage was never reached), extinct

Table 3: Deformation style recorded at SISs. Lines indicate the deformation mode at the time of SI. Columns list the spatial expression of the deformation at initiation. SC = Spreading Center; TF = Transform Fault; NF/DF = Normal Fault or Detachment Fault; SZ = Subduction Zone. Note that some SZs satisfy several settings or triggers either because there were multiple settings or triggers acting simultaneously or because initial settings or triggers are debated (see question marks in the supplementary Table). Colors and underlining codes are the same as in Table 1.

4.6 Global statement on Cenozoic subduction initiation characteristics

The exhaustive description of the 70 Cenozoic SISs at various stages of maturity allows us to provide a quantitative analysis of the conditions for their birth and evolution.

4.6.1. Importance of the SI process during the Cenozoic

The cumulated length of immature and mature subduction trenches created during the Cenozoic reaches 70350 km (see Table 1), i.e., ~28% more than the present cumulated length of active oceanic subduction zones. In terms of occurrences, 70 SISs were listed during the last 65 Ma, or on average nearly one per million years. A plot of SI ages (Fig.15) does not exhibit any particular pulse throughout the Cenozoic. It should be noted, however, a significant slowdown of initiations during the Oligocene and Early Miocene, i.e., only 5 occurrences within 15 Myr between 28 and 17 Ma. Crameri et al. (2020a&b), based on the study of thirteen subduction zone initiation (SZI) events that reached maturity during the last 100 Myrs, also noted two temporal clusters between ~55-40 Ma and between ~16-6 Ma. Incidentally, the rate of SI occurrences out of this period increased to 1.3 per million years. SI thus appears as a regular and quite continuous process at the global scale.

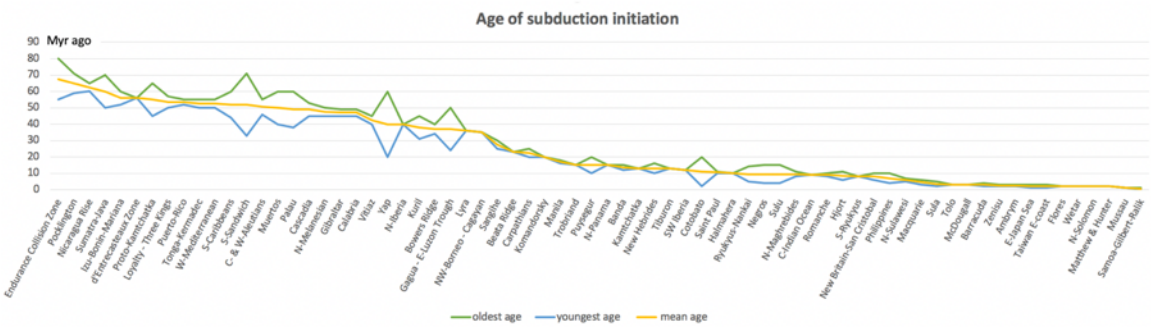

Fig.15: Distribution of SI ages throughout the Cenozoic. Ages are in Ma along the y-axis.

4.6.2. From immature to mature stage

	reached stages (70 occurrences - 70350 km)			
	incipient-diffuse #14 - 10390 km	incipient-localized #16 - 8120 km	achieved #11 - 6430 km	self-sustained #29 - 45410 km
still active #48 - 49260 km	Barracuda C-Indian Ocean E-Japan Sea Macquarie McDougall Mussau N-Maghrebides Saint Paul Samoa-Gilbert-Ralik Sula SW Iberia	Ambrym Cotobato Flores Hjort N-Panama N-Solomon Taiwan E-coast Tolo Wetar Yap Zenisu	Matthew & Hunter Negros N-Sulawesi Philippines Puysegur S-Caribbeans S-Ryukyus Sulu	Banda Calabria Cascadia C- & W-Aleutians Halmahera Izu-Bonin-Mariana Kamtchatka Kuril Manila New Britain-San Cristobal New Hebrides N-Melanesian Puerto-Rico Ryukyus-Nankai Sangihe S-Sandwich Sumatra-Java Tonga-Kermadec
	immature			mature
inactive today #22 - 21090 km	Beata Ridge Romanche Tiburon	Gagua - E-Luzon Trough Lyra Muertos N-Iberia Trobriand	d'Entrecasteaux Zone Komandorsky Nicaragua Rise	Bowers Ridge Carpathians Endurance Collision Zone Gibraltar Loyalty - Three Kings NW-Borneo - Cagayan Palau Pocklington Proto-Kamtchatka Vitiaz W-Mediterranean

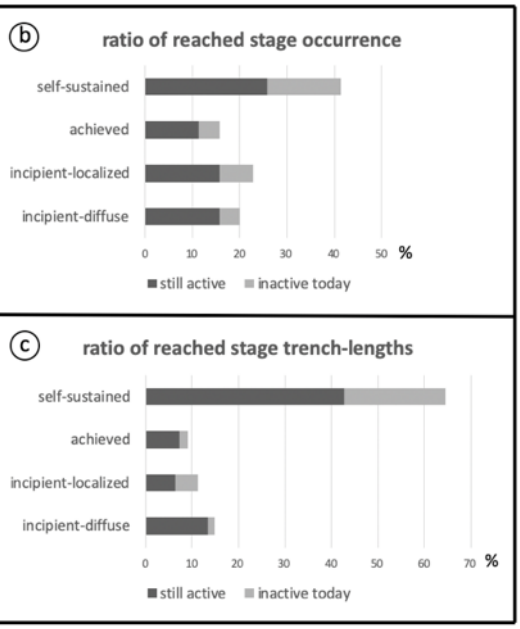

Fig.16: Distribution of reached stage (columns in (a) and bars in (b) and (c)) among the 70 studied Cenozoic SISs. The lists of SISs within the eight boxes of the table (a) correspond to the eight stages defined in Fig.3. Percentages of cases (b) or cumulated trench-length (c) on x-axes. Black and grey bars in (b) and (c) correspond to immature and mature subductions that are still active or have become inactive respectively.

We can estimate the prevalence of the different stages reached for every SIS following two complementary counting modes, either in terms of number of occurrences or cumulated trench-lengths. In the following, we have chosen to show both, stating either the ratio of occurrences over the total number of cases (nb / 70 cases, first value hereafter), or the ratio of the cumulated trench-length of occurrences over the total length of studied trenches (lg / 70350 km, second value hereafter with asterisk). We obtain: 20/15*% of incipient-diffuse SI stages, 23/11*% of incipient-localized SI stages, 16/9*% of achieved SI stages and 41/65*% of self-sustained subduction stages (Fig.16). Self-sustained (or mature) subduction is thus, by far, the most frequently reached stage during the Cenozoic, especially in terms of cumulated trench length.

Regarding the present-day status, 69/70*% of the SISs during the Cenozoic are still active, 16/8*% lapsed prematurely (later considered as aborted), and 16/22*% lapsed after reaching the self-sustained stage (later considered extinct). Taking away the 11 extinct and 11 aborted cases from the 70 Cenozoic SISs, 48 studied sites are still active, 30 being still immature and 18 being mature.

The average trench length of a mature SZ is at least twice larger than those of an immature SZ: ~1570 km vs ~800 km. This probably indicates that lateral propagation after initiation is very common. However, a careful analysis shows that the range of trench-lengths is wide for all stages: 100 to 4200 km for the incipient-diffuse SI stage, 100 to 900 km for the incipient-localized SI stage, 180 to 1700 km for the achieved SI stage and 200 to 3800 km for the self-sustained subduction stage. This suggests that SI does not systematically take place at a local scale before propagating sideways.

4.6.3. Duration of SI stages and subduction activity

Since we have only explored the Cenozoic period, we cannot account for time durations longer than 65 Myr. The analysis of the duration distribution in Fig.17 shows that ~60% of the cases had a duration shorter than 15 Myr, most of them having not reached the self-sustained subduction stage, and 40% lasted more than 15 Myr, including a few cases of immature stages. It should be noted that the 6 outliers (>15 Myr long immature stages: Nicaragua Rise, Beata Ridge, D'Entrecasteaux Zone, Yap, Muertos, S-Caribbeans) all present unclear or contradictory characters. Put another way, a SZ does not often stay immature after 15 Myr. Combined with the previous observation about SZs trench-lengths, we note that self-sustained SZs stay active longer and are wider than immature SZs.

Another interesting parameter that informs the process of SI is the time necessary to reach each stage. A lower bound can be reasonably constrained. Indeed, the shortest time to reach the achieved SI stage is recorded at Matthew & Hunter SZ: 1.8 Myr. The youngest age of a self-sustained SZ is presently observed at the active New Britain - San Cristobal SZ which initiated sometime between 6 Myr (Petterson et al., 1999, Mann and Taira, 2004) and 15 Myr (Wu et al., 2016). Given the uncertainty in the evaluation of the slab length based on tomography (900 km since 15 Ma for Wu et al., 2016 vs

575±100 km since 5-15 Ma for van der Meer et al., 2018), we can estimate the time at which the slab had a length of ~250 km, needed to reach the mature stage, considering a mean subduction rate of 9 - 10 cm/yr, i.e., 3 to 8 Myrs after onset (Fig. 18). Moreover, with the present length of the New Hebrides slab being ~750 km, it reached the 250 km length approximately 5 Myr ago using an average subduction rate of 10-12 cm/yr (Lallemand et al., 2005). Considering that the slab began to subduct 15 to 10 Myr ago, (van der Meer et al., 2018), we can infer that the self-sustained stage reached 5 to 10 Myr after the onset of SI.

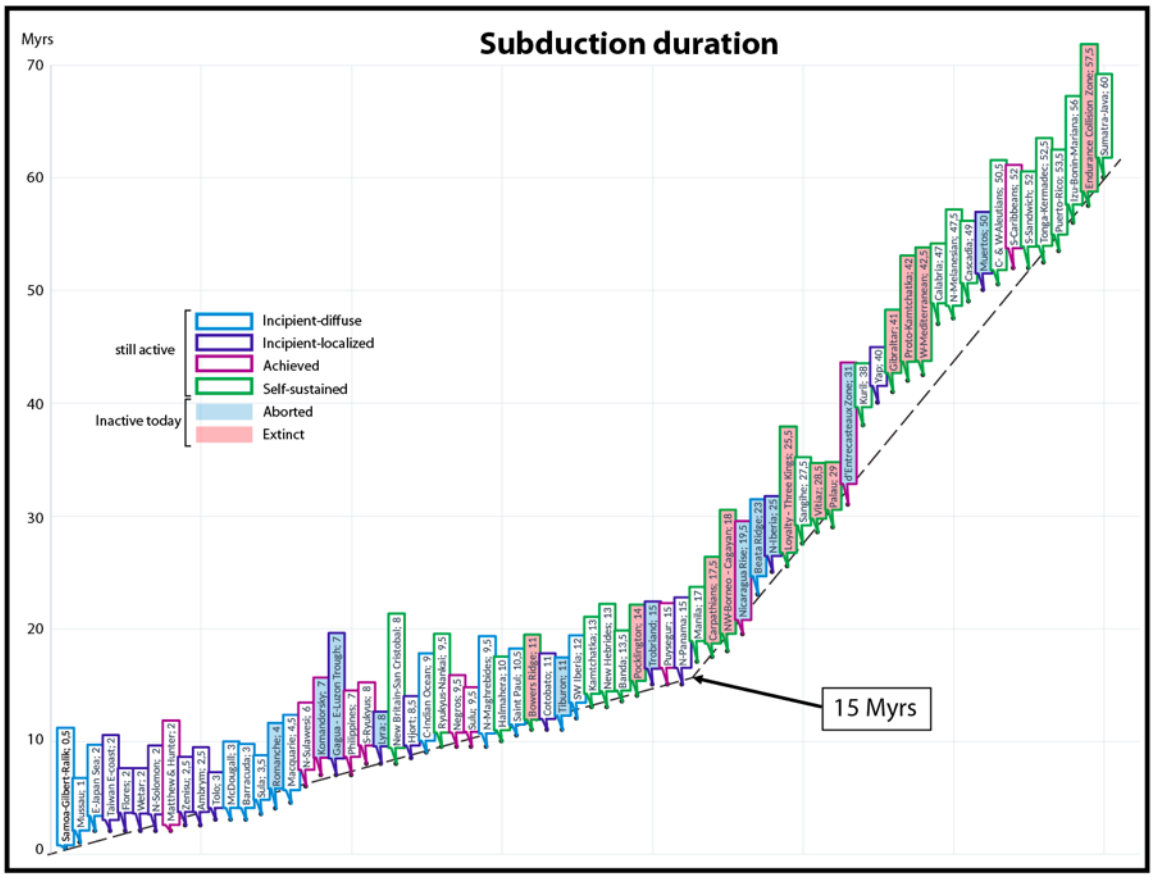

Fig.17: Duration of subduction activity at SISs during Cenozoic. The colors of the SZ name boxes are the same as in Tables 1, 2 and 3. Those with no background pattern are still active. Pink background pattern corresponds to extinct SZs. Blue background pattern indicates aborted SZs. Duration time in Myr on the y-axis.

Finally, we conclude that the timescales for localizing the subduction fault can be as short as ~1 Myr and ~1.8 Myr for generating arc volcanism (inferred from Matthew & Hunter). New Britain appears to be the fastest Cenozoic SI case to reach the self-sustained subduction stage within ~3-8 Myr. The SI process may abort at each preliminary step either soon or late (Fig.18). For example, there are cases like the Beata Ridge which apparently stayed at the incipient-diffuse SI stage for 23 Myr before stopping the process. Similarly, we note cases where SI was proceeding up to the incipient-localized stage and finally aborted after 25 Myr off N-Iberia, or even 50 Myr along the Muertos trench south of Puerto-Rico (Figs.17 & 18). Subduction aborted after reaching the achieved SI stage 31 Myr after initiation at the D'Entrecasteaux Zone and it

is still active along the S-Caribbeans after 52 Myr, but the situation there is ambiguous (see discussion in section 3.4). The upper bound for the time span to reach each stage of localization of the subduction fault, establishment of the primary volcanism or development of a self-sustained subduction is thus extremely variable depending on the regional geodynamic setting, and could sometimes reach tens of millions of years. Eleven mature SZs, initiated during the Cenozoic, ceased to be active, the shortest-lived one (Bowers Ridge) being active for only 11 Myr (Fig.17). We cannot provide any estimate for the longest-lived one since some of them like Sumatra-Java, IBM or Tonga-Kermadec are still active after 50-60 Myr of convergence. We also note 11 aborted cases of immature SZs after 4 to 50 Myr of activity, the shortest corresponding to a segment of the Romanche FZ and the longest being Muertos (Fig. 18).

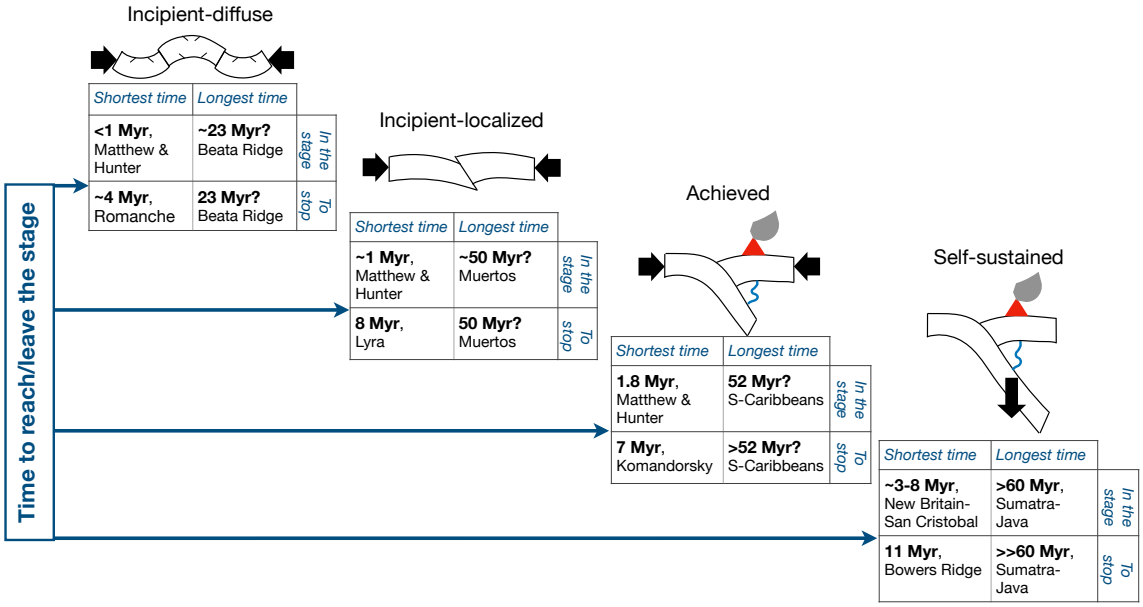

Fig.18: Time ranges inferred in the present compilation either to reach ("shortest time") each stage of the SI process (as defined in section 2 and sketched in Fig. 3), or to leave it ("longest time"). The second line of the time tables shows the equivalent time interval when SI aborted during the ongoing stage (first three immature stages), or died at a mature stage. Please note that the longest time for each immature stage corresponds to poorly constrained outliers ('?') and are not representative of the majority of immature stages (≤ 15 Myr).

4.6.4 Rate of success of SI

To estimate the rate of success of SI (meaning the opportunity to achieve a mature stage) within the time window of the Cenozoic time, we only consider the SZs for which the final "fate" of the maturation process is known, i.e., the cases having reached either the self-sustained subduction stage or which jammed prematurely, regardless of their present activity, i.e., 11 aborted plus 29 mature representing 40 cases. This gives us a rate of success of 72/89*%. Such a high rate of success must be put into perspective because we are reasoning within a limited time range, i.e., 65 Myr, to make statistics. Indeed, we ignore the fate of 20 immature but still active stages and we do not count the

self-sustained SZs that were initiated before, even shortly before the Cenozoic, like the Lesser Antilles SZ for example.

Similar estimates can be done concerning the immature stages. The population that we should consider to calculate the chances to reach the “achieved stage” includes the 40 SISs that reached the “achieved SI stage” and the 8 incipient SISs for which we know that they aborted. This gives us a rate of “achievement success” of 83/92*%. Using the same methodology, we obtain 95/98*% for the rate of success to reach the incipient-localized SI stage.

4.6.5 Geodynamic setting at the time of SI

60/57*% of SZs initiated at the transition between an ocean and a continent, plateau or arc (OT in this study), 29/24*% far from an OT and 11/19*% have an uncertain initial geodynamic setting (Fig. 19). Among those which initiated at an OT, 44/43*% correspond to rifted margins, 33/29*% to transform margins, 13/21*% to former SZs and 10/7*% to ridge flanks.

Among those which initiated far from an OT, 61/60*% correspond to the conversion of TFs or fracture zones, 31/27*% of spreading centers and 8/14*% of normal faults to subduction faults.

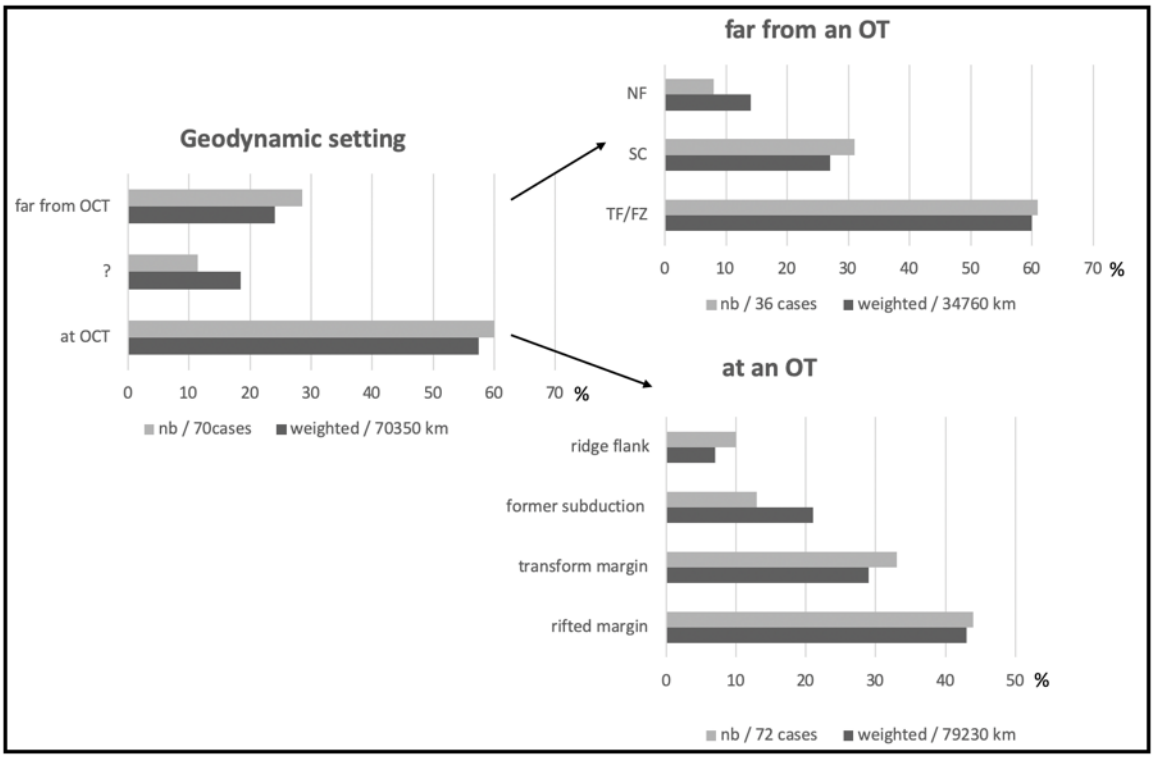

Fig.19: Distribution of geodynamic settings among SISsduring the Cenozoic. OT = Oceanic Transition, including Ocean-Continent, Ocean-Plateau and Ocean-Arc transitions; NF = normal fault; SC = spreading center, TF/FZ = transform fault or fracture zone. Note that the total number of cases or cumulated length differ from 70 cases and 70350 km in the two right-hand diagrams because they address sub-samples of the left-hand diagram and also because a given SZ may meet 2 or more criteria like for example “rifted margin” + “transform margin”. This is particularly true for the cases at an OT. Percentages of cases or cumulated trench-length on x-axes.

4.6.6. Suspected triggers of subduction

An important finding or confirmation is that lithospheric forcing seems ubiquitous in any SI. It is the only driving for 63/60*% of the SISs, whereas the remaining 37/40*% could be triggered by a combination of lithospheric and mantle forces (Fig. 20). SI thus seems to never be driven by mantle flows alone, which is consistent with Crameri et al. (2020a) findings that most SZI events among those studied are located outside the surface-projected area of the large-low-shear-wave velocity provinces, or along their edges, suggesting that both mantle upwelling and downwelling could play a significant role in fostering SZI. We also confirm their conclusion that in the last 100 Ma (65 Ma for us), only examples of SZI with either significant horizontal forcing, or else an additional vertical mantle-flow forcing, are observed. However, it must be remembered to note that the SZIs of Crameri et al. (2020a) are not equivalent to the SISs in our study as recalled in the glossary. Among the lithospheric forcings, ongoing collision (49/48*%) and kinematic changes (38/35*%) are dominant, then delamination (6/11*%) and sedimentary loading (6/6*%) can also arise but more rarely. Among additional mantle forcings, plume-induced or spreading center-related are mentioned in 43/41*% of the cases, slab breakoff-induced in 21/27*%, and other mantle flow-triggered forces in 36/32*%. In more than 50% of the cases, there are multiple, generally 2, up to 5 triggers, especially when mantle forcings are mentioned (collision and slab breakoff for example).

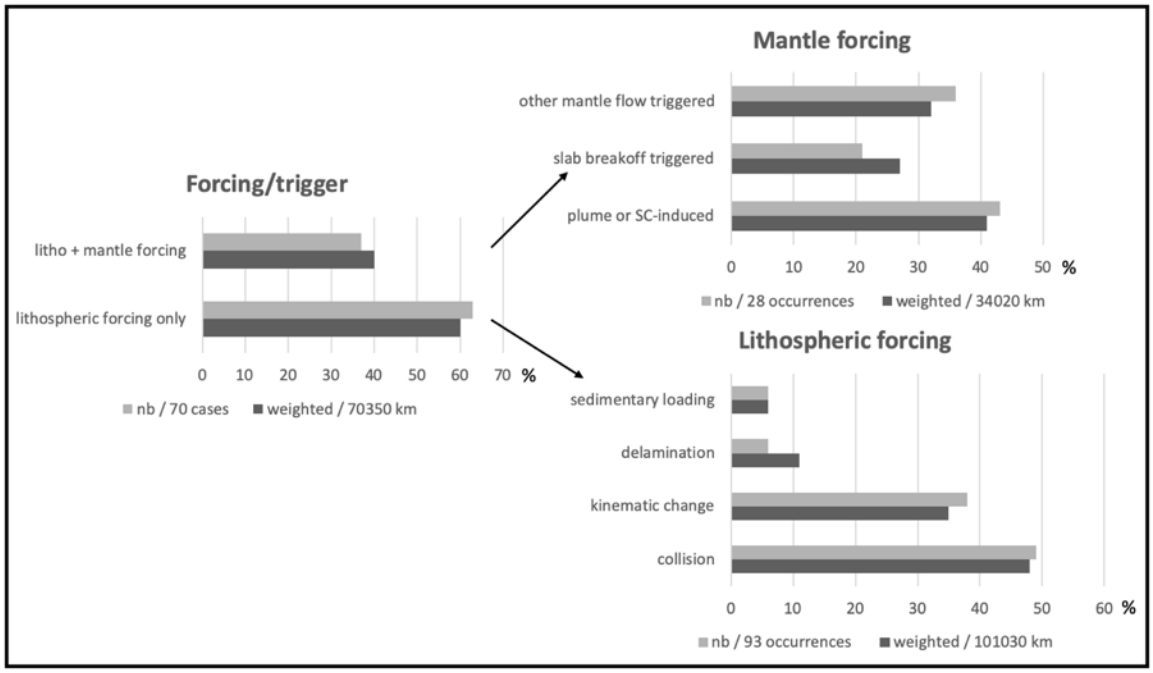

Fig.20: Distribution of forcings among SISs during the Cenozoic. See Fig.19 caption for more explanations. Percentages of cases or cumulated trench-length on x-axes.

4.6.7. Various modes of deformation

Conversion of a preexisting lithospheric fault to a subduction fault with a change in kinematics concerns 64/58*% of the cases, whereas reactivation of former reverse faults with the same kinematics is observed in only 12/18*% of the cases. In one out of four

cases (24%), we ignore if an inherited fault was reactivated because the initial setting has been obscured by the activity of the subduction since its birth. In this case, we cannot exclude the neoformation of the subduction fault. Let's reiterate that we classify the conversion of a transform to a subduction fault as a case of change of the kinematics of a preexisting fault even if part of the new fault is neoformed. This is because we consider that the transform fault helped localize the new fault and also because they intersect at depth.

The spatial expression of the deformation may take various forms, some of which either complement one another or were diversely interpreted by authors, so that the number of occurrences or cumulated lengths on the diagram (Fig.21) extends far beyond the 70 cases and 70350 km of cumulated length. This having been established, there are three main spatial expressions of SI: flip generally across an arc with a change of subduction polarity (19/24*%), conversion of a TF (23/22*%) and lateral propagation of an existing SZ (17/15*%). Then, we note two less observed situations: jump often back of a buoyant block that resists subduction keeping the same polarity (9%) and reactivation of a SZ (8/15*%). We also noted some rare spatial expressions such as: tectonic uplift (8/3*%), conversion of a spreading center (6/5*%), conversion of a normal or a detachment fault (4/3*%) and buckling (5/4*%). Again, multiple spatial expressions are the rule, generally a combination of 2 or 3 spatial expressions (lateral propagation and TF conversion for example).

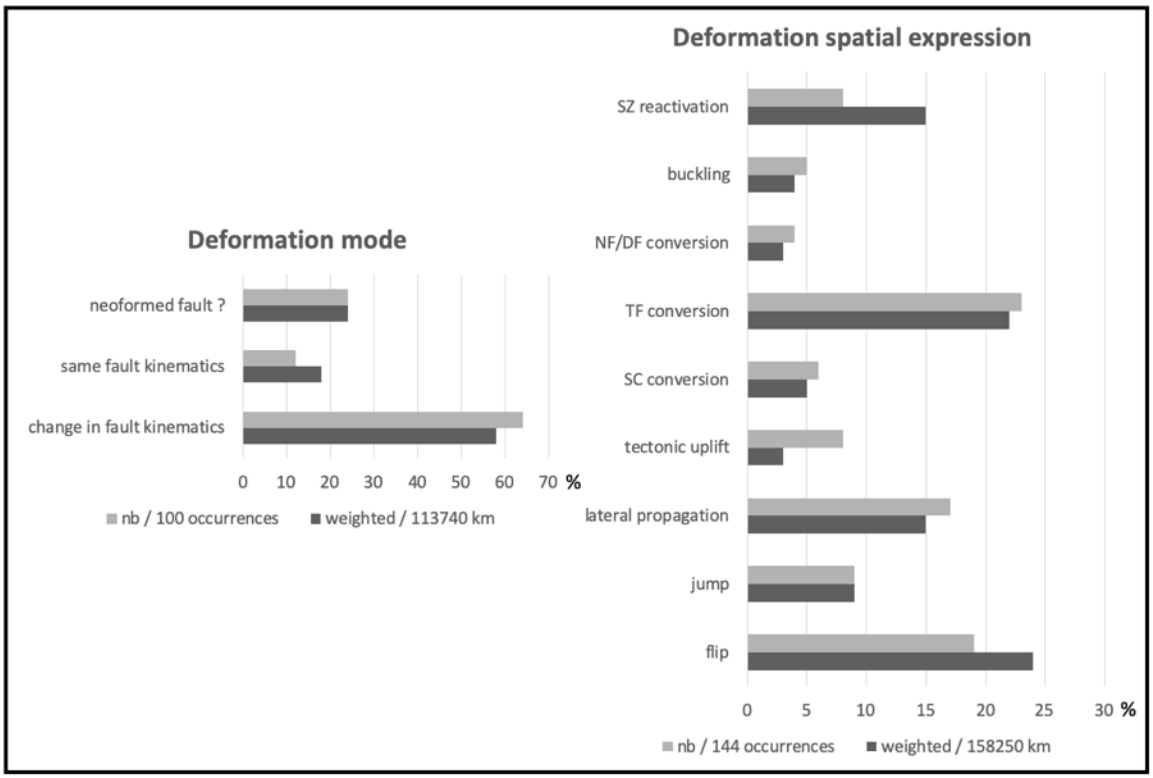

Fig.21: Distribution of compression localization modes and spatial expressions among SISs during the Cenozoic. See Fig.19 for more explanations. Percentages of cases or cumulated length on x-axes.

4.6.8. Respective age of subducting and overriding plates at SI

Excluding the oceanic plateaus or ridges which are buoyant (7 cases among 70, see P and R in Fig.22), the ages of the subducting plates (SP) at SI onset regularly distribute from 140 Myr (Gibraltar, SW-Iberia, Calabria, Samoa-Gilbert-Ralik) to 0 Ma (D'Entrecasteaux Zone, Loyalty-Three Kings). The subducting plate at SI onset was younger than 20 Myr for twenty-one cases (30%), younger than 40 Myr for thirty-five cases (50%), leading us to the conclusion that the subducting plate at initiation doesn't need to be old (Fig.22).
The age of the overriding plate is less easy to characterize because it consists, in two thirds of the study cases, of continents, arcs or plateaus which are intrinsically not prone to subduction. The age of the 22 remaining overriding oceanic plates (OP) at SI onset regularly distributes from 175 Myr (SW-Iberia) to 0 Myr (D'Entrecasteaux Zone, Loyalty-Three Kings). Seven of them were older than 67 Myr, attesting that they did not subduct despite their old age. In terms of age contrast between the subducting and overriding plates, it is almost equally distributed with positive and negative age contrasts. The SP is significantly younger than the OP at SI for SW-Iberia and Gagua-E-Luzon Trough and possibly Mussau depending on the authors (see section 3.1), slightly younger for C-Indian Ocean, Bowers Ridge and Hjort. The SP is significantly older than the OP at SI onset for Romanche, Gibraltar, Palau, Lyra and Cascadia, slightly older for Yap (Fig. 22). It is interesting to note that the ages of the converging plates are very close to each other within a few Myrs (small age offsets) in at least 10 of 22 sites.

Some cases were excluded like IBM or Matthew & Hunter because more than 50% of the overriding plate is composed of arc relics intermingled with very young oceanic basins. In both cases, the subducting plate is older than the very young oceanic basins opening throughout the relic arcs in the overriding plates.

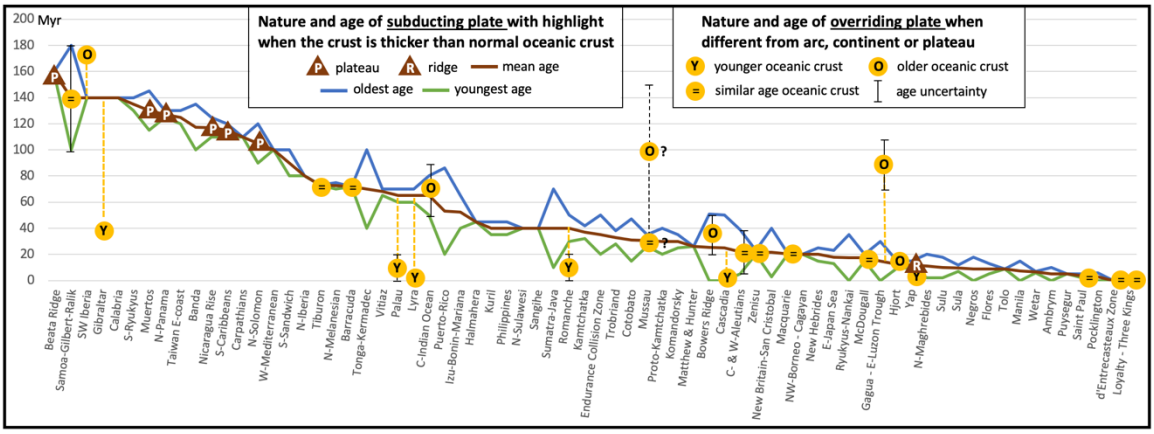

Fig.22: Distribution of ages of subducting plates in Myr and in descending order. When the oceanic crust is thicker than normal, the label P or R means plateau or ridge. A majority of overriding plates have an arc or a continental composition. For those having a typical oceanic composition, their age appears with yellow dots. O, Y and = mean that the overriding plate is respectively older, younger or has a similar age than the subducting plate.The length of the yellow dotted lines increases with the age offset between the overriding and the subducting oceanic plates.

4.6.9. State of stress at SI

The state of stress and the obliquity of convergence at initiation are difficult parameters to assess because they are model-dependent, assuming that models exist, which is not the case for several of the regions studied. We have therefore opted for a reading and interpretation of the literature reporting geological facts at the time of initiation allowing a rough estimate of the state of stress and the obliquity of convergence. All the sources used are listed in the table provided in the supplementary table. Given these uncertainties, we can say that the stress field at SI is compressive in 90% of the study cases as well as in terms of cumulated trench-length (Fig.23, panel 1). Moreover, no extensional stress was reported at SI but we recognize the difficulty to ascertain the state of stress at subduction initiation in the remaining 10%.

4.6.10. Azimuth and rate of convergence at SI

The direction of convergence at SI is supposed to be oblique in 59/52*% of cases, normal in 26/23*% of cases and unknown in the remaining 15/25*% of the cases.
The normal component of the convergence velocity at SI is estimated in only half of the study cases. When estimated, it is < 4 cm/yr in 83% of cases, < 6 cm/yr in 14% of cases and surprisingly reached 15 cm/yr in Sumatra-Java (Zahirowicz et al., 2014).

5. Discussion

5.1 Limits of the statistical approach and assets of the method

Compiling the events where SI is suspected is a huge challenge, even restraining the study to the Cenozoic, and no doubt that other investigators would obtain a different picture of the situation, but we trust that these differences would be minor. Surprisingly, our findings are often similar to those of Crameri et al. (2020a) despite the fact that the respective methodologies and criteria for selecting incipient subduction zones are significantly different. Only a thorough analysis of each of these studies can seriously compare the results. Reconstructions of past SI settings are often based on little evidence or models, but new evidence may arise and models are sometimes too simplistic. To overcome the perceptual difference between authors, we have decided to mention most hypotheses and often account for many of them that we consider plausible rather than choosing one scenario. By doing that, we have artificially multiplied some characters like the triggers for SI but we considered that it was the least bad option to reveal the uncertainties on some particular events. However, we were quite demanding on the definition of each maturation stage with due regard to the physics of the processes of SI (see sections 1.3 & 2), so that each studied case belongs to a single state (Figs. 3 & 16). In the same vein, our terminology for the settings, triggers or deformation modes for example (see section 4) may differ from other authors. We have, for example, extended the significance of the term OCT which generally means ocean-continent transition to the transition between an ocean and a continent, an arc or a plateau, by renaming it as OT (oceanic transition).
Plate tectonics is a continuous process meaning that some subduction zones initiated before the Cenozoic while others, which were initiated during the Cenozoic, are still ongoing. We thus face the same difficulty as seismologists trying to assess the

occurrence of great earthquakes, based only on instrumental records over the last century. We have decided to isolate the Cenozoic period for our quantitative analysis. Thus, we do not consider SZs initiated prior to the Cenozoic. Measuring the length of a subduction may depend on its age with respect to the time of its initiation if it propagated laterally, or vice versa if part of it has disappeared. We generally kept the present-day length of the subduction trenches. By doing this, we obviously introduce a bias in our statistics.

We chose to study SZ initiations occurring both at present-day and in the near past. The bunch of active Cenozoic SISs is made of 30 immature cases and 18 cases having already reached the self-sustained state. Since the evolution of the 30 immature SI events cannot be definitely stated, one could have concluded that the minimum rate of success of SI was approximately a bit more than 1/3, by assuming systematic abortion for the unknown SI fates in a conservative way. By also considering all SZ initiations beginning and ending during the Cenozoic, the SI rate of success rises to 72/89*% (section 4.6.4). This example highlights the advantages of having taken into account both ongoing and completed SZ initiations. Studying completed SZ initiation vallows for having a comprehensive view of the SI process, but the rather old age of these SISs implies that numerous crucial details of the conditions prevailing during the different stages of the SI process have been removed or overprinted through time, for instance when erased by the tectonic erosion of the initial forearc lithosphere. In contrast, SISs still active at present-day allow for a careful study to unravel the mechanisms involved in the immature stages of SI, but prevent from clearly forecasting the next stage (success or failure). We have designed an integrated approach offering a way to simultaneously limit all these drawbacks.

5.2 Initial settings and importance of rheological discontinuities

With regard to the importance of the SI phenomenon, we confirm the assertion by Gurnis et al. (2004) that about one half of the present-day mature SZs were initiated during the Cenozoic when counting their cumulative trench-lengths (~30,000 km). In our classification, about two thirds of the SZs initiate at the transition between an ocean and a continent, an arc or a plateau (OT). This result may seem to contradict some previous studies which concluded that SI in intra-oceanic settings prevailed. Mueller and Phillips (1991) predicted, for example, that transform faults and fracture zones - especially when sitting nearby a mature subduction zone where a buoyant feature is colliding - should represent the most likely sites of trench formation because of their intrinsic weakness. Gülcher et al. (2019), draw on the Middle Jurassic Neotethys case and 3D thermomechanical modeling to promote the role of intraoceanic extensional detachment faults which represent less than 3% of our Cenozoic settings. , based on the study of thirteen SZ initiations (2 or 3 of them being older than Cenozoic), concluded that they occur dominantly within oceanic plate settings in the presence of pre-existing volcanic arcs. They also indicate that SZs preferentially form within 1500 km (often less than 500 km) of a pre-existing plate weakness, while our study focuses on the nucleation zone sensu-stricto. Looking into more details, part of the discrepancy may come from the

respective definitions of oceanic settings and transition with an ocean (OT). Therefore, the comparison with other studies is not straightforward.
Using large-scale simulations of mantle convection featuring self-consistent plate-like lithospheric behaviour, Ulvrova et al. (2019) predicted that periods of continental dispersal, as the last ~100 Myr, are more favourable to SI close to continental margins. This is well-illustrated by the Cenozoic SISs distribution in Figs. 4-11. This tends to indicate that there are certainly periods prior to the Cenozoic when SI in intra-oceanic settings (understood far from the continents) were more frequent, especially those with supercontinents.

Our results also confirm the conclusions of most authors (e.g., Niu et al, 2003; Stern & Gerya, 2018; Gurnis et al., 2019) that large compositional differences or density contrasts favor SI if compressional stress occurs. Indeed, the great majority of the Cenozoic subduction zones are initiated either at an OT or active plate boundaries such as spreading centers. The Central Indian Ocean is a good illustration of a case where subduction is still at an incipient-diffuse stage after 9 Myr while the plate has probably been pre-stressed since ~35 Myr at the onset of the India-Eurasia collision. This slowness in the SI process may result from the absence of a pre-existing arc south of the collision zone and the orientation of the rifted margin southwest and southeast of India which might not be prone to host the future plate boundary (Zhong & Li, 2020). Even the physical models need a seed to localize the deformation within a homogeneous lithosphere under compression (Shemenda, 1992; Gurnis et al., 2004). Furthermore, the deformed area includes a pure shortening zone south of Ceylan around the Afanasy Nikitin Chain and a pure strike-slip zone within the Wharton Basin along the Ninety East Ridge accommodating the trenchward acceleration of Australia with respect to India (Delescluse et al., 2007). This shows that even in the absence of large compositional differences in intra-oceanic settings, weak zones are localizing the deformation as noted by most authors (e.g., Crameri et al., 2020a). According to Stern and Gerya (2018), large lateral density contrasts across profound lithospheric weaknesses of various origin favored spontaneous SI without pre-existing plate motion in opposition to induced SI. Here, we show that not only large compositional differences but also lithospheric weaknesses are crucial in forced SI settings. Indeed, more than 64/58*% of the deformation occurred via a change in pre-existing fault kinematics (see section 4.6.7).

There are countless examples in the literature where it is said explicitly or implicitly that old oceanic plates are more prone to subduction than young ones, generally arguing that their excess mass with respect to the underlying asthenosphere makes the difference. This statement is not true any more than saying that the slab dip increases with the slab age because of increasing slab pull (Lallemand et al., 2005). During the Cenozoic, the subducting plate was less than 40 Myr old at subduction onset in half of the cases. Interestingly, this age of ~40 Myr was suggested to be the threshold at which a cooling oceanic lithosphere can become denser than the underlying upper mantle (see section 1.3.5.1). This observation, as well as the lack of correlation between slab dip and age, show that prediction of which oceanic plate will subduct, or which dip angle will

characterize a slab of a given age, does not simply depend on gravitational forces. Furthermore, in many cases, the SI was successful and reached self-sustainability, even for an extremely young incoming plate at the onset of initiation (e.g., Loyalty-Three Kings). This suggests that the conditions prevailing at SI do not always govern the ones that will characterize the SZ at a later stage. In other words, it may not be straightforward to predict the final "fate" of a SIS by looking only at the age of the incoming plate at initiation (Gurnis et al., 2004). The Gagua Ridge, a former fracture zone juxtaposing an Early Cretaceous oceanic basin with an Eo-Oligocene basin, is an emblematic example. Despite an age contrast of more than 70 Myr, the younger basin subducted beneath the older one (Deschamps et al., 1998; Eakin et al., 2015; Qian et al., 2021). Zhong & Li (2019), based on numerical modeling, concluded that SI at a passive margin (understood rifted margin adjacent to a continent), representing nearly 30% of our Cenozoic cases, is not easy and requires special conditions. They go on to say that it is easier for younger oceanic plates to subduct at a passive margin under a given boundary force. Our analysis shows that for 66/60*% of the studied cases, the subducting oceanic plate at a rifted margin (including those adjacent to oceanic arcs) was younger than or equal to 40 Myr. Hall (2018) observed that marginal basins are the right place for initiating new SZ and their age doesn't matter. From the compilation shown in Fig.22, we observe as many cases where an old oceanic plate starts to subduct beneath a younger one than the opposite (Fig. 23, panel 2). It is likely that rheological contrasts may be a key ingredient not only to localize deformation, but also to select the easier plate (by minimizing the necessary energy) to deform, to strongly bend, and finally, to subduct. The subduction polarity might similarly result from a complex competition between (1) the respective ability of the two adjacent plates to be sheared on one hand, and to bend on the other hand, (2) their relative density contrast, and (3) the distribution of a weaker component located between them (typically, an inherited TF or a inherited arc), and the amount of rheological weakness that it represents with respect to the two lithospheres.

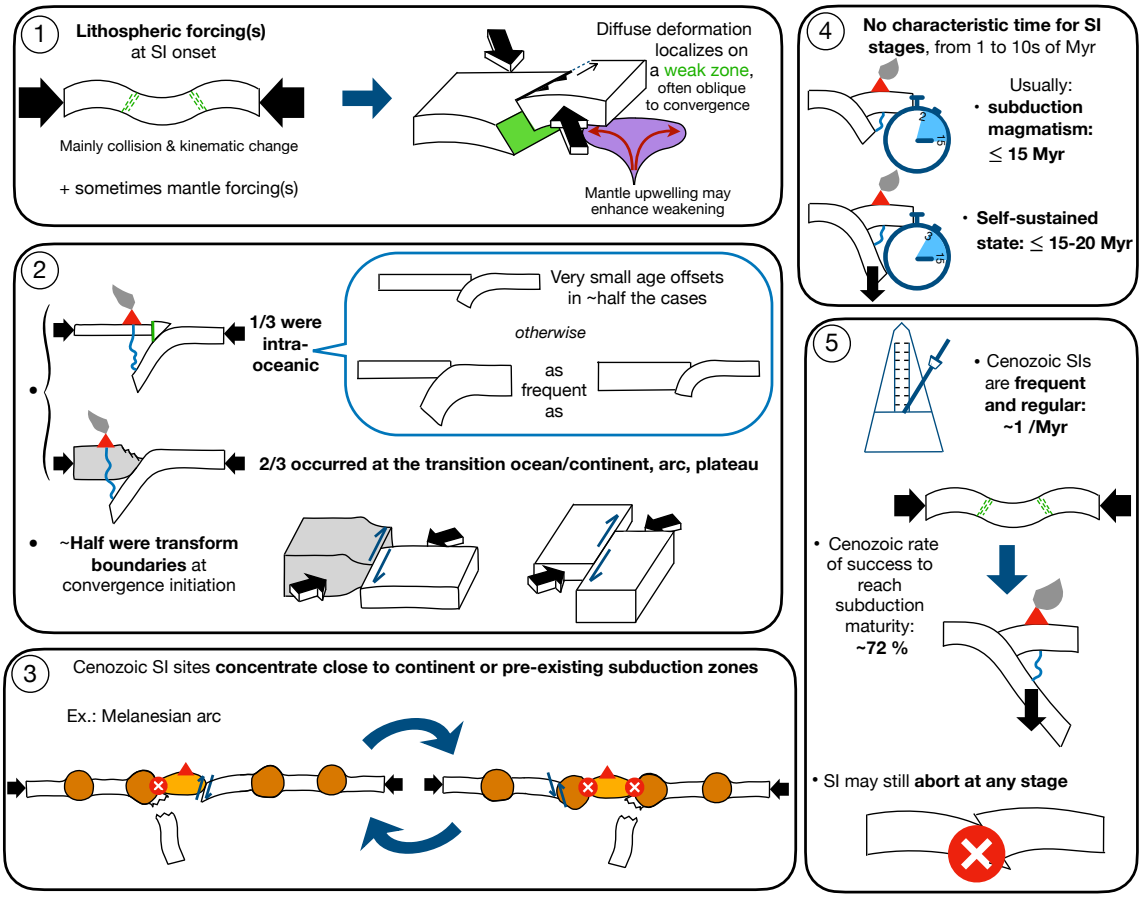

Fig.23: Graphical summary of the main results inferred from the compilation of 70 Cenozoic SISs, regarding the stress state at subduction onset and the main factors involved in deformation localization (1), the characteristics of the most frequent geodynamic settings of SI (2, 3), the critical time ranges the most frequently compiled (4), and the main characters suggesting the relative easiness of the SI process (5). See the captions of Figs. 1 and 14 for legend details.

5.3 Lithospheric forcings are necessary conditions

Supporting the conclusion of Crameri et al. (2020a) for the last ~100 Myr, our study highlights the prevalence of lithospheric forcing in the process of SI (Fig. 23, panel 1), collisions and kinematic changes being the main triggers far beyond delamination or sedimentary loading (Fig. 20). This doesn't exclude additional mantle forcings in many situations, but we show that these forces are just not enough to overcome the lithospheric resisting forces in the absence of compressive stress. Arcay et al. (2020), based on numerical simulations and natural examples, have demonstrated that spontaneous instability, even for a thick old oceanic plate at a TF evolving into a mature subduction, is unlikely in modern SI. By concluding this, they confirm McKenzie (1977) or Mueller and Phillips (1991) analytical predictions. Our conclusions differ significantly from those of Stern and Gerya (2018) who describe the two modes of SI with a large emphasis on the spontaneous mode in opposition to the induced one. We have discussed in section 1.2 the reasons for this discrepancy and specifically the overemphasis made by several authors on the IBM case while it represents only one over 70 Cenozoic cases. The fact that subduction cannot "spontaneously" initiate at an

oceanic TF in a modern Earth, even with a large age contrast, is attested by the failure of Cenozoic SI attempts even with moderate lithospheric forcings (Romanche, Lyra). Arcay et al. (2020) stated that the rheological necessary conditions to overcome the lithospheric resistance might have existed on a hot Earth during the Archean.

5.4 Multiple forcings favor subduction initiation

SI often results from a combination of two or more triggers. Collisions at pre-existing trenches often go along with kinematic changes at least at a local scale. Slab breakoff may follow soon after the collision, increasing the compressive stress within the colliding plates. Deformation then localizes at the most favourable nearby site either on the opposite side of the upper plate volcanic arc (flip) or less frequently back of the lower plate buoyant feature (jump or transference for some authors). The detachment and further sinking of the slab trigger a return asthenospheric flow which may indirectly contribute to the process of SI. This situation is presently observed beneath the Coastal Range east of Taiwan (Gautier et al., 2019) or beneath Sicily (Garzanti et al., 2018). The development of STEP Faults may also constitute an instance of multiplication of triggering forces that may lead to SI. Cenozoic natural examples include the North Maghrebides south of the Alboran Sea, the South Caribbeans south of the Grenada Basin, Matthew & Hunter region, the South Sandwich region or even the Southernmost Ryukyus. The relative plate motion may change with time from a direction parallel to the STEP Fault at initiation to an oblique converging direction across the strike-slip fault, allowing the existing subduction trench to propagate laterally (Matthew & Hunter, S-Ryukyus, see the next section) (Lallemand et al., 1997; 2001; Patriat et al., 2015). Sometimes, the lithospheric mantle of the continental plate can be entrained downward by the subducting oceanic plate resulting in its delamination in the vicinity of the plate boundary (Levander et al., 2014; van de Lagemaat et al., 2021). The thinning of the continental plate margin by delamination, as well as the specific mantle convection near the STEP fault, may create favourable conditions for SI as in the N-Maghrebides (Hamai et al., 2018; Aïdi et al., 2018) or the S-Caribbeans (Kroehler et al., 2011; Ayala et al., 2012). The presence of a plume or an active spreading-center is mentioned sometimes near or not far from a SI site. Some authors considering that it is the main trigger of SI like in Cascadia in Eocene or the Caribbeans in Cretaceous (Whattam and Stern, 2015; Stern and Dumitru, 2019), others that it is a secondary facilitating factor (Schmandt and Humphreys, 2011; Pindell and Kennan, 2009; Boschman et al., 2019), the main one being the plateau collision followed by a jump of the subduction zone. Whatever be the case, the proximity of a plume head or a spreading center at the start of SI in several cases (IBM, Cascadia, Manila, Negros, Yap, Palau, Lyra, Mussau, Pocklington, Matthew & Hunter, Loyalty - Three Kings, Saint Paul) certainly contributes in the weakening of the candidate plate for SI, possibly through heat conduction and magmatic fluid percolation (Fig. 23, panel 1). However, all these sites were subject to compressive stress often as a result of collisions or kinematic changes.

5.5 Oblique convergence facilitates subduction initiation

Notwithstanding the difficulty to precisely estimate the direction of the compressive stress with respect to the trend of the incipient subduction zone at the time of initiation,

the literature generally provides enough indications to state that it is oblique in the majority of cases (see section 4.6.10). This is not surprising if we consider that, by definition, the conversion of a TF or a transform margin to a subduction zone is progressive as observed nowadays for example along the Macquarie Ridge system from New Zealand to Hjort. The cumulative trench-length of the transform boundaries (oceanic TFs and transform margins) reaches 30910 km, i.e., 42/48*% of the total Cenozoic SI trench-length (Fig. 23, panel 2). On top of these initially-transform cases, there are many other cases where convergence obliquity prevailed (see attached supplementary Table). We analyze the importance of this character as an efficient catalyst for lateral propagation of the deformation as for example in the case of the growing Puerto-Rico SZ as the Caribbean plate obliquely overrides the North American plate.

5.6 Some regions are more prone to initiate multiple subduction cycles

Like many authors, we observe that SIs concentrate in specific areas often close to continents or pre-existing subduction zones (Ulvrova et al., 2019; Crameri et al., 2020a, Fig. 23, panel 3). This may be interpreted in two ways. One explanation could be the density of rheological discontinuities or weak zones there in opposition to the middle of the ocean. Another explanation has been suggested by Gurnis et al. (2004) who noticed that cumulative convergence, not the rate of convergence, is the dominant control on the force balance during SI. Their conclusion was based on numerical simulations. They explained that the force required for one plate to underthrust another depends on the elastoplastic state (i.e. total convergence), not the viscoelastic one (with pre-existing faults). A good example of a region prone to host a SZ is the Melanesian Arc. This arc has recorded alternative N- and S-dipping subduction zones throughout the Cenozoic starting with the E-Australian S-dipping subduction followed by the New Guinea - Pocklington N-dipping subduction, then by the N-Melanesian-Vitiaz S-dipping subduction, and finally by the New Britain - San Cristobal - New Hebrides N-dipping subduction (Petterson et al., 1999; Mann & Taira, 2004; Schellart et al., 2006; Schellart and Spakman, 2015). These successive flips of SZs across the composite arc mostly resulted from plateau or arc collisions which shutdowned the previous SZs.
It is noteworthy that more than two thirds of the subduction zones (67/70*%) were initiated in the West Pacific during the Cenozoic**.** This region also hosted most of the backarc basins during the same period suggesting either a common cause or a causal effect between the two. Gurnis et al. (2004) already noticed this common occurrence and proposed that back-arc extension might happen shortly (several tens of Myr) following SI. Their conclusion was supported by numerical models characterized by a high strain weakening factor and an upper plate without much strain resistance (nearly asthenosphere), making the causal effect questionable. The causal relation between SI and back-arc spreading has also been noticed by Faccenna et al. (2010) who suggested that magmatic pulses, prone to facilitate back-arc spreading, could originate from plumes triggered by the conjunction of newly formed facing SZs reproducing the scenarii of the North-Fidji and West-Philippine basin formation for example. In this study, the question should be phrased the other way: could the presence of young back-arc basins favor sideways SI? although these questions look like a chicken and egg problem, i.e.,

large rheological contrast between a young and old oceanic lithospheres favors strain localization and eventually SI under appropriate boundary forces, then the slab acceleration with increasing slab pull induces both a rollback and extension in the upper plate if some conditions are fulfilled (Arcay et al., 2008; Lallemand et al., 2008). Hall (2018), after detailed investigations of the eastern Sundaland region, observed that the main feature making this area the most active in terms of SI was a significant topographic difference between continent and ocean because of the anomalous larger depth of the marginal basins there. Subduction then commonly nucleates at the edge of an ocean basin close to a region of young arc magmatism. However, to reach a mature subduction stage, the thrust needs to cut through the entire lithosphere and a minimum lateral extent is needed (Hall, 2018). In this study, only three SZs narrower than 500 km reached maturity: Gibraltar (200 km), Palau (220 km) and Bowers Ridge (380 km). Gibraltar and Palau were part of a much wider subduction at the time of their initiation. Back to the first observation that a majority of SI occurred in the Western Pacific during the Cenozoic, one may suspect a large contribution of far-field tectonic forces resulting from the India-Eurasia collision (Jolivet et al., 2018) with strain localization where the largest density contrasts prevailed. The same happened when the Australia plate accelerated its northward motion and collisions occurred between its northern margin and eastern Sundaland in the Early Miocene (Hall, 2002; Zahirovic et al., 2016). This may also provide an explanation about the lower SI rate during the Oligocene (see section 4.6.1).

5.7 Factors likely to prevent SI success

A review of the eleven aborted Cenozoic cases shows that the SI process may cease at any stage (Fig. 16), regardless of the geodynamic setting or the deformation mode but with a dominance of transform settings. No additional mantle forcing, likely to help in the SI, was mentioned for those cases, indicating that lithospheric forcing (basically, nearby collision and kinematic changes) may not be sufficient.
The other most striking features that characterize SI failure are the following. Note however that a counterexample (having led to SI success) can be found for all criteria. When the convergence speed prevailing during incipient subduction could be inferred (5 cases: Beata Ridge, Romanche, Tiburon, N-Iberia, Nicaragua Rise), it appears that subduction abortion is systematically associated with slow (< 3 cm/yr) or very slow (<~5 mm/yr) convergence. This recalls that cold material advection competing against thermal assimilation must occur fast enough (>1 cm/yr) to be sustained (e.g., McKenzie 1977, see section 1.3.2). Subduction cessation occurring during the incipient stages is mainly observed when the subducting plate is significantly old (≥ 65 Myr, Romanche, N-Iberia, Tiburon, Lyra, Fig.21) sometimes also holding an oceanic plateau (Beata Ridge, Muertos). A significantly old incoming plate might thus be a hindering factor in some specific situations, possibly because it corresponds to a rather thick, cold and stiff lithosphere that cannot easily bend. Gibraltar or Calabria are, however, SI events where the subducting plate was thick without yielding SI failure. In contrast, SI stopped later (achieved SI stage) even for young subducting plates (Komandorsky, D'Entrecasteaux Zone). The overring plate is expected to be particularly thick in 9 cases of subduction

abortion, either because of the presence of an arc, continent or oceanic plateau, or of the age of the upper plate when typically oceanic (>70 Myr). This could underline the hindering effect of the overriding plate thickness, that rises the total amount of friction and shearing along the forming subduction plane. Nonetheless, it is not a systematic impeding parameter since Proto-Kamchatka and Endurance Collision zone including a thick upper plate (arc, continent) at SI onset reached the self-sustained stage (Fig. 16).

We notice that SI can also abort for young (<30 Myr old) and relatively thin overriding plates (D'Entrecasteaux Zone, Lyra, Romanche). Finally, we look at the plate age offset at the SI beginning when it could be defined, i.e. when both converging plates were typically oceanic (5 cases: Gagua, D'Entrecasteaux, Lyra, Romanche and Tiburon). It comes out that SI stops when the plate age offset is either very low (~0 Myr, 2 cases) or perhaps too high (≥ 50 Myr, 3 cases). These two extreme situations may thus be unfavorable regarding SI success. We acknowledge that other SI cases with similar plate age offsets succeeded in reaching the self-sustained stage (such as C- & W-Aleutians or Gibraltar, for extreme plate age offsets of ~0 Myr and >100 Myr, respectively).

To conclude, we do not identify unique and basic characteristics sufficient to stop SI when acting alone. The failure of a SI seems to result from a combination of hindering parameters (cooling, frictional resistance …) including insufficient external engines, possibly yielding a too low convergence velocity, and unfavorable plate ages.

Lastly, as aforementioned in section 4.6.3, the duration of the last SI stage when it aborted was usually longer than its equivalent one when it succeeded (Figs. 17 & 18). As discussed in section 4.6.3, the South Caribbeans again appear as an outlier, having reached the achieved SI stage since the Paleogene but being still active, whereas the longest aborted achieved SI case: D'Entrecasteaux Zone, occurred in the Oligocene. The S-Caribbeans case was not classified into the mature group, despite a slab longer than 800 km because we considered that the subduction of the buoyant Caribbean Plateau is sustained by far-field forces (relative plate motions between the Caribbean and America plates), rather than being self-sustained, according to our definition (see section 2).

5.8 No rule but a trend for SI to succeed

The total number of SISs and their rate of success, estimated from the Cenozoic occurrences only, are surprisingly high with ~95/98*% of success in localizing the shortening once enough compressive deformation is undergoing throughout a heterogeneous oceanic lithosphere, shrinking to ~83/92*% for the next stage of infant magmatism and to ~72/89*% for the final mature stage. Such high values denote the

propensity of the oceanic lithosphere to bend under normal conditions prevailing in the modern Earth and to develop a self-sustained SZ.

Except for a few outliers, most immature SZs are younger than 15 Myr (83%, Fig. 17). Furthermore, we have seen in section 4.6.2 that the shortest time taken by a Cenozoic SZ to reach the mature stage was ~3-8 Myr. We thus conclude that, most of the time, 3 to ~15 Myr are required for a SI to succeed (Fig. 23, panel 4). Values found in the literature for initiating a subduction generally fall in this range. Based on numerical models adapted for the case of the IBM trench inception from a TF, Leng et al. (2012) proposed a protracted period of ~10 Myr before the subduction reached the achieved state (infant magmatism). Similarly, Zhong and Li (2020), also based on numerical modeling, proposed the same duration after collision in a case of subduction jump, but they also specify that the SI process is strongly dependent on the convergent boundary force and weakly on the age of the lithosphere when a weak shear zone is imposed at the OCT.

6. Conclusion

The comprehensive examination of Cenozoic candidates for an initiation of subduction regardless of its fate lead us to the following conclusions:

- SI cases are frequent throughout the Cenozoic, with a mean rate of slightly more than once every Myr.
- Two thirds of them were completed in the Western Pacific area, close to the continents and/or pre-existing subduction zones. Even the intra-oceanic Samoa-Gilbert-Ralik system or the Macquarie Ridge Complex are connected at one of their edges with an arc or a continent.
- The rate of success from incipient to mature SZ exceeds 70%.
- It generally takes 3 to 15 Myr for a candidate area for subduction to reach the self-sustained stage.
- About half of the initial geodynamic settings were transform boundaries, either intra-oceanic or fringing continents.
- Lithospheric forcing is ubiquitous in the vast majority of the study cases, collision and kinematic changes being the main triggers.
- Multiple forcings including mantle forcings are very common, the proximity of a plume or a spreading-center being conspicuously a facilitating factor, but always within a compressional regime, oriented oblique to the nascent plate boundary in more than half of the cases.
- Large compositional, topographical differences and/or lithospheric weaknesses foster SI.
- Kinematic inversion of pre-existing faults is observed in ~60% of cases.
- Young oceanic plates are more prone to start subduction due to their smaller rigidity.
- The observation of SISs in the Cenozoic shows us that age contrast between convergent oceanic plates at initiation is often small and, if not, both situations (young beneath old or vice versa) are observed equally.

- Failure in SI results from a combination of hindering parameters (lithospheric strength, frictional resistance, unfavorable age contrasts for intra-oceanic SI,…) and insufficient external forcings probably yielding a too low convergence velocity.

Acknowledgements: Michel Peyret and Anne Delplanque provided assistance in the making of artworks by preparing the digital background topo-bathymetric file for the maps and making the final adjustments. We thank Fanny Garel and Sarah Abecassis for the times of sharing at the start of the project as well as all colleagues and friends with whom we had vigorous discussions on the Caribbean, Mediterranean or Western Pacific geodynamics, or "simply" models. We would like to thank Douwe van Hinsbergen and the reviewers, especially Fabio Crameri who devoted a lot of time to a thorough review of our study. Thanks to him, we have clarified our terminology in the hope that it will be clear to the reader. Finally, thanks to Tim Horscroft for his confidence when he invited the first author to submit this work to this journal.

Funding: The seeds of this research benefited from the SYSTER Program support of the CNRS-INSU funding agency in 2015 and 2016.

References

Abbott, M.J., Chamalaun, F.H., 1981. Geochronology of some Banda Arc volcanics. In: Barber, A.J., Wiryosujono, S. (Eds.), The Geology and Tectonics of Eastern Indonesia: Geological Research and Development Centre, Bandung, Special Publ. 2, 253–268.

Abratis, M., Wörner, G., 2001. Ridge collision, slab-window formation, and the flux of Pacific asthenosphere into the Caribbean realm. Geology 29 (2), 127-130.

Afonso, J. C., Ranalli, G., Fernández, M., 2007, Density structure and buoyancy of the oceanic lithosphere revisited, Geophys. Res. Lett., 34, L10302, doi:10.1029/2007GL029515.

Agard, P., Yamato, P., Soret, M., Prigent, C., Guillot, S., Plunder, A., B. Dubacq, A. Chauvet, Monié, P., 2016. Plate interface rheological switches during subduction infancy: Control on slab penetration and metamorphic sole formation. Earth Planet. Sci. Lett., 451, 208-220.

Agard, P., Prigent, C., Soret, M., Dubacq, B., Guillot, S., Deldicque, D., 2020. Slabitization: Mechanisms controlling subduction development and viscous coupling. Earth Sci. Rev. 208, 103259. https://doi.org/10.1016/j.earscirev.2020.103259.

Aïdi, C., Beslier, M., Yelles-Chaouche, A. K., Klingelhoefer, F., Bracene, R., Galve, A., Bounif, A., Schenini, L., Hamai, L., Schnurle, P., Djellit, H., Sage, F., Charvis, P., Deverchère, J., 2018. Deep structure of the continental margin and basin off Greater Kabylia, Algeria: New insights from wide-angle seismic data modeling and multichannel seismic interpretation. Tectonophysics 728–729, 1–22. https://doi.org/10.1016/j.tecto.2018.01.007.

Aitken, T., Mann, P., Escalona, A., Christeson, G., 2011. Evolution of the Grenada and Tobago basins and implications for arc migration. Mar. Petrol. Geol. 28 (1), 235–258. https://doi.org/10.1016/j.marpetgeo.2009.10.003.

Allen, R. W., Collier, J. S., Stewart, A. G., Henstock, T., Goes, S., & Rietbrock, A., 2019. The role of arc migration in the development of the lesser Antilles: A new

tectonic model for the Cenozoic evolution of the eastern Caribbean. Geology 47 (9), 891–895. https://doi.org/10.1130/G46708.1.

Alvarez-Marron, J., Rubio, E., Torne , M., 1997. Subduction- related structures in the north Iberian margin. J. Geophys. Res. 102, 22497–22511.

Arcay, D., 2017. Modelling the interplate domain in thermo-mechanical simulations of subduction: Critical effects of resolution and rheology, and consequences on wet mantle melting, Phys. Earth Planet. Inter., 269, 112–132, https://doi.org/10.1016/j.pepi.2017.05.008.

Arcay, D., Lallemand, S., Doin, M.-D., 2008. Back-arc strain in subduction zones : Statistical observations vs. numerical modeling. Geochem. Geophys. Geosyst. 9, Q05015. doi:10.1029/2007GC001875.

Arcay, D., Lallemand, S., Abecassis, S., Garel, F., 2020. Can subduction initiation at a transform fault be spontaneous? Solid Earth 11, 37–62.

Arculus, R. J., Ishizuka, O., Bogus, K. A., Gurnis, M., Hickey-Vargas, R., Aljahdali, M. H., Bandini-Maeder, A. N., Barth, A. P., Brandl, P. A., Drab, L., do Monte Guerra, R., Hamada, M., Jiang, F., Kanayama, K., Kender, S., Kusano, Y., Li, H., Loudin, L. C., Maffione, M., Marsaglia, K. M., McCarthy, A., Meffre, S., Morris, A., Neuhaus, M., Savov, I. P., Sena, C., Tepley III, F. J., van der Land, C., and Yogodzinski Zhang, G. M., 2015. A record of spontaneous subduction initiation in the Izu-Bonin-Mariana arc, Nat. Geosci. 8, 728–733, https://doi.org/10.1038/ngeo2515.

Arden, D.D., 1975. Geology of Jamaica and the Nicaragua Rise. In: Nairn A.E.M., Stehli F.G. (eds) The Gulf of Mexico and the Caribbean. Springer, Boston, MA. https://doi.org/10.1007/978-1-4684-8535-6_14.

Arndt, N., 2003. Komatiites, kimberlites, and boninites. J. Geophys. Res.108 (B6), 2293. doi:10.1029/2002JB002157.

Audemard, F. A., Castilla, R., 2016. Present-day stress tensors along the southern Caribbean plate boundary zone from inversion of focal mechanism solutions: A successful trial. J. South Am. Earth Sci. 71, 309-319. doi.org/10.1016/j.jsames.2016.06.005.

Authemayou, C., Pedoja, K., Heddar, A., Molliex, S., Boudiaf, A., Ghaleb, B., Van Vliet Lanoe, B., Delcaillau, B., 2017. Coastal uplift west of Algiers (Algeria): Pre and post Messinian sequences of marine terraces and rasas and their associated drainage patterns. Int. J. Earth Sci. 106, 19-41. DOI 10.1007/s00531-016-1292-5.

Auzemery, A., Willingshofer, E., Yamato, P., Duretz, T., Sokoutis, D., 2020. Strain localization mechanisms for subduction initiation at passive margins. Global and Planetary Change 195, 103323, doi: 1016/J.gloplacha.2020103323.

Auzende, J., Lafoy, Y., Marsset, B., 1988. Recent geodynamic evolution of the north Fiji basin (southwest Pacific). Geology 16, 925– 929.

Ayala, R. C., Bayona, G., Cardona, A., Ojeda, C., Montenegro, O. C., Montes, C., Valencia, V., Jaramillo, C., 2012. The paleogene synorogenic succession in the northwestern Maracaibo block: Tracking intraplate uplifts and changes in sediment delivery systems. J. South Am. Earth Sci. 39, 93-111. doi:10.1016/j.jsames.2012.04.005.

Baes, M., Govers, R., Wortel, R., 2011. Subduction initiation along the inherited weakness zone at the edge of a slab: insights from numerical models. Geophys. J. Int. 184, 991–1008.

Baes, M., Gerya, T., Sobolev, S. V., 2016. 3-d thermo-mechanical modeling of plume-induced subduction initiation. Earth Planet. Sci. Lett. 453, 193– 203.
Baes, M., Sobolev, S., 2017. Mantle Flow as a Trigger for Subduction Initiation: A Missing Element of the Wilson Cycle Concept. Geochem. Geophys. Geosyst. 18, 4469–4486. https://doi.org/10.1002/2017GC006962, 2017.
Baes, M., Sobolev, S. V., Quinteros, J., 2018. Subduction initiation in mid-ocean induced by mantle suction flow. Geophys. J. Int. 215, 1515–1522. doi: 10.1093/gji/ggy335.
Baes, M., Sobolev, S., Gerya, T., Brune, S., 2020. Plume-induced subduction initiation: Single-slab or multi-slab subduction?. Geochemistry, Geophysics, Geosystems 21, e2019GC008663. https://doi.org/10.1029/2019GC008663.
Baldwin, S.L., Fitzgerald, P.G., Webb, L.E., 2012. Tectonics of the New Guinea region: Ann. Rev. Earth Planet. Sci. 40, 495–520. doi: 10 .1146 /annurev-earth - 040809 -152540.
Barat, F., Mercier de Lépinay, B., Sosson, M., Müller, C., Baumgartner, P. O., Baumgartner-Mora, C., 2014. Transition from the Farallon Plate subduction to the collision between South and Central America: Geological evolution of the Panama Isthmus. Tectonophysics 622, 145-167. doi.org/10.1016/j.tecto.2014.03.008.
Barckhausen, U., Engels, M., Franke, D., Ladage, S., Pubellier, M., 2014. Evolution of the South China Sea: Revised ages for breakup and seafloor spreading. Mar. Pet. Geol. 58, 599-611. doi:10.1016/j.marpetgeo.2014.02.022.
Barker, P.F., Dalziel, I.W.D., Storey, B.C., 1991. Tectonic development of the Scotia Arc region. In: Tingey, R.J. (Ed.), The Geology of Antarctica. Oxford University Press, Oxford, 215–248.
Barker, P.F., 1995. Tectonic framework of the east Scotia Sea. In: Taylor, B. (Ed.), Backarc Basins: Tectonics and Magmatism. Plenum, New York, 281–314.
Barker, P.F., 2001. Scotia Sea regional tectonic evolution: implications for mantle flow and palaeocirculation. Earth-Sci. Rev. 55, 1-39.
Beaussier, S.J., Gerya, T.V., Burg, J., 2018. 3D numerical modelling of the Wilson cycle: structural inheritance of alternating subduction polarity. In: Wilson, W. (Ed.), Fifty Years of the Wilson Cycle Concept in Plate Tectonics. Geological Society of London, London. https://doi.org/10.1144/SP470.15.
Beaussier, S.J., Gerya, T.V., Burg, J., 2019. Near-ridge initiation of intraoceanic subduction: Effects of inheritance in 3D numerical models of the Wilson Cycle. Tectonophysics 763. https://doi.org/10.1016/j.tecto.2019.04.011.
Behn, M. D., Lin, J., Zuber, M. T., 2002. Evidence for weak oceanic transform faults. Geophys. Res. Lett. 29 (24), 2207. doi:10.1029/2002GL015612.
Bellon, H., Maury, R. C., Soeria-Atmadja, R., Cotten, J., Polvé, M., 2004. 65 my-long magmatic activity in Sumatra (Indonesia), from Paleocene to Present. Bull. Soc. Geol. Fr. 175, 61–72. doi:10.2113/175.1.61.
Bercovici, D., 1998. Generation of plate tectonics from lithosphere–mantle flow and void–volatile self-lubrication. Earth Planet. Sci. Lett., 154(1-4), 139-151.
Bercovici, D., Ricard, Y., 2005. Tectonic plate generation and two-phase damage: void growth versus grain size reduction. J. Geophys. Res. 110, B03401–B03401.

Billen, M. I., Arredondo, K. M., 2018. Decoupling of plate-asthenosphere motion caused by non-linear viscosity during slab folding in the transition zone. Phys. Earth Planet. Int., 281, 17-30, doi:10.1016/j.pepi.2018.04.011

Billi, A., Faccenna, C., Bellier, O., Minelli, L., Neri, G., Piromallo, C., Presti, D., Scrocca, D., Serpelloni, E., 2011. Recent tectonic reorganization of the Nubia-Eurasia convergent boundary heading for the closure of the western Mediterranean. Bull. Soc. Geol. Fr. 182, 279–303.

Bloomer, S., 1983. Distribution and origin of igneous rocks from the landward slopes of the Mariana Trench: Implications for its structure and evolution, J. Geophys. Res. 88, 7411–7428.

Boillot, G., Malod, J., 1988. The north and north-west Spanish continental margin: a review. Rev. Soc. Geol. Esp. 1, 295–316.

Bonatti, E., 1978. Vertical tectonism in oceanic fracture zones. Earth Planet. Sci. Lett. 37, 369-379.

Bonatti, E., Ligi, M., Gasperini, L., Peyve, A., Raznitsin, Y., Chen, Y. J., 1994. Transform migration and vertical tectonics at the Romanche fracture zone, Equatorial Atlantic. J. Geophys. Res. 99, 21779-21802.

Bonatti, E., 1996. Anomalous opening of the equatorial Atlantic due to an equatorial mantle thermal minimum. Earth Planet. Sci. Lett. 143, 147-160.

Booth-Rea, G., Ranero, C. S., Grevemeyer, I., 2018. The Alboran volcanic-arc modulated the Messinian faunal exchange and salinity crisis. Sci. Rep. 8, 13015. DOI:10.1038/s41598-018-31307-7.

Boschman, L. M., van Hinsbergen, D. J., Torsvik, T. H., Spakman, W., 2014. Kinematic reconstruction of the Caribbean region since the Early Jurassic. Earth-Science Reviews 138, 102-136. http://dx.doi.org/10.1016/j.earscirev.2014.08.007.

Boschman, L. M., van der Wiel, E., Flores, K. E., Langereis, C. G., van Hinsbergen, D. J. J., 2019. The Caribbean and Farallon plates connected: Constraints from stratigraphy and paleomagnetism of the Nicoya Peninsula, Costa Rica. J. Geophys. Res.: Solid Earth. 124, 6243–6266. https://doi.org/10.1029/2018JB016369.

Bougault, H., Maury, R.C., AzzouzI, M.E.R., Joron, J.-L., Gotten, J., Treuil, M., 1981. Tholeiites, basaltic andesites and andesites from Leg 60 sites: geochemistry, mineralogy and low partition coefficient elements. In: Hussong, D.M., Uyeda, S. et al. Initial Reports of the Deep Sea Drilling Project 60, 657~578.

Boutelier, D., Oncken, O., 2011. 3-D thermo-mechanical laboratory modeling of plate-tectonics: modeling scheme, technique and first experiments. *Solid Earth*, *2*(1), 35-51, doi:10.5194/se-2-35-2011..

Boutelier, D., Beckett, D., 2018. Initiation of Subduction Along Oceanic Transform Faults: Insights From Three-Dimensional Analog Modeling Experiments, Front. Earth Sci. 6, 204. https://doi.org/10.3389/feart.2018.00204.

Branlund, J., Regenauer-Lieb, K., Yuen, D., 2000. Fast ductile failure of passive margins from sediment loading. Geophys. Res. Lett. 27 (13), 1989-1992.

Briais, A., Patriat, P., Tapponnier, P., 1993. Updated interpretation of magnetic anomalies and seafloor spreading stages in the South China Sea: implications for the Tertiary tectonics of Southeast Asia. J. Geophys. Res. 98, 6299-6328. http://dx.doi.org/10.1029/92JB02280.

Calais, E., Béthoux, N., de Lépinay, B. M., 1992. From transcurrent faulting to frontal subduction: A seismotectonic study of the northern Caribbean plate boundary from Cuba to Puerto Rico. Tectonics 11(1), 114–123. https://doi.org/10.1029/91TC02364.

Calmant, S., Pelletier, B., Lebellegard, P., Bevis, M., Taylor, F. W., Phillips, D. A., 2003. New insights on the tectonics along the New Hebrides subduction zone based on GPS results, J. Geophys. Res. 108 (B6), 2319. doi:10.1029/2001JB000644.

Camacho, E., Hutton, W., Pacheco, J.F., 2010. A new look at evidence for a Wadati-Benioff zone and active convergence at the North Panama deformed belt. Bull. Seismol. Soc. Am. 100 (1), 343–348.

Cande, S., Stock, J., 2004. Pacific-Antarctic-Australia Motion and the formation of the Macquarie Plate, Geophys. J. Int. 157, 399–414.

Cardona, A., Valencia, V. A., Bayona, G., Duque, J., Ducea, M., Gehrels, G., Jaramillo, C., Montes, C., Ojeda, G., Ruiz, J., 2011. Early-subduction-related orogeny in the northern Andes: Turonian to Eocene magmatic and provenance record in the Santa Marta Massif and Rancheria Basin, northern Colombia. Terra Nova 23, 26-34. doi: 10.1111/j.1365-3121.2010.00979.x.

Carney, J.N., Macfarlane, A., 1982. Geological evidence bearing on the Miocene to recent structural evolution of the New Hebrides arc. Tectonophysics 87, 147–175.

Casey, J.F., Dewey, J.F., 1984. Initiation of subduction zones along transform and accreting plate boundaries, triple-junction evolution, and forearc spreading centres - implications for ophiolitic geology and obduction. Geol. Soc. Lond., Spec. Publ. 13, 269–290. https://doi.org/10.1144/GSL.SP.1984.013.01.22.

Cediel, F., Shaw, R. P., Caceres, C., 2003. Tectonic assembly of the Northern Andean Block. In: C. Bartolini, R. T. Buffler, and J. Blickwede, eds., The Circum-Gulf of Mexico and the Caribbean: Hydrocarbon habitats, basin formation, and plate tectonics: AAPG Memoir 79, 815– 848.

Cerpa, N.G., Hassani, R., Arcay, D., Lallemand, S., Garrocq, C., Philippon, M., Cornée, J.-J., Münch, P., Garel, F., Marcaillou, B., Mercier de Lépinay, B., Lebrun, J.-F., 2021. Caribbean plate boundaries control on the tectonic duality in the back-arc of the Lesser Antilles subduction zone during the Eocene. Tectonics, submitted, https://doi.org/10.31223/X5331R (available for downloading).

Chamot-Rooke, N., Le Pichon, X., 1989. Zenisu Ridge: a mechanical model of formation. Tectonophysics 160, 175-193.

Chemenda, A. I., Yang, R. K., Hsieh, C. -H., Groholsky, A. L., 1997. Evolutionary model for the Taiwan collision based on physical modelling. Tectonophysics 274, 253-274.

Chemenda, A. I., Yang, R.-K., Stephan, J.-F., Konstantinovskaya, E. A., Ivanov, G. M., 2001a. New results from physical modeling of arc-continent collision in Taiwan: evolutionary model. Tectonophysics 333, 159-178.

Chemenda, A. I., Hurpin, D., Tang, J.-C., Stephan, J.-F., Buffet, G., 2001b. Impact of arc-continent collision on the conditions of burial and exhumation of UHP/LT rocks: experimental and numerical modelling. Tectonophysics 342, 137-161.

Chiarabba, C., Palano, M., 2017. Progressive migration of slab break-off along the southern Tyrrhenian plate boundary: Constraints for the present day kinematics. J. Geodyn. 105, 51-61. doi.org/10.1016/j.jog.2017.01.006.

Choi, S. H., Mukasa, S. B., Shervais, J. W., 2008. Initiation of Franciscan subduction along a large-offset fracture zone: Evidence from mantle peridotites, Stonyford, California. Geology 36 (8), 595-598. doi: 10.1130/G24993A.1.

Chung, W.Y., Kanamori, H., 1978. A mechanical model for plate deformation associated with aseismic ridge subduction in the New Hebrides arc. Tectonophysics 50 (1), 29-40.

Civiero, C., Strak, V., Custódio, S., Silveira, G., Rawlinson, N., Arroucau, P., Corela, C., 2018. A common deep source for upper-mantle upwellings below the Ibero-western Maghreb region from teleseismic P-wave travel-time tomography. Earth Planet. Sci. Lett. 499, 157–172. https://doi.org/10.1016/j.epsl.2018.07.024.

Clift, P.D., Vannucchi, P., 2004. Controls on tectonic accretion versus erosion in subduction zones: Implications for the Origin and recycling of the continental crust. Rev. Geophys. 42, 1-31.

Cloetingh, S. A. P. L., Wortel, M. J. R., Vlaar, N. J., 1982. Evolution of passive continental margins and initiation of subduction zones, Nature 297, 139-142.

Cloetingh, S. A. P. L., Wortel, M. J. R., Vlaar, N. J., 1984. Passive margin evolution, initiation of subduction and the Wilson cycle. Tectonophysics 109, 147-163.

Cloetingh, S., Wortel, R., 1985. Regional stress field of the Indian plate. Geophys. Res. Lett. 12, 77-80.

Cloetingh, S., Wortel, R., 1986. Stress in the Indo-Australian plate. Tectonophysics 132, 49-67.

Cloetingh, S., Wortel, R., Vlaar, N.J., 1989. On the initiation of subduction zones. PAGEOPH. 129, 1/2, 7-25.

Cluzel, D., Aitchison, J. C., Picard, C., 2001. Tectonic accretion and underplating of mafic terranes in the late Eocene intraoceanic fore-arc of New Caledonia (Southwest Pacific): Geodynamic implications. Tectonophysics 340 (1-2), 23–59. https://doi.org/10.1016/S0040-1951(01)00148-2.

Cluzel, D., Meffre, S., Maurizot, P., Crawford, A.J., 2006. Earliest Eocene (53 Ma) convergence in the Southwest Pacific: evidence from pre-obduction dikes in the ophiolite of New Caledonia. Terra Nova 18 (6), 395-402.

Cluzel, D., Jourdan, F., Meffre, S., Maurizot, P. Lesimple, S., 2012. The metamorphic sole of New Caledonia ophiolite: 40Ar/39Ar, U-Pb, and geochemical evidence for subduction inception at a spreading ridge. Tectonics 31, TC3016. doi:10.1029/2011TC003085.

Collins, W. J., 2003. Slab pull, mantle convection, and Pangaean assembly and dispersal. Earth Planet. Sci. Lett. 205, 225-237.

Collot, J.Y., Daniel, J., Burne, R.V., 1985. Recent tectonics associated with the subduction / collision of the d'Entrecasteaux zone in the central New Hebrides. Tectonophysics 112, 325-356.

Collot, J.-Y., Lallemand, S.E., Pelletier, B., Eissen, J.-P., Glaçon, G., Fisher, M.A., Greene, H.G., Boulin, J., Daniel, J., Monzier, M., 1992. Geology of the d'Entrecasteaux - New Hebrides Island Arc collision zone: Results from a deep-sea submersible survey. Tectonophysics 212, 213-241.

Collot, J.-Y., Lamarche, G., Wood, R. A., Delteil, J., Sosson, M., Lebrun, J.-F., Coffin, M. F., 1995. Morphostructure of an incipient subduction zone along a transform plate boundary: Puysegur ridge and trench. Geology 23, 519–522.

Coltorti, M., Hasenaka, T., Briqueu, L., Baker, R. E., Siena, F., 1994. Petrology and magmatic affinity of the north D'Entrecasteaux Ridge, central New Hebrides Trench, site 828. Proc. Ocean Drill. Program Sci. Results 134, 353–362.

Crameri, F., Kaus, B. J. P., 2010. Parameters that control lithospheric-scale thermal localization on terrestrial planets. Geophys. Res. Lett. 37, L09308–L09308, doi: 10.1029/2010GL042921.

Crameri, F., Tackley, P.J., 2016. Subduction initiation from a stagnant lid and global overturn: new insights from numerical models with a free surface. Prog. in Earth and Planet. Sci. 3(1), 1-19, https://doi.org/10.1186/s40645-016-0103-8

Crameri, F., Magni, V., Domeier, M., Shephard, G. E., Chotalia, K., Cooper, G., Eakin, C. M., Grima, A. G., Gürer, D., Király, Á., Mulyukova, E., Peters, K., Robert, B., Thielmann, M. (2020a). A transdisciplinary and community-driven database to unravel subduction zone initiation. *Nature communications*, *11*(1), 1-14, doi:10.1038/s41467-020-17522-9.

Crameri, F., Magni, V., Domeier, M., Shephard, G.E., Chotalia, K., Cooper, G., Eakin, C., Grima, A.G., Gürer, D., Király, A., Mulyukova, E., Peters, K., Robert, B., Thielmann, M., 2020b. Subduction zone initiation (SZI) Database (Version 1.0.0) [Data set]. Zenodo. http://doi.org/10.5281/zenodo.3756716

Crawford, A.J., Falloon, T.J., Green, D.H., 1989. Classification, petrogenesis and tectonic setting of boninites. In: Crawford, A.J. (ed.) Boninites and Related Rocks. Unwin Hyman, London, 1-49.

Crawford, A.J., Meffre, S., Symonds, P.A., 2003. 120 to 0 Ma tectonic evolution of the Southwest Pacific and analogous geological evolution of the 600 to 220 Ma Tasman fold belt system. In: Hills, R.R., Müller, R.D. (Eds.), Evolution and dynamics of the Australian Plate. Geological Society of Australia Special Publication 22, 377–397.

d'Acremont, E., Lafosse, M., Rabaute, A., Teurquety, G., Do Couto, D., Ercilla,G., et al., 2020. Polyphase tectonic evolution of fore-arc basin related to STEP fault as revealed by seismic reflection data from the Alboran Sea (W Mediterranean). Tectonics 39, e2019TC005885. https://doi.org/10.1029/2019TC005885.

Daniel, J., Jouannic, C., Larue, B., Récy, J., 1977. Interpretation of d'Entrecasteaux Zone (north of New Caledonia). Int. Symp. on Geodynamics in South-West Pacific, Noumea 1976. Technip, Paris, 117-124.

Daniel, J., Jouannic, C., Larue, B. M., Récy, J., 1978. Marine Geology of Eastern Coral Sea (Eastern Margin of Indo-Australian Plate, North of New Caledonia). South Pac. Mar. Geol. Notes 1, CCOP-SOPAC, Suva, Fiji, 81–94.

Danyushevsky, L.V., Sobolev, A.V., Falloon, T.J., 1995. North Tongan high-Ca boninite petrogenesis; the role of Samoan plume and subduction- transform fault transition. J. Geodyn. 20, 219-241.

Danyushevsky, L.V., Crawford, A.J., Leslie, R.L., Tetroeva, S., Falloon, T.J., 2006. Subduction-related magmatism along the southeast margin of the North Fiji back-arc basin. Geochim. Cosmochim. Acta 69 (10), A633.

Danyushevsky, L. V., Falloon, T. J., Crawford, A. J., Sofia, A. T., Leslie, R. L., Verbeeten, A., 2008. High-Mg adakites from Kadavu Island Group, Fiji,

southwest Pacific: Evidence for the mantle origin of adakite parental melts. Geology, 36 (6), 499–502. doi:10.1130/G24349A.1.
Davaille, A., Smrekar, S. E., Tomlinson, S., 2017. Experimental and observational evidence for plume-induced subduction on Venus. Nat. Geosci., 10(5), 349-355.
Davies, G. F., 1980. Mechanics of subducted lithosphere. J. Geophys. Res., 85(B11), 6304-6318.
De Grave, J., Zhimulev, F. I., Glorie, S., Kuznetsov, G. V., Evans, N., Vanhaecke, F., McInnes, B., 2016. Late Palaeogene emplacement and late Neogene–Quaternary exhumation of the Kuril island-arc root (Kunashir island) constrained by multi-method thermochronometry. Geosci. Frontiers 7 (2), 211–220. https://doi.org/10.1016/j.gsf.2015.05.002
Delescluse, M., Chamot-Rooke, N., 2007. Instantaneous deformation and kinematics of the India–Australia Plate. Geophys. J. Int. 168, 818-842. doi: 10.1111/j.1365-246X.2006.03181.x.
Delescluse, M., Chamot-Rooke, N., 2008. Serpentinization pulse in the actively deforming Central Indian Basin. Earth Planet. Sci. Lett. 276, 140-151. doi:10.1016/j.epsl.2008.09.017.
Delescluse, M.,Montési, L. G. J., Chamot-Rooke, N., 2008. Fault reactivation and selective abandonment in the oceanic lithosphere. Geophys. Res. Lett. 35, L16312. http://dx.doi.org/10.1029/2008GL035066.
DeMets, C., Gordon, R. G., Argus, D. F., Stein, S., 1994. Effect of recent revisions to the geomagnetic reversal time scale on estimates of current plate motions. Geophys. Res. Lett. 21, 2191–2194.
Deschamps, A.E., Lallemand, S.E., Collot, J.-Y., 1998. A detailed study of the Gagua Ridge: A fracture zone ridge uplifted during a plate reorganisation in the mid-Eocene. Marine Geophysical Researches 20 (5), 403-423.
Deschamps, A., Monié, P., Lallemand, S., Hsu, S.-K., Yeh, K.-Y., 2000. Evidence for Early Cretaceous crust trapped in the Philippine Sea Plate. Earth Planet. Sci. Lett. 179, 503–516.
Deschamps, A., Lallemand, S., 2002. The West Philippine Basin: a Paleocene-Oligocene backarc basin opened between two opposed subduction zones. J. Geophys. Res. 107(12), 2322. doi:10.1029/2001JB001706.
Deschamps, A., Lallemand, S., 2003. Geodynamic setting of Izu-Bonin-Mariana boninites. In: Larter RD & Leat PT (eds) Intra-oceanic subduction systems: tectonic and magmatic processes. Geol. Soc. London Spe. Publ. 219, 163–185.
Dessa, J.-X., S. Operto, S. Kodaira, A. Nakanishi, G. Pascal, K. Uhira, Kaneda, Y., 2004. Deep seismic imaging of the eastern Nankai trough, Japan, from multifold ocean bottom seismometer data by combined travel time tomography and prestack depth migration. J. Geophys. Res. 109, B02111. doi:10.1029/2003JB002689.
Deverchère, J., Yelles, K., Domzig, A., Mercier de Lépinay, B., Bouillin, J.-P., Gaullier, V., Bracène, R., Calais, E., Savoye, B., Kherroubi, A., Le Roy, P., Pauc, H., Dan, G., 2005. Active thrust faulting offshore Boumerdés, Algeria, and its relations to the 2003 Mw 6.9 earthquake. Geophys. Res. Lett. 32, L04311. doi:10.1029/2004GL021646.
Deville, E., Mascle, A., 2012. The Barbados ridge: A mature accretionary wedge in front of the Lesser Antilles active margin. In: Roberts, D. G. and Bally, A. W.

(eds) Regional Geology and Tectonics: Principles of Geologic Analysis, 581-607. DOI: 10.1016/B978-0-444-53042-4.00021-2
Dewey, J. F., 1969. Continental margins: a model for conversion of Atlantic-type to Andean type. Earth Planet. Sci. Lett. 6, 189-197.
Dewey, J., Spall, H., 1975. Pre-Mesozoic plate tectonics: How far back in Earth history can the Wilson Cycle be extended ? Geology, 422-424.
Dickinson, W.R., Seely, D.R., 1979. Structure and stratigraphy of forearc regions. Amer. Assoc. Petrol. Geol. Bull. 63, 2–31.
Diebold, J.B., 2009. Submarine volcanic stratigraphy and the Caribbean LIP's formational environment. In: James, K.H., Lorente, M.A., Pindell, J.L. (Eds.), The Origin and Evolution of Caribbean Plate. Geol. Soc. London Spec. Publ. 328, 799–808.
Doin, M.-P., Henry, P., 2001. Subduction initiation and continental crust recycling: the roles of rheology and eclogitization. Tectonophysics, 342(1-2), 163-191.
Domeier, M., Shephard, G. E., Jakob, J., Gaina, C., Doubrovine, P. V., Torsvik, T. H., 2017. Intraoceanic subduction spanned the Pacific in the Late Cretaceous-Paleocene. Sci. Adv. 3, eaao2303.
Driscoll, N. W., Diebold, J. B., 1998. Deformation of the Caribbean region: One plate or two?. Geology 26, 1043–1046.
Duarte, J. C., Rosas, F. M., Terrinha, P., Schellart, W. P., Boutelier, D., Gutscher, M.-A., Ribeiro, A., 2013. Are subduction zones invading the Atlantic? Evidence from the southwest Iberia margin. Geology 41 (8), 839-842. doi:10.1130/G34100.1.
Duarte, J., Riel, N., Civiero, C., Rosas, F., Schellart, W., Almeida, J., Silva, S., Terrinha, P., 2019. Delamination of oceanic lithosphere in SW Iberia: a key for subduction initiation?. Geophys. Res. Abstracts 21, EGU2019-6001.
Duggen S., Hoernle, K., van den Bogaard, P., Garbe-Schönberg, D., 2005. Post-Collisional Transition from Subduction-to Intraplate-type Magmatism in the Westernmost Mediterranean: Evidence for Continental-Edge Delamination of Subcontinental Lithosphere. J. Pet. 46 (6), 1155-1201. doi:10.1093/petrology/egi013.
Duncan, R.A., 1982. A captured island chain in the Coast Range of Oregon and Washington. Journal of Geophysical Research 87, 10,827–10,837. https:// doi .org /10 .1029 /JB087iB13p10827.
Dürkefälden, A., Hoernle, K., Hauff, F., Wartho, J.-A., van den Bogaard, P., Werner, R., 2019a. Age and geochemistry of the Beata Ridge: Primary formation during the main phase (~89 Ma) of the Caribbean Large Igneous Province. Lithos 328–329, 69–87. doi.org/10.1016/j.lithos.2018.12.021.
Dürkefälden, A., Hoernle, K., Hauff, F., Werner, R., Garbe-Schönberg, D., 2019b. Caribbean Large Igneous Province volcanism: the depleted Icing on the enriched Cake. Chem. Geol. 509, 45–63. https://doi.org/10.1016/j.chemgeo.2019.01.004.
Dymkova, D., Gerya, T., 2013. Porous fluid flow enables oceanic subduction initiation on Earth, Geophys. Res. Lett. 40, 5671–5676. https://doi.org/10.1002/2013GL057798.
Eagles, G., 2010. Age and origin of the central Scotia Sea. Geophys. J. Int. 183, 587–600. http://dx.doi.org/10.1111/j.1365-246X.2010.04781.x.

Eagles, G., Jokat,W., 2014. Tectonic reconstructions for paleobathymetry in Drake Passage. Tectonophysics 611, 28–50. http://dx.doi.org/10.1016/j.tecto.2013.11.021.

Eakin, D. H., McIntosh, K. D., Van Avendonk H. J. A., Lavier, L., 2015. New geophysical constraints on a failed subduction initiation: The structure and potential evolution of the Gagua Ridge and Huatung Basin. Geochem. Geophys. Geosyst. 16, 1–21. doi:10.1002/2014GC005548.

Ellis, M., 1988. Lithospheric strength in compression: Initiation of subduction, flake tectonics, foreland migration of thrusting, and an origin of displaced terranes. J. Geol., 96(1), 91-100.

Ely, K. S., Sandiford, S., Hawke, M. L., Phillips, D., Quigley, M., Edmundo dos Reis, J., 2011. Evolution of Ataúro Island: Temporal constraints on subduction processes beneath the Wetar zone, Banda Arc. J. Asian Earth Sci. 41, 477–493. doi:10.1016/j.jseaes.2011.01.019.

Encarnación, J. P., Essene, E. J., Mukasa, S. B., Hall, C. H., 1995. High-Pressure and Temperature Subophiolitic Kyanite-Garnet Amphibolites Generated during Initiation of Mid-Tertiary Subduction, Palawan, Philippines. J Petrol 36 (6),1481–1503.

Erickson, S.G., 1993. Sedimentary loading, lithospheric flexure, and subduction initiation at passive margins. Geology 21, 125–128.

Erickson, S. G., Arkani-Hamed, J., 1993. Subduction initiation at passive margins: The Scotian Basin, eastern Canada as a potential example. Tectonics, 12(3), 678-687.Escalona, A., Mann, P., 2011. Tectonics, basin subsidence mechanisms, and paleogeography of the Caribbean-South American plate boundary zone. Mar. Petrol. Geol. 28 (1), 8–39. https://doi.org/10.1016/j.marpetgeo.2010.01.016.

Faccenna, C., Giardini, D., Devy, P., Argentiri, A., 1999. Initiation of subduction at Atlantic-type margins: insights from laboratory experiments. J. Geophys. Res. 104, 2749–2766.

Faccenna, C., Becker, T.W., Lucente, F.P., Jolivet, L., Rossetti, F., 2001. History of subduction and back arc extension in the Central Mediterranean. Geophys. J. Int. 145, 809-820.

Faccenna, C., Piromallo, C., Crespo-Blanc, A., Jolivet, L., 2004. Lateral slab deformation and the origin of the western Mediterranean arcs. Tectonics, 23, TC1012. doi:10.1029/2002TC001488.

Faccenna, C., Becker, T. W., Lallemand, S., Lagabrielle, Y., Funiciello, F., Piromallo, C., 2010. Subduction-triggered magmatic pulses: a new class of plumes?. Earth Planet. Sci. Lett. 299, 54–68. doi:10.1016/j.epsl.2010.08.012.

Faccenna, C., Becker, T. W., Lallemand, S., Steinberger, B., 2012. On the role of slab pull in the Cenozoic motion of the Pacific plate. Geophys. Res. Lett. 39, L03305. doi:10.1029/2011GL050155.

Faccenna, C., Becker, T. W., Auer, L., Billi, A., Boschi, L., Brun, J.-P., Capitanio, F. A., Funiciello, F., Horvath, F., Jolivet, L., Piromallo, C., Royden, L., Rossetti, F., Serpelloni, E., 2014. Mantle dynamics in the Mediterranean. Rev. Geophys. 52, doi:10.1002/ 2013RG000444.

Faccenna, C., Holt, A., Becker, T., Lallemand, S., Royden, L., 2018. Dynamics of the Ryukyu / Izu-Bonin-Marianas double subduction system. Tectonophysics. doi.org/10.1016/j.tecto.2017.08.011.

Faure, M., Monié, P., Fabbri, O., 1988. Microtectonics and 39Ar-40Ar dating of high pressure metamorphic rocks of the south Ryukyu Arc and their bearings on the pre-Eocene geodynamic evolution of Eastern Asia. Tectonophysics 156, 133-143.

Fernandez-Viejo, G., Pulgar, J. A., Gallastegui, J., Quintina, L., 2012. The Fossil Accretionary Wedge of the Bay of Biscay: Critical Wedge Analysis on Depth-Migrated Seismic Sections and Geodynamical Implications. J. Geol. 120. DOI: 10.1086/664789.

Foley, F. V., Pearson, N. J., Rushmer, T., Turner, S., Adam, J., 2013. Magmatic evolution and magma mixing of Quaternary adakitic rocks at Solander and Little Solander Islands, New Zealand. J. Petrol. 54, 703–744. doi:10.1093/petrology/egs082.

Forsyth, D. W., Uyeda, S., 1975. On the relative importance of the driving forces of plate motion, Geophys. J. R. Astron. Soc., 43, 163–200.

Fournier, M., Chamot-Rooke, N., Petit, C., Huchon, P., Al-Kathiri, A., Audin, L., Beslier, M.O., d'Acremont, E., Fabbri, O., Fleury, J.M., Khanbari, K., Lepvrier, C., Leroy, S., Maillot, B., Merkouriev, S., 2010. Arabia–Somalia plate kinematics, evolution of the Aden-Owen- Carlsberg triple junction, and opening of the Gulf of Aden. J.Geophys. Res. 115, B04102. doi:10.1029/2008JB006257.

Fournier, M., Chamot-Rooke, N., Rodriguez, M., Huchon, P., Petit, C., Beslier, M., Zaragosi, S., 2011. Owen Fracture Zone: The Arabia–India plate boundary unveiled. Earth Planet. Sci. Lett. 302, 247–252.

Fujiwara, T., Tamura, C., Nishizawa, A., Fujioka, K., Kobayashi, K., Iwabuchi, Y., 2000. Morphology and tectonics of the Yap Trench. Mar. Geophys. Res. 21 (1–2), 69–86.

Fukao, Y., 1973. Thrust faulting at a lithospheric plate boundary, the Portugal earthquake of 1969. Earth Planet. Sci. Lett. 18, 205–216. doi: 10.1016/0012-821X(73)90058-7.

Fullea, J., Fernadez, M., Afonso, J. C., Verges, J., Zeyen, H., 2010. The structure and evolution of the lithosphere–asthenosphere boundary beneath the Atlantic–Mediterranean Transition Region. Lithos 120, 74-95. doi.org/10.1016/j.lithos.2010.03.003.

Gaina, C., Müller, D., 2007. Cenozoic tectonic and depth/age evolution of the Indonesian gateway and associated back-arc basins. Earth Sci. Rev. 83,177–203. doi:10.1016/j.earscirev.2007.04.004.

Gallastegui, J., Pulgar, J. A., 2002. Initiation of an active margin at the North Iberian continent-ocean transition. Tectonics 21 (4), 10.1029/2001TC901046.

Garrocq, C., Lallemand, S., Marcaillou, B., Lebrun, J.-F., Padron, C., Klingelhoefer, F., Laigle, M., Münch, P., Gay, A., Schenini, L., Beslier, M.-O., Mercier de Lépinay, B., Quillévéré, F., Boudhager-Fadel, M., the Garanti cruise team, 2021. Genetic relations between the Aves Ridge and the Grenada back-arc basin, East Caribbean Sea. J. Geophys. Res. 126. DOI: 10.1029/2020JB020466.

Garzanti, E., Radeff, G., Malusa, M. G., 2018. Slab breakoff: A critical appraisal of a geological theory as applied in space and time. Earth-Sci. Rev. 177, 303-319. doi.org/10.1016/j.earscirev.2017.11.012.

Gautier, S., Tiberi, C., Lopez, M., Foix, O., Lallemand, S., Theunissen, T., Hwang, C., Chang, E., 2019. Detailed lithospheric structure of an arc-continent collision

beneath Taiwan revealed by joint inversion of seismological and gravity data, Geophys. J. Int. https://doi.org/10.1093/gji/ggz159.
Gerbault, M., Burov, E. B., Poliakov, A. N. B., Daignières, M., 1999. Do faults trigger folding in the lithosphere?. Geophys. Res. Lett. 26 (2), 271-274.
Gerbault, M., 2000. At what stress level is the central Indian Ocean lithosphere buckling? Earth Planet. Sci. Lett. 178, 165-181.
Gerya, T.V., Connolly, J.A.D., Yuen, D.A., 2008. Why is terrestrial subduction one-sided? Geology 36 (1), 43–46.
Gerya, T., 2011. Future directions in subduction modeling. J. Geodyn. 52, 344–378.
Gerya, T., Stern, R., Baes, M., Sobolev, S., Whattam, S., 2015. Plate tectonics on the Earth triggered by plume- induced subduction initiation. Nature 527, 221–225. doi:10.1038/nature15752.
Ghiglione, M.C., Yagupsky, D., Ghidella, M., Ramos, V.A., 2008. Continental stretching preceding the opening of the Drake Passage: evidence from Tierra del Fuego. Geology 36 (8), 643–646.
Gomez, S., Bird, D., Mann, P., 2018. Deep crustal structure and tectonic origin of the Tobago-Barbados ridge. Interpretation 6 (2), T471–T484. doi.org/10.1190/INT-2016-0176.1.
Gómez de la Peña, L., Ranero, C. R., Gràcia, E., 2018. The crustal domains of the Alboran Basin (western Mediterranean). Tectonics 37, 3352–3377. https://doi.org/10.1029/2017TC004946.
Gong, Z. Langereis, C. G., Mullender, T. A. T., 2008. The rotation of Iberia during the Aptian and the opening of the Bay of Biscay. Earth Planet. Sci. Lett. 273, 80–93.
Goren, L., Aharonov, E., Mulugeta, G., Koyi, H.A. & Mart, Y., 2008. Ductile deformation of passive margins: a new mechanism for subduction initiation, J. Geophys. Res. 113. doi:10.1029/2005JB004179.
Govers, R., Wortel, M. J. R., 2005. Lithosphere tearing at STEP faults: Response to edges of subduction zones. Earth Planet. Sci. Lett. 236, 505-523.
Granja-Bruna, J. L., Carbo-Gorosabel, A., Llanes Estrada, P., Munoz-Martin, A., ten Brink, U. S., Gomez Ballesteros, M., Druet, M., Pazos, A., 2014. Morphostructure at the junction between the Beata ridge and the Greater Antilles island arc (offshore Hispaniola southern slope). Tectonophysics 618, 138-163. doi.org/10.1016/j.tecto.2014.02.001.
Greene, H. G., Collot, J.-Y., 1994. Ridge-arc collision: timing and deformation determined by leg 134 drilling, central New Hebrides Island Arc. Proceedings of the Ocean Drilling Program. Scientific results 134, 609-621.
Guilmette, C., Smit, M.A., van Hinsbergen, D.J., Gürer, D., Corfu, F., Charette, B., Maffione, M., Rabeau, O., Savard, D., 2018. Forced subduction initiation recorded in the sole and crust of the Semail Ophiolite of Oman. Nat. Geosci. 11, 688–695.
Gülcher, A. J. P., Beaussier, S. J., Gerya, T. V., 2019. On the formation of oceanic detachment faults and their influence on intra-oceanic subduction initiation: 3D thermomechanical modeling. Earth Planet. Sci. Lett. 506, 195-208. https://doi.org/10.1016/j.epsl.2018.10.042
Gurnis, M., Hall, C., Lavier, L., 2004. Evolving force balance during incipient subduction. Geochem. Geophys. Geosyst., 5, Q07001, https://doi.org/10.1029/2003GC000681.

Gurnis, M., van Avendonk, H., Gulick, S. P. S., Stock, J., Sutherland, R., Hightower, E., Shuck, B., Patel, J., Williams, E., Kardell, D., Herzig, E., Idini, B., Graham, K., Estep, J., Carrington, L., 2019. Incipient subductionat the contact with stretched continental crust: The Puysegur Trench. earth Planet. Sci. Lett. 520, 212-219. doi.org/10.1016/j.epsl.2019.05.044.

Gutscher, M.-A., Spakman, W., Bijwaard, H., Engdahl, E. R., 2000. Geodynamics of flat subduction: Seismicity and tomographic constraints from the Andean margin. Tectonics 19, 814–833.

Gutscher, M.-A., Malod, J., Rehault, J.-P., Contrucci, I., Klingelhoefer, F., Mendes-Victor, L., Spakman, W., 2002. Evidence for active subduction beneath Gibraltar. Geology 30, 1071–1074. doi: 10.1130/0091-7613(2002)030<1071:EFASBG>2.0.CO;2.

Gutscher, M.-A., Dominguez, S., Westbrook, G. K., Le Roy, P., Rosas, F., Duarte, J. C., Terrinha, P., Miranda, J. M., Graindorge, D., Gailler, A., Sallares, V., Bartolome, R., 2012. The Gibraltar subduction: A decade of new geophysical data. Tectonophysics 574–575, 72–91. doi.org/10.1016/j.tecto.2012.08.038.

Hall, C. E., Gurnis, M., Sdrolias, M., Lavier, L. L., Müller, R. D., 2003. Catastrophic initiation of subduction following forced convergence across fractures zones. Earth Planet. Sci. Lett. 212, 15–30. https://doi.org/10.1016/S0012-821X(03)00242-5.

Hall, R., 1987. Plate boundary evolution in the Halmahera region, Indonesia. Tectonophysics 144, 337–352.

Hall, R., 1996. Reconstructing Cenozoic SE Asia. In: Tectonic Evolution of SE Asia, Geol. Soc. London Spec. Publ. 106, 153–184.

Hall, R., 2002. Cenozoic geological and plate tectonic evolution of SE Asia and the SW Pacific: computer-based reconstructions, model and animations. J. Asian Earth Sci. 20, 353–434.

Hall, R., Morley, C.K., 2004. Sundaland Basins. In: Clift, P.,Wang, P., Kuhnt,W., Hayes, D.E. (Eds.), Continent–Ocean Interactions within the East Asian Marginal Seas. Geophysical Monograph, 149. American Geophysical Union,Washington, D.C., 55–85.

Hall, R., 2012. Late Jurassic–Cenozoic reconstructions of the Indonesian region and the Indian Ocean. Tectonophysics 570-571, 1–41.

Hall, R., Spakman, W., 2015. Mantle structure and tectonic history of SE Asia. Tectonophysics 658, 14–45.

Hall, R., 2018. The subduction initiation stage of the Wilson cycle**.** Geological Society, London, Special Publications 470, 415-437. https://doi-org.insu.bib.cnrs.fr/10.1144/SP470.3

Hamai, L., Petit, C., Abtout, A., Yelles-Chaouche, A., Déverchère, J., 2015. Flexural behaviour of the north Algerian margin and tectonic implications. Geophys. J. Int. 201, 1426–1436. https://doi .org /10 .1093 /gji /ggv098.

Hamai, L., Petit, C., Le Pourhiet, L., Yelles-Chaouche, A., Deverchère, J., Beslier, M.-O., Abtout, A., 2018. Towards subduction inception along the inverted North African margin of Algeria? Insights from thermo-mechanical models. Earth Planet. Sci. Lett. 501, 13-23.

Hamilton, W., 1979. Tectonics of the Indonesian region. In: U.S. Geological Survey Professional Paper 1078, 345p.

Handy, M.R., Schmid, S.M., Bousquet, R., Kissling, E., Bernoulli, D., 2010. Reconciling plate-tectonic reconstructions of Alpine Tethys with the geological-geophysical record of spreading and subduction in the Alps. Earth-Sci. Rev. 102, 121-158.

Harris, C. W., Miller, M. S., Porritt, R. W., 2018. Tomographic imaging of slab segmentation and deformation in the Greater Antilles. Geochemistry, Geophysics, Geosystems 19, 2292–2307. https://doi.org/10.1029/2018GC007603.

Hassani, R., Jongmans, D., Chéry, J., 1997. Study of plate deformation and stress in subduction processes using two-dimensional numerical models. J. Geophys. Res. 102, 17951-17965.

Hastie, A.R., Mitchell, S.F., Treloar, P.J., Kerr, A.C., Neill, I., Barfod, D.N., 2013. Geochemical components in a Cretaceous island arc: the Th/La-(Ce/Ce*)Nd diagram and implications for subduction initiation in the inter-American region. Lithos 162-163, 57–69. http://dx.doi.org/10.1016/j.lithos.2012.12.001.

Hastie, A.R., Cox, S., Kerr, A.C., 2021. Northeast- or southwest-dipping subduction in the Cretaceous Caribbean gateway? Lithos 386-387, https://doi.org/10.1016/j.lithos.2021.105998.

Hawkins, J.W., Castillo, P.R., 1998. Early history of the Izu–Bonin–Mariana Arc System — evidence from Belau and the Palau Trench. Island Arc 7 (3), 559–578.

Hayes, G. P., Furlong, K. P., Ammon, C. J., 2009. Intraplate deformation adjacent to the Macquarie ridge south of New Zealand—The tectonic evolution of a complex plate boundary. Tectonophysics 463(1-4), 1–14. https://doi.org/10.1016/j.tecto.2008.09.024.

Hayward, N., Watts, A.B., Westbrook, G.K., and Collier, J.S., 1999. A seismic reflection and GLORIA study of compressional deformation in the Gorringe Bank region, eastern North Atlantic. Geophys. J. Int. 138, 831–850. doi:10.1046/j.1365-246x.1999.00912.x.

Hegarty, K.A., Weissel, J.K., Hayes, D.E., 1983. Convergence at the Caroline-Pacific plate boundary: collision and subduction. In: Hayes, D.E. (Ed.), Tectonic and Geologic Evolution of Southeast Asian Seas and Islands. Geophysical Monograph. American Geophysical Union, Washington, D.C., 326–348.

Hensen, C., Duarte, J. C., Vannucchi, P., Mazzini, A., Lever, M. A., Terrinha, P., Géli, L., Henry, P., Villinger, H., Morgan, J., Schmidt, M., Gutscher. M.-A., Bartolome, R., Tomonaga, Y., Polonia, A., Gràcia, E., Tinivella, U., Lupi, M., Çagatay, M. N., Elvert, M., Sakellariou, D., Matias, L., Kipfer, R., Karageorgis, A. P., Ruffine, L., Liebetrau, V., Pierre, C., Schmidt, C., Batista, L., Gasperini, L., Burwicz, E., Neres, M., Nuzzo, M., 2019. Marine Transform Faults and Fracture Zones: A Joint Perspective Integrating Seismicity, Fluid Flow and Life. Front. Earth Sci. 7, 39. doi: 10.3389/feart.2019.00039.

Hickey-Vargas, R., 2005. Basalt and tonalite from the Amami Plateau, northern West Philippine Basin: new Early Cretaceous ages and geochemical results, and their petrologic and tectonic implications. Isl. Arc 14,653–665.

Hilairet, N., Reynard, B., Wang, Y., Daniel, I., Merkel, S., Nishiyama, N., and Petitgirard, S. (2007). High-pressure creep of serpentine, interseismic deformation, and initiation of subduction. Science, 318(5858), 1910–1913.

Hilde, T., Uyeda, S., Kroenke, L., 1977. Evolution of the western pacific and its margin. Tectonophysics, 38(1), 145 – 165.
Hinschberger, F., Malod, J.A., Dyment, J., Honthaas, C., Réhault, J.P., Burhanuddin, S., 2001. Magnetic lineation constraints for the back-arc opening of the Late Neogene south Banda Basin (eastern Indonesia). Tectonophysics 333, 47– 59.
Hinschberger, F., Malod, Réhault, J.P., Villeneuve, M., Royer, J.-Y., Burhanuddin, S., 2005. Late Cenozoic geodynamic evolution of eastern Indonesia. Tectonophysics 404, 91-118. doi:10.1016/j.tecto.2005.05.005.
Hsieh, Y.-H., Liu, C.-S., Suppe, J., Byrne, T. B., Lallemand, S., 2020. The Chimei submarine canyon and fan: A record of Taiwan arc-continent collision on the rapidly deforming overriding plate. Tectonics 39, e2020TC006148. https://doi.org/10.1029/2020TC006148.
Huang, C.-Y., Chen, W.-H., Wang, M.-H., Lin, C.-T., Yang, S., Li, X., Yu, M., Zhao, X., Yang, K.-M., Liu, C.-S., Hsieh, Y.-H., Harrish, R., 2018. Juxtaposed sequence stratigraphy, temporal-spatial variations of sedimentation and development of modern-forming forearc Lichi Mélange in North Luzon Trough forearc basin onshore and offshore eastern Taiwan: An overview. Earth-Science Reviews 182, 102-140. https://doi.org/10.1016/j.earscirev.2018.01.015.
Huang, C.-Y., Wang, P., Yu, M., You, C.-F., Liu, C.-S., Zhao, X., Shao, L., Zhong, G., Yumul Jr., G. P., 2019. Potential role of strike-slip faults in opening up the South China Sea. Natl Sci Rev. https://doi.org/10.1093/nsr/nwz119.
Hughes, G., Turner, C., 1977. Upraised Pacific Ocean floor, southern Malaita. Geol. Soc. Am. Bull. 88, 412–424.
Hynes, A., 1982. Stability of the oceanic tectosphere a model for early Proterozoic intercratonic orogeny. Earth Planet. Sci. Lett. 61, 333–345.
Ishizuka, O., Tani, K., Reagan, M. K., Kanayama, K., Umino, S., Harigane, Y., Sakamoto, I., Miyajima, Y., Yuasa, M., Dunkley, D. J., 2011. The timescales of subduction initiation and subsequent evolution of an oceanic island arc. Earth Planet. Sci. Lett. 306, 229–240. doi:10.1016/j.epsl.2011.04.006.
Ishizuka, O., Taylor, R.N., Ohara, Y., Yuasa, M., 2013. Upwelling, rifting and age-progressive magmatism from the Oki-Daito mantle plume. Geology 41, 1011–1014. http://dx.doi.org/10.1130/G34525.1.
Ishizuka, O., Tani, K., Reagan, M. K., 2014. Izu-Bonin-Mariana forearc crust as a modern ophiolite analogue. Elements 10,115–120. doi:10.2113/gselements.10.2.115.
Ishizuka, O., Hickey-Vargas, R., Arculus, R. J., Yogodzinski, G. M., Savov, I. P., Kusano, Y., McCarthy, A., Brandl, P. A., Sudo, M., 2018. Age of Izu-Bonin-Mariana arc basement, Earth Planet. Sci. Lett. 481, 80–90. https://doi.org/10.1016/j.epsl.2017.10.023.
Jicha, B. R., Scholl, D. W., Singer, B. S., Yogodzinski, G. M., Kay, S. M., 2006. Revised age of Aleutian Island Arc formation implies high rate of magma production. Geology 34 (8), 661. https://doi.org/10.1130/G22433.1.
Johnston, M. D., Long, M. D., Silver, P. G., 2011. State of stress and age offsets at oceanic fracture zones and implications for the initiation of subduction. Tectonophysics 512, 47-59. doi:10.1016/j.tecto.2011.09.017.
Jolivet, L., Faccenna, C., Becker, T., Tesauro, M., Sternai, P., Bouilhol, P., 2018. Mantle Flow and Deforming Continents: From India-Asia Convergence to

Pacific Subduction. Tectonics 37, 2887–2914. https://doi.org/10.1029/2018TC005036.
Kamenetsky, V.S., Crawford, A.J., Eggins, S., Muhe, R., 1997. Phenocryst and melt inclusion chemistry of near-axis seamounts, Valu Fa Ridge, Lau Basin: insight into mantle wedge melting and the addition of subduction components. Earth Planet. Sci. Lett. 151, 205-223.
Karig, D.E., 1982. Initiation of subduction zones: implications for arc evolution and ophiolite development. In Leggett, J.K. (Ed.), Trench-Forearc Geology. Geol. Soc. Spec. Publ. 10, 563–576.
Keenan, T. E., Encarnacion, J., Buchwaldt, R., Fernandez, D., Mattinson, J., Rasoazanamparany, C., Luetkemeyer, P. B., 2016. Rapid conversion of an oceanic spreading center to a subduction zone inferred from high-precision geochronology. PNAS, E7359–E7366. doi/10.1073/pnas.1609999113.
Keller, W. R., 2004. Cenozoic plate tectonic reconstructions and plate boundary processes in the southwest Pacific. Ph.D. dissertation, Calif. Inst. of Technol., Pasadena.
Kemp, D.V., Stevenson, D.J., 1996. A tensile, flexural model for the initiation of subduction. Geophys. J. Int. 125, 73–93.
Kerr, A., Tarney, J., Marriner, G., Nivia, A., Saunders, A., 1997. The Caribbean – Colombian Cretaceous igneous province: the internal anatomy of an oceanic plateau. In: Mahoney, J., Coffin, M. (Eds.), Large Igneous Provinces: Continental, Oceanic, and Planetary Flood Volcanism. American Geophysical Union, Washington, DC, 123– 144.
Kherroubi, A., Déverchère, J., Yelles, A. K., Mercier de Lépinay, B., Domzig, A., Cattaneo, A., Bracene, R., Gaullier, V., Graindorge, D., 2009. Recent and active deformation pattern off the easternmost Algerian margin, western Mediterranean Sea: New evidence for contractional tectonic reactivation. Mar. Geol. 261 (1–4), 17–32. doi:10.1016/j.margeo.2008.05.016.
Kim, Y.-M., Lee, S.-M., Okino, K., 2009. Comparison of gravity anomaly between mature and immature intra-oceanic subduction zones in the western Pacific. Tectonophysics 474, 657-673. doi:10.1016/j.tecto.2009.05.004.
Kimura, J.-I., Stern, R. J., Yoshida, T., 2005. Reinitiation of subduction and magmatic responses in SW Japan during Neogene time. Geol. Soc. Am. Bull. 117 (7–8), 969–986.
Kimura, G., Y. Hashimoto, Y. Kitamura, A. Yamaguchi, Koge, H., 2014. Middle Miocene swift migration of the TTT triple junction and rapid crustal growth in southwest Japan: A review. Tectonics 33, 1219–1238. doi:10.1002/2014TC003531.
Kiraly, A., Capitanio, F.A., Funiciello, F., Faccenna, C., 2017. Subduction induced mantle flow: Length-scales and orientation of the toroidal cell. Earth Planet. Sci. Lett. 479, 284-297. http://dx.doi.org/10.1016/j.epsl.2017.09.017.
Kizaki, K., 1986. Geology and tectonics of the Ryukyu Islands. Tectonophysics 125, 193-207.
Kobayashi, Y., 1983. Initiation of subduction of plates. Chikyuu (Earth Monthly) 3, 510-518.
Kobayashi, K., 2004. Origin of the Palau and Yap trench–arc systems. Geophys. J. Int. 157 (3), 1303–1315.

Kodaira, S., Iidaka, T., Kato, A., Park, J.-O., Iwasaki, T., Kaneda, Y., 2004. High Pore Fluid Pressure May Cause Silent Slip in the Nankai Trough. Science 304, 1295-1298.

Konecny, V., Kovac, M., Lexa, J., Sefara, J., 2002. Neogene evolution of the Carpatho-Pannonian region: an interplay of subduction and back-arc uprise in the mantle. EGU Stephan Mueller Spec. Publ. Ser. 1, 105–23.

Konstantinovskaya, E., 2001. Arc–continent collision and subduction reversal in the Cenozoic evolution of the Northwest Pacific: An example from Kamchatka (NE Russia). Tectonophysics 333, 75–94.

Konstantinovskaya, E., 2011. Early Eocene arc–continent collision in Kamchatka, Russia: Structural evolution and geodynamic model, Arc-Continent Collision, Springer, 247–277.

Koppers, A. P., 2014. On the Ar/Ar dating of low-potassium ocean crust basalt from IODP Expedition 349, South China Sea. Abstract in AGU Fall Meeting, T31E-03.

Koulali, A., Ouazar, D., Tahayt, A., King, R. W., Vernant, P., Reilinger, R. E., McClusky, S., Mourabit, T., Davila, J. M., Amraoui, N., 2011. New GPS constraints on active deformation along the Africa–Iberia plate boundary. Earth Planet. Sci. Lett. 308, 211-217. doi:10.1016/j.epsl.2011.05.048.

Koulali, A., Susilo, S., McClusky, S., Meilano, I., Cummins, P., Tregoning, P., Lister, G., Efendi, J., Syafi'i, M. A., 2016. Crustal strain partitioning and the associated earthquake hazard in the eastern Sunda-Banda Arc. Geophys. Res. Lett. 43, 1943–1949. doi:10.1002/2016GL067941.

Krishna, K.S., Ramana, M.V., Gopala Rao, D., Murthy, K.S.R., Malleswara Rao, M., Subrahmanyam, V., Sarma, K.V.L.N.S., 1998. Periodic deformation of oceanic crust in the central Indian Ocean. J. Geophys. Res. 103, 17 859–17 875.

Kroehler, M. E., Mann, P., Escalona, A., Christeson, G. L., 2011. Late Cretaceous-Miocene diachronous onset of back thrusting along the South Caribbean deformed belt and its importance for understanding processes of arc collision and crustal growth. Tectonics 30, TC6003. doi:10.1029/2011TC002918.

Kroenke, L., Resig, J., Cooper, P., 1986. Tectonics of the southeastern Solomon Islands: formation of the Malaita anticlinorium. In: Vedder, J., Pound, K., Boundy, S. (Eds.), Geology and Offshore Resources of the Pacific Island Arcs-Central and Western Solomon Islands. Circum-Pacific Council for Energy and Mineral Resources 4. Earth Science Series, Houston, TX, 109–116.

Kroenke, L.W., Walker, D.A., 1986. Evidence for the formation of a new trench in the Western Pacific, Eos, Trans. Am. Geophys. Union 67, 145-146.

Lagabrielle, Y., Pelletier, B., Cabioch, G., Régnier, M., Calmant, S., 2003. Coseismic and long-term vertical displacement due to back arc shortening, central Vanuatu: Offshore and onshore data following the Mw 7.5, 26 November 1999 Ambrym earthquake. J. Geophys. Res., 108 (B11), 2519. doi:10.1029/2002JB002083.

Lagabrielle, Y., Goddéris, Y., Donnadieu, Y., Malavieille, J., Suarez, M., 2009. The tectonic history of Drake Passage and its possible impacts on global climate. Earth Planet. Sci. Lett. 279, 197–211. doi.org/10.1016/j.epsl.2008.12.037.

Lai, C.-K., Xia, X.-P., Hall, R., Meffre, S., Tsikouras, B., Rosana Balangue-Tarriela, M. I., et al., 2021. Cenozoic evolution of the Sulu Sea arc-basin system: An overview. Tectonics, 40, e2020TC006630. doi.org/10.1029/2020TC006630.

Lallemand, S., Okada, H., Otsuka, K., Labeyrie L. , 1985. Tectonique en compression sur la marge est de la mer du Japon: mise en évidence de chevauchements à vergence orientale. C. R. Acad. Sc. Paris 301 (II-3), 201-206 (in french with english abstract).

Lallemand, S., Jolivet, L., 1985. Japan Sea: A pull-apart basin, Earth Planet. Sci. Lett. 76, 375-389.

Lallemand, S. E., Malavieille, J., Calassou, S., 1992. Effects of oceanic ridge subduction on accretionary wedges: Experimental modeling and marine observations. Tectonics 11, 1301-1321.

Lallemand, S. E., 1995. High rates of arc consumption by subduction processes: some consequences. Geology 23, 551–554.

Lallemand, S.E., Liu, C.-S., Font, Y., 1997. A tear fault boundary between the Taiwan orogen and the Ryukyu subduction zone. Tectonophysics 274, 1/3, 171-190.

Lallemand, S. E., 1998. Possible interaction between mantle dynamics and high rates of arc consumption by subduction processes in circum-Pacific area. In: M.F.J. Flower, Sun-Lin Chung, Ching-Hua Lo, and Tung-Yi Lee, eds, Mantle dynamics and plate interactions in East Asia, *Geodynamic Series AGU* 27, 1-10.

Lallemand, S. E., Popoff, M., Cadet, J.-P., Deffontaines, B., Bader, A.-G., Pubellier, M., Rangin C., 1998. Genetic relations between the central & southern Philippine Trench and the Philippine Trench. J. Geophys. Res. 103, B1, 933-950.

Lallemand, S., 1999. La subduction océanique. Gordon and Breach Science Publishers, 208 pp. (in French).

Lallemand, S., Liu, C. -S., Dominguez, S., Schnürle, P., Malavieille, J., and the ACT scientific crew, 1999. Trench parallel stretching and folding of forearc basins and lateral migration of the accretionary wedge in the southern Ryukyus: a case of strain partition caused by oblique convergence. Tectonics 8, 231-247.

Lallemand, S., Font, Y., Bijwaard, H., Kao, H., 2001. New insights on 3-D plates interaction near Taiwan from tomography and tectonic implications. Tectonophysics 335 (3-4), 229-253.

Lallemand, S., Heuret, A., Boutelier, D., 2005. On the relationships between slab dip, back-arc stress, upper plate absolute motion and crustal nature in subduction zones; Geochem. Geophys. Geosyst., 6, 1, doi :10.1029/2005GC000917.

Lallemand S., Heuret A., Faccenna C., Funiciello, F., 2008. Subduction dynamics revealed by trench migration. Tectonics 27, TC3014. doi:10.1029/2007TC002212.

Lallemand, S., Theunissen, T., Schnürle, P., Lee, C.-S., Liu, C.-S., Font Y., 2013. Indentation of the Philippine Sea Plate by the Eurasia Plate in Taiwan: details from recent marine seismological experiments. Tectonophysics 594, 60-79. http://dx.doi.org/10.1016/j.tecto.2013.03.020.

Lallemand, S., 2014. Strain modes within the forearc, arc and back-arc domains in the Izu (Japan) and Taiwan arc-continent collisional settings. J. Asian Earth Sci. 86, 1-11. doi.org/10.1016/j.jseaes.2013.07.043.

Lallemand, S., 2016a. Philippine Sea Plate inception, evolution and consumption with special emphasis on the early stages of Izu-Bonin-Mariana subduction. Prog. Earth Planet. Sci. 3, 15. https://doi.org/10.1186/s40645-016-0085-6.

Lallemand, S., 2016b. Subduction. In Encyclopedia of Marine Geosciences, Springer Science, Eds : Harff, J., Meschede, M., Petersen, S., and Thiede, J., 793-803, DOI 10.1007/978-94-007-6644-0_103-1

Lamarche, G., Collot, J.-Y., Wood, R. A., Sosson, M., Sutherland, R., Delteil J., 1997. The Oligo-Miocene Pacific-Australia plate boundary, south of New Zealand: Evolution from oceanic spreading to strike-slip faulting. Earth Planet. Sci. Lett.. 148 (1/2), 129–139.

Lamarche, G., Lebrun, J.-F., 2000. Transition from strike-slip faulting to oblique subduction: Active tectonics at the Puysegur Margin, South New Zealand. Tectonophysics 316, 67–89.

Larue, D.K., 1994. Puerto Rico and the Virgin Islands. In: Donovan, S.K., and Jackson, T.A., eds., Caribbean Geology; An Introduction: Kingston, University of the West Indies Publisher's Association, 151–165.

Lebrun, J.-F., Lamarche, G., Collot, J.-Y., 2003. Subduction Initiation at a Strike-Slip Plate Boundary: the Cenozoic Pacific - Australian Plate Boundary, South of New Zealand. J. Geophys. Res. 108, B9, 2453. doi:10.1029/2002JB002041.

Legendre, L., Philippon, M., Münch, P., Leticée, J. L., Noury, M., Maincent, G., Cornée, J.-J., Caravati, A., Lebrun, J.-F., Mazabraud, Y., 2018. Trench bending initiation: Upper plate strain pattern and volcanism. Insights from the Lesser Antilles arc, St. Barthelemy Island, French West Indies. Tectonics 37 (9), 2777–2797. doi.org/10.1029/2017TC004921.

Leng, W., Gurnis, M., 2011. Dynamics of subduction initiation with different evolutionary pathways. Geochem. Geophys. Geosyst. 12, Q12018. doi:10.1029/2011GC003877.

Leng, W., Gurnis, M., Asimow, P., 2012. From basalts to boninites: The geodynamics of volcanic expression during induced subduction initiation. Lithosphere, 4(6), 511-523.

Leng, W., Gurnis, M., 2015. Subduction initiation at relic arcs. Geophys. Res. Lett. 42, 7014–7021. http://dx.doi.org/10.1002/2015GL064985.

Le Pichon, X., Sibuet, J. C., 1971. Western extension of boundary between European and Iberian plates during the Pyrenean orogeny. Earth Planet Sci. Lett. 12, 83-88.

Le Pichon, X., Iiyama, T., Boulegue, J., Charvet, J., Faure, M., Kenichi, K., Lallemant, S., Okada, S., Rangin, C., Renard, V., Taira, A., Urabe, T., Uyeda, S., 1987. Nankai Trough and Zenisu Ridge: a deep-submersible survey. Earth Planet. Sci. L.ett. 83, 285-299.

Leprêtre, A., Klingelhoefer, F., Graindorge, D., Schnurle, P., Beslier, M. O., Yelles, K., Déverchère, J., Bracene, R., 2013. Multiphased tectonic evolution of the Central Algerian margin from combined wide-angle and reflection seismic data off Tipaza, Algeria. J. Geophys. Res. Solid Earth 118, 3899–3916. doi:10.1002/jgrb.50318.

Leroy, S., Mauffret, A., Patriat, P., Mercier de Lepinay, B., 2000. An alternative interpretation of the Cayman trough evolution from a reidentification of magnetic anomalies. Geophys. J. Int. 141 (3), 539–557.

Levander, A., Bezada, M. J., Niu, F., Humphreys, E. D., Palomeras, I., Thurner, S. M., Masy, J., Schmitz, M., Gallart, J., Carbonell, R., Miller, M. S., 2014. Subduction-driven recycling of continental margin lithosphere. Nature 515, 253-257. doi:10.1038/nature13878.

Lévy, F., Jaupart, C., 2012. The initiation of subduction by crustal extension at a continental margin. Geophys. J. Int. 188, 779–797. doi: 10.1111/j.1365-246X.2011.05303.x.

Lewis, S. E., Hayes, D. E., 1983. The tectonics of northward propagating subduction along Eastern Luzon, Philippine Islands. In: Hayes DE (ed) The tectonic and geologic evolution of SE Asian seas and islands: Part II, Geol Monogr 27. AGU, Washington DC, 57–78.

Li, C. F., Xu, X., Lin, J., Sun, Z., Zhu, J., Yao, Y., et al., 2014. Ages and magnetic structures of the South China Sea constrained by deep tow magnetic surveys and IODP Expedition 349. Geochemistry, Geophysics, Geosystems 15, 4958–4983. https://doi.org/10.1002/2014GC005567

Lin, S.-C., Kuo, B.-Y., 2016. Dynamics of the opposite-verging subduction zones in the Taiwan region: Insights from numerical models. J. Geophys. Res. Solid Earth 121, doi:10.1002/2015JB012784.

Linckens, J., Herwegh, M., Müntener, O., and Mercolli, I. (2011), Evolution of a polymineralic mantle shear zone and the role of second phases in the localization of deformation, J. Geophys. Res., 116, B06210, doi:10.1029/2010JB008119.

Linthout, K., Helmers, H., Sopaheluwakan, J., 1997. Late Miocene obduction and microplate migration around the southern Banda Sea and the closure of the Indonesian Seaway. Tectonophysics 281, 17-30.

Livermore, R.A., McAdoo, D., Marks, K., 1994. Scotia Sea tectonics from high-resolution satellite gravity. Earth Planet. Sci. Lett. 123, 255–268.

Livermore, R.A., Nankivell, A.P., Eagles, G., Morris, P., 2005. Paleogene opening of Drake Passage. Earth Planet. Sci. Lett. 236, 459–470.

Lock, J., Davies, H. L., Tiffin, D. L., Murakami, F., Kisimoto, K., 1987. The Trobriand Subduction System in the Western Solomon Sea. Geo-Mar. Lett. 7, 129-134.

Louat, R., Pelletier, B., 1989. Seismotectonics and present-day relative plate motion in the New Hebrides arc-North Fiji basin region. Tectonophysics 167, 41–55.

Lowrie, A., Smoot, C., Batiza, R., 1986. Are oceanic fracture zones locked and strong or weak?: New evidence for volcanic activity and weakness. Geology 14, 242-245.

Lu, C. -Y., Hsü, K. -J., 1992. Tectonic evolution of the Taiwan mountain belt. Petroleum Geology of Taiwan 27, p. 21-46.

Lu, G., Kaus, B.J.P., Zhao, L., Zheng, T., 2015. Self-consistent subduction initiation induced by mantle flow. Terra Nova 27 (2), 130–138.

Lustrino, M, Morra, V, Fedele, L, Franciosi, L., 2009. Beginning of the Apennine subduction system in central western Mediterranean: constraints from Cenozoic “orogenic” magmatic activity of Sardinia (Italy). Tectonics 28, TC5016.

Macpherson, C.G., Hall, R., 2001. Tectonic setting of Eocene boninite magmatism in the Izu–Bonin–Mariana forearc. Earth Planet. Sci. Lett. 186 (2), 215–230.

Macpherson, C. G., 2008. Lithosphere erosion and crustal growth in subduction zones: Insights from initiation of the nascent East Philippine Arc. Geology 36 (4), 311–314. doi: 10.1130/G24412A.1.

Magni, V., 2019. The effects of back-arc spreading on arc magmatism. Earth Planet. Sci. Lett. 519, 141-151. https://doi.org/10.1016/j.epsl.2019.05.009

Maffione, M., Thieulot, C., van Hinsbergen, D.J.J., Morris, A., Plümper, O., Spakman, W., 2015. Dynamics of intraoceanic subduction initiation: 1. Oceanic detachment fault inversion and the formation of supra-subduction zone ophiolites. Geochem. Geophys. Geosyst. 16, 1753–1770. https://doi.org/10.1002/2015GC005746.

Maffione, M., van Hinsbergen, D. J. J., 2018. Reconstructing plate boundaries in the Jurassic Neo-Tethys from the East and West Vardar Ophiolites (Greece and Serbia). Tectonics, 37, 858–887. https://doi.org/10.1002/2017TC004790

Mahatsente, R., Ranalli, 2004. Time evolution of negative buoyancy of an oceanic slab subducting with varying velocity, J. Geodyn., 38, 117-129.

Maia, M., Sichel, S., Briais, A., Brunelli, D., Ligi, M., Ferreira, N., Campos, T., Mougel, B., Brehme, I., Hémond, C., Motoki, A., Moura, D., Scalabrin, C., Pessanha, I., Alves, E., Ayres, A., Oliveira, P., 2016. Extreme mantle uplift and exhumation along a transpressive transform fault. Nat. Geosci. 9 (8), 619–623. https://doi.org/10.1038/ngeo2759.

Maillet, P., Monzier. M., Selo, M., Storzer, D., 1983. The d'Entrecasteaux Zone (South-West Pacific) - a petrological and geochronological reappraisal. Mar. Geol. 53, 179-198.

Malahoff, A., Hammonds, J., Feden, R.H., 1979. Back arc spreading. Volcanism and evolution of the Havre trough-Lau basin-Fiji plateau. Proceedings, Hawaii Symposium on Intraplate Volcanism and Submarine Volcanism, Hilo, Hawaii, 113.

Malavieille, J., Lallemand, S., Dominguez, S., Deschamps, A., Lu, C.-Y., Liu, C.S., Schnurle, P., Scientific Crew, 2002. Arc-continent collision in Taiwan: new marine observations and tectonic evolution. Geol. Soc. Amer. Special Paper 358, 187–211.

Malavieille, J., Molli, G., 2014. La Corse alpine. Géochronique 132, 12-25 (in french).

Maldonado, A., Bohoyo, F., Galindo-Zaldivar, J., Hernandez-Molina, J., Lobo, F. J., Lodolo, E., Martos, Y. M., Perez, L. F., Schreider, A. A., Somoza, L., 2014. A model of oceanic development by ridge jumping: Opening of the Scotia Sea. Global Planet. Change 123, 152-173. doi.org/10.1016/j.gloplacha.2014.06.010.

Mann, P., Taira, A., 2004. Global tectonic significance of the Solomon Islands and OntongJava Plateau convergent zone. Tectonophysics 389, 137-190. doi:10.1016/j.tecto.2003.10.024.

Mann, P., 2007. Overview of the tectonic history of northern Central America. Geol. Soc. Am. Spec. Pap. 428, 1–19. https://doi.org/10.1130/2007.2428(01)

Marques, F.O, Cabral, F. R., Gerya, T. V., Zhu, G., May, D. A., 2014. Subduction initiates at straight passive margins. Geology 42, 331-334. doi:10.1130/G35246.1.

Marques, F. O., & Kaus, B. J. P. (2016). Speculations on the impact of catastrophic subduction initiation on the earth system. J. Geodyn., 93, 1-16.

Mart, Y., Aharonov, E., Mulugeta, G., Ryan, W., Tentler, T. & Goren, L., 2005. Analogue modelling of the initiation of subduction, Geophys. J. Int. 160, 1081–1091.

Martínez-Loriente, S., Gracia, E., Bartolome, R., Sallarès, V., Connors, C., Perea, H., Lo Iacono, C., Klaeschen, D., Terrinha, P., Danobeitia, J. J., Zitellini, N., 2013. Active deformation in old oceanic lithosphere and significance for earthquake hazard: Seismic imaging of the Coral Patch Ridge area and neighboring abyssal plains (SW Iberian Margin). Geochem. Geophys. Geosyst. 14, 2206–2231, doi: 10.1002/ggge.20173.

Martínez-Loriente, S., Sallarès, V., Gràcia, E., Bartolome, R., Dañobeitia, J. J., Zitellini, N., 2014. Seismic and gravity constraints on the nature of the basement in the Africa-Eurasia plate boundary: New insights for the geodynamic evolution of the SW Iberian margin, J. Geophys. Res. Solid Earth 119, 127–149, doi:10.1002/2013JB010476.

Martínez-Loriente, S., Gracia, E., Bartolome, Perea, H., Klaeschen, D., Danobeitia, J. J., Zitellini, N., Wynn, R. B., Masson, D. G., 2018. Morphostructure, tectono-sedimentary evolution and seismic potential of the Horseshoe Fault,SW Iberian Margin. Basin Res. 30 (1), 382–400. doi: 10.1111/bre.12225.

Martinod, J., Davy, P., 1992. Periodic Instabilities During Compression or Extension of the Lithosphere: 1. Deformation Modes From an Analytical Perturbation Method. J. Geophys. Res. 97 (B2), 1999-2014.

Massell, C., Coffin, M. F., Mann, P., Mosher, S., Frohlich, C., Duncan, C. S., Karner, G., Ramsay, D., Lebrun, J.-F., 2000. Neotectonics of the Macquarie Ridge Complex, Australia-Pacific plate boundary. J. Geophys. Res. 105 (6), 13,457–13,480.

Matsuda, J., Saito, K., Zasu, S., 1975. K-Ar age and Sr isotope ratio of the rocks in the manganese nodules obtained from the Amami Plateau, Western Philippine Sea. In: Symposium on Geological Problems of the Philippine Sea. Geol. Soc. Japan, 91–98.

Matsumoto, T., Tomoda, Y., 1983. Numerical-simulation of the initiation of subduction at the fracture-zone. J. Phys. Earth 31, 183–194.

Matthews, K.J., Williams, S.E., Whittaker, J.M., Müller, R.D., Seton, M., Clarke, G.L., 2015. Geologic and kinematic constraints on Late Cretaceous to mid Eocene plate boundaries in the southwest Pacific. Earth-Science Reviews 140, 72–107.

Mauffret, A., Leroy, S., 1999. Neogene intraplate deformation of the Caribbean plate at the Beata Ridge. In: Sedimentary Basins of the World 4, Caribbean Basins, edited by P. Mann, Elsevier Sci., 627–669.

Mauffret, A., Leroy, S., d'Acremont, E., Maillard, A., Mercier de Lépinay, B., Tadeu dos Reis, A., Miller, N., Nercessian, A., Perez-Vega, R., Perez, D., 2001. Une coupe de la province volcanique Caraïbe : premiers résultats de la campagne sismique Casis 2. C. R. Acad. Sci. Paris 333, 659-667.

Maunder, B., Prytulak, J., Goes, S., Reagan, M., 2020. Rapid subduction initiation and magmatism in the Western Pacific driven by internal vertical forces. Nature comm. 11, 1874. https://doi.org/10.1038/s41467-020-15737-4.

Mazzotti, S., Lallemant, S. J., Henry, P., Le Pichon, X., Tokuyama, H., Takahashi, N., 2002. Intraplate shortening and underthrusting of a large basement ridge in the eastern Nankai subduction zone. Mar. Geol. 187, 63-88.

McCaffrey, R., Nabelek, J., 1984. The geometry of back-arc thrusting along the eastern Sunda Arc, Indonesia: constraints from earthquake and gravity data. J. Geophys. Res. 89 (B7), 6171–6179.

McKenzie, D., 1977. The initiation of trenches: a finite amplitude instability. In Island Arcs, Deep Sea Trenches and Back-Arc Basins, Maurice Ewing Series 1, eds Talwani, M. & Pitman, W., American Geophysical Union, Washington, DC., 57–61.

McNutt, M. K., Menard, H. W.,1982. Constraints on yield strength in the oceanic lithosphere from observations of flexure, Geophys.or.R. Astron. Soc., 71, 363-394.

Meckel, T. A., Coffin, M. F., Mosher, S., Symonds, P., Bernardel, G., Mann, P., 2003. Underthrusting at the Hjort Trench, Australian-Pacific plate boundary: Incipient subduction?. Geochem. Geophys. Geosyst. 4 (12), 1099. doi:10.1029/2002GC000498.

Meckel, T. A., Mann, P., Mosher, S., Coffin, M. F., 2005. Influence of cumulative convergence on lithospheric thrust fault development and topography along the Australian-Pacific plate boundary south of New Zealand. Geochem. Geophys. Geosyst., 6, Q09010. doi:10.1029/2005GC000914.

Meffre, S., Falloon, T. J., Crawford, T. J., Hoernle, K., Hauff, F., Duncan, R. A., Bloomer, S. H., Wright, D. J., 2012. Basalts erupted along the Tongan fore arc during subduction initiation: Evidence from geochronology of dredged rocks from the Tonga fore arc and trench. Geochem. Geophys. Geosyst. 13, Q12003. doi:10.1029/2012GC004335.

Milia, A., Iannace, P., Tesauro, M., Torrente, M. M., 2018. Marsili and Cefalù basins: The evolution of a rift system in the southern Tyrrhenian Sea (Central Mediterranean). Global Planet. Change 171, 225-237. doi.org/10.1016/j.gloplacha.2017.12.003.

Mitchell, A. H. G., 1984. Initiation of subduction by post-collision foreland thrusting and back-thrusting. J. Geodyn. 1, 103-120.

Miura, S., Suyehiro, K., Shinohara, M., Takahashi, N., Araki, E., Taira, A., 2004. Seismological structure and implications of collision between the Ontong Java Plateau and Solomon Island Arc from ocean bottom seismometer–airgun data. Tectonophysics 389, 191-220. doi:10.1016/j.tecto.2003.09.029.

Molli, G., Malavieille, J., 2010. Orogenic processes and the Corsica/Apennines geodynamic evolution: insights from Taiwan. Int. J. Earth Sci. 100, 1207-1224.

Monna, S., Argnani, A., Cimini, G. B., Frugoni, F., Montuori, C., 2015. Constraints on the geodynamic evolution of the Africa-Iberia plate margin across the Gibraltar Strait from seismic tomography. Geosci. Frontiers 6, 39-48. doi.org/10.1016/j.gsf.2014.02.003.

Montes, C., Hatcher, R.D., Restrepo-Pace, P., 2005. Tectonic reconstruction of the northern Andean blocks: oblique convergence and rotations derived from the kinematics of the Piedras-Girardot area, Colombia. Tectonophysics 399, 221–250.

Montes, C., Rodriguez-Corcho, A. F., Bayona, G., Hoyos, N., Zapata, S., Cardona, A., 2019. Continental margin response to multiple arc-continent collisions: The northern Andes-Caribbean margin. Earth-Sci. Rev. 198, 102903. doi.org/10.1016/j.earscirev.2019.102903.

Monzier, M., Danyushevsky, L. V., Crawford, A. J., Bellon, H., Cotten, J., 1993. High-Mg andesites form the southern termination of the New Hebrides island arc (SW Pacific). J. Volcanol. Geotherm. Res. 57, 193–217.

Morency, C., Doin, M.-P., 2004. Numerical simulations of the mantle delamination. J. Geophys. Res. 109, 3410. https://doi.org/10.1029/2003JB002414.
Mortimer, N., Gans, P. B., Foley, F. V., Turner, M. B., Daczko, N., Robertson, M., Turnbull, I. M., 2013. Geology and Age of Solander Volcano, Fiordland, New Zealand. The Journal of Geology 121, 475–487. DOI: 10.1086/671397.
Mortimer, N., Gans, P. B., Palin, J. M., Herzer, R. H., Pelletier, B., Monzier, M., 2014. Eocene and Oligocene basins and ridges of the Coral Sea-New Caledonia region: Tectonic link between Melanesia, Fiji, and Zealandia. Tectonics 33, 1386–1407. doi:10.1002/2014TC003598.
Mueller, S., Phillips, R.J., 1991. On the initiation of subduction. J. Geophys. Res. 96, 651–665.
Müller, R.D., Smith, W.H.F., 1993. Deformation of the oceanic crust between the North American and SouthAmerican plates. J. Geophys. Res. 98, 8275–8291.
Müller, R.D., Royer, J.-Y., Cande, S.C., Roest, W.R., Maschenkov, S., 1999. New constraints on the Late Cretaceous–Tertiary plate tectonic evolution of the Caribbean. In: Mann, P., ed., Caribbean Basins: Amsterdam, Elsevier, Sedimentary Basins of the World 4, 33–57.
Mrozowski, C. L., Lewis, S. D., Hayes, D. E., 1982. Complexities in the tectonic evolution of the West Philippine Basin. Tectonophysics 82, 1–24.
Mulyukova, E., Bercovici, D., 2018. Collapse of passive margins by lithospheric damage and plunging grain size. Earth Planet. Sci. Lett. 484, 341-352. https://doi.org/10.1016/j.epsl.2017.12.022.
Nakamura, K., 1983. Possible nascent trench along the eastern Japan sea as the convergent boundary between Eurasian and North American plates. Bull. Earthquake Res. Inst. Univ. Tokyo 58, 721-732 (in japanese with english abstract).
Nakanishi, A., Shibara, H., Hino, R., Kodaira, S., Kanazawa, T., Shimamura, H., 1998. Detailed subduction structure across the eastern Nankai Trough obtained from ocean bottom seismographic profiles. J. Geophys. Res. 103, 27151-27168.
Nakanishi, A., Shiobara, H., Hino, R., Mochizuki, K., Sato, T., Kasahara, J., Takahashi, N., Suyehiro, K., Tokuyama, H., Segawa, J., Shinohara, M., Shimahura, H., 2002. Deep crustal structure of the Eastern Nankai trough and the Zenisu ridge by dense airgun-OBS seismic profiling. Mar. Geol. 187, 47-62.
Neill, I., Kerr, A. C., Hastie, A. R., Stanek, K.-P., Millar, I. L., 2011. Origin of the Aves Ridge and Dutch–Venezuelan Antilles: Interaction of the Cretaceous 'Great Arc' and Caribbean–Colombian Oceanic Plateau?. J. Geol. Soc. 168 (2), 333–348. doi.org/10.1144/0016-76492010-067.
Nerlich, R., Clark, S. R., Bunge, H.-P., 2014. Reconstructing the link between the Galapagos hotspot and the Caribbean Plateau. GeoResJ 1-2. http://dx.doi.org/10.1016/j.grj.2014.02.001.
Nicolas, A., Boudier, F., 1995. Mapping oceanic ridge segments in Oman ophiolite. J. Geophys. Res.100, B4, 6179-6197. https://doi.org/10.1029/94JB01188
Nikolaeva, K., Gerya, T.V., Connolly, J.A.D., 2008. Numerical modelling of crustal growth in intraoceanic volcanic arcs. Phys. Earth Planet. Inter. 171, 336–356.
Nikolaeva, K., Gerya, T.V., Marques, F.O., 2010. Subduction initiation at passive margins: numerical modeling. J. Geophys. Res. 115, B03406.

Niu, Y., O'Hara, M.J., Pearce, J.A., 2003. Consequence of lateral compositional buoyancy contrast within the lithosphere: a petrological perspective. J. Petrol. 44, 851–866.
Nocquet, J. M., Calais, E., 2004. Geodetic measurements of crustal deformation in the Western Mediterranean and Europe, Pure Appl. Geophys. 161, 661–681.
Nocquet, J.-M., 2012. Present-day kinematics of the Mediterranean: A comprehensive overview of GPS results. Tectonophysics 579, 220–242. doi:10.1016/j.tecto.2012.03.037.
Nugroho, H., Harris, R., Lestariya, A. W., Maruf, B., 2009. Plate boundary reorganization in the active Banda Arc–continent collision: Insights from new GPS measurements. Tectonophysics 479, 52-65. doi:10.1016/j.tecto.2009.01.026.
Nunez, D., Cordoba, D., Cotilla, M. O., Pazos, A., 2016. Modeling the Crust and Upper Mantle in Northern Beata Ridge (CARIBE NORTE Project). Pure Appl. Geophys. 173, 1639–1661. DOI 10.1007/s00024-015-1180-0.
Ohara, Y., Fujioka, K., Ishizuka, O., Ishii, T., 2002. Peridotites and volcanics from the Yap arc system; implications for tectonics of the southern Philippine Sea Plate. Chem. Geol. 189 (1–2), 35–53.
Okada, H., Lallemand, S., Otsuka, K., Labeyrie, L., 1985. Submarine geologic structure of the eastern margin of the Sea of Japan with special reference to the nascent trench problem. Geosc. Rep. of Shizuoka University 11, 119-133 (in Japanese with english abstract).
Okal, E. A., Woods, D. F., Lay, T., 1986. Intraplate deformation in the Samoa-Gilbert-Ralik area: a prelude to a change of plate boundaries in the Southwest Pacific?. Tectonophysics 132, 69-77.
Okamura, Y., Watanabe, M., Morijiri, R., Satoh, M., 1995. Rifting and basin inversion in the eastern margin of the Japan Sea. Island Arc 4, 166-181.
Okamura, Y., Satake, K., Ikehara, K., Takeuchi, A., Arai, K. 2005. Paleoseismology of deep-sea faults based on marine surveys of northern Okushiri ridge in the Japan Sea. J. Geophys. Res. 110, B09105. doi:10.1029/2004JB003135.
Okino, K., Kasuga, S., Ohara, Y., 1998. A new scenario of the Parece Vela basin genesis. Mar. Geophys. Res. 20 (1),21–40.
Oxburgh, E. R., Parmentier, E. M., 1977. Compositional and density stratification in oceanic lithosphere - causes and consequences. J. Geol. Soc. London 133, 343-355.
Ozima, M., Kaneoka, I., Ujie, H., 1977. 40Ar/39Ar age of rocks and development mode of the Philippine Sea. Nature 267, 816–818.
Padron, C., Klingelhoefer, F., Marcaillou, B., Lebrun, J.-F., Lallemand, S., Garrocq, C., Laigle, M., Roest, W., Beslier, M.-O., Schenini, L., Graindorge, D., Gay, A., Audemard, F., Münch, P., the GARANTI Cruise team, 2021a. Deep structure of the Grenada Basin from wide-angles seismic, bathymetric and gravity data. J. Geophys. Res.: Solid Earth 126. DOI: 10.1029/2020JB020472.
Padron, C., Deville, E., Huyghe, P., Lallemant, S., Lebrun, J. F., 2021b. Diffuse deformation processes at the southeastern boundary of the Caribbean plate. In C. Bartolini, ed., South America–Caribbean–Central Atlantic plate boundary: Tectonic evolution, basin architecture, and petroleum systems. AAPG Memoir 123. DOI: 10.1306/13692261M1233854.

Park, J.-O., Moore, G. F., Tsuru, T., Kodaira, S., Kaneda, Y., 2003. Earth Planet. Sci. Lett. 217, 77-84.

Parsons, B., Richter, F. M., 1980. A relation between the driving force and geoid anomaly associated with mid-ocean ridges. Earth Planet. Sci. Lett., *51*(2), 445-450.

Patocka, V., Cizkova, H., Tackley, P. J., 2019. Do elasticity and a free surface affect lithospheric stresses caused by upper-mantle convection?. 2019. Geophys. J. Int. 216, 1740–1760. doi: 10.1093/gji/ggy513.

Patriat, M., Pichot, T., Westbrook, G.K., Umber, M., Deville, E., Bénard, F., Roest, W.R., Loubrieu, B., the Antiplac cruise party, 2011. Evidence for Quaternary convergence between the North American and South American plates, east of the Lesser Antilles. Geology 39 (10), 979–982.

Patriat, M., Collot, J., Danyushevsky, L., Fabre, M., Meffre, S., Falloon, T., Rouillard, P., Pelletier, B., Roach, M., Fournier, M., 2015. Propagation of back-arc extension into the arc lithosphere in the southern New Hebrides volcanic arc. Geochem. Geophys. Geosyst. 16, 3142–3159. https://doi.org/10.1002/2015GC005717.

Patriat, M., Collot, J., Etienne, S., Poli, S., Clerc, C., Mortimer, N., Pattier, F., Juan, C., Roest, W. R., VESPA Scientific voyage team, 2018. New Caledonia obducted peridotite nappe: Offshore extent and implications for obduction and postobduction processes. Tectonics 37, 1077–1096. https://doi.org/10.1002/2017TC004722.

Patriat, M., Falloon, T., Danyushevsky, L., Collot, J., Jean, M.M., Hoernle, K., Hauff, F., Maas, R., Woodhead, J.D., Feig, S.T., 2019. Subduction initiation terranes exposed at the front of a 2 Ma volcanically-active subduction zone. Earth Planet. Sci. Lett. 508, 30–40.

Pelletier, B., Meschede, M., Chabernaud, T., Roperch, R., Zhao,X., 1994. Tectonics of the central New Hebrides arc, North Aoba basin. Proc. Ocean Drill. Program Sci. Results 134, 431– 444.

Pelletier, B., Calmant, S., Pillet, R., 1998. Current tectonics of the Tonga–New Hebrides region. Earth and Planetary Science Letters 164, 263– 276.

Perez, A., Umino, S., Yumul Jr, G. P., Ishizuka, O., 2018. Boninite and boninite-series volcanics in northern Zambales ophiolite: doubly vergent subduction initiation along Philippine Sea plate margins. Solid Earth 9, 713–733. https://doi.org/10.5194/se-9-713-2018.

Pérez-Díaz, L., Eagles, G., Sigloch, K., 2020. Indo-Atlantic plate accelerations around the Cretaceous-Paleogene boundary: A time-scale error, not a plume-push signal. Geology 48(12), 1169-1173. doi: https://doi.org/10.1130/G47859.1

Petterson, M., Babbs, T., Neal, C., Mahoney, J., Saunders, A., Duncan, R., Tolia, D., Magu, R., Qopoto, C., Mahoa, H., Natogga, D., 1999. Geological-tectonic framework of Solomon Islands, SW Pacific: crustal accretion and growth within an intra-oceanic setting. Tectonophysics 301, 35–60.

Phinney, E., Mann, P., Coffin, M., Shipley, T., 1999. Sequence stratigraphy, structure, and tectonics of the southwestern Ontong Java Plateau adjacent to the North Solomon trench and Solomon Islands arc. J. Geophys. Res. 104, 20449– 20466.

Phinney, E.J., Mann, P., Coffin, M.F., Shipley, T.H., 2004. Sequence stratigraphy, structural style, and age of deformation of the Malaita accretionary prism

(Solomon arc-Ontong Java Plateau convergent zone). Tectonophysics 389, 221–246.
Pichot, T., Patriat, M., Westbrook, G., Nalpas, T., Gutscher, M., Roest, W., Deville, E., Moulin, M., Aslanian, D., Rabineau, M., 2012. The Cenozoic tectonostratigraphic evolution of the Barracuda Ridge and Tiburon Rise, at the western end of the North America – South America plate boundary zone. Mar. Geol. 303-306, 154-171. https://doi.org/10.1016/j.margeo.2012.02.001.
Pindell, J.L., Barrett, S.F., 1990. Geological evolution of the Caribbean region: A plate tectonic perspective. In: Dengo, G., and Case, J.E., eds., The Caribbean region: Boulder, Colorado, Geological Society of America, Geology of North America, 405–432.
Pindell, J. L., Kennan, L., 2001. Processes and events in the terrane assembly of Trinidad and eastern Venezuela. In: Fillon, R. H., Rosen, N. C. et al. (eds) Transactions of the 21st GCSSEPM Annual Bob F. Perkins Research Conference: Petroleum Systems of Deep-Water Basins, 159–192.
Pindell, J. L., Kennan, L., Stanek, K.-P., Maresch, W. V., Draper, G., 2006. Foundations of Gulf of Mexico and Caribbean evolution: Eight controversies resolved. Geologica Acta 4, 89-128.
Pindell, J. L., Kennan, L., 2009. Tectonic evolution of the Gulf of Mexico, Caribbean and northern South America in the mantle reference frame: an update. Geol. Soc. London, Spe. Publ. 328 (1), 1.1–1.55. https://doi.org/10.1144/SP328.1.
Pindell, J., Maresch, W. V., Martens, U., Stanek, K., 2012. The Greater Antillean Arc: Early Cretaceous origin and proposed relationship to Central American subduction mélanges: implications for models of Caribbean evolution. Int. Geol. Rev. 54 (2), 131-143. DOI: 10.1080/00206814.2010.510008
Pubellier, M., Meresse, F., 2013. Phanerozoic growth of Asia; geodynamic processes and evolution. J. Asian Earth Sc. 72, 118-128.
Pubellier, M., Morley, C. K., 2014. The basins of Sundaland (SE Asia): Evolution and boundary conditions. Mar. Petrol. Geol. 58, 555-578. http://dx.doi.org/10.1016/j.marpetgeo.2013.11.019.
Pysklywec, R. N., Mitovica, J. X., Ishii, M., 2003. Mantle avalanche as a driving force for tectonic reorganization in the southwest Pacific. Earth Planet. Sci. Lett. 209, 29-38. doi:10.1016/S0012-821X(03)00073-6.
Qian, S., Zhang, X., Wu, J., Lallemand, S., Nichols, A. R. L., Huang, C.-Y., Miggins, D.P., Zhou, H., 2021. First identification of a Cathaysian continental fragment beneath the Gagua Ridge, Philippine Sea, and its tectonic implications. Geology 49. https://doi.org/10.1130/G48956.1.
Qing, J., Liao, J., Li L., Gao, R., in press. Dynamic evolution of induced subduction through the inversion of spreading ridges. J. Geophys. Res. Solid Earth. doi: 10.1029/2020JB020965.
Rangin, C., Jolivet, L., Pubellier, M., Tethys Pacific working Group, 1990. A simple model for the tectonic evolution of southeast Asia and Indonesia region for the past 43 m.y.. Bull. Soc. géol. France (6), 889-905.
Rangin, C., Spakman, W., Pubellier, M., Bijwaard, H., 1999. Tomographic and geological constraints on subduction along the eastern Sundaland continental margin (South-East Asia). Bull. Soc. Geol. Fr. 170, 775–788.
Reagan, M. K., Ishizuka, O., Stern, R. J., Kelley, K. A., Ohara, Y., Blichert-Toft, J., Bloomer, S. H., Cash, J., Fryer, P., Hanan, B. B., Hickey-Vargas, R., Ishii, T.,

Kimura, J. I., Peate, D. W., Rowe, M. C., Woods, M., 2010. Fore-arc basalts and subduction initiation in the Izu–Bonin–Mariana system. Geochem Geophys Geosyst 11, Q03X12. doi.org/10.1029/2009GC002871.

Reagan, M. K., McClelland, W. C., Girard, G., Goff, K. R., Peate, D. W., Ohara, Y., Stern, R. J., 2013. The geology of the southern Mariana fore-arc crust: Implications for the scale of Eocene volcanism in the western Pacific. Earth Planet Sci Lett 380, 41–51. doi:10.1016/j.epsl.2013.08.013.

Reagan, M. K., Heaton, D. E., Schmitz, M. D., Pearce, J. A., Shervais, J. W., and Koppers, A. A., 2019. Forearc ages reveal extensive short-lived and rapid seafloor spreading following subduction initiation. Earth Planet. Sc. Lett. 506, 520–529. https://doi.org/10.1016/j.epsl.2018.11.020.

Regenauer-Lieb, K., Yuen, D.A., Branlund, J., 2001. The initiation of subduction: critically by addition of water? Science 294, 578–580.

Régnier, M., Calmant, S., Pelletier, B., Lagabrielle, Y., Cabioch, G., 2003. The Mw 7.5 1999 Ambrym earthquake, Vanuatu: A back arc intraplate thrust event. Tectonics 22 (4), 1034. doi:10.1029/2002TC001422.

Révillon, S., Hallot, E., Arndt, N.T., Chauvel, C., and Duncan Jr., A., 2000. A Complex History for the Caribbean Plateau: Petrology, Geochemistry, and Geochronology of the Beata Ridge, South Hispaniola. J. Geol. 108, 641–661.

Ribeiro, J.M., Stern, R.J., Kelley, K., Shaw, A., Martinez, F., Ohara, Y., 2015. Composition of the slab-derived fluids released beneath the Mariana fore-arc: evidence for shallow dehydration of the subducting plate. Earth Planet. Sci. Lett. 418, 136-148. http://dx.doi.org/10.1016/j.epsl.2015.02.018.

Rodriguez, M., Chamot-Rooke, N., Fournier,M., Huchon, P., Delescluse, M., 2013. Mode of opening of an oceanic pull-apart: The 20 °N Basin along the Owen Fracture Zone (NW Indian Ocean). Tectonics 32, 1343–1357. doi:10.1002/tect.20083.

Rodriguez, M., Arnould, M., Coltice, N., Soret, M., 2021. Long-term evolution of a plume-induced subduction in the Neotethys realm. Earth Planet. Sci. Lett. 561, 116798. https://doi.org/10.1016/j.epsl.2021.116798.

Rodriguez-Zurrunero, A., Granja-Bruna, J.L., Munoz-Martin, A., Leroy, S., ten Brink, U., Gorosabel-Araus, J.M., Gomez de la Pena, L., Druet, M., Carbo-Gorosabel, A., 2020. Along-strike segmentation in the northern Caribbean plate boundary zone (Hispaniola sector): Tectonic implications. Tectonophysics 776, https://doi.org/10.1016/j.tecto.2020.228322.

Roest, W.R., Collette, B.J., 1986. The Fifteen-Twenty fracture zone and the North American-South American plate boundary. J. Geol. Soc. London 143 (5), 833–843.

Roest, W. R., Srivastava, S. P., 1991. Kinematics of the plate boundaries between Eurasia, Iberia, and Africa in the north Atlantic from the Late Cretaceous to the present. Geology 19, 613–616.

Roland, E., Behn, M. D., Hirth, G., 2010. Thermal-mechanical behavior of oceanic transform faults: Implications for the spatial distribution of seismicity. Geochem. Geophys. Geosyst. 11, Q07001. doi:10.1029/2010GC003034.

Roman, Y.A., Pujols, E.J., Cavosie, A.J., Stockli, D.F., 2020. Timing and magnitude of progressive exhumation and deformation associated with Eocene arc-continent collision in the NE Caribbean plate. GSA Bulletin, https://doi.org/10.1130/B35715.1.

Rosenbaum, G., 2014. Geodynamics of oroclinal bending: Insights from the Mediterranean. J. Geodyn. 82, 5-15. doi.org/10.1016/j.jog.2014.05.002.
Royden, L., Faccenna, C., 2018. Subduction Orogeny and the Late Cenozoic Evolution of the Mediterranean Arcs. Annu. Rev. Earth Planet. Sci. 46, 261–89. https://doi.org/10.1146/annurev-earth-060115-012419.
Sallarès, V., Gailler, A., Gutscher, M.-A., Graindorge, D., R Bartolome, R., Gràcia, E., Díaz, J., Dañobeitia, J. J., Zitellini, N., 2011. Seismic evidence for the presence of Jurassic oceanic crust in the central Gulf of Cadiz (SW Iberia margin). Earth Planet. Sci. Lett. 311, 112–123, doi:10.1016/j.epsl.2011.09.003.
Sallarès, V., Martínez-Loriente, S., Prada, M., Gràcia, E., Ranero, C., Gutscher, M.-A., Bartolome, R., Gailler, A., Danobeitia, J. J., Zitellini, N., 2013. Seismic evidence of exhumed mantle rock basement at the Gorringe Bank and the adjacent Horseshoe and Tagus abyssal plains (SW Iberia). Earth Planet. Sci. Lett. 365, 120–131. doi: 10.1016/j.epsl.2013.01.021.
Sanchez, J., Mann, P., Carvajal-Arenas, L. C., Bernal-Olaya, R., 2019. Regional transect across the western Caribbean Sea based on integration of geologic, seismic reflection, gravity, and magnetic data. AAPG Bulletin 103, (2), 303–343. DOI:10.1306/05111816516.
Sandiford, D., Moresi, L., 2019. Improving subduction interface implementation in dynamic numerical models. Solid Earth, 10(3), 969-985, doi:10.5194/se-10-969-2019.
Sartori, R., 1990. The main results of ODP Leg 107 in the frame of Neogene to recent geology of peri-tyrrhenian areas. Proc. ODP Sci. Res. 107, 715–30.
Sato, T., No, T., Kodaira, S., Takahashi, N., Kaneda, Y., 2014. Seismic constraints of the formation process on the back-arc basin in the southeastern Japan Sea. J. Geophys. Res. Solid Earth 119, 1563–1579. doi:10.1002/2013JB010643.
Scalabrino, B., Lagabrielle, Y., de la Rupelle, A., Malavieille, J., Polvé, M., Espinoza, M., Morata, D., Suarez, M., 2009. Subduction of an active spreading ridge beneath southern South America: a review of the Cenozoic geological records from the Andean foreland, Central Patagonia (46–47°S). In: Lallemand, S., Funiciello, F., (Eds.), Subduction Zone Dynamics, vol. 225. International Journal of Earth Sciences, Springer-Verlag Berlin Heidelberg. doi:10.1007/978-3-540-87974-9.
Schellart, W.P., Lister, G. S., Toy, V. G., 2006. A Late Cretaceous and Cenozoic reconstruction of the Southwest Pacific region: Tectonics controlled by subduction and slab rollback processes. Earth-Sci. Rev. 76, 191-233. doi:10.1016/j.earscirev.2006.01.002.
Schellart, W. P., Kennett, B. L. N., Spakman, W., Amaru, M., 2009. Plate reconstructions and tomography reveal a fossil lower mantle slab below the Tasman Sea. Planet. Sci. Lett. 278, 143-151. doi:10.1016/j.epsl.2008.11.004.
Schellart, W. P., Spakman, W., 2012. Mantle constraints on the plate tectonic evolution of the Tonga–Kermadec–Hikurangi subduction zone and the South Fiji Basin region. Australian J. Earth Sci. 59, 933–952. doi.org/10.1080/08120099.2012.679692.
Schellart, W. P., Sapkman, W., 2015. Australian plate motion and topography linked to fossil New Guinea slab below Lake Eyre. Earth Planet. Sci. Lett. 421, 107-116. http://dx.doi.org/10.1016/j.epsl.2015.03.036.

Schellart, W. P., 2017. A geodynamic model of subduction evolution and slab detachment to explain Australian plate acceleration and deceleration during the latest Cretaceous–early Cenozoic. Lithosphere 9 (6), 976–986. doi .org /10 .1130 /L675 .1.

Schellart, W. P., 2020. Control of Subduction Zone Age and Size on Flat Slab Subduction. Front. Earth Sci. 8 (26). doi: 10.3389/feart.2020.00026.

Schettino, A., Scotese, C., 2002. Global kinematic constraints to the tectonic history of the Mediterranean region and surrounding areas during the Jurassic and Cretaceous. In: Rosenbaum, G. and Lister, G. S. 2002. Reconstruction of the evolution of the Alpine-Himalayan Orogen. J. Virtual Explorer 8, 149-168.

Schmandt, B., Humphreys, E., 2011. Seismically imaged relict slab from the 55 Ma Siletzia accretion to the northwest United States. Geology 39, 175–178. https:// doi .org /10.1130/G31558 .1.

Schmid, S. M., Bernoulli, D., Fügenschuh, B. , Scheffer, S., Matenco, L., Schuster, R., Tischler, M., Ustaszewski, K., 2008. The Alpine-Carpathian-Dinaridic orogenic system: correlation and evolution of tectonic units. Swiss J. Geosci. 101,139–83. DOI 10.1007/s00015-008-1247-3.

Scholl, D. W., Vallier, T. L., Stevenson, A. J., 1986. Terrane accretion, production, and continental growth—a perspective based on the origin and tectonic fate of the Aleutian-Bering Sea region. Geology 14, 43–47.

Scholl, D. W., Stevenson, A. J., Mueller, S., Geist, E. L., Engebretson, D. C., Vallier, T. C., 1992. Exploring the notion that southeast-Asian-type escape tectonics and trench clogging are involved in regional-scale deformation of Alaska and the formation of the Aleutian-Bering Sea region. In: M. Flower, R. McCabe and T. Hilde, (editors), Southeast Asia Structure, Tectonics, and Magmatism: Proceedings of the Geodynamics Research Institute Symposium, Texas A & M University, College Station, Texas, 57–63.

Searle, R., 1983. Multiple, closely spaced transform faults in fast-slipping fractures zones. Geology, 11, 607–610

Seno, T., 1983. A consideration on the "Japan sea subduction hypothesis" seismic slip vector along the Japan trench. Jishin (J. Geol. Soc. Jpn.) 36, 227-273 (in Japanese).

Seranne, M., 1999. The Gulf of Lion continental margin (NW Mediterranean) revisited by IBS: an overview. In: The Mediterranean Basins: Tertiary Extension Within the Alpine Orogen, ed. B. Durand, L. Jolivet, F. Horvath, M. Seranne, Geol. Soc. Spec. Publ. 156. Geol. Soc. London, 21–53.

Serpelloni, E., Vannucci, G., Pondrelli, S., Argnani, A., Casula, G., Anzidei, M., Baldi, P., Gasperini, P., 2007. Kinematics of the Western Africa-Eurasia plate boundary from focal mechanisms and GPS data. Geophys. J. Int. 169, 1180–1200. doi: 10.1111/j.1365-246X.2007.03367.x.

Seton, M., Müller, R. D., Zahirovic, S., Gaina, C., Torsvik, T., Shephard, G., Talsma, A., Gurnis, M., Turner, M., Maus, S., Chandler, M., 2012. Global continental and ocean basin reconstructions since 200 Ma. Earth-Sci. Rev., 113 (3-4), 212–270. https://doi.org/10.1016/j.earscirev.2012.03.002

Seton, M., Flament, N., Whittaker, J., Müller, R. D., Gurnis, M., Bower, D. J., 2015. Ridge subduction sparked reorganization of the Pacific plate-mantle system 60–50 million years ago. Geophys. Res. Lett. 42, 1732–1740. https://doi.org/10.1002/2015GL063057.

Seton, M., Mortimer, N., Williams, S., Quilty, P., Gans, P., Meffer, S., Micklethwaite, S., Zahirovic, S., Moore, J., Matthews, K. J., 2016. Melanesian back-arc basin and arc development: Constraints from the eastern Coral Sea. Gondwana Res. 39, 77-95. doi.org/10.1016/j.gr.2016.06.011.

Shao, W.-Y., Chung, S.-L., Chen, W.-S., Lee, H.-Y., Xie, L.-W., 2015. Old continental zircons from a young oceanic arc, eastern Taiwan: Implications for Luzon subduction initiation and Asian accretionary orogeny. Geology 43 (6), 479-482.

Sharp, W.D., Clague, D.A., 2006. 50-Ma initiation of Hawaiian-Emperor bend records major change in Pacific plate motion. Science 313, 1281–1284, doi: 10 .1126 /science .1128489.

Shemenda, A., Grocholsky, A. L., 1986. Geodynamics of the South Antilles Region. Geotectonics 20, 58-66.

Shemenda A,. I., 1989. Results from physical modeling of horizontal compression in the lithosphere. Dokl. Akad. Nauk SSSR 307, 345-350 (in Russian).

Shemenda, A. I., 1992. Horizontal lithosphere compression and subduction: Constraints provided by physical modeling. J. Geophys. Res. 97, 11097-11116.

Shemenda, A.I., 1994. Subduction: Insights from Physical Modeling. Kluwer Academic Publishers.

Shimabukuro, D. H., Wakabayashi, J., Alvarez, W., Chang, S. C., 2012. Cold and old: The rock record of subduction initiation beneath a continental margin, Calabria, southern Italy. Lithosphere 4(6), 524-532.

Shinjo, R., Chung, S.-L., Kato, Y., Kimura, M., 1999. Geochemical and Sr-Nd isotopic characteristics of volcanic rocks from the Okinawa Trough and Ryukyu Arc: Implications for the evolution of a young, intracontinental back arc basin. J. Geophys. Res. 104, 10591-10608.

Sibuet, J.-C., Hsu, S.-K., Shyu, C.-T., Liu, C.-S., 1995. Structural and kinematic evolution of the Okinawa trough backarc basin. In Backarc Basins: Tectonics and Magmatism, ed. by B. Taylor, Plenum, New York, 343-378.

Sibuet, J.-C., Srivastava, S. P., Spakman, W., 2004. Pyrenean orogeny and plate kinematics. J. Geophys. Res. 109, B08104. doi:10.1029/2003JV002514.

Sibuet, J.-C., Yeh, Y.-C., Lee, C.-S., 2016. Geodynamics of the South China Sea. Tectonophysics 692, 98–119. doi:10.1016/j.tecto.2016.02.022.

Sigurdsson, I. A., Kamenetsky, V. S., Crawford, A. J., Eggins, S. M., Zlobin, S. K., 1993. Primitive island arc and oceanic lavas from the Hunter Ridge-Hunter Fracture Zone. Evidence from glass, olivine and spinel compositions. Mineral. Petrol. 47, 149–169.

Silver, E.A., Moore, J.C., 1978. The Molucca Sea collision zone, Indonesia. J. Geophys. Res. 83, 1681–1691.

Silver, E.A., Reed, D., McCaffrey, R., 1983. Back arc thrusting in the Eastern Sunda Arc, Indonesia: a consequence of arc-continent collision. J. Geophys. Res. 88, B9, 7429-7448.

Silver, E.A., Reed, D.L., Tagudin, J.E., Heil, D.J., 1990. Implications of the north and South Panama thrust belts for the origin of the Panama orocline. Tectonics 9 (2), 261–281.

Simons, W.J.F., Socquet, A., Vigny, C., Ambrosius, B.A.C., Abu, S.H., Promthong, C., Subarya, Sarsito, D.A., Matheussen, S., Morgan, P., Spakman, W., 2007. A

decade of GPS in Southeast Asia: resolving Sundaland motion and boundaries. J. Geophys. Res. 112, B06420. http://dx.doi.org/10.1029/2005JB003868.
Smrekar, S. E., Davaille, A., Sotin, C., 2018. Venus Interior Structure and Dynamics. Space Sci. Rev. 214 (88). https://doi.org/10.1007/s11214-018-0518-1.
Solomatov, V. S., 2004a. Initiation of subduction by small-scale convection. J. Geophys. Res., 109, B01412. doi:10.1029/2003JB002628.
Solomatov, V. S., 2004b. Correction to ‘‘Initiation of subduction by small-scale convection’’. J. Geophys. Res. 109, B05408, doi:10.1029/2004JB003143.
Soret, M., Agard, P., Dubacq, B., Vitale-Brovarone, A., Monié, P., Chauvet, A., Whitechurch, H., and Villemant, B., 2016. Strain localization and fluid infiltration in the mantle wedge during subduction initiation: Evidence from the base of the new caledonia ophiolite. Lithos, 244, 1 – 19.
Spakman, W., Wortel, R., 2004. A tomographic view on Western Mediterranean geodynamics. In: The TRANSMED Atlas - The Mediterranean Region From Crust to Mantle, edited by W. Cavazza et al., Springer, Berlin, Heidelberg, 31–52.
Srivastava, S. P., Schouten, H., Roest, E. R., Klitgord, K. D., Kovacs, L. C., Verhoef J., Macnab, R., 1990. Iberian plate kinematics: a jumping plate boundary between Eurasia and Africa. Nature 344, 756–759.
Stampfli, G.M., 2000. Tethyan oceans. In: E. Bozkurt, J.A. Winchester, J.D.A. Piper (Eds.), Tectonics and Magmatism in Turkey and Surrounding Area, Geol. Soc. London Spec. Publ. 173, 163-185.
Stanek, K. P., Maresch, W. V., Pindell, J. L., 2009. The geotectonic story of the northwestern branch of the Caribbean Arc: Implications from structural and geochronological data of Cuba. Geol. Soc. London Spec. Publ. 328 (1), 361–398. doi.org/10.1144/SP328.15.
Stern, R., Bloomer, S., 1992. Subduction zone infancy: examples from the Eocene Izu- Bonin-Mariana and Jurassic California arcs. Geol. Soc. Am. Bull. 104, 1621–1636. https://doi.org/10.1130/0016-7606(1992)104.
Stern, R.J., 2004. Subduction initiation: spontaneous and induced. Earth Planet. Sci. Lett. 226, 275–292.
Stern, R.J., Reagan, M., Ishizuka, O., Ohara, Y., Whattam, S., 2012. To understand subduction initiation, study forearc crust; to understand forearc crust, study ophiolites. Lithosphere 4, 469–483.
Stern, R. J., Gerya, T., 2018. Subduction initiation in nature and models: A review. Tectonophysics 746, 173–198. https://doi.org/10.1016/j.tecto.2017.10.014, 2018.
Stern, R.J., Dumitru, T.A., 2019. Eocene initiation of the Cascadia subduction zone: a second example of plume-induced subduction initiation? Geosphere. https://doi.org/10.1130/GES02050.1.
Strzerzynski, P., Déverchère, J., Cattaneo, A., Domzig, A., Yelles, K., Mercier de Lépinay, B., Babonneau, N., Boudiaf, A., 2010. Tectonic inheritance and Pliocene-Pleistocene inversion of the Algerian margin around Algiers: Insights from multibeam and seismic reflection data. Tectonics 29, TC2008. doi:10.1029/2009TC002547.
Sutherland, R., 1995. The Australia-Pacific boundary and Cenozoic plate motions in the SW Pacific: Some constraints from Geosat data. Tectonics 14 (4), 819–831. doi:10.1029/95TC00930.

Sutherland, R., Barnes, P., Uruski, C., 2006. Miocene-Recent deformation, surface elevation, and volcanic intrusion of the overriding plate during subduction initiation, offshore southern Fiordland, Puysegur margin, southwest New Zealand. NZ J. Geol.Geophys. 49 (1), 131-149. DOI: 10.1080/00288306.2006.9515154.

Sutherland, R., Collot, J., Lafoy, Y., Logan, G. A., Hackney, R., Stagpoole, V., Uruski, C., Hashimoto, T., Higgins, K., Herzer, R. H., Wood, R., Mortimer, N., Rollet, N., 2010. Lithosphere delamination with foundering of lower crust and mantle caused permanent subsidence of New Caledonia Trough and transient uplift of Lord Howe Rise during Eocene and Oligocene initiation of Tonga-Kermadec subduction, western Pacific. Tectonics 29, TC2004. doi:10 .1029 /2009TC002476.

Sutherland, R., Collot, J., Bache, F., Henrys, S., Barker, D., Browne, G. H., Lawrence, M. J. F., Morgans, H. E. G., Hollis, C. J., Clowes, C., Mortimer, N., Rouillard, P., Gurnis, M., Etienne, S., Stratford, W., 2017. Widespread compression associated with Eocene Tonga-Kermadec subduction initiation. Geology 45 (4), 355–358. https://doi.org/10.1130/G38617.1

Taboada, A., Rivera, L. A., Fuenzalida, A., Cisternas, A., Philip, H., Bijwaard, H., Olaya, J., Rivera, C., 2000. Geodynamics of the northern Andes: subductions and intracontinental deformation (Colombia). Tectonics 19 (5), 787-813.

Tamaki, K., Honza, E., 1985. Incipient subduction and obduction along the eastern margin of the Japan Sea. Tectonophysics 119, 381-406.

Tang, J.-C., Chemenda, A. I., 2000. Numerical modelling of arc–continent collision: application to Taiwan. Tectonophysics 325, 23-42.

Tang, J.-C., Chemenda, A.I., Chéry, J., Lallemand, S., Hassani, R., 2002. Compressional subduction regime and initial arc-continent collision : Numerical modeling. Geol. Soc. Am. Spec. Paper 358, 177-186.

Tao, W. C., O'connell, R. J., 1992. Ablative subduction: A two-sided alternative to the conventional subduction model. J. Geophys. Res, 97(B6), 8877-8904.

Tapster, S., Roberts, N. M. W., Petterson, M. G., Naden, J., 2014. From continent to intra-oceanic arc: Zircon xenocrysts record the crustal evolution of the Solomon island arc. Geology 42 (12), 1087–1090. doi:10.1130/G36033.1.

Taylor, F. W., Frohlich, C., Lecolle, J., Strecker, M., 1987. Analysis of partially emerged corals and reef terraces in the central Vanuatu arc: Comparison of contemporary co-seismic and non seismic with Quaternary vertical movements. J. Geophys. Res. 92, 4905– 4933.

Taylor, B., Goodliffe, A., Martinez, F., Hey, R., 1995. Continental rifting and initial sea-floor spreading in the Woodlark Basin. Nature 374, 534–537.

ten Brink, U. S., Marshak, S., Granja Bruna, J.-L., 2009. Bivergent thrust wedges surrounding oceanic island arcs: Insight from observations and sandbox models of the northeastern Caribbean plate. Geol. Soc. Am. Bull. 121 (11/12), 1522-1536. doi: 10.1130/B26512.1.

Terrinha, P., Matias, L., Vicente, J., Duarte, J., Luíse, J., Pinheiro, L., Lourenço, N., Diez, S., Rosas, F., Magalhaes, V., Valadares, V., Zitellini, N., Roque C., Mendes Victor, L., MATESPRO Team, 2009. Morphotectonics and strain partitioning at the Iberia–Africa plate boundary from multibeam and seismic reflection data. Mar. Geol. 267, 156–174.

Thielmann, M., Kaus, B. J., 2012. Shear heating induced lithospheric-scale localization: does it result in subduction? Earth Planet. Sci. Lett. 359, 1–13.
Toth, J., Gurnis, M., 1998. Dynamics of subduction initiation at preexisting fault zones, J. Geophys. Res., 103, 18,053–18,067.
Tortella, D., Torne, M., Perez-Estaun, A., 1997. Geodynamic Evolution of the Eastern Segment of the Azores-Gibraltar Zone: The Gorringe Bank and the Gulf of Cadiz Region. Mar. Geophys. Res. 19, 211–230.
Turcotte, D. L., Haxby, W. F., Ockendon, J. R., 1977. Lithospheric Instabilities, Maurice Ewing Series - American Geophysical Union I, 63-69.
Turcotte, G., Schubert, G., 1982. Geodynamics: Application of Continuum Physics to Geological Problems, John Wiley, New York, NY.
Turner, S., Rushmer, T., Reagan, M., Moyen, J.-F., 2014. Heading down early on? Start of subduction on Earth. Geology 42 (2), 139-142. doi:10.1130/G34886.1.
Ueda, K., Gerya, T. V., Sobolev, S. V., 2008. Subduction initiation by thermal–chemical plumes: Numerical studies. Physics of the Earth and Planetary Interiors 171 (1), 296–312.
Ulvrova, M. M., Coltice, N., Williams, S., Tackley, P. J., 2019. Where does subduction initiate and cease? A global scale perspective. Earth Planet. Sci. Lett., 528, 115836.
Ustaszewski, K., Schmid, S., Fügenschuh, M., Tischler, M., Kissling, E., Spakman, W., 2008. A map-view restoration of the Alpine-Carpathian-Dinaridic system for the early Miocene. Swiss J. Geosci. 101 (1), 273-94.
Uyeda, S., Ben-Avraham, Z., 1972. Origin and development of the Philippine Sea. Nature 240, 176-178.
Uyeda, S., Kanamori, H., 1979. Back-arc opening and the mode of subduction. J. Geophys. Res. 84, 1049-1061.
Vaes, B., van Hinsbergen, D. J. J., Boschman, L. M., 2019. Reconstruction of subduction and back-arc spreading in the NW Pacific and Aleutian Basin: Clues to causes of Cretaceous and Eocene plate reorganizations. Tectonics 38, 1367–1413. https://doi.org/10.1029/2018TC005164.
Vallejo, C., Spikings, R. A., Luzieux, L., Winkler, W., Chew, D., Page, L., 2006. The early interaction between the Caribbean Plateau and the NW South American Plate. Terra Nova 18, 264-269. doi: 10.1111/j.1365-3121.2006.00688.x.
van Benthem, S., Govers, R., Spakman, W., Wortel, R., 2013. Tectonic evolution and mantle structure of the Caribbean, J. Geophys. Res. Solid Earth 118, 3019–3036. doi:10.1002/jgrb.50235.
van de Lagemaat, S. H. A., van Hinsbergen, D. J. J., Boschman, L. M., Kamp, P. J. J., Spakman, W., 2018. Southwest Pacific absolute plate kinematic reconstruction reveals major Cenozoic Tonga-Kermadec slab dragging. Tectonics 37, 2647–2674. https://doi.org/10.1029/2017TC004901.
van de Lagemaat, S. H. A., Swart, M. L. A., Kosters, M. E., Vaes, B., Boschman, L. M., Burton-Johnson, A., Bijl, P. K., Spakman, W., and van Hinsbergen, D. J. J., 2021. From subduction initiation to extension in the Scotia Sea region and the opening of the Drake Passage: when and why?. Earth-Science Reviews 215. doi.org/10.1016/j.earscirev.2021.103551.
van der Meer, D. G., van Hinsbergen, D. J. J., Spakman, W., 2018. Atlas of the underworld: slab remnants in the mantle, their sinking history, and a new

outlook on lower mantle viscosity. Tectonophysics 723, 309–448. doi:10.1016/j.tecto.2017.10.004
van der Werff, W., 2000. Backarc deformation along the eastern Japan Sea margin, offshore northern Honshu. J. Asian Earth Sci. 18, 71-95.
van Fossen, M. C., Channell, J. E. T., 1988. Paleomagnetism of Late Cretaceous and Eocene limestones and chalks from Haiti: Tectonic interpretations. Tectonics 7 (3), 601-612.
van Hinsbergen, D.J.J., Vissers, R.L., Spakman,W., 2014. Origin and consequences of western Mediterranean subduction, rollback, and slab segmentation. Tectonics 33, 393-419.
van Hinsbergen, D.J.J., Torsvik, T.H., Schmidt, S.M., Matenco, L.C., Maffione, M., Visers, R.L.M., Gürer, D., Spakman, W., 2020. Orogenic architecture of the Mediterranean region and kinematic reconstruction of its tectonic evolution since the Triassic. Gondwana Res. 81, 79-229. https://doi.org/10.1016/j.gr.2019.07.009
van Hinsbergen, D. J.J., Steinberger, B., Guilmette, C., Maffione, M., Gürer, D., Peters, K., Plunder, A., McPhee, P. J., Gaina, C., Advokaat, E. L., Vissers, R. L.M., Spakman, W., in press. A record of plume-induced plate rotation triggering seafloor spreading and subduction initiation. Nature Geoscience.
Vérard, Ch., Flores, K., Stampfli, G., 2012. Geodynamic reconstructions of the South America–Antarctica plate system. J. Geodyn. 53, 43–60. http://dx.doi.org/10.1016/j. jog.2011.07.007.
Vlaar, N. J., Wortel, M. J. R., 1976. Lithospheric aging instability and subduction, Tectonophysics 32, 331-351.
von Huene, R., Lallemand, S., 1990. Tectonic erosion along the Japan and Peru convergent margin. Geol. Soc. Am. Bull. 102, 704–720.
von Huene, R., Scholl, D. W., 1991. Observations at convergent margins concerning sediment subduction, subduction erosion, and the growth of continental crust. Rev. Geophys. 29,279–316.
Wanke, M., Portnyagin, M., Hoernle, K., Werner, R., Hauff, F., van den Bogaard, P., Garbe-Schonberg, D., 2012. Bowers Ridge (Bering Sea): An Oligocene-Early Miocene island arc. Geology 40, 687–690.
Weber, M., Gomez-Tapias, J., Cardona, A., Duarte, E., Pardo-Trujillo, A., Valencia, V. A., 2015. Geochemistry of the Santa Fé Batholith and Buritica Tonalite in NW Colombia - Evidence of subduction initiation beneath the Colombian Caribbean Plateau. J. South Am. Earth Sci. 62, 257-274. doi.org/10.1016/j.jsames.2015.04.002.
Wei, D., Seno, T., 1998. Determination of the Amurian Plate Motion. In: M.F.J. Flower, Sun-Lin Chung, Ching-Hua Lo, and Tung-Yi Lee, eds, Mantle dynamics and plate interactions in East Asia, *Geodynamic Series AGU* 27. https://doi.org/10.1029/GD027p0337.
Weissel, J.K., Anderson, R.N., Geller, C.A., 1980. Deformation of the Indo-Australian plate. Nature 287, 284–291.
Wells, R., Bukry, D., Friedman, R., Pyle, D., Duncan, R., Haeussler, P., Wooden, J., 2014. Geologic history of Siletzia, a large igneous province in the Oregon and Washington Coast Range: Correlation to the geomagnetic polarity time scale and implications for a long-lived Yellowstone hotspot. Geosphere 10, 692–719. https:// doi .org /10 .1130 /GES01018 .1.

Whattam, S.A., Stern, R.J., 2011. The ‘subduction initiation rule’: a key for linking ophiolites, intra-oceanic forearcs and subduction initiation. Contrib. Mineral. Petrol. 162, 1031–1045.
Whattam, S.A., Stern, R.J., 2015. Late Cretaceous plume-induced subduction initiation along the southern margin of the Caribbean and NW South America: The first documented example with implications for the onset of plate tectonics. Gondwana Research 27, 38–63. https://doi .org /10 .1016 /j .gr .2014 .07 .011.
Whattam, S. A., Montes, C., Stern, R. J., 2020. Early central American forearc follows the subduction initiation rule. Gondwana Res. 79, 283-300.
White, W., Copeland, P., Gravatt, D. R., Devine, J. D., 2017. Geochemistry and geochronology of Grenada and Union islands, Lesser Antilles: The case for mixing between two magma series generated from distinct sources. Geosphere 13 (5), 1359–1391. doi.org/10.1130/GES01414.1.
Whittaker, J., Müller, R. D., Leitchenkov, G., Stagg, H., Sdrolias. M., Gaina, C., Goncharov, A., 2007. Major Australian–Antarctic plate reorganization at Hawaiian–Emperor bend time. Science 318, 83–86. doi:10.1126/science.1143769
Wiens, D. A., Stein, S., 1983. Age dependence of oceanic intraplate seismicity and implications for lithospheric evolution, J. Geophys. Res., 88, 6455-6468.
Wilson JT. 1968. Static or mobile earth: the current scientific revolution. Proc. Am. Philos. Soc. 112(5), 309–20.
Wilson, M., Bianchini, G., 1999. Tertiary–Ouaternary magmatism within the Mediterranean and surrounding regions. In: Durand, B., Jolivet, L., Horvath, F., Séranne, M. (Eds.), The Mediterranean Basins: Tertiary Extension within the Alpine Orogen: Geol. Soc. London Spec. Publ. 156, 141–168.
Wolfson-Schwehr, M., Boettcher, M. S., McGuire, J. J., Collins, J. A. , 2014. The relationship between seismicity and fault structure on the Discovery transform fault, East Pacific Rise. Geochem. Geophys. Geosyst. 15, 3698– 3712, doi:10.1002/2014GC005445.
Wong, T., Solomatov, V., 2015. Towards scaling laws for subduction initiation on terrestrial planets: constraints from two-dimensional steady-state convection simulations. Progress Earth Planet. Sci. 2, 18. DOI 10.1186/s40645-015-0041-x.
Wong, T., Solomatov, V., 2016. Constraints on plate tectonics initiation from scaling laws for single-cell convection. Physics Earth Planet. Sci. Int. 257, 128-136. https://doi.org/10.1016/j.pepi.2016.05.015.
Wortel, M. J. R., Spakman, W., 2000. Subduction and slab detachment in the Mediterranean-Carpathian region. Science 290,1910–17.
Worthing, M.A., Crawford, A.J., 1996. The igneous geochemistry and tectonic setting of metabasites from the Emo metamorphics, Papua New Guinea; a record of the evolution and destruction of a backarc basin. Mineralogy and Petrology 58, 79–100. doi:10 .1007 /BF01165765.
Wright, J. E., Wyld, S. J., 2011. Late Cretaceous subduction initiation on the eastern margin of the Caribbean-Colombian Oceanic Plateau: One Great Arc of the Caribbean?. Geosphere, 7(2), 468–493. https://doi.org/10.1130/GES00577.1
Wu, J., Suppe, J., Lu, R., Kanda, R., 2016. Philippine Sea and East Asian plate tectonics since 52 Ma constrained by new subducted slab reconstruction

methods. J. Geophys. Res. Solid Earth 121, 4670–4741. doi:10.1002/2016JB012923.
Yan, C., Kroenke, L.W., 1993. A plate tectonic reconstruction of the Southwest Pacific, 0–100 Ma. Proc. ODP Sci. Results 130, 697–709.
Yang, T. F., Tien, J.-L., Chen, C.-H., Lee, T., Punongbayan, R. S., 1995. Fission-track dating of volcanics in the northern part of the Taiwan-Luzon Arc: eruption ages and evidence for crustal contamination. J. Southeast Asian Earth Sci. 11 (2), 81-93.
Yang, T. F., Lee, T., Chen, C.-H., Cheng, S. N., Knittel, U., Punongbayan, R. S., Rasdas, A. R., 1996. A double island arc between Taiwan and Luzan: tectonic manifestation of ridge subduction. Tectonophysics 258, 85-101.
Yang, T., Gurnis, M., Zahirovic, S., 2016. Mantle-induced subsidence and compression in SE Asia since the early Miocene. Geophys. Res. Lett. 43, 1901–1909. doi:10.1002/2016GL068050.
Yoneshima, S., Mochizuki, K., Araki, E., Hino, R., Shinohara, M., Suyehiro, K., 2005. Subduction of the Woodlark Basin at New Britain Trench, Solomon Islands region. Tectonophysics 397, 225-239. doi:10.1016/j.tecto.2004.12.008.
Yu, S.-B., Hsu, Y.-J., Bacolcol, T., Yang, C.-C., Tsai, Y.-C., Solidum, R., 2013. Present-day crustal deformation along the Philippine Fault in Luzon, Philippines. J. Asian Earth Sci. 65, 64-74.
Yu, M., Yan, Y., Huang, C.-Y., Zhang, X., Tian, Z., Chen, W.-H., & Santosh, M., 2018. Opening of the South China Sea and upwelling of the Hainan plume. Geophysical Research Letters 45, 2600–2609. https://doi.org/10.1002/2017GL076872.
Yuen, D., Fleitout, L., Schubert, G. & Froidevaux, C. Shear deformation zones along major transform faults and subducting slabs. Geophys. J. Int. 54, 93–119 (1978).
Yumul, G. P. Jr, Dilamanta, C. B., Tamayo, R. A. Jr, Maury, R. C., 2003. Collision, subduction and accretion events in the Philippines: A synthesis. Island Arc 12, 77–91.
Zahirovic, S., Seton, M., Müller, R. D., 2014. The Cretaceous and Cenozoic tectonic evolution of Southeast Asia. Solid Earth 5, 227–273. doi:10.5194/se-5-227-2014.
Zahirovic, S., Matthews, K.J., Flament, N., Müller, R.D., Hill, K.C., Seton, M., Gurnis, M., 2016. Tectonic evolution and deep mantle structure of the eastern Tethys since the latest Jurassic. Earth-Science reviews 162, 293-337. doi.org/10.1016/j.earscirev.2016.09.005.
Zhao, M., He, E., Sibuet, J.-C., Sun, L., Qiu, X., Tan, P., Wang, J., 2018. Post-seafloor spreading volcanism in the central east South China Sea and its formation through an extremely thin oceanic crust. Geochem. Geophys. Geosyst., https://doi. org/10.1002/2017GC007034.
Zhang, L., Zlotnik, S., Li, C.-F., 2021. Anomalous subduction initiation: Young under old oceanic lithosphere. Geochemistry, Geophysics, Geosystems, 22, e2020GC009549. https://doi.org/10.1029/2020GC009549
Zhang, S., Leng, W., 2021. Subduction polarity reversal: Induced or spontaneous? Geophysical Research Letters, 48, e2021GL093201. https://doi.org/10.1029/2021GL093201

Zhong, X., Li, Z.-H., 2019. Forced subduction initiation at passive continental margins: Velocity-driven versus stress-driven. Geophys. Res. Lett., 46, 11054–11064. https://doi.org/10.1029/2019GL084022.

Zhong, X., Li, Z.-H., 2020. Subduction initiation during collision-induced subduction transference: Numerical modeling and implications for the Tethyan evolution. J. Geophys. Res., 125, e2019JB019288. https://doi. org/10.1029/2019JB019288

Zhou, X., Li, Z.-H., Gerya, T. V., Stern, R. J., Xu, Z., Zhangi, J., 2018. Subduction initiation dynamics along a transform fault control trench curvature and ophiolite ages. Geology 46, 607–610. https://doi.org/10.1130/G40154.1.

Zhou, X., Li, Z.-H., Gerya, T. V., Stern, R. J., 2020. Lateral propagation–induced subduction initiation at passive continental margins controlled by preexisting lithospheric weakness. Sci. Adv. 6, eaaz1048.

Zhou, X., Wada, I., 2021. Differentiating induced versus spontaneous subduction initiation using thermomechanical models and metamorphic soles. Nature Communications 12, 4632. doi.org/10.1038/s41467-021-24896-x

Zhu, G., Gerya, T.V., Yuen, D.A., Honda, S., Yoshida, T., Connolly, J.A.D., 2009. 3-D Dynamics of hydrous thermal chemical plumes in oceanic subduction zones. Geochem. Geophys. Geosyst. 10, Q11006.

Zhu, G., Gerya, T. V., Honda, S., Tackley, P. J., and Yuen, D. A., 2011. Influences of the buoyancy of partially molten rock on 3-d plume patterns and melt productivity above retreating slabs. Phys. Earth Planet. Int., 185(3), 112 – 121.

Zitellini, N., Gracia, E., Matias, L., Terrinha, P., Abreu, M. A., DeAlteriis, G., Henriet, J.-P., Danobeitia, J.-J., Masson, D. G., Mülder, T., Ramella, R., Somoza, L., Diez, S., 2009. The quest for the Africa–Eurasia plate boundary west of the Strait of Gibraltar. Earth Planet. Sci. Lett. 280, 13-50. doi:10.1016/j.epsl.2008.12.005.